ADAPTOR PROTEIN REGULATION IN IMMUNE SIGNALLING

EDITED BY: Navin Kumar Verma, Dermot Kelleher and Thai Tran
PUBLISHED IN: Frontiers in Immunology

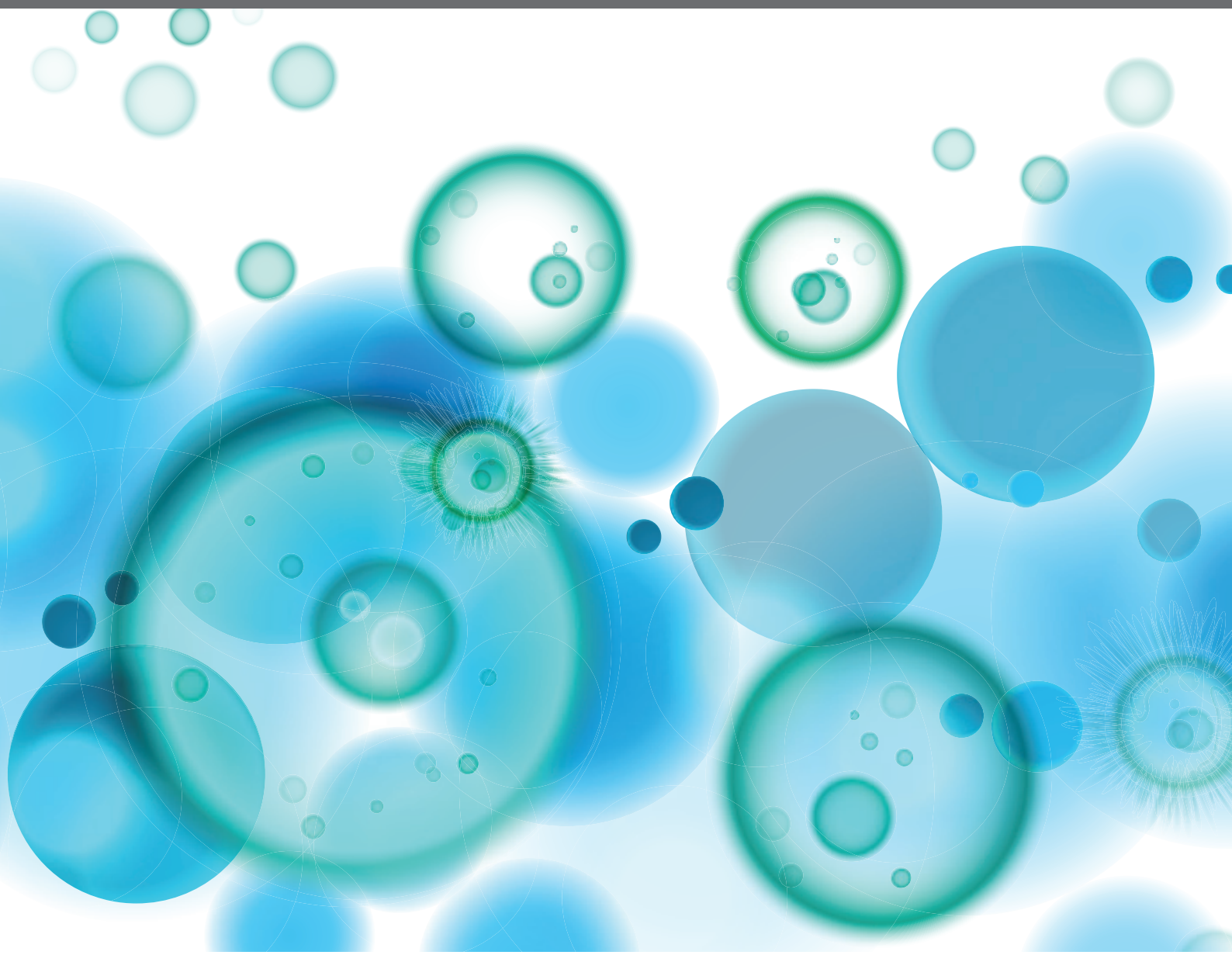

frontiers Research Topics

frontiers

ISSN 1664-8714
ISBN 978-2-88963-703-4
DOI 10.3389/978-2-88963-703-4

About Frontiers

Frontiers is more than just an open-access publisher of scholarly articles: it is a pioneering approach to the world of academia, radically improving the way scholarly research is managed. The grand vision of Frontiers is a world where all people have an equal opportunity to seek, share and generate knowledge. Frontiers provides immediate and permanent online open access to all its publications, but this alone is not enough to realize our grand goals.

Frontiers Journal Series

The Frontiers Journal Series is a multi-tier and interdisciplinary set of open-access, online journals, promising a paradigm shift from the current review, selection and dissemination processes in academic publishing. All Frontiers journals are driven by researchers for researchers; therefore, they constitute a service to the scholarly community. At the same time, the Frontiers Journal Series operates on a revolutionary invention, the tiered publishing system, initially addressing specific communities of scholars, and gradually climbing up to broader public understanding, thus serving the interests of the lay society, too.

Dedication to Quality

Each Frontiers article is a landmark of the highest quality, thanks to genuinely collaborative interactions between authors and review editors, who include some of the world's best academicians. Research must be certified by peers before entering a stream of knowledge that may eventually reach the public - and shape society; therefore, Frontiers only applies the most rigorous and unbiased reviews.
Frontiers revolutionizes research publishing by freely delivering the most outstanding research, evaluated with no bias from both the academic and social point of view. By applying the most advanced information technologies, Frontiers is catapulting scholarly publishing into a new generation.

What are Frontiers Research Topics?

Frontiers Research Topics are very popular trademarks of the Frontiers Journals Series: they are collections of at least ten articles, all centered on a particular subject. With their unique mix of varied contributions from Original Research to Review Articles, Frontiers Research Topics unify the most influential researchers, the latest key findings and historical advances in a hot research area! Find out more on how to host your own Frontiers Research Topic or contribute to one as an author by contacting the Frontiers Editorial Office: researchtopics@frontiersin.org

ADAPTOR PROTEIN REGULATION IN IMMUNE SIGNALLING

Topic Editors:
Navin Kumar Verma, Nanyang Technological University, Singapore
Dermot Kelleher, University of British Columbia, Canada
Thai Tran, National University of Singapore, Singapore

Citation: Verma, N. K., Kelleher, D., Tran, T., eds. (2020). Adaptor Protein Regulation in Immune Signalling. Lausanne: Frontiers Media SA. doi: 10.3389/978-2-88963-703-4

Table of Contents

frontiers in Immunology

EDITORIAL
published: 13 March 2020
doi: 10.3389/fimmu.2020.00441

Editorial: Adaptor Protein Regulation in Immune Signalling

Navin Kumar Verma[1]*, *Thai Tran*[2]* and *Dermot Kelleher*[1,3]*

[1] Lee Kong Chian School of Medicine, Nanyang Technological University Singapore, Singapore, Singapore, [2] Department of Physiology, Yong Loo Lin School of Medicine, National University of Singapore, Singapore, Singapore, [3] Departments of Medicine and Biochemistry and Molecular Biology, University of British Columbia, Vancouver, BC, Canada

Keywords: innate and adaptive immunity, leukocyte motility, T cells, B cells, NK cells, mast cells, monocytes, CG-NAP

Editorial on the Research Topic

Adaptor Protein Regulation in Immune Signalling

OPEN ACCESS

Edited and reviewed by:
Francesca Granucci,
University of Milano Bicocca, Italy

***Correspondence:**
Navin Kumar Verma
nkverma@ntu.edu.sg
Thai Tran
phstt@nus.edu.sg
Dermot Kelleher
dermot.kelleher@ubc.ca

Specialty section:
This article was submitted to Molecular Innate Immunity, a section of the journal Frontiers in Immunology

Received: *17 February 2020*
Accepted: *26 February 2020*
Published: *13 March 2020*

Citation:
Verma NK, Tran T and Kelleher D (2020) Editorial: Adaptor Protein Regulation in Immune Signalling. Front. Immunol. 11:441. doi: 10.3389/fimmu.2020.00441

Adaptor proteins are essential cellular components that govern signaling cross-talks in time and space with precise specificity. They contain multiple protein-binding modules that bring cellular enzymes and effector molecules into close proximity to their targets, controlling their activities. These proteins add another layer to the specificity of signaling by the type of protein-binding modules they engage in and their subcellular localization. Several adaptor proteins have been identified that coordinate signal transduction cascades in immune cells for their effector functions, including motility, activation, proliferation, and differentiation.

This Research Topic is a collection of work that aims to provide an overview of emerging roles of adaptor proteins in immune functions. We invited several immunologists and scientists to update the knowledge about adaptor proteins in immune signaling. A total of six original research papers and three insightful reviews in this collection provide meaningful insights toward the roles of adaptor proteins in the functioning of various immune cell types, including T cells, B cells, natural killer (NK) cells, mast cells, and monocytes.

The topic starts with a primary article by Böning et al. in which authors demonstrate a crucial role of the adhesion and degranulation-promoting adapter protein (ADAP) in NK cell priming, cytokine production, and cytotoxicity in an *in vivo* setting. Using an intracellular pathogen *Listeria monocytogenes*, they show that infection-primed NK cells lacking ADAP produce inefficient amounts of perforin and have impaired cytotoxic capacity. In another original article, Rudolph et al. demonstrate that T cell-specific conditional ADAP knockout mice display less severe experimental autoimmune encephalomyelitis (EAE). They propose that ADAP-expressing NK cells and myeloid cells might synergistically contribute to the observed mild EAE. These datasets expand the knowledge about roles of the cytosolic adapter protein ADAP in immune cell functions.

The review by Verma et al. summarizes the role of CG-NAP/kinase interactions in T cell homeostasis and functions. Due to its ability to dynamically and spatial-temporally interact with multiple kinases, CG-NAP appears central to the functional regulation of T cell activation,

proliferation, differentiation, and migration. They suggest exploiting CG-NAP/kinase interactions as tunable therapeutic targets for T cell-mediated diseases.

In the next very informative review, Yablonski describes the biological and functional roles of the Grb2-related adaptor downstream of Shc (Gads) in regulating allergy and T cell-mediated immunity. She expounds that linker for activation of T cells (LAT), Gads, and Src homology 2 (SH2) domain-containing leukocyte phosphoprotein of 76 kDa (SLP-76) form heterotrimeric microclusters that mediate signal transduction *via* the T cell receptor (TCR) and the mast cell high-affinity IgE receptor FcεRI. The review sheds light on additional Gads-binding molecules, including co-stimulatory proteins CD28 and CD6, adaptor protein Shc, deubiquitinating enzymes USP8 and AMSH, the serine/threonine hematopoietic progenitor kinase 1 (HPK1) and the tyrosine kinase BCR-ABL.

Natural killer T (NKT) cells are a distinct subset of T cells sharing phenotypic and functional characteristics common to both conventional T cells and NK cells. They can recognize lipid antigens presented by the major histocompatibility complex (MHC) class I-like CD1d molecules (1). The review by Gerth and Mattner drives the reader into the intracellular processes mediated by adaptor proteins, in particular the adaptor protein SLP-76, in the unique biology of NKT cells, such as selection, differentiation, and activation.

The toll-like receptor (TLR) eight is a known endosomal sensor of degraded RNA in human phagocytes and is involved in the recognition of viruses, bacteria, and mitochondria (2, 3). Using a TLR8 antagonist in their original article, Moen et al. demonstrate an important role of TLR8 in human monocytes challenged with *Staphylococcus aureus*, *Streptococcus agalactiae*, *Streptococcus pneumonia*, *Pseudomonas aeruginosa*, and *Escherichia coli*. They propose a novel signaling model where TLRs rapidly recruit and modify the interleukin-1 receptor-associated kinase 1 (IRAK-1) pool in monocytes, which may also sequester the adaptor protein MyD88 and/or IRAK-4, attenuating the interferon regulatory factor 5 (IRF5)-dependent cytokine induction and TLR8 /IRF5 signaling.

The next original article by Zhou et al. demonstrates a vital role of the mitochondrial serine/threonine kinase phosphatase and tensin homolog (PTEN)-induced putative kinase 1 (PINK1) in innate antiviral immunity. The authors highlight that PINK1 positively regulates the retinoic acid-inducible gene I (RIG-I) triggered antiviral immunity by preventing the degradation of TNF receptor-associated factor 3 (TRAF3) and reducing the inhibition of the cellular responses mediated *via* the yes-associated protein (YAP).

Studies indicate that large antigen-containing particles, such as vaccinia virus, bacteria, and multicellular parasites, induce T cell-dependent B cell high-affinity antibody responses (4). Such responses require the internalization of large particulate antigens after the recognition by the B cell receptor (BCR). Using high-throughput quantitative image analysis and a panel of small molecule inhibitors, Verstegen et al. show that human B cells require IgM-BCR signaling *via* PI3K to efficiently engulf large anti-IgM-coated particles. This signaling cascade involves the cytoplasmic adaptor protein NCK in addition to the co-receptor CD19. They further demonstrate that the IgM-BCR/NCK signaling facilitates the activation of Rho family GTP-binding protein RAC1 to promote actin cytoskeleton remodeling necessary for particle internalization. They propose the NCK/PI3K/RAC1 signaling axis as an attractive target for biological intervention to prevent undesired antibody response to large particulate antigens.

The Skp1/Cul1/F-box ubiquitin ligase, β transducin repeat-containing protein (β-TrCP), regulates a diverse range of intracellular signaling pathways (5, 6). In this collection, Liu et al. demonstrate how β-TrCP restricts signal transduction *via* the TNF receptor-associated factor 6/IκB kinase (TRAF6/IKK) upstream of IκBα signaling induced by bacterial lipopolysaccharide, which is implicated in the regulation of inflammatory signaling by TLRs.

In conclusion, the collection of original articles and reviews provide new and valuable insight about the complex roles of adaptor proteins in immune regulation and also illustrate the important roles that these molecules play in immune function. We hope that this collection would inspire future research employing advance molecular and genetic tools to further dissect the interplay between adaptor proteins and their interacting partners in immune cells. In the near future, we anticipate much progress in this area of research, a greater appreciation of adaptor protein regulation of immune cells and the emergence of adaptor proteins as potential new targets for therapy.

AUTHOR CONTRIBUTIONS

All authors listed have made a substantial, direct and intellectual contribution to the work, and approved it for publication.

FUNDING

This work was supported, in part, by the Lee Kong Chian School of Medicine, Nanyang Technological University Singapore Start-Up Grant (L0412290), and the Singapore Ministry of Education (MOE) under its Singapore MOE Academic Research Fund (AcRF) Tier 2 Grant (MOE2017-T2-2-004) to NV and the Singapore MOE AcRF Tier 2 grant (MOE2019-T2-1-059) and Tier 1 grant (NUHSRO/2019/048/T1/SEED-MAR/01) to TT.

ACKNOWLEDGMENTS

We thank all the authors for contributing to this Research Topic.

REFERENCES

1. Krovi SH, Gapin L. Invariant natural killer T cell subsets-more than just developmental intermediates. *Front Immunol.* (2018) 9:1393. doi: 10.3389/fimmu.2018.01393
2. Krüger A, Oldenburg M, Chebrolu C, Beisser D, Kolter J, Sigmund AM, et al. Human TLR8 senses UR/URR motifs in bacterial and mitochondrial RNA. *EMBO Rep*. (2015) 16:1656–63. doi: 10.15252/embr.201540861
3. de Marcken M, Dhaliwal K, Danielsen AC, Gautron AS, Dominguez-Villar M. TLR7 and TLR8 activate distinct pathways in monocytes during RNA virus infection. *Sci Signal.* (2019) 12:605. doi: 10.1126/scisignal.aaw1347
4. Catron DM, Pape KA, Fife BT, van Rooijen N, Jenkins MK. A protease-dependent mechanism for initiating T-dependent B cell responses to large particulate antigens. *J Immunol.* (2010) 184:3609–17. doi: 10.4049/jimmunol.1000077
5. Kanemori Y, Uto K, Sagata N. Beta-TrCP recognizes a previously undescribed nonphosphorylated destruction motif in Cdc25A and Cdc25B phosphatases. *Proc Natl Acad Sci USA*. (2005) 102:6279–84. doi: 10.1073/pnas.0501873102
6. Tang W, Li Y, Yu D, Thomas-Tikhonenko A, Spiegelman VS, Fuchs SY. Targeting beta-transducin repeat-containing protein E3 ubiquitin ligase augments the effects of antitumor drugs on breast cancer cells. *Cancer Res.* (2005) 65:1904–8. doi: 10.1158/0008-5472.CAN-04-2597

Conflict of Interest: The authors declare that the research was conducted in the absence of any commercial or financial relationships that could be construed as a potential conflict of interest.

frontiers in Immunology

ORIGINAL RESEARCH
published: 13 December 2018
doi: 10.3389/fimmu.2018.02930

β-TrCP Restricts Lipopolysaccharide (LPS)-Induced Activation of TRAF6-IKK Pathway Upstream of IκBα Signaling

Jin Liu[1,2†], Yukang Yuan[1,2†], Jing Xu[1†], Kui Xiao[3†], Ying Xu[4], Tingting Guo[1,2], Liting Zhang[1,2], Jun Wang[4] and Hui Zheng[1,2*]*

[1] Institutes of Biology and Medical Sciences, Soochow University, Suzhou, China, [2] Jiangsu Key Laboratory of Infection and Immunity, Soochow University, Suzhou, China, [3] Department of Respiratory Medicine, The Second Xiangya Hospital, Institute of Respiratory Disease, Central South University, Changsha, China, [4] Department of Intensive Care Medicine, The First Affiliated Hospital of Soochow University, Suzhou, China

OPEN ACCESS

Edited by:
Navin Kumar Verma,
Nanyang Technological University,
Singapore

Reviewed by:
Marco Di Gioia,
Harvard Medical School,
United States
Eswari D-M,
University of California, San Francisco,
United States

***Correspondence:**
Hui Zheng
huizheng@suda.edu.cn
Jun Wang
wjsdfyy@163.com

[†] These authors have contributed equally to this work

Specialty section:
This article was submitted to Molecular Innate Immunity, a section of the journal Frontiers in Immunology

Received: 03 October 2018
Accepted: 29 November 2018
Published: 13 December 2018

Citation:
Liu J, Yuan Y, Xu J, Xiao K, Xu Y, Guo T, Zhang L, Wang J and Zheng H (2018) β-TrCP Restricts Lipopolysaccharide (LPS)-Induced Activation of TRAF6-IKK Pathway Upstream of IκBα Signaling. Front. Immunol. 9:2930. doi: 10.3389/fimmu.2018.02930

β transducin repeat-containing protein (β-TrCP) is a Skp1-Cul1-F-box ubiquitin ligase, which plays important roles in controlling numerous signaling pathways. Notably, β-TrCP induces ubiquitination and degradation of inhibitor of NF-κB (IκBα), thus triggering activation of NF-κB signaling. Here, we unexpectedly find that β-TrCP restricts TRAF6-IKK signaling upstream of IκBα induced by lipopolysaccharide (LPS). In LPS-Toll-like receptor 4 (TLR4) pathway, protein kinase D1 (PKD1) is essential for activation of TRAF6-IKK-IκBα signaling including TRAF6 ubiquitination, IKK phosphorylation and subsequent IκBα degradation. We found that LPS promotes binding of β-TrCP to PKD1, and results in downregulation of PKD1 and recovery of IκBα protein level. Knockdown of β-TrCP blocks LPS-induced downregulation of PKD1. Supplement of enough PKD1 in cells inhibits recovery of IκBα protein levels during LPS stimulation. Furthermore, we demonstrate that β-TrCP inhibits LPS-induced TRAF6 ubiquitination and IKK phosphorylation. Taken together, our findings identify β-TrCP as an important negative regulator for upstream signaling of IκBα in LPS pathway, and therefore renew the understanding of the roles of β-TrCP in regulating TLRs inflammatory signaling.

Keywords: ubiquitination, E3 ligase, β-TrCP, protein kinase D1, LPS

INTRODUCTION

The protein kinase D (PKD) family is a group of serine/threonine protein kinases that are comprised of three members (PKD1/PKCμ, PKD2, and PKD3/PKCν) (1). PKD family members have been shown to be essential for various cellular signaling pathways including activation of NF-κB and MAPKs, cell motility and adhesion, gene expression, and ROS (Reactive oxygen species) generation (2–5). PKD family is also involved in regulation of immune and inflammatory responses. It has been reported that PKD2 promotes phosphorylation and degradation of interferon alpha receptor 1 (IFNAR1), thus restricting interferon-mediated antiviral immunity (6). In addition, increasing evidence demonstrates that PKD family plays important roles in regulating Toll-like receptor (TLR)-mediated inflammatory signaling (7, 8). Recent studies found that a PKC/PKD inhibitor is able to inhibit lipopolysaccharide (LPS)-TLR4-mediated p38 activation and TNF-α secretion (9). PKD1, but not PKD2 and PKD3, is essential for MyD88-dependent

ubiquitination of TNF-α receptor-associated factor 6 (TRAF6), phosphorylation of IKK, and subsequent activation of NF-κB and MAPKs in TLRs signaling (7). However, in spite of many important effects of PKD family on numerous signaling pathways, how cellular PKD protein levels are regulated remains largely unexplored.

Ubiquitin-mediated proteolysis is indispensable in regulating cellular levels and stabilities of diverse proteins, and therefore plays crucial roles in controlling cell signaling and human disease progression (10). There are three types of enzymes which catalyze the conjugation of ubiquitin to its substrates: ubiquitin-activating enzyme (E1), ubiquitin-conjugating enzyme (E2), and ubiquitin ligases (E3). To date, more than 600 human ubiquitin E3 ligases have been identified. The ubiquitin E3 ligases are the key determiners for the substrate specificity. Among these ubiquitin E3 ligases, β transducin repeat-containing protein (β-TrCP) has been clearly described, and regulates many important signaling proteins (11–16). Notably, β-TrCP induces ubiquitination and degradation of inhibitor of NF-κB (IκBα), which results in NF-κB release from the IκBα-NF-κB complex, and finally triggers activation of NF-κB signaling (11, 12). Thus, β-TrCP is recognized as a positive regulator for NF-κB-related inflammatory signaling pathway.

In the present study, we unexpectedly found that β-TrCP negatively regulates TRAF6-IKK signaling upstream of IκBα induced by LPS. LPS is a kind of endotoxin secreted by Gram-negative bacteria. As an activation model of inflammation, LPS is widely used for studying the regulation mechanisms of inflammatory signaling pathways. LPS activates TLR4 signaling by recruiting MyD88 to form the TLR4/MyD88/IRAK receptor complex, which promotes PKD1 activation and subsequent TRAF6 ubiquitination (8). Ubiquitinated TRAF6 then leads to phosphorylation and activation of TAK1 and IKK. Activated IKK induces IκB phosphorylation, which recruits β-TrCP to target IκB for ubiquitination and degradation. Finally, NF-κB is released from the IκB-NF-κB complex and translocates into the nucleus in an activated status.

Here, we revealed that β-TrCP can also target PKD1, a signaling molecule upstream of IκBα in LPS signaling, and promotes PKD1 ubiquitination and degradation. We found that LPS promoted interaction between β-TrCP and PKD1, and results in downregulation of PKD1 and recovery of IκBα protein level. Knockdown of β-TrCP blocks LPS-induced downregulation of PKD1. Consistently, β-TrCP attenuates LPS-induced TRAF6 ubiquitination and IKK phosphorylation. Collectively, our findings uncover that β-TrCP acts as an important negative regulator for upstream signaling of IκBα in LPS signaling.

MATERIALS AND METHODS

Cell Culture

Human embryonic kidney cells (HEK293T) and RAW264.7 cell lines were obtained from ATCC. All cells were cultured at 37°C under 5% CO_2 in Dulbecco's modified Eagle's medium (DMEM; Hyclone) supplemented with 10% FBS (GIBCO, Life Technologies), 100 units/mL penicillin, and 100 μg/mL streptomycin. According to the manufacturer's recommendation, plasmids were transfected into cells by using Longtrans (Ucallm).

Expression Constructs and Reagents

Plasmids encoding β-TrCP and HA-β-TrCP were gifts from Dr. Serge Y. Fuchs (University of Pennsylvania). Expression plasmids HA- or GST-tagged PKD1, PKD2 and PKD3 were generated using PCR amplified from a HEK293T cDNA library. HA-Ub, HA-Ub-R48K, and HA-Ub-R63K were described previously (17). Myc-His-PKD1(1–444) and Myc-His-PKD1(445–912) were generated using PCR amplified from HA-PKD1. Myc-PKD1-Δ(172–312) and Myc-PKD1-Δ(311–444) were generated using PCR amplified from Myc-His-PKD1(1–444). Shβ-TrCP were purchased from GENECHEM (Shanghai, China). All mutations were generated by QuickChange site-Directed Mutagenesis Kit (Stratagene). All the plasmids were confirmed by DNA sequencing. Cycloheximide, MG132 and LPS were purchased from Sigma.

RNA Isolation and Real-Time PCR

Total RNAs were extracted from HEK293T cells using TRIzol reagent (Invitrogen). The cDNA was produced by reverse transcription using oligo (dT) and analyzed by quantitative real-time PCR (qPCR) with PKD1, β-actin primers using SYBR Green Supermix (Bio-Rad Laboratories). The primer sequences were as follows: PKD1, 5′-GCCAACAGAACCATCAGTCC-3' and 5′-CTCCAATAGTGCCGTTTCCG-3′; β-actin, 5′-ACCAACTGGGACGACATGGAGAAA-3′ and 5′-ATAGCACAGCCTGGATAGCAACG-3′. The relative expression of the target genes mRNA was normalized to β-actin mRNA. The results were analyzed from three independent experiments and are shown as the average mean ± SD.

Immunoblotting and Immunoprecipitation

Immunoblotting and immunoprecipitation were performed as described previously (17, 18). Briefly, all cells were harvested on ice using lysis buffer. N-ethylmaleimide (10 mM) was added to the lysis buffer when protein ubiquitination was detected. Immunoprecipitation was performed using specific antibodies overnight on a rotor at 4°C. Equivalent quantity of proteins were subjected to SDS-PAGE followed by transferring to PVDF membranes (Millipore). Then membranes were blocked with 5% non-fat milk or 5% BSA, and incubated with the corresponding primary antibodies, followed by the respective HRP-conjugated Goat anti-mouse or Goat anti-rabbit (Bioworld) secondary antibodies. Immunoreactive bands were depicted using SuperSignal West Dura Extended kits (Thermo Scientific). The following antibodies specific for GST (1:2000, HaiGene, M0301), PKD1 (1:500, Santa Cruz, sc-639), β-TrCP (1:1000, Cell signaling, #4394), HA (1:2000, abcam, ab9110), K63Ub (1:500, Cell signaling, D7A11), tubulin (1:5000, Proteintech, 66031-1-Ig), β-actin (1:5000, Proteintech, 66009-1-Ig), Myc (1:1000, abmart, #284566), IκBα (1:2000, Cell signaling, #4814), TRAF6 (1:500, Santa Cruz, sc-8409), Ubiquitin (1:1000, Santa Cruz, sc-8017), IKK (1:1000, Cell signaling, #2682), and pS176/18-IKK (1:1000, Cell signaling, #2697) have been used.

Cycloheximide Chase Assay

The half-life of proteins was determined by cycloheximide (CHX) chase assay. HEK293T cells were transfected with GST-PKD1, with or without shβ-TrCP in 6-well culture plates. Seventy two hours after transfection, cells were treated with DMSO or CHX (50 mg/mL) for 0, 6, 12 h. Furthermore, cells were harvested on ice and subjected to analysis by western blotting.

LPS Stimulation

RAW264.7 cells were treated with LPS (2.5 μg/mL) for different times. Cells were then harvested on ice using lysis buffer containing 150 mM NaCl, 20 mM Tris-HCl (pH 7.4), 1% Nonidet P-40, 0.5 mM EDTA, PMSF (50 μg/ml), and protease inhibitor mixtures (Sigma) and subjected to analysis by immunoblotting or immunoprecipitation.

CRISPR-Cas9-Mediated Genome Editing

Small guide RNAs targeting mus PKD1: $1^{\#}$ (5′-GCCCAGTCCGCTGCTGCCCG-3') and $2^{\#}$ (5′-GCCGCACTGGTCCCAGGGTC-3′) were cloned into the lentiCRISPRv2 vector and were transfected into HEK293T cells. Forty eight hours after transfection, the supernatant was used to infect RAW264.7 cells. Then the RAW264.7 cells were cultured under puromycin selection until further experiments.

In vivo Ubiquitination Assay

To analyze ubiquitination of TRAF6 in LPS signaling, RAW264.7 cells were treated with LPS (2.5 μg/mL) for 0, 15, 30 min. Cells were harvested in lysis buffer containing 150 mM NaCl, 20 mM Tris-HCl (PH 7.4), 1% NonidetP-40, 0.5 mM EDTA, PMSF (50 μg/ml), N-ethylmaleimide (10 mM) and protease inhibitors mixtures (Sigma). Endogenous TRAF6 proteins were immunoprecipitated using a specific TRAF6 antibody and then subjected to ubiquitination analysis using a specific ubiquitin (Ub) antibody by western blotting.

Statistical Analysis

Comparison between different groups was analyzed by using a two-tailed Student's *T*-test. All differences were considered that $p < 0.05$ represent statistically significant.

RESULTS

β-TrCP Negatively Regulates Protein Levels of PKD1, but Not PKD2 and PKD3

To explore the ubiquitin-mediated regulation of PKD family, we firstly analyzed the amino acid sequences of PKD family. We noted that PKD family members possess a putative $DSG(X)_{2+n}S$ motif, which has been demonstrated to be a characteristic of substrates for ubiquitin E3 ligase β-TrCP. Thus, we hypothesized that PKD family members could be potential substrates of β-TrCP. To determine the possible effect of β-TrCP on PKD family, we firstly analyzed the effects of β-TrCP overexpression on exogenous PKD family members. The results showed that overexpression of β-TrCP significantly downregulated protein levels of exogenous GST-PKD1 (**Figure 1A**), but not GST-PKD2 (**Figure 1B**) and GST-PKD3 (**Figure 1C**). To confirm the effect of β-TrCP on endogenous PKD1, we transfected cells with increasing amount of β-TrCP. We found that overexpression of β-TrCP gradually lowered protein levels of endogenous PKD1 (**Figure 1D**). Furthermore, endogenous β-TrCP was knocked down by shRNAs against β-TrCP (shβ-TrCP). We found that knockdown of β-TrCP upregulated protein levels of endogenous PKD1 in cells (**Figure 1E**). In addition, we found that overexpression of β-TrCP did not decrease PKD1 mRNA levels (**Figure 1F**), suggesting that β-TrCP regulates PKD1 at protein level. Taken together, our results suggest that β-TrCP is a negative regulator of cellular PKD1 protein.

β-TrCP Promotes PKD1 Ubiquitination and Accelerates PKD1 Degradation

To explore the mechanisms of PKD1 downregulation mediated by β-TrCP, we firstly took advantage of a proteasomal inhibitor MG132. Our results showed that MG132 inhibited β-TrCP-mediated PKD1 downregulation (**Figure 2A**), suggesting that β-TrCP promotes PKD1 downregulation via the proteasome pathway. Thus, we next analyzed whether β-TrCP is capable of regulating ubiquitination levels of PKD1. We found that overexpression of β-TrCP obviously promoted ubiquitination of GST-PKD1, but not GST-PKD2 and GST-PKD3 (**Figure 2B**), suggesting that β-TrCP specifically targets PKD1 member of PKD family. Furthermore, knockdown of β-TrCP upregulated PKD1 protein levels (**Figure 2C**, left panel) and significantly downregulated ubiquitination levels of PKD1 (**Figure 2C**, right panel). Next, we tried to determine whether β-TrCP induces K48-linked or K63-linked ubiquitination of PKD1. To this end, Ub-R48K (all lysines in Ub are mutated to arginines except lysine 48 residue) and Ub-R63K (all lysines in Ub are mutated to arginines except lysine 63 residue) were used to analyze the types of PKD1 ubiquitination. Our data showed that overexpression of β-TrCP significantly increased K48-linked polyubiquitination of PKD1 (**Figure 2D**). However, β-TrCP did not obviously affect K63-linked ubiquitination of PKD1 (**Figure 2E**).

Given that β-TrCP induces K48-linked ubiquitination of PKD1, we speculated that the protein stability of PKD1 could be regulated by β-TrCP. To address this hypothesis, we carried out cycloheximide (CHX) pulse chase analysis of PKD1 protein. Cells transfected with control vector (shCON) or shβ-TrCP were treated with protein synthesis inhibitor CHX. We found that knockdown of β-TrCP in cells substantially inhibited PKD1 degradation (**Figure 2F**), suggesting that β-TrCP knockdown enhances PKD1 protein stability. Furthermore, overexpression of β-TrCP accelerated the degradation of endogenous PKD1 protein (**Figure 2G**). In conjunction with the above observation showing that β-TrCP induces PKD1 K48-linked polyubiquitination, we think that β-TrCP can specifically promote PKD1 ubiquitination and degradation.

$NS_{354}G$ Motif of PKD1 Is Required for β-TrCP Binding and Degradation of PKD1

Previous studies have demonstrated that the conserved $DSG(X)_{2+n}S$ motif is an important characteristic of protein substrates for β-TrCP binding and subsequent protein substrates

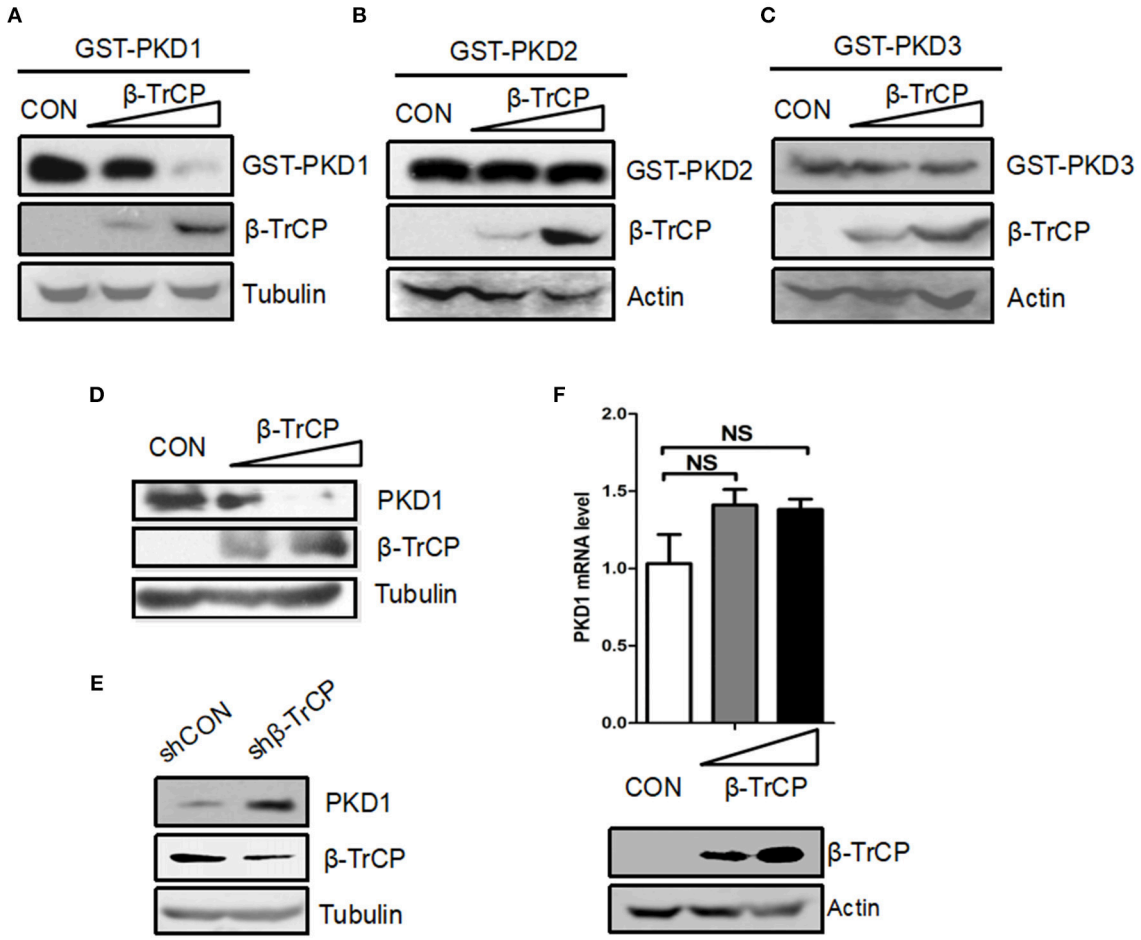

FIGURE 1 | β-TrCP specifically promotes downregulation of PKD1. **(A–C)** HEK293T cells were transfected with either an empty vector or increasing doses of β-TrCP, together with GST-PKD1 **(A)** or GST-PKD2 **(B)** or GST-PKD3 **(C)**. Protein levels of GST-PKD1/2/3, β-TrCP and Tubulin were analyzed by immunoblotting as indicated. **(D)** HEK293T cells were transfected with increasing doses of β-TrCP. Protein levels of PKD1, β-TrCP, and Tubulin were analyzed by immunoblotting as indicated. **(E)** HEK293T cells were transfected with control shRNAs (shCON) or shRNAs against β-TrCP (shβ-TrCP). Protein levels of PKD1, β-TrCP and Tubulin were analyzed by immunoblotting as indicated. **(F)** HEK293T cells were transfected with empty vector or increasing doses of β-TrCP. The mRNA levels of endogenous PKD1 were measured by qRT-PCR. β-TrCP was analyzed by immunoblotting.

degradation. And mutation of the first serine (S) in this $DSG(X)_{2+n}S$ motif of a protein substrate will result in its inability to bind with β-TrCP. By analyzing the amino acid sequences of PKD1, we found that PKD1 does possess this $DSG(X)_{2+n}S$ motif. Therefore, we firstly determined the interaction between β-TrCP and PKD1. By co-immunoprecipitation assays, we found that β-TrCP is able to interact with PKD1 (**Figure 3A**). To our surprise, mutation of this serine 380 in $DSG(X)_{2+n}S$ motif of PKD1 did not obviously affect the binding of β-TrCP to PKD1-S_{380}A (**Figure 3B**), indicating that β-TrCP interacts with PKD1 in an non-canonical manner.

We noticed that recent studies have reported several "atypical" substrates of β-TrCP, including STAT1 (19), Weel (20), GHR (21), ELAVL1/huR, CDC25B, and TP53 (22), which do not contain the classic $DSG(X)_{2+n}S$ motif. Instead, most of these atypical substrates have the $XSG(X)_{2+n}S$ motif. Therefore, we analyzed the potential $XSG(X)_{2+n}S$ motif in various species of PKD1 including Homo Sapiens, Mus Musculus, Rattus norvegicus, Desmodus rotundus, Pongoabelii, Chrysemys picta bellii (**Figure 3C**). To determine which $XSG(X)_{2+n}S$ motif of PKD1 is pivotal for binding with β-TrCP, we firstly constructed two PKD1 deletion mutants, PKD1 (1–444) and PKD1 (445–912) (**Figure 3D**). The ability of β-TrCP to downregulate two PKD1 mutants was analyzed. Our results showed that PKD1 (1–444), but not PKD1 (445–912), can be downregulated by β-TrCP overexpression (**Figure 3E**), indicating that the potential $XSG(X)_{2+n}S$ motif locates in PKD1 (1–444). PKD1 (1–444) possesses three conserved $XSG(X)_{2+n}S$ motifs (**Figure 3D**). Thus, we constructed another two PKD1 mutants, PKD1-Δ(172–312) and PKD1-Δ(311–444) (**Figure 3D**). We found that deletion of the 311–444 motif, but not the 172–312 motif, abolished β-TrCP-mediated downregulation of PKD1 (**Figure 3F**). These results suggested that the key $XSG(X)_{2+n}S$ motif locates in PKD1-Δ(311–444), which has two

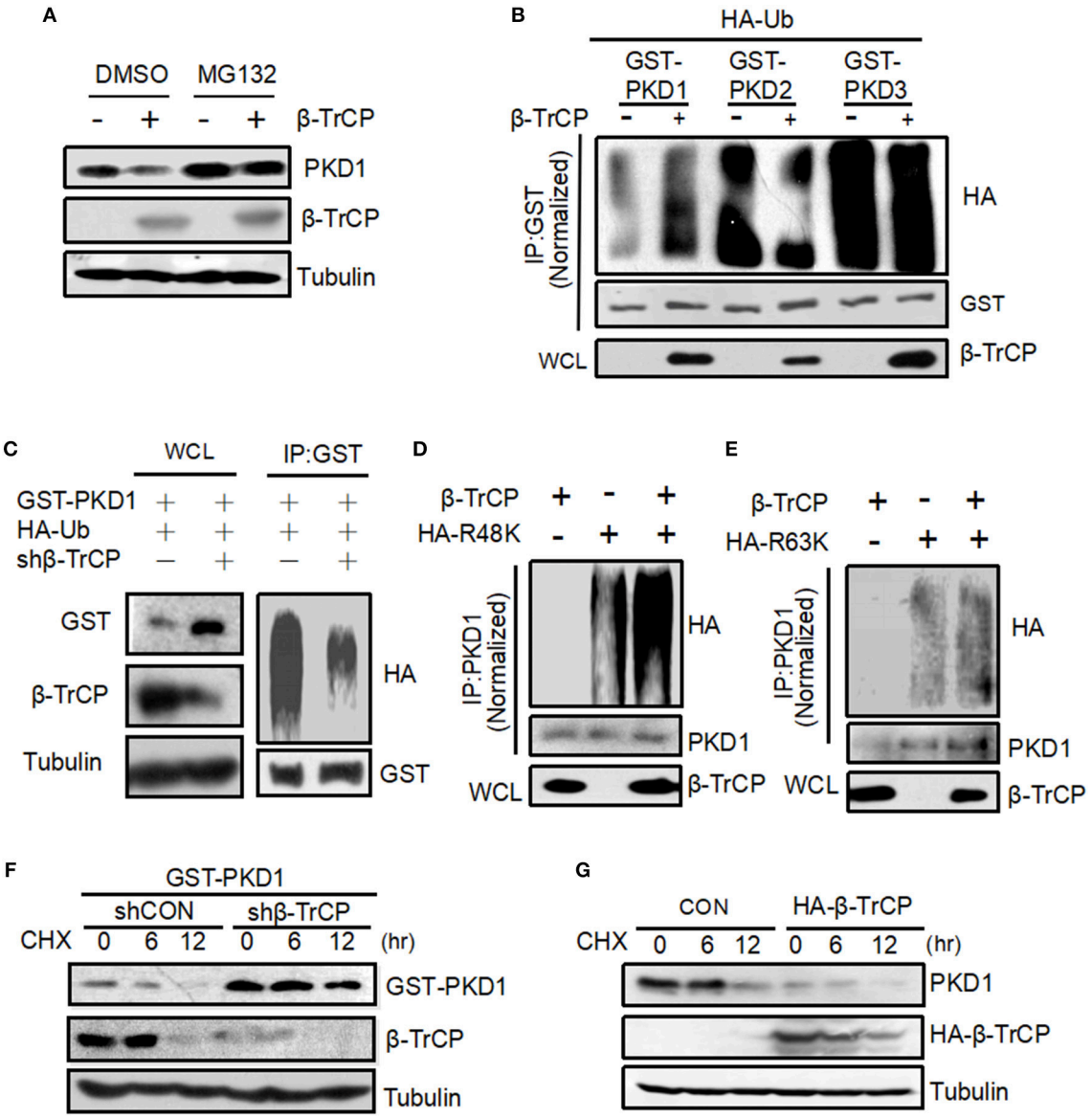

FIGURE 2 | β-TrCP promotes PKD1 ubiquitination and accelerates PKD1 degradation. **(A)** HEK293T cells transfected with empty vector or β-TrCP were treated with or without MG132 (10 μM) for 12 h. Endogenous PKD1 levels were analyzed by immunoblotting as indicated. **(B)** HEK293T cells were transfected as indicated. GST-PKD1, GST-PKD2, and GST-PKD3 proteins were immunoprecipitated by a GST antibody. Ubiquitination and protein levels were analyzed using indicated antibodies. **(C)** HEK293T cells were transfected with shCON or shβ-TrCP, together with HA-Ub and GST-PKD1. Cells then were treated with MG132 (10 μM) for 4 h. Immunoprecipitation (IP) and immunoblotting (IB) were performed as indicated. **(D,E)** 293T cells were transfected with β-TrCP, together with HA-ub-K48 (R48K) **(D)** or HA-ub-K63 (R63K) **(E)** as indicated. PKD1 proteins were immunoprecipitated and then PKD1 ubiquitination was analyzed by indicated antibodies. **(F)** HEK293T cells were transfected with either shCON or shβ-TrCP, together with GST-PKD1. Seventy two hours after transfection, cells were treated with CHX (50 μg/mL) for 0, 6, and 12 h. Whole cell extracts were analyzed by immunoblotting using indicated antibodies. **(G)** HEK293T cells transfected with HA-β-TrCP. Forty eight hours after transfection, cells were treated with CHX (50 μg/mL) for 0, 6, and 12 h. Whole cell extracts were analyzed by immunoblotting using indicated antibodies.

$XSG(X)_{2+n}S$ motifs, $NS_{354}G$ and $DS_{380}G$. Our previous data have demonstrated that the $DS_{380}G$ motif of PKD1 is not essential for interaction between β-TrCP and PKD1 (**Figure 3B**). Therefore, we made a new PKD mutant, PKD1-$S_{354}A$. Our data showed that mutation of serine 354 of PKD1 abolished the binding of β-TrCP to PKD1 (**Figure 3G**). Consistently, β-TrCP cannot downregulate PKD1-$S_{354}A$ protein, as compared with PKD1-wild type (WT) (**Figure 3H**). Taken together, we demonstrate that the $NS_{354}G$ motif of PKD1 is required for β-TrCP binding and PKD1degradation.

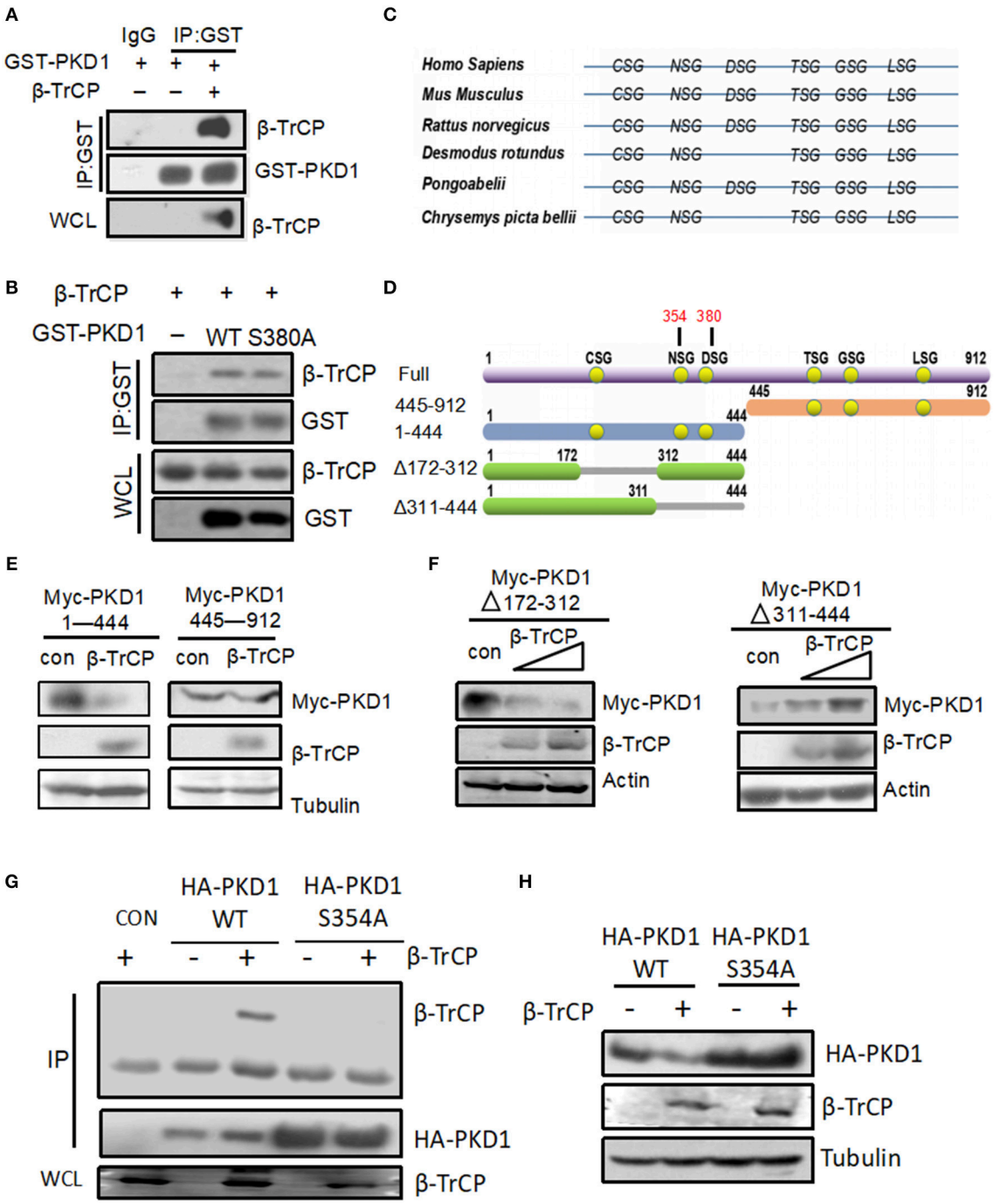

FIGURE 3 | NSG motif of PKD1 is required for β-TrCP binding and degradation of PKD1. **(A)** HEK293T cells were transfected with GST-PKD1, together with or without β-TrCP. GST-PKD1 proteins were immunoprecipitated by a GST antibody, and protein levels of GST-PKD1, β-TrCP, and Tubulin were analyzed using indicated antibodies. **(B)** HEK293T cells were transfected with β-TrCP, together with GST-PKD1-WT or GST-PKD1-S380A. Whole cell lysates were subjected to IP-IB analysis as indicated. **(C)** XSG motifs in various species of PKD1. **(D)** Mapping of PKD1 full length and different mutants. **(E)** HEK293T cells were transfected with β-TrCP, together with either Myc-PKD1(1–444) or Myc-PKD1(445–912). Protein levels of Myc-PKDs mutants, β-TrCP and Tubulin were measured by immunoblotting with indicated antibodies. **(F)** HEK293T cells were transfected with either an empty vector or increasing doses of β-TrCP, together with Myc-PKD1-Δ(172–312) or Myc-PKD1-Δ(311–444). Immunoblotting was performed using indicated antibodies. **(G)** HEK293T cells were transfected with β-TrCP, together with HA-PKD1 (WT or S354A). Immunoprecipitation (IP) and immunoblotting were performed using indicated antibodies. **(H)** HEK293T cells were transfected with or without β-TrCP, together with HA-PKD1 (WT or S354A). Protein levels of HA-PKD1, β-TrCP, and Tubulin were analyzed by immunoblotting as indicated.

LPS Promotes Binding of β-TrCP to PKD1 and Downregulates PKD1 Protein Levels

Our above findings reveal that β-TrCP interacts with PKD1, and promotes PKD1 ubiquitination and degradation. Interestingly, we noticed that both β-TrCP and PKD1 are involved in LPS induced inflammatory signaling pathway (**Figure 4A**). Thus, we sought to determine whether the regulation of β-TrCP on PKD1 occurs in LPS inflammatory signaling. To this end, the interaction between β-TrCP and PKD1 in LPS signaling was analyzed. We found that LPS significantly promoted binding of β-TrCP to PKD1 (**Figure 4B**), and simultaneously upregulated PKD1 ubiquitination (**Figure 4B**). These data suggest that β-TrCP could interact with and regulate PKD1 during LPS stimulation.

To further study the possible regulation of LPS stimulation on PKD1, we analyzed protein levels of PKD1 in RAW264.7 cells under the conditions of LPS treatment for various times. Using a specific antibody against PKD1, we found that PKD1 protein levels were significantly reduced at 90 min and 180 min stimulation by LPS, whereas IκBα levels gradually increased simultaneously (**Figure 4C**). Importantly, when β-TrCP was knocked down, LPS-induced downregulation of PKD1 was markedly inhibited (**Figure 4D**), suggesting that β-TrCP is responsible for PKD1 downregulation in LPS signaling. Collectively, we demonstrate that LPS stimulation can promote binding of β-TrCP to PKD1, and results in PKD1 downregulation.

Supplement of PKD1 in Cells Inhibits Recovery of IκBα Protein Levels in LPS Signaling

Interestingly, from the above results we observed a negative correlation between PKD1 and IκBα protein levels in LPS signaling (**Figure 4C**). It is actually not difficult to understand. It has been clearly demonstrated that LPS stimulation can activate TLR4 signaling and lead to IκBα protein degradation very rapidly. In conjunction with our findings here showing that the upstream signaling molecule PKD1 can be downregulated after LPS stimulation, we speculate that the LPS-TLR4 signaling could be inhibited during the PKD1 downregulation stage, which could result in decrease of IκBα phosphorylation and recovery of IκBα protein levels. That is, PKD1 downregulation during LPS stimulation could contribute to recovery of IκBα protein levels. Next, we try to provide more evidence for this speculation. Given that manipulation of β-TrCP could directly affect IκBα, which impedes the observation of the dynamic changes of IκBα protein levels during LPS stimulation, we took advantage of PKD1 overexpression to supplement PKD1 levels in cells. Firstly, RAW264.7 cells were transfected with increasing dose of PKD1. Cells were then treated with LPS for 90 min. Our data showed that PKD1 overexpression continuously lowered IκBα protein levels in a dose-dependent manner (**Figure 5A**). Conversely, knockout of PKD1 in RAW264.7 cells by CRISPR–Cas9 genome editing substantially upregulated IκBα protein levels in LPS signaling (**Figure 5B**). Furthermore, we analyzed

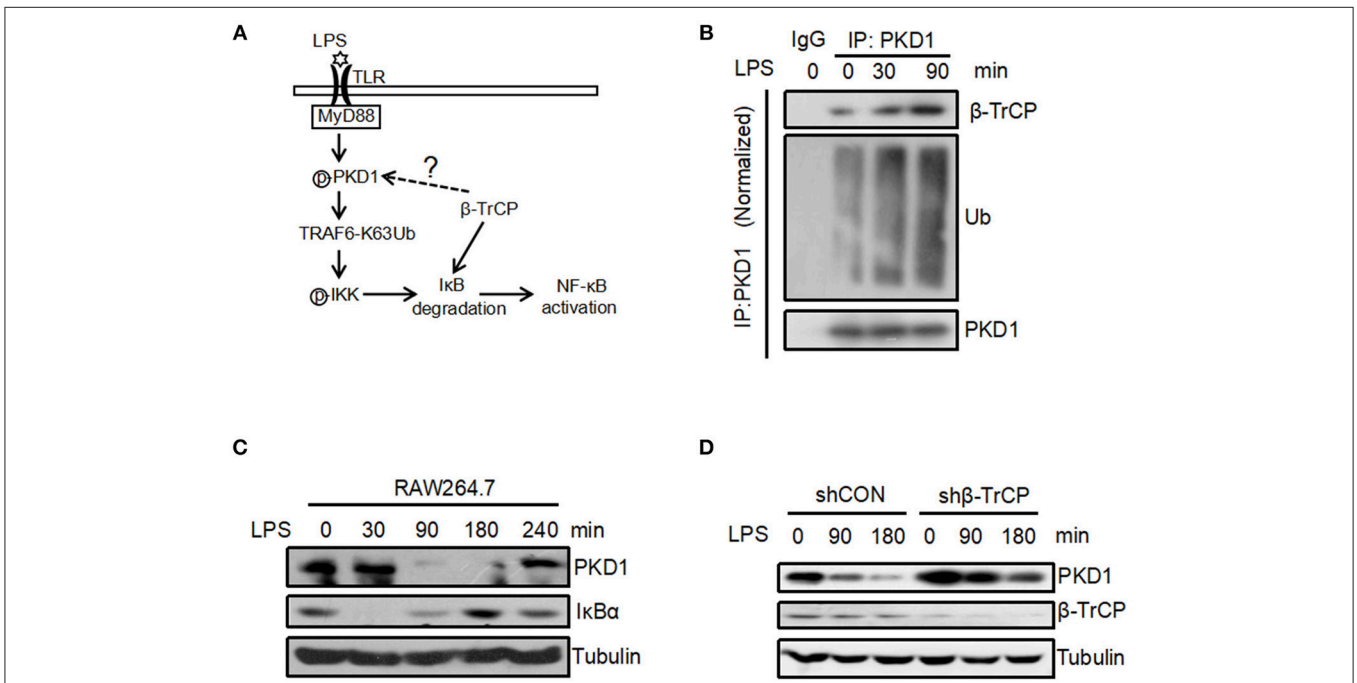

FIGURE 4 | LPS promotes binding of β-TrCP to PKD1 and downregulates PKD1 protein levels. **(A)** The model for LPS-induced inflammatory signaling. **(B)** RAW264.7 cells were treated with LPS (2.5 μg/mL) for 0, 30, 90 min. PKD1 were immunoprecipitated and then immunoblotting was performed using indicated antibodies. **(C)** RAW264.7 cells were stimulated with LPS (2.5 μg/mL) for 0, 30, 90, 180, 240 min. The protein levels of PKD1, IκBα and Tubulin were analyzed by immunoblotting as indicated. **(D)** RAW264.7 cells were transfected with either shCON or shβ-TrCP. Seventy two hours after transfection, cells were stimulated with LPS (2.5 μg/mL) for 0, 90, 180 min. The protein levels of PKD1, β-TrCP and Tubulin were analyzed by immunoblotting as indicated.

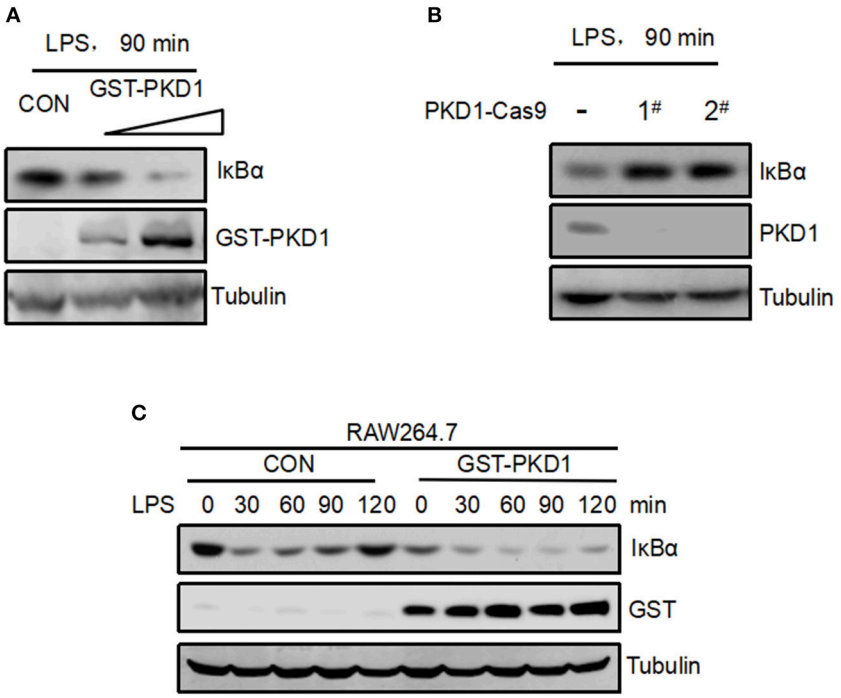

FIGURE 5 | Supplement of PKD1 in cells inhibits recovery of IκBα protein levels in LPS signaling. **(A)** RAW264.7 cells were transfected with increasing does of GST-PKD1. 48 h after transfection, cells were stimulated with LPS (2.5 μg/mL) for 90 min. Protein levels of GST-PKD1, IκBα, and Tubulin were analyzed by immunoblotting as indicated. **(B)** PKD1 in RAW264.7 cells was knocked out by CRISPR–Cas9 genome editing. Two guide RNAs were designed to target PKD1 (1# and 2#). RAW264.7PKD1-Cas9 cells were stimulated with LPS (2.5 μg/mL) for 90 min. Protein levels of PKD1, IκBα, and Tubulin were analyzed by immunoblotting as indicated. **(C)** RAW264.7 cells were transfected with either empty vector or GST-PKD1. Forty eight hours after transfection, cells were stimulated with LPS (2.5 μg/mL) for 0, 30, 60, 90, 120 min. Protein levels of GST-PKD1, IκBα, and Tubulin were analyzed by immunoblotting as indicated.

the dynamic changes of IκBα protein levels in LPS signaling. The result showed that during LPS stimulation, IκBα protein levels significantly decreased at 30 min time point. After that, IκBα protein levels were gradually recovered (**Figure 5C**, left panel). When cells were supplemented with PKD1, the recovery of IκBα protein levels was dramatically delayed (**Figure 5C**, right panel). Collectively, we believe that PKD1 downregulation could contribute to recovery of IκBα protein levels in LPS signaling.

β-TrCP Negatively Regulates LPS-Induced TRAF6 Ubiquitination and IKK Activation

Given that we have demonstrated that β-TrCP promotes PKD1 downregulation in LPS signaling, we further study whether β-TrCP can regulate the signaling pathway downstream of PKD1 and upstream of IκBα. In LPS signaling, PKD1 activation leads to TRAF6 polyubiquitination and subsequent IKK phosphorylation and activation. Therefore, we analyzed the roles of β-TrCP in regulating TRAF6 ubiquitination and IKK phosphorylation in LPS signaling. Our data showed that β-TrCP overexpression significantly inhibited LPS-stimulated ubiquitination of TRAF6 (**Figure 6A**). Conversely, knockdown of β-TrCP remarkably promoted TRAF6 ubiquitination induced by LPS (**Figure 6B**). Furthermore, we found that overexpression of β-TrCP reduced K63-linked polyubiquitination of TRAF6 (**Figure 6C**), but had no obvious effect on TRAF6 protein levels (**Figure 6D**), suggesting that β-TrCP inhibits TRAF6 signaling activation. Next, we studied whether β-TrCP could regulate IKK phosphorylation. Using a specific antibody against activated IKK at Ser176/180 site, we found that β-TrCP obviously inhibited LPS-stimulated IKK phosphorylation (**Figure 6E**). Taken together, our findings demonstrate that β-TrCP negatively regulates LPS-induced TRAF6 K63-linked ubiquitination and IKK activation.

DISCUSSION

PKD1, as a ubiquitous serine-threonine protein kinase, plays crucial roles in multiple biological processes, including cell growth, adhesion, motility, and angiogenesis (2–5). Stable PKD1 levels in cells are extremely important for normal physiology functions of cells. Dysregulated PKD1 expression could result in the pathogenesis of some cancers. PKD1 could be activated by various stimuli including growth factor (23), oxidative stress (24), and apoptotic signaling (25). Thus far, the regulation of PKD1 expression remains largely unexplored. It has been reported that PKD1 expression is gradually reduced during breast cancer progression, which could be directly associated with hypermethylation of PKD1 promoter (26). Recent studies demonstrated that there is a correlation between the expression of PKD1 and ERα in breast cancer

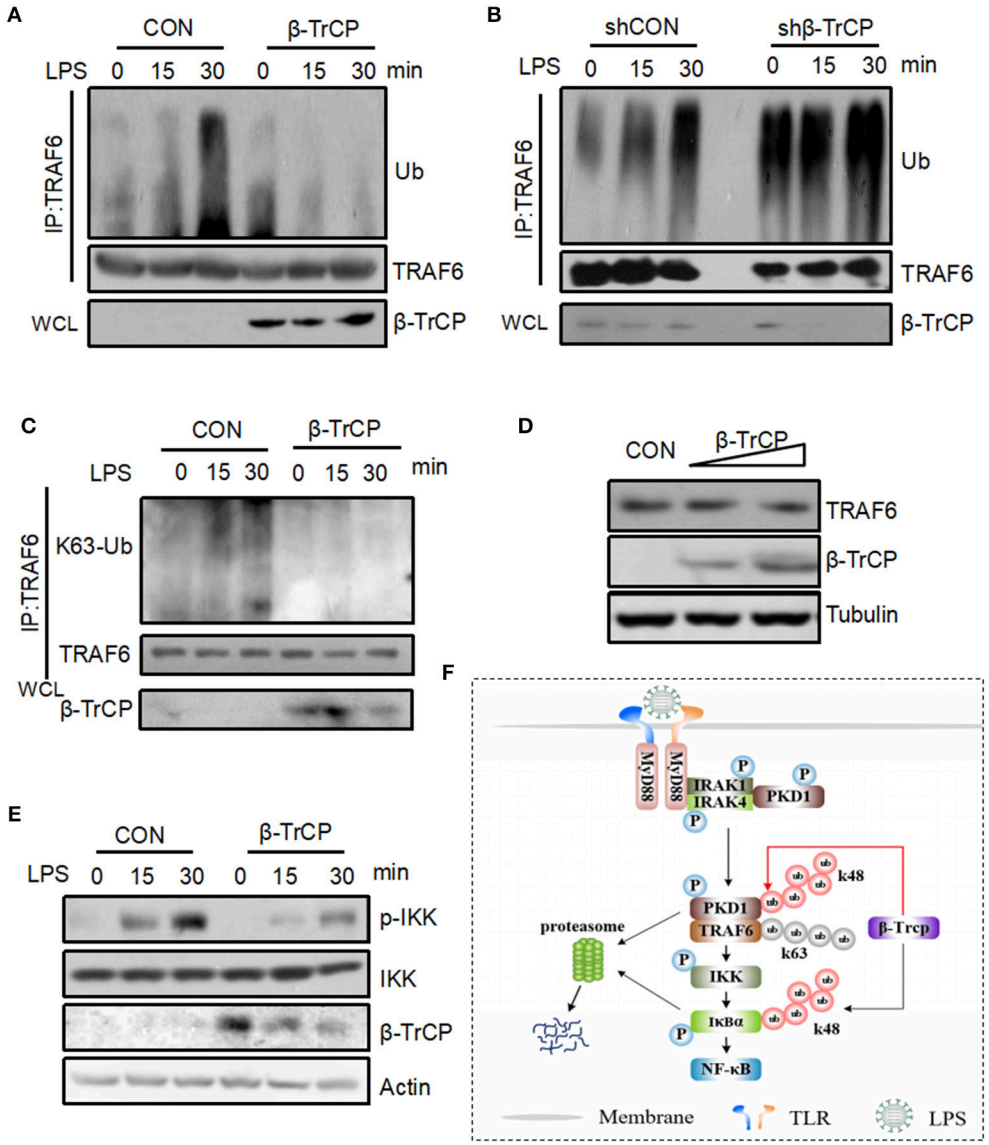

FIGURE 6 | β-TrCP negatively regulates LPS-induced TRAF6 ubiquitination and IKK activation. **(A)** RAW264.7 cells were transfected with β-TrCP. Forty eight hours after transfection, cells were stimulated with LPS (2.5 μg/mL) for 0, 15, 30 min. Endogenous TRAF6 were pulled down, and ubiquitination and protein levels of TRAF6 were analyzed using indicated antibody. **(B)** RAW264.7 cells were transfected with either shCON or shβ-TrCP. Seventy two hours after transfection, cells were stimulated with LPS (2.5 μg/mL) for 0, 15, 30 min. ubiquitination and protein levels of TRAF6 were analyzed as **(A)**. **(C)** RAW264.7 cells were transfected with β-TrCP. Forty eight hours after transfection, cells were stimulated with LPS (2.5 μg/mL) for 0, 15, 30 min. Endogenous TRAF6 were immunoprecipitated, and K63-linked polyubiquitination and protein levels of TRAF6 were analyzed using indicated antibody. **(D)** Total protein levels of TRAF6 were analyzed using indicated antibodies. **(E)** RAW264.7 cells were transfected with or without β-TrCP. Forty eight hours after transfection, cells were stimulated with LPS (2.5 μg/mL) for 0, 15, 30 min. The levels of p-IKK, IKK, β-TrCP, and Actin were analyzed by immunoblotting as indicated. **(F)** Hypothetical model for β-TrCP-mediated regulation of LPS inflammatory signaling pathway. LPS stimulation activates TLR4-PKD1-TRAF6-IKK signaling, which rapidly induces IκBα phosphorylation and subsequent IκBα ubiquitination and degradation mediated by β-TrCP. Finally, NF-κB inflammatory signaling was activated. During LPS stimulation, β-TrCP also interacts with PKD1, which results in PKD1 ubiquitination and degradation, and leads to inhibition of LPS-TLR4-PKD1-TRAF6-IKK signaling. Together, β-TrCP plays both promotion and brake roles in LPS-induced inflammatory signaling.

cells (27). However, ubiquitination-mediated regulation of PKD1 remains unknown so far. In this study, we for the first time reveal that ubiquitin E3 ligase β-TrCP regulates PKD1 protein levels in cells. We clearly demonstrated that in LPS signaling β-TrCP can interact with PKD1, which leads to PKD1 downregulation. Furthermore, β-TrCP-mediated downregulation of PKD1 restricts LPS-induced TRAF6 K63-linked polyubiquitination and IKK phosphorylation. Thus, our findings uncover the novel regulation mediated by the β-TrCP-PKD1 axis in LPS inflammatory signaling. In addition,

it has been reported that PKD1 can be activated by TLR-mediated MyD88 signaling pathway. Thus, it could be interesting to observe the effects of β-TrCP on PKD1 levels in different TLR ligands-activated signaling pathways in the future.

It has been well-characterized that β-TrCP's substrates contain a consensus D<u>S</u>G$(X)_{2+n}$S degron. The serine residues in this degron could be phosphorylated by certain protein kinases, which results in β-TrCP recognition and subsequent ubiquitination of the substrates (28–30). In this study, we found that PKD1 does possess a potential D<u>S</u>G$(X)_{2+n}$S motif. However, this D<u>S</u>G$(X)_{2+n}$S motif of PKD1 is not important for β-TrCP binding and PKD1 degradation. Through analyzing all conserved X<u>S</u>G$(X)_{2+n}$S motif in various species of PKD1, we finally found the NSG$(X)_{2+n}$S motif of PKD1 is essential for β-TrCP binding and subsequent degradation of PKD1. As a matter of fact, some studies have reported several "atypical" substrates of β-TrCP, including STAT1 (19), Weel (20), and GHR (21), which do not have the classic DSG$(X)_{2+n}$S motif. Here, our study uncovers a new "atypical" degron in PKD1 for β-TrCP-mediated degradation.

Prevailing thought holds that β-TrCP is a positive regulator for TLRs-NF-κB inflammatory signaling, because β-TrCP induces IκBα degradation and NF-κB release. In this study, we demonstrate that β-TrCP could be a negative regulator for upstream signaling of TLRs-NF-κB pathway. LPS stimulation activates TLR4-PKD1-TRAF6-IKK-IκBα signaling, which leads to β-TrCP-mediated ubiquitination and degradation of IκBα rapidly. Unexpectedly, we find that during LPS stimulation β-TrCP also binds to PKD1, which results in PKD1 ubiquitination and degradation. PKD1 downregulation inhibits further activation of LPS-PKD1-TRAF6-IKK signaling (**Figure 6F**). As observed in this study, β-TrCP-mediated PKD1 downregulation inhibits TRAF6 K63-linked polyubiquitination and subsequent IKK phosphorylation. Also, we observed that PKD1 protein levels are negatively correlated with IκBα levels in LPS signaling, and supplement of PKD1 in cells significantly delays recovery of IκBα protein levels. Taken together, we think that β-TrCP plays both promotion and brake roles in LPS-induced inflammatory signaling. The dual effects of β-TrCP may provide the balance for LPS inflammatory signaling. Based on the dual effects of β-TrCP, we focus on studying LPS-IKK upstream signaling, rather than analyzing cytokines production downstream of IκBα signaling.

In summary, we demonstrate that β-TrCP specifically targets PKD1 for K48 ubiquitination and degradation in an "atypical" binding manner. Furthermore, we uncover that during LPS stimulation β-TrCP can interact with PKD1 and promotes PKD1 downregulation, which in turn restricts TRAF6-IKK signaling upstream of IκBα in LPS inflammatory pathway. Our findings reveal that β-TrCP is an important negative regulator for upstream signaling of IκBα in LPS signaling, and therefore renew our understanding of the roles of β-TrCP in TLRs inflammatory signaling.

AUTHOR CONTRIBUTIONS

HZ, JW, and JL designed the research. JL, YY, JX, KX, and YX performed the experiments. HZ and JL wrote the manuscript. YX, LZ, and TG provided expertise and advice. HZ supervised the project.

FUNDING

This study was funded by National Natural Science Foundation of China (31570865, 31770177 and 31501139), the Program of 1000 Young Talents, Jiangsu Provincial Distinguished Young Scholars (BK20130004), and Changjiang scholars and Innovative Research Team in University of Ministry of Education of China (PCSIRT-IRT1075).

ACKNOWLEDGMENTS

We thank Dr. Serge Y. Fuchs from University of Pennsylvania for important plasmids, and also thank all members of Hui lab for helpful discussions.

REFERENCES

1. Rozengurt E, Rey O, Waldron RT. Protein kinase D signaling. *J Biol Chem.* (2005) 280:13205–8. doi: 10.1074/jbc.R500002200
2. Arnold R, Patzak IM, Neuhaus B, Vancauwenbergh S, Veillette A, Van Lint J, et al. Activation of hematopoietic progenitor kinase 1 involves relocation, autophosphorylation, and transphosphorylation by protein kinase D1. *Mol Cell Biol.* (2005) 25:2364–83. doi: 10.1128/MCB.25.6.2364-2383.2005
3. Dequiedt F, Van Lint J, Lecomte E, Van Duppen V, Seufferlein T, Vandenheede JR, et al. Phosphorylation of histone deacetylase 7 by protein kinase D mediates T cell receptor-induced Nur77 expression and apoptosis. *J Exp Med.* (2005) 201:793–804. doi: 10.1084/jem.20042034
4. Storz P, Doppler H, Toker A. Protein kinase D mediates mitochondrion-to-nucleus signaling and detoxification from mitochondrial reactive oxygen species. *Mol Cell Biol.* (2005) 25:8520–30. doi: 10.1128/MCB.25.19.8520-8530.2005
5. Matthews SA, Liu P, Spitaler M, Olson EN, McKinsey TA, Cantrell DA, et al. Essential role for protein kinase D family kinases in the regulation of class II histone deacetylases in B lymphocytes. *Mol Cell Biol.* (2006) 26:1569–77. doi: 10.1128/MCB.26.4.1569-1577.2006
6. Zheng H, Qian J, Varghese B, Baker DP, Fuchs S. Ligand-stimulated downregulation of the alpha interferon receptor: role of protein kinase D2. *Mol Cell Biol.* (2011) 31:710–20. doi: 10.1128/MCB.01154-10
7. Park JE, Kim YI, Yi AK. Protein kinase D1: a new component in TLR9 signaling. *J Immunol.* (2008) 181:2044–55. doi: 10.4049/jimmunol.181.3.2044
8. Park JE, Kim YI, Yi AK. Protein kinase D1 is essential for MyD88-dependent TLR signaling pathway. *J Immunol.* (2009) 182:6316–27. doi: 10.4049/jimmunol.0804239
9. Jeohn GH, Cooper CL, Jang KJ, Liu B, Lee DS, Kim HC, et al. Go6976 inhibits LPS-induced microglial TNFalpha release by suppressing p38 MAP kinase activation. *Neuroscience* (2002) 114:689–97. doi: 10.1016/S0306-4522(02)00356-1
10. Bedford L, Lowe J, Dick LR, Mayer RJ, Brownell JE. Ubiquitin-like protein conjugation and the ubiquitin-proteasome system as drug targets. *Nat Rev Drug Discov.* (2011) 10:29–46. doi: 10.1038/nrd3321

11. Yaron A, Hatzubai A, Davis M, Lavon I, Amit S, Manning AM, et al. Identification of the receptor component of the IkappaBalpha-ubiquitin ligase. *Nature* (1998) 396:590–4. doi: 10.1038/25159
12. Fuchs SY, Chen A, Xiong Y, Pan ZQ, Ronai Z. HOS, a human homolog of Slimb, forms an SCF complex with Skp1 and Cullin1 and targets the phosphorylation–dependent degradation of IkappaB and beta-catenin. *Oncogene* (1999) 18:2039–46. doi: 10.1038/sj.onc.1202760
13. Hart M, Concordet JP, Lassot I, Albert I, del los Santos R, Durand H, et al. The F-box protein beta-TrCP associates with phosphorylated beta-catenin and regulates its activity in the cell. *Curr Biol.* (1999) 9:207–10. doi: 10.1016/S0960-9822(99)80091-8
14. Lassot I, Segeral E, Berlioz-Torrent C, Durand H, Groussin L, Hai T, et al. ATF4 degradation relies on a phosphorylation-dependent interaction with the SCF(betaTrCP) ubiquitin ligase. *Mol Cell Biol.* (2001) 21:2192–202. doi: 10.1128/MCB.21.6.2192-2202.2001
15. Guardavaccaro D, Kudo Y, Boulaire J, Barchi M, Busino L, Donzelli M, et al. Control of meiotic and mitotic progression by the F box protein beta-Trcp1 *in vivo*. *Dev Cell* (2003) 4:799–812. doi: 10.1016/S1534-5807(03)00154-0
16. Kumar KG, Tang W, Ravindranath AK, Clark WA, Croze E, Fuchs SY. SCF(HOS) ubiquitin ligase mediates the ligand-induced down-regulation of the interferon-alpha receptor. *EMBO J.* (2003) 22:5480–90. doi: 10.1093/emboj/cdg524
17. Ren Y, Zhao P, Liu J, Yuan Y, Cheng Q, Zuo Y, et al. Deubiquitinase USP2a sustains interferons antiviral activity by restricting ubiquitination of activated STAT1 in the nucleus. *PLoS Pathog.* (2016) 12:e1005764. doi: 10.1371/journal.ppat.1005764
18. Li L, Qian G, Zuo Y, Yuan Y, Cheng Q, Guo T, et al. Ubiquitin-dependent turnover of adenosine deaminase acting on RNA 1 (ADAR1) is required for efficient antiviral activity of type I interferon. *J Biol Chem.* (2016) 291:24974–85. doi: 10.1074/jbc.M116.737098
19. Soond SM, Townsend PA, Barry SP, Knight RA, Latchman DS, Stephanou A. ERK and the F-box protein betaTRCP target STAT1 for degradation. *J Biol Chem.* (2008) 283:16077–83. doi: 10.1074/jbc.M800384200
20. Watanabe N, Arai H, Nishihara Y, Taniguchi M, Hunter T, Osada H. M-phase kinases induce phospho-dependent ubiquitination of somatic Wee1 by SCFbeta-TrCP. *Proc Natl Acad Sci USA.* (2004) 101:4419–24. doi: 10.1073/pnas.0307700101
21. van Kerkhof P, Putters J, Strous GJ. The ubiquitin ligase SCF(betaTrCP) regulates the degradation of the growth hormone receptor. *J Biol Chem.* (2007) 282:20475–83. doi: 10.1074/jbc.M702610200
22. Low TY, Peng M, Magliozzi R, Mohammed S, Guardavaccaro D, Heck AJ. A systems-wide screen identifies substrates of the SCFbetaTrCP ubiquitin ligase. *Sci Signal.* (2014) 7:rs8. doi: 10.1126/scisignal.2005882
23. Waldron RT, Iglesias T, Rozengurt E. The pleckstrin homology domain of protein kinase D interacts preferentially with the eta isoform of protein kinase C. *J Biol Chem.* (1999) 274:9224–30. doi: 10.1074/jbc.274.14.9224
24. Storz P, Toker A. Protein kinase D mediates a stress-induced NF-kappaB activation and survival pathway. *EMBO J.* (2003) 22:109–20. doi: 10.1093/emboj/cdg009
25. Endo K, Oki E, Biedermann V, Kojima H, Yoshida K, Johannes FJ, et al. Proteolytic cleavage and activation of protein kinase C [micro] by caspase-3 in the apoptotic response of cells to 1-beta -D-arabinofuranosylcytosine and other genotoxic agents. *J Biol Chem.* (2000) 275:18476–81. doi: 10.1074/jbc.M002266200
26. Borges S, Doppler H, Perez EA, Andorfer CA, Sun Z, Anastasiadis PZ, et al. Pharmacologic reversion of epigenetic silencing of the PRKD1 promoter blocks breast tumor cell invasion and metastasis. *Breast Cancer Res.* (2013) 15:R66. doi: 10.1186/bcr3460
27. Karam M, Bieche I, Legay C, Vacher S, Auclair C, Ricort JM. Protein kinase D1 regulates ERalpha-positive breast cancer cell growth response to 17beta-estradiol and contributes to poor prognosis in patients. *J Cell Mol Med.* (2014) 18:2536–52. doi: 10.1111/jcmm.12322
28. Frescas D, Pagano M. Deregulated proteolysis by the F-box proteins SKP2 and beta-TrCP: tipping the scales of cancer. *Nat Rev Cancer* (2008) 8:438–49. doi: 10.1038/nrc2396
29. Lau AW, Fukushima H, Wei W. The Fbw7 and betaTRCP E3 ubiquitin ligases and their roles in tumorigenesis. *Front Biosci.* (2012) 17:2197–212. doi: 10.2741/4045
30. Wang Z, Liu P, Inuzuka H, Wei W. Roles of F-box proteins in cancer. *Nat Rev Cancer* (2014) 14:233–47. doi: 10.1038/nrc3700

Conflict of Interest Statement: The authors declare that the research was conducted in the absence of any commercial or financial relationships that could be construed as a potential conflict of interest.

frontiers in Immunology

ORIGINAL RESEARCH
published: 13 March 2019
doi: 10.3389/fimmu.2019.00415

Human B Cells Engage the NCK/PI3K/RAC1 Axis to Internalize Large Particles via the IgM-BCR

Niels J. M. Verstegen[1,2†], Peter-Paul A. Unger[1†], Julia Z. Walker[1], Benoit P. Nicolet[1], Tineke Jorritsma[1], Jos van Rijssel[3], Robbert M. Spaapen[1], Jelle de Wit[1], Jaap D. van Buul[3], Anja ten Brinke[1] and S. Marieke van Ham[1,4]*

[1] Department of Immunopathology, Sanquin Research and Landsteiner Laboratory, Amsterdam UMC, University of Amsterdam, Amsterdam, Netherlands, [2] Synthetic Systems Biology and Nuclear Organization, Swammerdam Institute for Life Sciences, University of Amsterdam, Amsterdam, Netherlands, [3] Department of Molecular Cell Biology, Sanquin Research and Landsteiner Laboratory, Amsterdam UMC, University of Amsterdam, Amsterdam, Netherlands, [4] Swammerdam Institute for Life Sciences, University of Amsterdam, Amsterdam, Netherlands

Growing evidence indicate that large antigen-containing particles induce potent T cell-dependent high-affinity antibody responses. These responses require large particle internalization after recognition by the B cell receptor (BCR) on B cells. However, the molecular mechanisms governing BCR-mediated internalization remain unclear. Here we use a high-throughput quantitative image analysis approach to discriminate between B cell particle binding and internalization. We systematically show, using small molecule inhibitors, that human B cells require a SYK-dependent IgM-BCR signaling transduction via PI3K to efficiently internalize large anti-IgM-coated particles. IgM-BCR-mediated activation of PI3K involves both the adaptor protein NCK and the co-receptor CD19. Interestingly, we here reveal a strong NCK-dependence without profound requirement of the co-receptor CD19 in B cell responses to large particles. Furthermore, we demonstrate that the IgM-BCR/NCK signaling event facilitates RAC1 activation to promote actin cytoskeleton remodeling necessary for particle engulfment. Thus, we establish NCK/PI3K/RAC1 as an attractive IgM-BCR signaling axis for biological intervention to prevent undesired antibody responses to large particles.

Keywords: B cell, CRISPR, internalization, signaling pathway, large antigen-containing particle

OPEN ACCESS

Edited by:
Thai Tran,
National University of Singapore, Singapore

Reviewed by:
Michael Reth,
University of Freiburg, Germany
Aaron James Marshall,
University of Manitoba, Canada

****Correspondence:***
S. Marieke van Ham
m.vanham@sanquin.nl

† These authors have contributed equally to this work

Specialty section:
This article was submitted to B Cell Biology, a section of the journal Frontiers in Immunology

Received: *24 October 2018*
Accepted: *18 February 2019*
Published: *13 March 2019*

Citation:
Verstegen NJM, Unger P-PA, Walker JZ, Nicolet BP, Jorritsma T, van Rijssel J, Spaapen RM, de Wit J, van Buul JD, ten Brinke A and van Ham SM (2019) Human B Cells Engage the NCK/PI3K/RAC1 Axis to Internalize Large Particles via the IgM-BCR. Front. Immunol. 10:415. doi: 10.3389/fimmu.2019.00415

INTRODUCTION

The first step in induction of antibody production is binding of external antigen to the B cell receptor (BCR) on naive B cells. BCR ligation by antigen results in BCR-mediated transmembrane signaling and antigen internalization, followed by proteolytic degradation and presentation of antigen-derived peptides through major histocompatibility complex class II (MHCII) molecules on the B cell plasma membrane (1–3). MHCII/antigen complexes are recognized by antigen-specific T cell receptors expressed by $CD4^+$ T cells (4). After formation of a stable antigen-specific interaction, B cells receive help from $CD4^+$ T cells via co-stimulatory molecules and soluble cytokines to promote B cell differentiation into high-affinity antibody-producing plasma cells during germinal center (GC) reactions in secondary lymphoid organs.

The BCR consists of a membrane-bound immunoglobulin associated with a CD79a and CD79b heterodimer containing intracellular immunoreceptor tyrosine activation motifs (ITAMs) (5). Upon cognate antigen recognition, phosphorylation of the ITAMs is initiated by the SRC family

kinase LYN and spleen tyrosine kinase (SYK) (6–8). These phosphorylated motifs recruit several adaptor and effector proteins that make up the signalosome, containing SYK, B cell linker (BLNK), bruton's tyrosine kinase (BTK), phospholipase C-γ2 (PLCγ2), and the co-receptor CD19. The signalosome drives activation of multiple downstream effector pathways to amplify the signal from the BCR that results in changes in cell metabolism, gene expression, and cytoskeletal organization. Many of proteins required for transmembrane signaling are also involved in antigen internalization and the subsequent intracellular trafficking of the antigen-BCR complex (9). Most studies describing signaling components and molecular mechanisms that control BCR-mediated antigen internalization use small soluble antigens or antigen tethered to planer lipid bilayer surfaces or plasma membrane sheets that is extracted though force-dependent extraction or enzymatic liberation (10–13). B cells are, however, also able to internalize large particles. This ability has long been disregarded, but in recent years, multiple groups, including our own, have demonstrated the existence of this cell biological process for internalization of large particles including anti-IgM-coated bacteria and beads (14–17). The physiological importance of this pathway was recently demonstrated by showing that internalization of large particles by follicular B cells resulted in a strong GC response and the generation of high-affinity class-switched antibodies in mice (16). Of added importance in large particle uptake is the process of epitope spreading. Epitope spreading is a process in which antigens distinct from the antigen that was recognized by the antigen-specific BCR are presented on the B cells plasma membrane (18–20). As such, B cells and $CD4^+$ T cells with different specificity can interact to drive the ongoing immune response. This process is highly desirable if it targets foreign antigens during infection to broadening the B cell response. In contrast, in cases of self-reactivity in autoimmune reactions or alloimmunization against transfused blood products, epitope spreading is a clinical problem in much need of targeted therapy.

Here we investigated the molecular mechanisms that mediate internalization and antigen presentation of large particles in human B cells. A high-throughput quantitative image analysis approach was employed using inactivated anti-IgM-coated *Salmonella typhimurium* as a model particle to quantify IgM-BCR-mediated internalization. We show that phosphoinositide-3 kinase (PI3K) is the main driver of actin-dependent large particle acquisition by human B cells. IgM-BCR-mediated activation of PI3K involves both the adaptor protein NCK and the co-receptor CD19 (21–24). We demonstrate that the IgM-BCR/NCK axis is required for internalization of large particles in human B cells. This axis drives internalization via activation of the actin cytoskeleton modulator RAC1. Collectively, our data reveal that the NCK-PI3K-RAC1 axis is essential to mount a humoral immune response to large particles.

MATERIALS AND METHODS

Purification of $CD19^+$ B and $CD4^+$ T Cells

Human buffy coats were obtained from healthy blood donors after informed consent, in accordance with the protocol of the local institutional review board, the Medical Ethics Committee of Sanquin Blood Supply, and conforms to the principles of the Declaration of Helsinki. Peripheral blood mononuclear cells (PBMCs) were isolated through standard gradient centrifugation using Ficoll-lymphoprep (Axis-Shield). $CD19^+$ B cells and $CD4^+$ T cells were purified from PBMCs with anti-CD19 and anti-CD4 Dynabeads, respectively, and DETACHaBEAD (Invitrogen) following the manufacturer's instructions. Purity was typically > 98% as assessed by flow cytometry.

Cell Cultures

HEK293T cells were grown in IMDM (Lonza) supplemented with 10% fetal calf serum (FCS; Bodinco), 100 U/ml penicillin and 100 μg/ml streptomycin (Thermo Fisher Scientific). Ramos B cells were grown in B cell medium that consists of RPMI 1640 medium (Life Technologies) supplemented with 5% FCS, 100 U/ml penicillin and 100 μg/ml streptomycin, 2 mM L-glutamine (Invitrogen), 50 μM β-mercaptoethanol (Sigma) and 20 μg/ml human apotransferrin [Sigma; depleted for human IgG with protein G Sepharose (Amersham Biosciences)]. The HLA-DOβ-GFP Ramos cell line has been described before (17) and was cultured in B cell medium in the presence of 2 mg/ml G418 (Life Technologies).

gRNA Design and Plasmids

Guide sequences with homology to *CD19* (5′-AAGCGGGGACTCCCGAGACC-3′), *NCK1* (5′-GGTCATAGAGACGTTCCCCT-3′) and *NCK2* (5′-CGGTAC ATAGCCCGTCCTGT-3′) were designed using CRISPR design, and subsequently cloned into the lentiCRISPRv2 backbone containing puromycin resistance gene (25). The Lifeact-GFP and DORA RAC1-sensor constructs in a lentiviral backbone have been described before (26, 27).

Lentiviral Vector Construction

Lentiviral vectors were produced by co-transfecting HEK293T cells with the lentiviral transfer plasmids gRNA/Cas9-expressing lentiCRISPRv2, Lifeact-GFP, or DORA RAC1-sensor, and the packaging plasmids pVSVg, psPAX2, and pAdv (28, 29) using polyethylenimine (PEI, Polysciences). Virus-containing supernatant was harvested 48 and 72 h after transfection, then frozen and stored in −80°C.

Cell Lines and Transduction

Transduction of lentiviral vector into Ramos B cells was performed with 8 μg/ml protamine sulfate (Sigma). CRISPR-mediated knockout cells were enriched by culturing in B cell medium supplemented with 1–2 μg/ml puromycin (Invitrogen). CD19 knockout Ramos B cells were purified using a FACSAria II (BD Bioscience). For this, cells were washed and then stained with anti-CD19 APC (clone SJ25-C1; BD Bioscience) in phosphate buffered saline (PBS; Fresenius Kabi) supplemented with 0.1% bovine serum albumin (BSA; Sigma). The NCK1/2 double-knockout cell line was obtained by single cell sorting using a FACSAria II (BD Bioscience). After clonal expansion, cells were screened for complete knockout using an immunoblot assay (as described below). Ramos B cells that stably expressed

Lifeact-GFP or RAC1 biosensor were sorted by flow cytometry-based sorting using a FACSAria II (BD Bioscience).

Serum Preparation

Blood samples were drawn from healthy volunteers after informed consent (Sanquin). Serum was obtained by collecting blood, allowing it to clot for 1 h at room temperature (RT) and collecting the supernatant after centrifugation at 3,000 rpm for 15 min. Serum of sixteen healthy donors was mixed and stored in small aliquots at −80°C to avoid repetitive freeze/thawing.

Labeling of Antibodies and Beads

Mouse monoclonal anti-human IgG (MH16-1; Sanquin Reagents), mouse monoclonal anti-human C3d (C3-19; Sanquin Reagents) and mouse monoclonal anti-human IgM (MH15-1, Sanquin Reagents) were labeled with DyLight 650, DyLight 488 or DyLight 405, respectively, according to manufacturer's instructions (Thermo Fisher Scientific). To get rid of excess dye, the antibodies were washed extensively using an Amicon Ultra centrifugal filter (10K; Merck Milipore). The labeling rate was around 7 fluorochromes per antibody, as determined by UV-VIS spectroscopy on a Nanodrop ND1000 spectrophotometer (Thermo Scientific).

Goat-anti-mouse IgG (Fc) polystyrene beads (3 μm, Spherotech) were washed twice with PBS containing 0.1% BSA and labeled overnight with anti-human IgM-DyLight405. The beads were stored at 4°C until further use. Before use, the beads were washed twice with PBS supplemented with 0.1% normal mouse serum (in house), and once with PBS supplemented with 0.1% BSA.

Bacterial Strains

Salmonella typhimurium SL1344 has been described before (30). *S. typhimurium* SL1344 that constitutively express the dsRed protein were generated by electroporating bacteria with a pMW211 plasmid. Bacteria were grown overnight shaking at 37°C in Luria-Bertani (LB) medium broth with 50 μg/ml carbenicillin (Invitrogen). To reach mid-log growth phase, the overnight grown bacteria were diluted 1/33 in fresh LB medium and incubated at 37°C for 3 h while shaking. Subsequently, bacteria were washed twice with PBS and inactivated through incubation at 65°C for 15 min, or through incubation with 4% paraformaldehyde (PFA; Sigma) in PBS for 20 min. To block the free aldehyde groups of PFA, bacteria were incubated with 0.02 M glycine (Merck). Mouse monoclonal anti-human IgM (Fc) (clone MH15-1; Sanquin) or mouse monoclonal anti-human CD19 (clone LT19; Miltenyi Biotec) was mixed with mouse monoclonal anti-*S. typhimurium* LPS (clone 1E6; Biodesign International) and rat anti-mouse IgG1 (clone RM161-1; Sanquin) to generate anti-LPS/IgM (17, 31–33) or anti-LPS/CD19 antibody complexes. Inactivated bacteria were coated with these antibody complexes in the dark for 30 min, while rotating. Subsequently, the bacteria were washed with PBS and kept at 4°C until further use.

For complement/antibody opsonization, *S. typhimurium* was incubated with 10% freshly thawed or heat-inactivated serum in PBS supplemented with 10 mM $CaCl_2$ and 2mM $MgCl_2$ at 37°C for 30 min. Heat-inactivation of the serum was performed by incubation at 56°C for 30 min. After incubation, bacteria were washed thoroughly with PBS to wash away all non-bound serum components. To asses *S. typhimurium*-reactive antibody and complement opsonization, bacteria were washed and stained with anti-human IgG-DyLight650 and anti-human C3d-DyLight488 in PBS supplemented with 0.1% BSA for 20 min in the dark at RT and measured on a FACSCanto II (BD Bioscience). The acquired data was analyzed using FlowJo Software version 10 (Tree Star).

Soluble Anti-IgM or Large Particle Challenge

Primary human B cells or Ramos B cells were left untreated or incubated with vehicle (DMSO) or small molecule inhibitors (**Supplementary Table 1**) in B cell medium without antibiotics for 15 min at 37°C. Subsequently, cells were incubated with soluble anti-IgM (5 μg/mL), uncoated or antibody complex-coated PFA-inactivated *S. typhimurium,* or anti-IgM-coated 3 μm polystyrene beads for 30 min at 37°C. Ice cold PBS was added to halt internalization. Alternatively, B cells were incubated with anti-IgM-coated PFA-inactivated *S. typhimurium* for 30 min in B cell medium without antibiotics on ice to allow particle binding but not internalization (**Figures 3F,G**, **5G,H**). Subsequently, the B cells were washed extensively to remove unbound particles, then incubated at 37°C for the time indicated, after which ice cold PBS was added to halt internalization.

ImageStream^X Analysis

Cells were stained with anti-HLA-DR APC (clone L243; BD Bioscience) in PBS supplemented with 0.1% BSA for 30 min in the dark on ice and fixed for 20 min in PBS with 4% PFA. Primary human B cells or Ramos B cells were washed and 4′,6′-diamidino-2-phenylindole (DAPI; Sigma) was added to stain the cell nucleus. Large particle internalization by human B cells was evaluated on an ImageStream^X mark II imaging flow cytometer (Merck). The acquired data was analyzed using IDEAS V6.2 Software (Merck) and FlowJo Software version 10 (**Supplementary Figures 1A**, **4**).

CD4$^+$ T Cell Proliferation Assay

Primary human B cells were incubated with vehicle (DMSO) or small molecule inhibitors (**Supplementary Table 1**) for 15 min at 37°C before being challenged with uncoated (control) or anti-IgM-coated heat-inactivated *S. typhimurium*. Heat-inactivated *S. typhimurium* was used instead of PFA-inactivated *S. typhimurium* to allow antigenic peptide presentation. B cells were primed with *S. typhimurium* for 30 min at 37°C and then washed in medium containing 100 μg/ml gentamicin (Invitrogen) to eliminate non-internalized bacteria (17). To allow antigenic peptide presentation, cells were cultured in B cell medium with 10 μg/ml gentamicin, supplemented with small molecule inhibitors (**Supplementary Table 1**) for 20 h at 37°C/5% CO_2. Subsequently, *S. typhimurium*-primed B cells were washed extensively and irradiated with 60 Gy to halt antigen processing before incubation with autologous CD4$^+$ T cells that were labeled with Cell Trace CFSE according to manufacturer's instructions

(Invitrogen). 10×10^4 B cells and 5×10^4 $CD4^+$ T cells were cocultured in 200 µl B cell medium at 37°C/5% CO_2 in 96-well round-bottom plates (Greiner Bio-One) for 6 days. Cells were then stained with anti-CD4 APC (clone SK3; BD Bioscience) to separate $CD4^+$ T cells from the remaining $CD19^+$ B cells and $CD4^+$ T cell proliferation was measured on a FACSLSRII (BD Bioscience). DAPI was added to exclude dead cells. The acquired data was analyzed using FlowJo Software version 10.

Lifeact-Imaging

For confocal laser scanning microscopy analysis, Lab-Tec 8-well chamber slides (Thermo Fisher Scientific) were coated with 1 mg/ml poly-L-lysine (Sigma) for 1 h, washed thoroughly with Aquadest and air-dried. Ramos B cells expressing Lifeact-GFP were allowed to bind to the coated slides for 15 min at 37°C before being challenged with anti-human IgM-coated polystyrene beads (3 µm). For real-time imaging

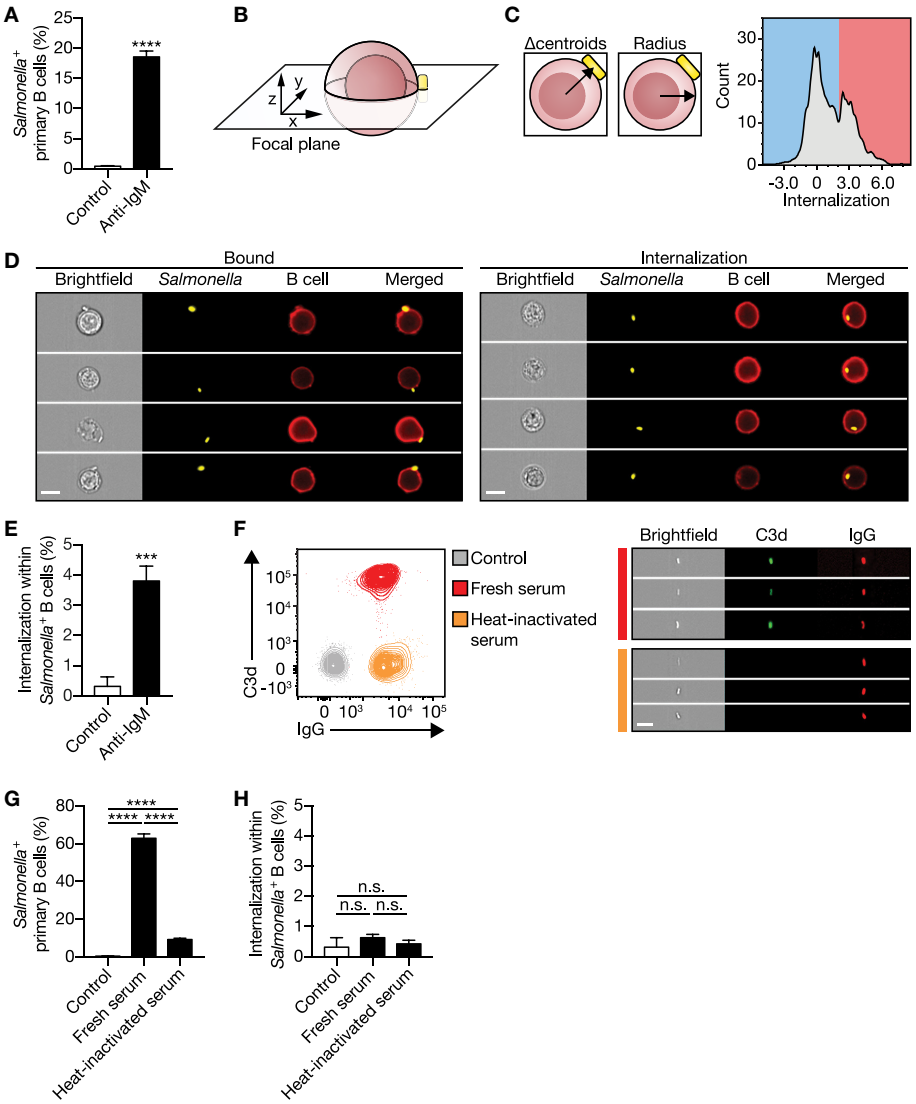

FIGURE 1 | IgM-BCR stimulation specifically promotes large particle internalization. **(A)** Proportion of primary human B cells interacting with control or anti-IgM-coated *S. typhimurium* ($n = 9$). **(B)** Schematics of a B cell:*S. typhimurium* interaction. Internalization was assessed using a high-throughput quantitative image analysis approach for *S. typhimurium* located in the same focal plane as the human B cell only. **(C)** To discriminate between bound and internalized *S. typhimurium*, analysis masks were generated to determine the center of both the B cell and *S. typhimurium.* Internalization was defined as the distance between the two centroids (left) after correction for the B cell radius as a measure for the cell size (middle). Internalization was plotted against the event count (right). The red/blue shadings behind the plot indicate the portion of cells that bound (blue) or internalized (red) large particles. Events that had a calculated value similar to or >2 were defined as being internalized. **(D)** Representative images of primary human B cells containing bound (left) or internalized (right) *S. typhimurium*. Bar, 7 µm. **(E)** Proportion of internalization of control or anti-IgM-coated *S. typhimurium* within *Salmonella*$^+$ primary human B cells ($n = 9$). **(F)** Representative plots (left) and images (right) of *S. typhimurium* opsonized with antibodies (IgG) or together with complement (C3d) derived from human serum. Bar, 7 µm. **(G–H)** Proportion of primary human B cells that interacted with **(G)** and internalized **(H)** serum-opsonized *S. typhimurium* ($n = 9$). Bars depict mean values and error bars are SEM. ***$P < 0.001$; ****$P < 0.0001$; n.s., not significantly different by paired *t*-test **(A,E)** or repeated-measures one-way ANOVA with Sidak post-test **(G,H)**.

a LEICA TCS SP8 confocal microscope system equipped with a 63 × 1.4 NA oil objective and 405 nm diode, 488 nm argon, 594 nm HeNe, and 633 nm HeNe laser, was used. Images were processed using ImageJ software (National Institutes of Health).

Fluorescence Resonance Energy Transfer (FRET)-Based Biosensor Analysis

RAC1 activity was measured in Ramos B cells after stimulation with anti-IgM-coated *S. typhimurium* by monitoring yellow fluorescent protein (YFP) FRET over donor cyan fluorescent protein (CFP) intensities as described before (27). Lab-Tec 8-well chamber slides were prepared as described above. A Zeiss Observer Z1 microscope equipped with a 63x NA1.3 oil immersion objective, an HXP 120-V excitation light source, a Chroma 510 DCSP dichroic splitter, and two Hamamatsu ORCA-R2 digital charge-coupled device cameras was used for simultaneous monitoring Cerulean3 and Venus emission. Zeiss Zen 2012 microscope software was used to control the system. Offline ratio analyses between Cerulean3 and Venus images were processed using the ImageJ software. Image stacks were background corrected, stacks were aligned, and a smooth filter was applied to both image stacks to improve image quality by reducing noise. FRET ratios were bleed-through corrected (62%) for the CFP leakage into the YFP channel. An image threshold was applied exclusively to the Venus image stack, converting background pixels to "not a number" (NaN) allowing elimination of artifacts in ratio image stemming from the background noise. Finally, the Venus/Cerulean3 ratio was calculated and the Parrot-2 look-up table (created by dr. J. Goedhart) was applied to generate a heatmap.

Immunoblot Analysis

Ramos B cells (10×10^6) were lysed in 50 mM Tris, pH 7.6, 20 mM $MgCl_2$, 150 mM NaCl, 1% (v/v) Triton X-100, 0.5% (w/v) deoxycholic acid (DOC) and 0.1% (w/v) SDS supplemented with a phosphatase inhibitor cocktail (Sigma) and fresh protease-inhibitor-mixture tablets (Roche Applied Science). Cell lysates were then centrifuged at 14,000 rpm for 15 min at 4°C, and supernatants were recovered and boiled in SDS sample buffer containing 4% β-mercaptoethanol. Samples were analyzed using 12.5% SDS-Page. Proteins were transferred onto a 0.2 μm nitrocellulose membrane (Whatman), subsequently membranes were blocked with 5% (w/v) BSA (**Figures 2E**, **3K**) or 5% (w/v) milk powder (**Figures 3B**, **5G**) in Tris-buffered saline with Tween 20 (TBST). The nitrocellulose membrane was incubated for 1 h at RT with mouse monoclonal anti-NCK (clone 108; BD Bioscience), rabbit polyclonal anti-cofilin (cat #ab42823; Abcam), rabbit polyclonal anti-pAKT (Ser473) (cat #9271; Cell Signaling Technology) or rabbit monoclonal anti-AKT (pan) (clone C67E7; Cell Signaling Technology), followed by incubation for 1 h at RT with HRP-conjugated rat monoclonal anti-mouse kappa (RM-19; Sanquin Reagents) or HRP-conjugated goat anti-rabbit IgG (cat #ab205718; Abcam) in TBST. Between the incubation steps, the membranes were washed with TBST. Antibody staining was visualized with the Pierce enhanced chemiluminescence (ECL) 2 Western Blotting substrate kit (Thermo Fisher Scientific) according to manufacturer's instructions and analyzed using ChemiDoc MP System (BioRad). Brightness/contrast parameters were adjusted globally across the entire image using Image Lab software (BioRad).

RacGTP Pulldown Assay

Cells were lysed in 50 mM Tris, pH 7.6, 20 mM $MgCl_2$, 150 mM NaCl, 1% (v/v) Triton X-100, 0.5% (w/v) DOC and 0.1% (w/v) SDS supplemented with protease inhibitors. Cell lysates were then centrifuged at 14,000 rpm for 15 min at 4°C. Supernatants were recovered and GTP-bound RAC1 was isolated by rotating supernatants at 4°C for 30 min with 5 μg biotinylated PAK-CRIB peptide coupled to streptavidin agarose as described before (27). Beads were centrifuged at 5,000 rpm for 20 s at 4°C, washed five times in 50 mM Tris, pH 7.6, 10 mM $MgCl_2$, 150 mM NaCl, 1% (v/v) Triton X-100 and boiled in SDS-sample buffer containing 4% β-mercaptoethanol. Samples were then analyzed by 12.5% SDS-Page as described in the immunoblot section above using mouse monoclonal anti-RAC1 (clone 102; BD Transduction Laboratories) and HRP-conjugated rat monoclonal anti-mouse kappa (RM-19; Sanquin Reagents).

Statistical Analyses

Statistical analyses were performed using Prism 7 (Graphpad). The statistical tests used are indicated in the figure descriptions. Differences were considered statistically significant when $p \leq 0.05$.

RESULTS

Internalization of Large Particles by Primary Human B Cells Is Mediated via the IgM-B Cell Receptor (BCR) and Not by Antibody and Complement Receptors

To evaluate internalization of large particles by primary human B cells, a high-throughput quantitative image analyses approach was established using ImageStream^X, as this combines visual analysis with the statistical power of flow cytometry. Inactivated *S. typhimurium* was used as a model particle. Primary human B cells isolated from blood displayed a low proportion of B cells associating with our model particle (**Figure 1A**), in line with the low numbers of primary human B cells expressing a BCR that specifically binds *S. typhimurium,* as observed before (17). *S. typhimurium* was coated with a monoclonal antibody specific for immunoglobulin M (anti-IgM) allowing association irrespective of the B cells antigen specificity. Indeed, anti-IgM coating markedly enhanced particle binding as compared with uncoated control (**Figure 1A**). Subsequently, a custom feature was generated to quantify the relative particle internalization distance into B cells, only taking cells into account in which both particle and B cell were imaged in the same focal plane (**Figures 1B,C**; **Supplementary Figures 1A,B**). This allowed us to distinguish between B cells having membrane-bound particles from B cells that completely internalized the particles (**Figures 1C,D**). Using this approach, we demonstrated that IgM-BCR-mediated internalization of large antigen-coated

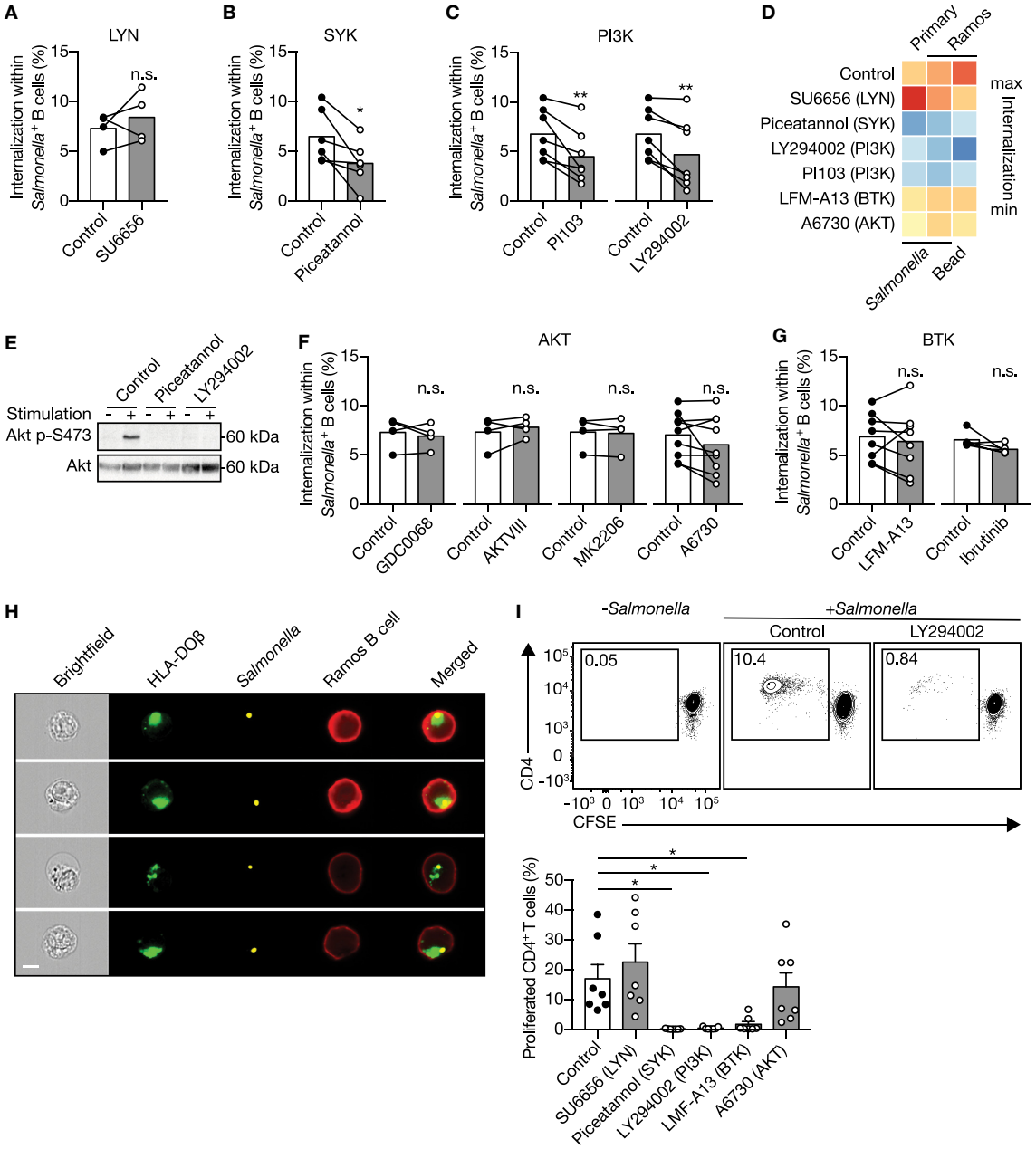

FIGURE 2 | IgM-BCR-mediated signaling through SYK and PI3K facilitate large particle internalization. **(A–C)** Proportion of internalization within *S. typhimurium*$^+$ primary human B cells after treatment with inhibitors of LYN [**(A)**; $n = 4$], SYK [**(B)**; $n = 6$] or PI3K [**(C)**; $n = 7$]. **(D)** Heatmap of the mean proportion of internalization within *S. typhimurium*$^+$ or 3μm polystyrene bead$^+$ primary human B cells and Ramos B cells after treatment with inhibitors of LYN, SYK, PI3K, BTK, or AKT. Heatmap colors indicate effect on internalization. **(E)** Immunoblot of whole cell extracts from Ramos B cells that were unstimulated (–) or stimulated (+) with *S. typhimurium* after incubation with inhibitors of SYK (Piceatannol) or PI3K (LY294002). The blots were probed with specific antibodies for pAKT at S473 and AKT. **(F,G)** Proportion of internalization within *S. typhimurium*$^+$ primary human B cells after treatment with inhibitors of AKT [**(F)**; $n = 4$ and 9] or BTK [**(G)**; $n = 8$ and 5]. **(H)** Representative images of Ramos B cells expressing GFP-tagged HLA-DOβ having internalized *S. typhimurium*. *S. typhimurium*-containing phagosomes localize to the HLA-DOβ-containing MHC class II-antigen loading compartments. Bar, 7μm. **(I)** Representative plots (top) and quantification (bottom) of the proportion of proliferated CD4$^+$ T cells after co-culture with *S. typhimurium*-primed autologous primary human B cells that were treated with inhibitors ($n = 7$). All data points represent the mean of an individual experiment with duplicate measurements. Error bars indicate SEM. *$P < 0.05$; **$P < 0.01$; n.s., not significantly different by paired *t* test **(A–C, F, G)** or repeated-measures one-way ANOVA with Dunnett's post-test **(I)**.

particles occurred within 30 min of incubation with primary human B cells (**Figure 1E**), confirming earlier observations (17, 31). To validate this property of the IgM-BCR in large particle internalization, particles were opsonized with serum derived complement and/or antibodies to bind complement- and Fcγ receptors expressed by primary human B cells,

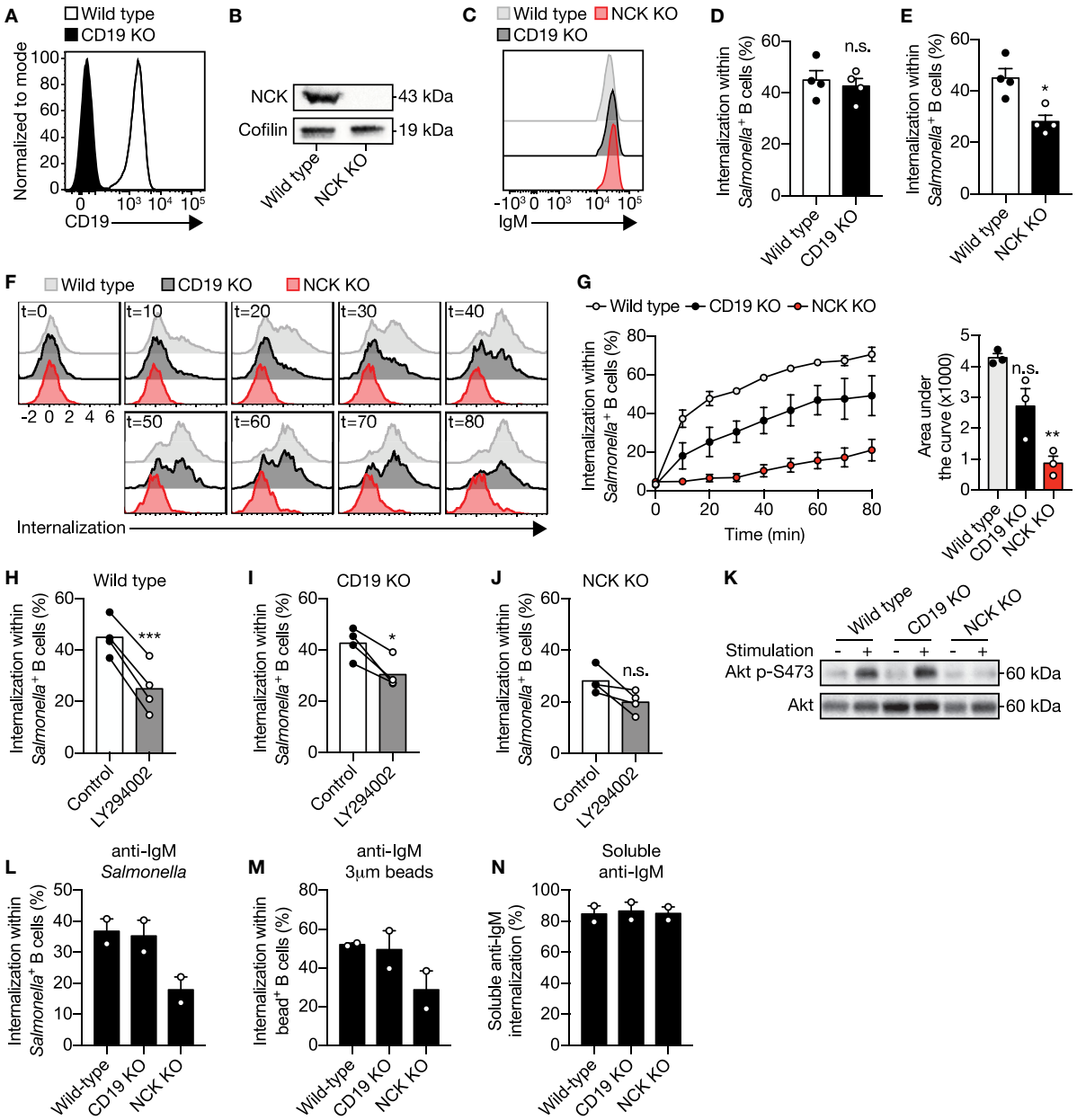

FIGURE 3 | The adaptor protein NCK is required for PI3K activity to facilitate IgM-BCR-induced internalization of large particles. **(A)** Representative histogram of CD19 expression in wild type and CD19 KO Ramos B cells. **(B)** Immunoblot of whole cell extracts from wild type and NCK KO Ramos B cells probed with NCK- or cofilin-specific (loading control) antibodies. **(C)** Representative histogram of surface IgM expression in wild type, CD19 KO and NCK KO Ramos B cells. **(D,E)** Proportion of internalization within *S. typhimurium*$^+$ CD19 KO **(D)** and NCK KO **(E)** Ramos B cells compared with wild type ($n = 4$). **(F,G)** Representative histograms **(F)** and quantification [**(G)**; left] of the proportion of internalization within *S. typhimurium*$^+$ wild type, CD19 KO and NCK KO Ramos B cells in time ($n = 3$). The area under the curve was obtained to quantify internalization in time [**(G)**; right]. **(H–J)** Proportion of internalization within *S. typhimurium*$^+$ wild type **(H)**, CD19 KO **(I)** and NCK KO **(J)** Ramos B cells after treatment with a PI3K inhibitor ($n = 4$). **(K)** Immunoblot of whole cell extracts from wild type, CD19 KO and NCK KO Ramos B cells that were unstimulated (–) or stimulated (+) with *S. typhimurium*. The blots were probed with specific antibodies against pAKT at S473 and AKT. **(L,M)** Proportion of internalization within *S. typhimurium*$^+$ **(L)**, 3μm polystyrene bead$^+$ **(N)** and soluble anti-IgM$^+$ **(M)** wild type, CD19 KO and NCK KO Ramos B cells ($n = 2$). Each data point represents the mean of an individual experiment with duplicate measurements. Error bars indicate SEM. $^*P < 0.05$; $^{**}P < 0.01$; $^{***}P < 0.001$; n.s., not significantly different by paired *t*-test **(B, D, G–I)** or repeated-measures one-way ANOVA with Dunnett's post-test **(F)**.

respectively (**Figure 1F**; **Supplementary Figure 2**). Interestingly, complement and antibody opsonization both mediate particle binding (**Figure 1G**), but did not facilitate internalization (**Figure 1H**). Together, these data demonstrate that large particle internalization by human B cells is specifically induced after IgM-BCR-mediated particle binding.

SYK and PI3K Are Important Signaling Components to Mediate IgM-BCR-Mediated Particle Internalization

To understand the mechanism by which human B cells facilitate IgM-BCR-mediated internalization of large particles, small molecule inhibitors that decrease activity of signaling proteins downstream of the IgM-BCR were used. Two major players in the signaling cascade downstream of the IgM-BCR include SRC-family protein tyrosine kinase LYN and SYK, which both mediate phosphorylation of conserved ITAMs contained within the cytoplasmic domains of CD79a and CD79b associated with the IgM-BCR (34, 35). The LYN inhibitor SU6656 did not affect internalization by primary human B cells (**Figure 2A**), whereas the SYK inhibitor piceatannol significantly reduced internalization (**Figure 2B**), suggesting that large particle uptake is SYK-dependent. A well-known signaling protein that becomes activated after SYK recruitment to the IgM-BCR is PI3K (36). The PI3K inhibitors PI103 and LY294002 significantly reduced internalization of large anti-IgM-coated particles in both primary and Ramos B cells (**Figures 2C,D**). In line with the fact that PI3K drives AKT phosphorylation (37), inhibition of SYK or PI3K abrogated phosphorylation of AKT at S473 after stimulation with anti-IgM-coated *S. typhimurium* (**Figure 2E**). In contrast, inhibition of AKT did not affect large particle internalization, indicating that although being activated AKT is not essential for internalization (**Figures 2D,F**). In addition, inhibition of BTK known to amplify the signal from the IgM-BCR also did not affect large particle internalization, both in primary B cells and in the Ramos B cell line (**Figures 2D,G**). To assess potential involvement of bacterial virulence factors or pathogen associated molecular patterns (PAMPs) that may engage additional receptors to affect IgM-BCR signaling pathways, inert polystyrene beads were coated with anti-IgM. Anti-IgM-coated polystyrene beads were internalized by Ramos B cells similar to anti-IgM-coated *S. typhimurium* (**Figure 2D**). Additionally, internalization of polystyrene beads was equally dependent on SYK and PI3K as compared to anti-IgM-coated *S. typhimurium* indicative of a shared mechanism underlying large particle internalization (**Figure 2D**). Together, these data systematically show that IgM-BCR-mediated uptake of large particles by human B cells is initiated by SYK and requires activation of PI3K irrespective of downstream signaling through AKT or BTK.

Inhibition of Large Particle Uptake Impairs Presentation to CD4$^+$ T Cells

Visualization of internalization of large particles by Ramos B cells revealed that after uptake the particle-containing phagosomes colocalized with HLA-DOβ-containing MHC class II antigen-loading compartments (**Figure 2H**). To establish whether large particle internalization by primary human B cells led to MHC class II antigen-derived peptide loading and presentation, we assessed their capacity to stimulate autologous CD4$^+$ T cells. Particle-primed, but not control primary human B cells induced CD4$^+$ T cell proliferation (**Figure 2I**). Consistent with the effects on large particle internalization, inhibition of SYK and PI3K, in contrast to LYN and AKT in primary human B cells diminished the ability of particle-primed B cells to activate CD4$^+$ T cells (**Figure 2I**). Of note, while BTK inhibition did not affect antigenic particle internalization (**Figure 2G**), it did significantly abolish CD4$^+$ T cells activation (**Figure 2I**), suggesting that BTK is involved in antigen presentation after large particle internalization.

Large Particle Induced IgM-BCR Activation of PI3K Strongly Depends on the Adaptor Protein NCK

PI3K can be activated through two pathways after IgM-BCR-mediated recognition of antigen. Direct signaling downstream of the IgM-BCR is propagated by the adaptor protein NCK via B cell adaptor for PI3K (BCAP) bound to PI3K (21). Alternatively, the activation of PI3K has been shown to be mediated by CD19 as part of the IgM-BCR co-receptor complex (22–24). To determine which pathway is involved in PI3K-driven uptake of large anti-IgM-coated particles by B cells, CD19 and NCK knockout (KO) Ramos B cells were generated using CRISPR-Cas9 (**Figures 3A,B**). Plasma membrane IgM expression was not affected upon CD19 or NCK KO (**Figure 3C**). Targeting of the large particle to the co-receptor CD19 did not induce internalization (**Supplementary Figures 3A,B**). Remarkably, deletion of NCK and not CD19 significantly decreased IgM-BCR-mediated uptake of large anti-IgM-coated particles as compared to wild type control Ramos B cells (**Figures 3D,E**). To further assess the role of CD19 and NCK in the dynamics of large particle internalization, internalization of IgM-BCR-bound particles was analyzed in time. In confirmation, absence of NCK strongly and significantly reduced internalization of large anti-IgM-coated particles in Ramos B cells at different time points after particle binding, whereas absence of CD19 did not significantly affect internalization efficiency, although an inhibitory trend was visible (**Figures 3F,G**). In line with the efficient uptake of large anti-IgM-coated particles in absence of CD19, inhibition of PI3K still significantly decreased internalization in the CD19 KO Ramos B cells, demonstrating a continued dependence on PI3K in the absence of CD19 similar to wild type control (**Figures 3H,I**). In contrast, inhibition of PI3K along with NCK KO had no significant effect on large anti-IgM-coated particle internalization, suggesting that the adaptor protein NCK is responsible for the recruitment of PI3K into the signalosome to drive large particle internalization (**Figure 3J**). Indeed, NCK KO, but not CD19 KO Ramos B cells exhibit a lack of phosphorylation of AKT at S473 following stimulation with large particles, which is indicative of diminished PI3K activity (**Figure 3K**). To determine whether the adaptor protein NCK is required for internalization of large particle in general, the internalization efficiency of anti-IgM-coated *S. typhimurium*, inert anti-IgM-coated polystyrene beads and soluble anti-IgM were compared. Interestingly, absence of NCK strongly reduced internalization of both anti-IgM-coated particles, whereas internalization of soluble anti-IgM was unaffected (**Figures 3L–N**; **Supplementary Figure 4**). Altogether, these data

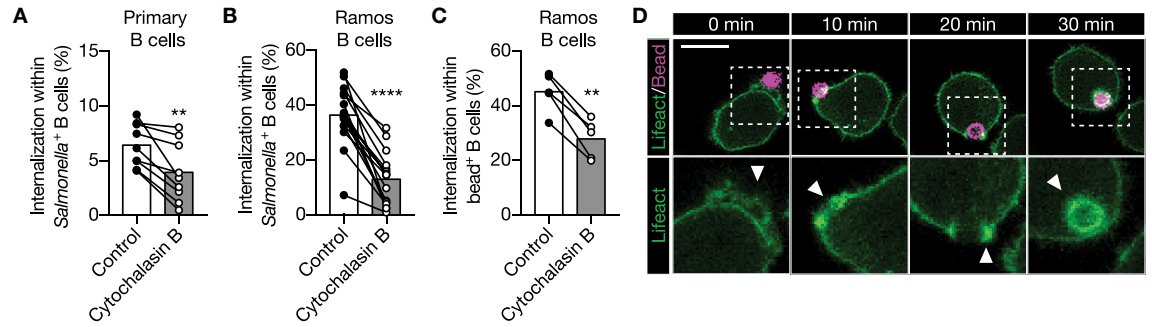

FIGURE 4 | IgM-BCR-mediated large particle internalization is an actin-dependent process. **(A–C)** Proportion of internalization within *S. typhimurium*$^+$ **(A,B)** or polystyrene bead$^+$ **(C)** primary human B cells [**(A)**; $n = 9$], and Ramos B cells [**(B)**; $n = 16$, **(C)**; $n = 5$] after treatment with cytochalisin **(B)**. **(D)** Representative confocal still-images at different time points imaging internalization of anti-IgM-coated polystyrene beads by Ramos B cells expressing Lifeact-GFP. Arrowhead, clusters of actin driving internalization. Bar, 10 μm. The boxed region at the upper panels is enlarged at the lower panels. Each data point represents the mean of an individual experiment with duplicate measurements. $^{**}P < 0.01$; $^{****}P < 0.0001$ by paired *t*-test.

demonstrate that uptake of large anti-IgM-coated particles, and not soluble anti-IgM, by the IgM-BCR requires the adaptor protein NCK.

Actin Polymerization Drives IgM-BCR-Mediated Large Particle Internalization

We then asked how PI3K induces internalization of large anti-IgM-coated particles. PI3K is a modulator of actin cytoskeleton rearrangement, which is important for BCR mobility and micro cluster formation (12, 38–42). Although disruption of the actin cytoskeleton by cytochalasin B did not alter membrane IgM expression (**Supplementary Figures 5A–C**), it did significantly decreased internalization of large anti-IgM-coated particles in primary human B cells and in the Ramos B cell line (**Figures 4A–C**). To further assess the role of the actin cytoskeleton, Ramos B cells expressing Lifeact-GFP were used to effectively visualize actin cytoskeleton remodeling during large particle internalization. Formation of F-actin containing pod-like structure that extends the plasma membrane and surrounds the particle immediately upon contact were visualized using anti-IgM-coated polystyrene beads. F-actin further accumulated during uptake and encircled the particle-containing phagosome long after antigen uptake, which suggests that actin mediates intracellular antigen trafficking (**Figure 4D**). These data show that BCR-induced internalization of large particles is dependent on actin polymerization.

NCK Facilitates RAC1 Activity During Internalization of Large Anti-IgM-Coated Particles

We established that NCK/PI3K signaling is required for IgM-BCR-mediated internalization of large particles, which is further propagated irrespective of BTK and AKT. How does PI3K then promote downstream signaling transduction to facilitate actin-dependent internalization? The potential involvement of RAC1 was investigated as RAC1 is a key regulator of the actin cytoskeleton organization in mammalian cells, and its activity is modulated by various guanine nucleotide exchange factors (GEFs) and GTPase-activating proteins (GAPs) that are recruited to phosphorylated lipids produces by PI3K (43–45). Internalization of large anti-IgM-coated particles was significantly affected in both primary and Ramos B cells upon inhibition of RAC1 activity (**Figures 5A,B**). To further elucidate the role of RAC1 in internalization, a DORA-based RAC1 biosensor was used to visualize RAC1 activity during internalization (**Figure 5C**). This revealed enhanced RAC1 activity near the particle binding site during particle engulfment, which faded once the particle was fully internalized (**Figures 5D–F**). In contrast, RAC1 activity in the cytosol was largely unaffected (**Figures 5D–F**). To establish further a mechanistic link between upstream NCK-dependent PI3K recruitment and downstream RAC1 activity to modulate actin organization, we performed a pull-down assay with the biotinylated CDC42/RAC1-interactive binding (CRIB) domain of PAK1 that binds activated RAC1 from stimulated cells. This analysis validated upregulation of RAC1 activity upon stimulation with large anti-IgM-coated particles in wild type Ramos B cells (**Figures 5G,H**). In contrast, RAC1 activity was markedly decreased after stimulation of NCK KO Ramos B cells (**Figures 5G,H**). Together, these data demonstrate a requirement for NCK-mediated signaling in BCR-induced activation of RAC1 during large particle engulfment by human B cells.

DISCUSSION

BCR engagement with antigen initiates two critical cellular processes in B cells. On the one hand, triggering of the signaling receptor induces B cell activation. On the other hand, antigen encounter promotes internalization and efficient antigen-derived peptide presentation to facilitate an interaction with CD4$^+$ T cell help. Over the past decades it has become evident that CD4$^+$ T cell help is essential to the development of high affinity, class switched IgG antibody responses (46–52).

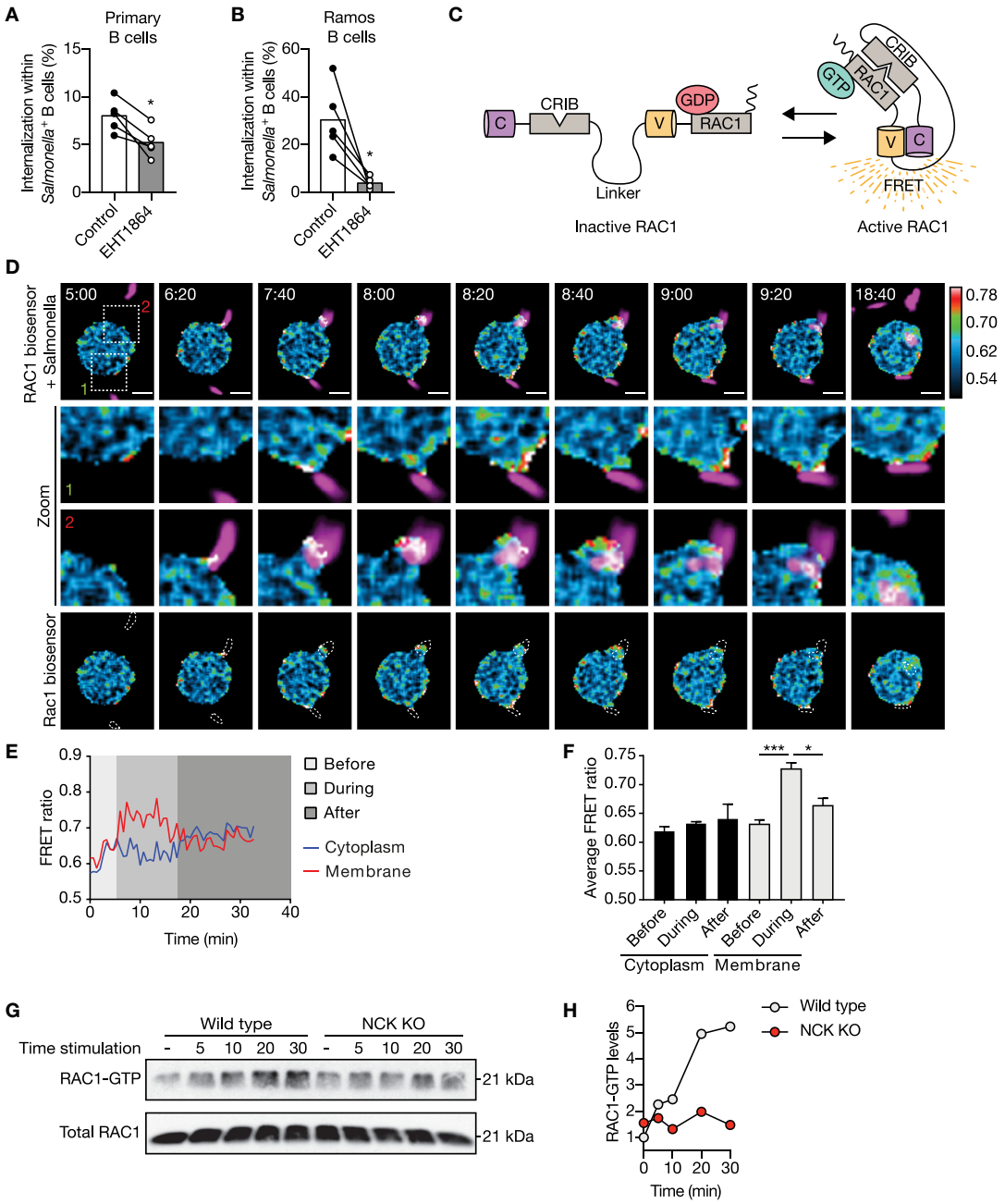

FIGURE 5 | NCK facilitates IgM-BCR-mediated activation of RAC1 subsequent large particle binding. **(A,B)** Proportion of internalization within *S. typhimurium*$^+$ primary human B cells **(A)** and Ramos B cells **(B)** after treatment with a RAC1 inhibitor ($n = 5$). **(C)** Schematic illustration of the Cerulean3-CRIB-Venus-RAC1 FRET sensor. Inactive GDP-bound RAC1 results in a large distance between the two fluorescent proteins without a FRET signal. Active GTP-bound RAC1 binds the CDC42/RAC1-interactive binding (CRIB) motif of PAK1, which brings the two fluorescent proteins into close proximity resulting in high FRET efficiency. **(D)** Time-lapse Venus/Cerulean3 ratio images of the RAC1 DORA biosensor showing spatiotemporal RAC1 activation upon stimulation with anti-IgM-coated *S. typhimurium* expressing dsRed (magenta). Bar, 5 μm. The boxed region at the upper panel is enlarged at the middle panels. Lower panels show RAC1 biosensor FRET ratio images with dashed lines marking *S. typhimurium* localization. Time indicated in minutes. Calibration bar shows RAC1 activation (red) relative to basal RAC1 activity (blue). **(E,F)** Representative activation ratio **(E)** and quantification **(F)** of the RAC1 biosensor in time. The activation ratio was assessed at the membrane as compared to the cytoplasm in close proximity to the particle contact area before, during and after *S. typhimurium* internalization ($n = 3$ independent experiments). **(G,H)** Immunoblot and quantification of GTP-bound RAC1 precipitated from whole cell extracts of wild type and NCK KO Ramos B cells that were unstimulated (–) or stimulated with anti-IgM-coated *S. typhimurium* for 5, 10, 20, and 30 min. Total Rac1 levels from whole cell extracts were determined to control precipitation input (representative of $n = 2$ independent experiments). Bars depict mean values and error bars are SEM. Each data point represents the mean of an individual experiment with duplicate measurements. $^*P < 0.05$; $^{***}P < 0.001$ by paired *t*-test.

In the current study, we aimed to identify the molecular mechanisms that govern internalization of large particles and bacteria by human B cells, as this process enables B cells that recognize one antigen to attract broad T cell help directed against other antigens in the particle, and yields broad undesired antibody responses in autoimmunity and blood transfusion. We present data that demonstrate that human B cells take up large particles via the IgM-BCR-induced NCK/PI3K/RAC1 axis to drive actin cytoskeleton modulation, without a requirement for the co-receptor CD19 (**Figure 6**). Using our high-throughput quantitative image analysis approach, we established that complement and antibodies opsonization both induce large particle binding, whereas particle internalization was exclusively achieved when the IgM-BCR is engaged. The ability to bind complement and/or antibody-opsonized particles is likely used for antigen transfer. Indeed, non-cognate B cells carry complement-opsonized antigen on their plasma membrane in a CR2-dependent manner to transfer and deposit these antigens onto follicular dendritic cells (FDC) (53). In confirmation with previous observations, we here demonstrate that IgM-BCR-mediated large particle internalization is highly dependent on active transmembrane signaling, which reflects a need for functional intracellular immunoreceptor tyrosine activation motifs (ITAMs) (16, 54). By using small molecule inhibitors, we demonstrate that the signaling protein SYK, and not LYN, is required for large particle internalization. The observation that LYN is not essential in IgM-BCR signaling has been made previously in B cells from *lyn*$^{-/-}$ mice that were found to be hyperresponsive to BCR ligation (55). As strength of the initial BCR signaling correlates with the stability of clustered antigenic receptor molecules, our data suggest that upon proper cross-linking of the IgM-BCR by large particles, signaling can be transmitted independent of LYN, whereas SYK, the protein required for the initiation of the multimolecular signalosome that activates distinct and inter-related signaling pathways, cannot be bypassed (42). BTK inhibition did not affect internalization of large particles, whereas it greatly inhibited particle-dependent CD4^{+} T cell proliferation. This suggests that BTK regulates other intracellular processes that are necessary to mount a proper CD4^{+} T cell response. Indeed, BTK was found to promote the rate of BCR internalization and the movement of the internalized antigen-BCR complex to late endosomes and peptide presentation in splenic mouse B cells (56). This suggests that small soluble antigen and large particles require distinct molecular pathways downstream of the BCR to be internalized, but once internalized similar molecular events are activated, that are dependent on BTK and regulate antigen processing and presentation.

The involvement of the co-receptor CD19 in PI3K recruitment and its central role in BCR signaling are well-known (57, 58). Since PI3K activity was key in the internalization process, the finding that PI3K activity was not profoundly dependent on CD19 was unexpected. It has been observed before that CD19 does not fully account for PI3K translocation to the BCR since PI3K activity is still present in B cells from CD19$^{-/-}$ mice after BCR stimulation (59), as also determined in the current study. Previously, it was shown that BCR signaling in response to small soluble antigen is independent of the co-receptor, whereas CD19 is essential in potentiation BCR-mediated signaling transduction in response to membrane-bound antigen stimulation (42). This may suggest that the co-receptor CD19 is only required for antigen internalization when the antigen is linked to a membrane. Here we demonstrate that PI3K-dependent internalization of large anti-IgM-coated particles is strongly promoted by the adaptor protein NCK, in line with the recent finding that NCK can also propagate BCR-mediated activation of PI3K (21). Although, NCK can be recruited to participate in BCR signaling through the BLNK complex in B cells (60), Castello and colleagues demonstrate that NCK is recruited to a non-ITAM phosphorylated tyrosine on the BCR-associated Igα to participate in BCR signaling in a BTK- and SYK-independent manner. As large particle internalization is dependent on SYK, this may suggest that NCK recruitment is facilitated by the SYK-dependent BLNK route.

It has been described previously that actin cytoskeleton rearrangements are required for internalization of soluble antigen (56). We have extended on this observation by showing that internalization of large particles by human B cells is mediated by the actin cytoskeleton, as also observed for murine follicular B cells (16). Furthermore, we show that actin cytoskeleton rearrangements are modulated by IgM-BCR-induced NCK-PI3K axis via the small GTPase RAC1. PI3K facilitates RAC1 activation through the generation of lipids that can bind and recruit PH-domain-containing guanine nucleotide exchange factors (GEFs) that control RAC1 activation (61). A well-known GEF that might

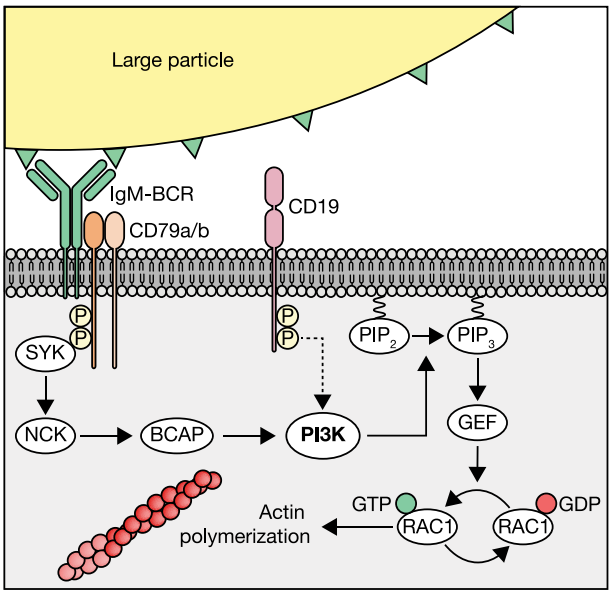

FIGURE 6 | Schematic of IgM-BCR-induced PI3K-driven internalization of large particles. Human B cells internalize large particles though IgM-BCR activation of PI3K via NCK without profound requirement of the co-receptor CD19 (dotted arrow). PI3K facilitates internalization though the conversion of phosphatidylinositol 4,5-biphosphate (PIP_2) to phosphatidylinositol 3,4,5-triphosphate (PIP_3) to recruit guanine nucleotide exchange factors (GEFs) that modulate RAC1-dependent activation of the actin cytoskeleton.

be the bridge between PI3K and RAC1 is VAV, which was shown to activate RAC1 and regulate cytoskeletal structures after BCR activation (34, 62). VAV would be of particular interest since it is the predominant RAC1 GEF expressed in B cells (63) In addition, other PI3K dependent adaptors such as Bam32 have been shown to be an important regulator for RAC1 activation and actin remodeling, warranting future research (64).

In conclusion, we provide evidence for the first time that internalization of large anti-IgM-coated particles by human B cells occurs via the SYK/NCK/PI3K/RAC1-actin axis, which may be susceptible to regulation. SYK and PI3K are both targets of clinically-approved inhibitors that are currently used in clinical trials against autoimmune thrombocytopenia (ITP), leukemia and lymphomas (65, 66). It is important to realize that these patients may be more susceptible to microbial infections due to reduced B cell humoral immune response against microbes as a result of the affected ability to internalize large particles and to attract the $CD4^+$ T cell help required for class switching, somatic hypermutation, and plasma cell differentiation.

ETHICS STATEMENT

Approval by local ethical committee (Sanquin Research, Amsterdam) and in line with the Declaration of Helsinki.

AUTHOR CONTRIBUTIONS

NV, P-PU, AtB, and SvH conceived the ideas and designed the experiments. NV, P-PU, JW, BN, TJ, and JvR performed the experiments. NV, P-PU, JW, BN, TJ, JvR, RS, JdW, JvB, AtB, and SvH analyzed the data. NV, P-PU, AtB, and SvH wrote the manuscript. All authors have read and approved the manuscript.

ACKNOWLEDGMENTS

We thank M.L.M. Jongsma for assistance on the generation of CRISPR/Cas9 induced knockout cells; M. Fernandez-Borja for kindly providing the Lifeact-GFP construct; G. Marsman and Y.E. Bar-Ephraïm for titrating the small molecule inhibitors; Y. Wu (UConn Health, Farminton, CT) for longstanding collaboration on the DORA sensor; and E.P.J. Mul, M. Hoogenboezem and S. Tol for technical support.

SUPPLEMENTARY MATERIAL

The Supplementary Material for this article can be found online at: https://www.frontiersin.org/articles/10.3389/fimmu.2019.00415/full#supplementary-material

REFERENCES

1. Tulp A, Verwoerd D, Dobberstein B, Ploegh HL, Pieters J. Isolation and characterization of the intracellular MHC class II compartment. *Nature.* (1994) 369:120–6. doi: 10.1038/369120a0
2. Qiu Y, Xu X, Wandinger-Ness A, Dalke DP, Pierce SK. Separation of subcellular compartments containing distinct functional forms of MHC class II. *J Cell Biol.* (1994) 125:595–605. doi: 10.1083/jcb.125.3.595
3. Amigorena S, Drake JR, Webster P, Mellman I. Transient accumulation of new class II MHC molecules in a novel endocytic compartment in B lymphocytes. *Nature.* (1994) 369:113–20. doi: 10.1038/369113a0
4. Lanzavecchia A. Antigen-specific interaction between T and B cells. *Nature.* (1985) 314:537–9. doi: 10.1038/314537a0
5. Reth M. Antigen receptor tail clue. *Nature.* (1989) 338:383–4. doi: 10.1038/338383b0
6. Dal Porto JM, Gauld SB, Merrell KT, Mills D, Pugh-Bernard AE, Cambier J. B cell antigen receptor signaling 101. *Mol Immunol.* (2004) 41:599–613. doi: 10.1016/j.molimm.2004.04.008
7. Kuokkanen E, Šuštar V, Mattila PK. Molecular control of B cell activation and immunological synapse formation. *Traffic.* (2015) 16:311–26. doi: 10.1111/tra.12257
8. Woyach JA, Johnson AJ, Byrd JC. The B-cell receptor signaling pathway as a therapeutic target in CLL. *Blood.* (2012) 120:1175–84. doi: 10.1182/blood-2012-02-362624
9. Hoogeboom R, Tolar P. Molecular mechanisms of B cell antigen gathering and endocytosis. *Curr Top Microbiol Immunol.* (2015) 393:45–63. doi: 10.1007/82_2015_476
10. Tolar P, Sohn HW, Liu W, Pierce SK. The molecular assembly and organization of signaling active B-cell receptor oligomers. *Immunol Rev.* (2009) 232:34–41. doi: 10.1111/j.1600-065X.2009.00833.x
11. Spillane KM, Tolar P. B cell antigen extraction is regulated by physical properties of antigen-presenting cells. *J Cell Biol.* (2017) 216:217–30. doi: 10.1083/jcb.201607064
12. Natkanski E, Lee W-Y, Mistry B, Casal A, Molloy JE, Tolar P. B cells use mechanical energy to discriminate antigen affinities. *Science.* (2013) 340:1587–90. doi: 10.1126/science.1237572
13. Nowosad CR, Spillane KM, Tolar P. Germinal center B cells recognize antigen through a specialized immune synapse architecture. *Nat Immunol.* (2016) 17:870–7. doi: 10.1038/ni.3458
14. Gao J, Ma X, Gu W, Fu M, An J, Xing Y, et al. Novel functions of murine B1 cells: active phagocytic and microbicidal abilities. *Eur J Immunol.* (2012) 42:982–92. doi: 10.1002/eji.201141519
15. Parra D, Rieger AM, Li J, Zhang Y-A, Randall LM, Hunter CA, et al. Pivotal advance: peritoneal cavity B-1 B cells have phagocytic and microbicidal capacities and present phagocytosed antigen to CD4+ T cells. *J Leukoc Biol.* (2012) 91:525–36. doi: 10.1189/jlb.0711372
16. Martínez-Riaño A, Bovolenta ER, Mendoza P, Oeste CL, Martín-Bermejo MJ, Bovolenta P, et al. Antigen phagocytosis by B cells is required for a potent humoral response. *EMBO Rep.* (2018) 19:1–15. doi: 10.15252/embr.201846016
17. Souwer Y, Griekspoor A, Jorritsma T, de Wit J, Janssen H, Neefjes J, et al. B cell receptor-mediated internalization of salmonella: a novel pathway for autonomous B cell activation and antibody production. *J Immunol.* (2009) 182:7473–81. doi: 10.4049/jimmunol.0802831
18. Vanderlugt CJ, Miller SD. Epitope spreading. *Curr Opin Immunol.* (1996) 8:831–6. doi: 10.1016/S0952-7915(96)80012-4
19. Cornaby C, Gibbons L, Mayhew V, Sloan CS, Welling A, Poole BD. B cell epitope spreading: mechanisms and contribution to autoimmune diseases. *Immunol Lett.* (2015) 163:56–68. doi: 10.1016/j.imlet.2014.11.001
20. Degn SE, van der Poel CE, Firl DJ, Ayoglu B, Al Qureshah FA, Bajic G, et al. Clonal evolution of autoreactive germinal centers. *Cell.* (2017) 170:913–26.e19. doi: 10.1016/j.cell.2017.07.026
21. Castello A, Gaya M, Tucholski J, Oellerich T, Lu KH, Tafuri A, et al. Nck-mediated recruitment of BCAP to the BCR regulates the PI(3)K-Akt pathway in B cells. *Nat Immunol.* (2013) 14:966–75. doi: 10.1038/ni.2685
22. Beckwith M, Jorgensen G, Longo DL. The protein product of the proto-oncogene c-cbl forms a complex with phosphatidylinositol 3-kinase p85 and CD19 in anti-IgM-stimulated human B-lymphoma cells. *Blood.* (1996) 88:3502–7.
23. Weng WK, Jarvis L, LeBien TW. Signaling through CD19 activates Vav/mitogen-activated protein kinase pathway and induces formation of a

CD19/Vav/phosphatidylinositol 3-kinase complex in human B cell precursors. *J Biol Chem.* (1994) 269:32514–21.
24. Tuveson DA, Carter RH, Soltoff SP, Fearon DT. CD19 of B cells as a surrogate kinase insert region to bind phosphatidylinositol 3-kinase. *Science.* (1993) 260:986–9.
25. Sanjana NE, Shalem O, Zhang F. Improved vectors and genome-wide libraries for CRISPR screening. *Nat Methods.* (2014) 11:783–4. doi: 10.1038/nmeth.3047
26. Riedl J, Crevenna AH, Kessenbrock K, Yu JH, Neukirchen D, Bista M, et al. Lifeact: a versatile marker to visualize F-actin. *Nat Methods.* (2008) 5:605–7. doi: 10.1038/nmeth.1220
27. Timmerman I, Heemskerk N, Kroon J, Schaefer A, van Rijssel J, Hoogenboezem M, et al. A local VE-cadherin and Trio-based signaling complex stabilizes endothelial junctions through Rac1. *J Cell Sci.* (2015) 128:3041–54. doi: 10.1242/jcs.168674
28. Carette JE, Guimaraes CP, Varadarajan M, Park AS, Wuethrich I, Godarova A, et al. Haploid genetic screens in human cells identify host factors used by pathogens. *Science.* (2009) 326:1231–5. doi: 10.1126/science.1178955
29. Shalem O, Sanjana NE, Hartenian E, Shi X, Scott DA, Mikkelson T, et al. Genome-scale CRISPR-Cas9 knockout screening in human cells. *Science.* (2014) 343:84–7. doi: 10.1126/science.1247005
30. Martínez-Lorenzo MJ, Méresse S, de Chastellier C, Gorvel JP. Unusual intracellular trafficking of *Salmonella typhimurium* in human melanoma cells. *Cell Microbiol.* (2001) 3:407–16. doi: 10.1046/j.1462-5822.2001.00123.x
31. Souwer Y, Griekspoor A, de Wit J, Martinoli C, Zagato E, Janssen H, et al. Selective infection of antigen-specific B lymphocytes by Salmonella mediates bacterial survival and systemic spreading of infection. *PLoS ONE.* (2012) 7:e50667. doi: 10.1371/journal.pone.0050667
32. de Wit J, Souwer Y, Jorritsma T, Klaasse Bos H, ten Brinke A, Neefjes J, et al. Antigen-specific B cells reactivate an effective cytotoxic T cell response against phagocytosed Salmonella through cross-presentation. *PLoS ONE.* (2010) 5:e13016. doi: 10.1371/journal.pone.0013016
33. de Wit J, Jorritsma T, Makuch M, Remmerswaal EBM, Klaasse Bos H, Souwer Y, et al. Human B cells promote T-cell plasticity to optimize antibody response by inducing coexpression of TH1/TFH signatures. *J Allergy Clin Immunol.* (2015) 135:1053–60. doi: 10.1016/j.jaci.2014.08.012
34. Niiro H, Clark EA. Regulation of B-cell fate by antigen-receptor signals. *Nat Rev Immunol.* (2002) 2:945–56. doi: 10.1038/nri955
35. Rolli V, Gallwitz M, Wossning T, Flemming A, Schamel WWA, Zürn C, et al. Amplification of B cell antigen receptor signaling by a Syk/ITAM positive feedback loop. *Mol Cell.* (2002) 10:1057–69. doi: 10.1016/S1097-2765(02)00739-6
36. Beitz LO, Fruman DA, Kurosaki T, Cantley LC, Scharenberg AM. SYK is upstream of phosphoinositide 3-kinase in B cell receptor signaling. *J Biol Chem.* (1999) 274:32662–6. doi: 10.1074/jbc.274.46.32662
37. Hamman BD, Pollok BA, Bennett T, Allen J, Heim R. Binding of a pleckstrin homology domain protein to phosphoinositide in membranes: a miniaturized FRET-based assay for drug screening. *J Biomol Screen.* (2002) 7:45–55. doi: 10.1177/108705710200700107
38. Schlam D, Bagshaw RD, Freeman SA, Collins RF, Pawson T, Fairn GD, et al. Phosphoinositide 3-kinase enables phagocytosis of large particles by terminating actin assembly through Rac/Cdc42 GTPase-activating proteins. *Nat Commun.* (2015) 6:8623. doi: 10.1038/ncomms9623
39. Tolar P, Hanna J, Krueger PD, Pierce SK. The constant region of the membrane immunoglobulin mediates B cell-receptor clustering and signaling in response to membrane antigens. *Immunity.* (2009) 30:44–55. doi: 10.1016/j.immuni.2008.11.007
40. Liu W, Won Sohn H, Tolar P, Meckel T, Pierce SK. Antigen-induced oligomerization of the B cell receptor is an early target of Fc gamma RIIB inhibition. *J Immunol.* (2010) 184:1977–89. doi: 10.4049/jimmunol.0902334
41. Treanor B, Depoil D, Gonzalez-Granja A, Barral P, Weber M, Dushek O, et al. The membrane skeleton controls diffusion dynamics and signaling through the B Cell Receptor. *Immunity.* (2010) 32:187–99. doi: 10.1016/j.immuni.2009.12.005
42. Depoil D, Fleire S, Treanor BL, Weber M, Harwood NE, Marchbank KL, et al. CD19 is essential for B cell activation by promoting B cell receptor-antigen microcluster formation in response to membrane-bound ligand. *Nat Immunol.* (2008) 9:63–72. doi: 10.1038/ni1547
43. Campa CC, Ciraolo E, Ghigo A, Germena G, Hirsch E. Crossroads of PI3K and Rac pathways. *Small GTPases.* (2015) 6:71–80. doi: 10.4161/21541248.2014.989789
44. Guo F, Debidda M, Yang L, Williams DA, Zheng Y. Genetic deletion of Rac1 GTPase reveals its critical role in actin stress fiber formation and focal adhesion complex assembly. *J Biol Chem.* (2006) 281:18652–9. doi: 10.1074/jbc.M603508200
45. Welch HCE, Coadwell WJ, Stephens LR, Hawkins PT. Phosphoinositide 3-kinase-dependent activation of Rac. *FEBS Lett.* (2003) 546:93–7. doi: 10.1016/S0014-5793(03)00454-X
46. Shulman Z, Gitlin AD, Targ S, Jankovic M, Pasqual G, Nussenzweig MC, et al. T follicular helper cell dynamics in germinal centers. *Science.* (2013) 341:673–7. doi: 10.1126/science.1241680
47. Gitlin AD, Shulman Z, Nussenzweig MC. Clonal selection in the germinal centre by regulated proliferation and hypermutation. *Nature.* (2014) 509:637–40. doi: 10.1038/nature13300
48. Shulman Z, Gitlin AD, Weinstein JS, Lainez B, Esplugues E, Flavell RA, et al. Dynamic signaling by T follicular helper cells during germinal center B cell selection. *Science.* (2014) 345:1058–62. doi: 10.1126/science.1257861
49. Gitlin AD, Mayer CT, Oliveira TY, Shulman Z, Jones MJK, Koren A, et al. HUMORAL IMMUNITY. T cell help controls the speed of the cell cycle in germinal center B cells. *Science.* (2015) 349:643–6. doi: 10.1126/science.aac4919
50. Kräutler NJ, Suan D, Butt D, Bourne K, Hermes JR, Chan TD, et al. Differentiation of germinal center B cells into plasma cells is initiated by high-affinity antigen and completed by Tfh cells. *J Exp Med.* (2017) 214:1259–67. doi: 10.1084/jem.20161533
51. Allen CDC, Ansel KM, Low C, Lesley R, Tamamura H, Fujii N, et al. Germinal center dark and light zone organization is mediated by CXCR4 and CXCR5. *Nat Immunol.* (2004) 5:943–52. doi: 10.1038/ni1100
52. Mesin L, Ersching J, Victora GD. Germinal center B cell dynamics. *Immunity.* (2016) 45:471–82. doi: 10.1016/j.immuni.2016.09.001
53. Phan TG, Grigorova I, Okada T, Cyster JG. Subcapsular encounter and complement-dependent transport of immune complexes by lymph node B cells. *Nat Immunol.* (2007) 8:992–1000. doi: 10.1038/ni1494
54. Batista FD, Neuberger MS. B cells extract and present immobilized antigen: implications for affinity discrimination. *EMBO J.* (2000) 19:513–20. doi: 10.1093/emboj/19.4.513
55. Xu Y, Harder KW, Huntington ND, Hibbs ML, Tarlinton DM. Lyn tyrosine kinase: Accentuating the positive and the negative. *Immunity.* (2005) 22:9–18. doi: 10.1016/j.immuni.2004.12.004
56. Sharma S, Orlowski G, Song W. Btk regulates B cell receptor-mediated antigen processing and presentation by controlling actin cytoskeleton dynamics in B cells. *J Immunol.* (2009) 182:329–39. doi: 10.4049/jimmunol.182.1.329
57. Fearon DT, Carroll MC. Regulation of B lymphocyte responses to foreign and self-antigens by the CD19/CD21 complex. *Annu Rev Immunol.* (2000) 18:393–422. doi: 10.1146/annurev.immunol.18.1.393
58. Tedder TF, Inaoki M, Sato S. The CD19-CD21 complex regulates signal transduction thresholds governing humoral immunity and autoimmunity. *Immunity.* (1997) 6:107–18. doi: 10.1016/S1074-7613(00)80418-5
59. Otero DC, Omori SA, Rickert RC. CD19-dependent Activation of Akt Kinase in B-lymphocytes. *J Biol Chem.* (2001) 276:1474–1478. doi: 10.1074/jbc.M003918200
60. Cannons JL, Zhao F, Schwartzberg PL. Ncking BCR-mediated PI3K activation. *EMBO Rep.* (2013) 14:852–3. doi: 10.1038/embor.2013.133
61. Jellusova J, Rickert RC. The PI3K pathway in B cell metabolism. *Crit Rev Biochem Mol Biol.* (2016) 51:359–378. doi: 10.1080/10409238.2016.1215288
62. Malhotra S, Kovats S, Zhang W, Coggeshall KM. B cell antigen receptor endocytosis and antigen presentation to T cells require Vav and dynamin. *J Biol Chem.* (2009) 284:24088–97. doi: 10.1074/jbc.M109.014209
63. Turner M, Billadeau DD. VAV proteins as signal integrators for multi-subunit immune-recognition receptors. *Nat Rev Immunol.* (2002) 2:476–86. doi: 10.1038/nri840
64. Allam A, Niiro H, Clark EA, Marshall AJ. The adaptor protein Bam32 regulates Rac1 activation and actin remodeling through a

phosphorylation-dependent mechanism. *J Biol Chem.* (2004) 279:39775–82. doi: 10.1074/jbc.M403367200

65. Podolanczuk A, Lazarus AH, Crow AR, Grossbard E, Bussel JB. Of mice and men: an open-label pilot study for treatment of immune thrombocytopenic purpura by an inhibitor of Syk. *Blood.* (2009) 113:3154–60. doi: 10.1182/blood-2008-07-166439
66. Okkenhaug K, Graupera M, Vanhaesebroeck B. Targeting PI3K in cancer: impact on tumor cells, their protective stroma, angiogenesis, and immunotherapy. *Cancer Discov.* (2016) 6:1090–105. doi: 10.1158/2159-8290.CD-16-0716

Conflict of Interest Statement: The authors declare that the research was conducted in the absence of any commercial or financial relationships that could be construed as a potential conflict of interest.

frontiers in Immunology

ORIGINAL RESEARCH
published: 14 May 2019
doi: 10.3389/fimmu.2019.01069

Mitochondrial Protein PINK1 Positively Regulates RLR Signaling

Jun Zhou[1,2*†], *Rui Yang*[3†], *Zhaoru Zhang*[1,2], *Qianru Liu*[1,2], *Yuanyuan Zhang*[4], *Qingqing Wang*[5] *and Hongbin Yuan*[3*]

[1] Department of Cell Biology, School of Basic Medical Sciences, Zhejiang University, Hangzhou, China, [2] The Key Laboratory of Reproductive Genetics, Ministry of Education, Zhejiang University, Hangzhou, China, [3] Department of Anesthesiology, Changzheng Hospital, Second Military Medical University, Shanghai, China, [4] The Children's Hospital, Zhejiang University School of Medicine, Hangzhou, China, [5] Institute of Immunology, Zhejiang University School of Medicine, Hangzhou, China

The serine/threonine kinase phosphatase and tensin homolog (PTEN)-induced putative kinase 1(PINK1) controls mitochondrial quality and plays a vital role in the pathogenesis of early-onset Parkinson's disease. However, whether PINK1 has functions in innate antiviral immunity is largely unknown. Here, we report that viral infection down regulates PINK1 expression in macrophages. PINK1 knockdown results in decreased cytokine production and attenuated IRF3 and NF-κB activation upon viral infection. PINK1 promotes the retinoic-acid-inducible gene I (RIG-I)-like receptors (RLR)-triggered immune responses in a kinase domain-dependent manner. Furthermore, PINK1 associates with TRAF3 via the kinase domain and inhibits Parkin-mediated TRAF3 K48-linked proteasomal degradation. In addition, PINK1 interacts with Yes-associated protein 1 (YAP1) upon viral infection and impairs YAP1/IRF3 complex formation. Collectively, our results demonstrate that PINK1 positively regulates RIG-I triggered innate immune responses by inhibiting TRAF3 degradation and relieving YAP-mediated inhibition of the cellular antiviral response.

Keywords: PINK, RLR, TRAF3, ubiquitination, YAP1, antiviral immune response, macrophages, IRF3

OPEN ACCESS

Edited by:
Thai Tran,
National University of Singapore, Singapore

Reviewed by:
Junji Xing,
Houston Methodist Research Institute, United States
Kushagra Bansal,
Harvard Medical School, United States

***Correspondence:**
Jun Zhou
zhjjwm300@zju.edu.cn
Hongbin Yuan
jfjczyy@163.com

[†]These authors have contributed equally to this work

Specialty section:
This article was submitted to Molecular Innate Immunity, a section of the journal Frontiers in Immunology

Received: *05 December 2018*
Accepted: *26 April 2019*
Published: *14 May 2019*

Citation:
Zhou J, Yang R, Zhang Z, Liu Q, Zhang Y, Wang Q and Yuan H (2019) Mitochondrial Protein PINK1 Positively Regulates RLR Signaling. Front. Immunol. 10:1069. doi: 10.3389/fimmu.2019.01069

INTRODUCTION

As the host's first line of defense, innate immunity detects, and fights against pathogen invasion. The recognition of viral infection by the innate immune system depends on germline-encoded pattern-recognition receptors, including TLRs (Toll-like receptors), RLRs (retinoic-acid-inducible gene I (RIG-I)-like receptors), Nod-like receptors, and DNA sensors (1, 2). TLRs (TLR3, TLR7/8, and TLR9) recognize virus-derived RNA and DNA in the endosome. The RLR members RIG-I and MDA5 (melanoma differentiation-associated gene 5) sense viral RNAs in the cytoplasm, whereas cGAS (cyclic GMP-AMP synthase) is responsible for the recognition of viral DNA in the cytoplasm (3, 4).

RIG-I, the most important RLR family member, recognizes viral RNA such as vesicular stomatitis virus (VSV), respiratory syncytial virus (RSV), and Sendai virus (SeV) and induces IFN-β production (5). After recognition of invading viruses, RIG-I recruits adaptors, including MAVS, TRAF3, and results in TRAF3 ubiquitination, which provides docking sites for the formation of the TBK1/IKKε complex. The activated complex subsequently phosphorylates the transcription

factors IRF3/IRF7 and induces the nuclear translocation of IRF3/IRF7 dimers to trigger type I IFNs and proinflammatory cytokine production (6). Aberrant RLR signaling is associated with autoimmune and/or inflammatory diseases such as systemic lupus erythematosus (3), chronic obstructive pulmonary disease (COPD) (7); hence, moderate activation of RLRs signaling is critical for efficient viral clearance without harmful immunopathology.

PINK1 [phosphatase and tensin homolog (PTEN)-induced putative kinase 1] is a serine/threonine kinase that is responsible for the pathogenesis of early-onset Parkinson's disease (PD) (8). PINK1 can act upstream of Parkin to remove damaged mitochondria via mitophagy (9). Aside from its role in neurodegeneration and mitophagy, PINK1 has multiple distinct functions in regulating cell metabolism, cancer development and inflammation (10). PINK1 can promote hepatic insulin resistance (IR) via JNK and ERK signaling in palmitate (PA)-treated HepG2 cells (11). PINK1 suppresses MDV (mitochondrial-derived vesicles) formation and MitAP (mitochondrial antigen presentation) provoked by inflammation (12). PINK1 has also been implicated in liver inflammation due to hepatitis B (HBV) or C virus (HCV) infection (13–15). In addition, a review discussed the neurological sequelae of infection by viruses known to induce parkinsonism, including influenza virus, Coxsackie, Japanese encephalitis B, and HIV viruses (16). Recent epidemiologic studies have revealed that patients with HCV infection might be at an increased risk of PD (17, 18). These data suggest that virus infection might be involved in the pathogenesis of PD. However, the role of PINK1 in antiviral immunity has not been reported.

Here, we report that viral infection downregulates PINK1 expression in macrophages. PINK1 enhances RLR-triggered type I interferon and proinflammatory cytokine production in a kinase domain dependent manner. PINK1 associates with TRAF3, inhibiting TRAF3 proteasomal degradation after conjugation to K48-linked ubiquitin by Parkin. Furthermore, PINK1 inhibits the interaction between Yes-associated protein 1 (YAP1) and IRF3, leading to increased IRF3 activation. Our data demonstrate that PINK1 functions as a positive regulator of the antiviral immune response by regulating TRAF3 degradation and YAP1/IRF3 complex formation.

MATERIALS AND METHODS

Cells and Virus Infection

RAW264.7 macrophages and HEK293T cells were obtained from the American Type Culture Collection (ATCC, Rockville, MD, USA) and maintained in DMEM supplemented with 10% fetal bovine serum (FBS). For stable cell lines, RAW264.7 macrophages were transfected with jetPRIME reagent (Polyplus) according to manufacturer's instructions, and then were selected with puromycin (8 μg/ml) and pooled for further experiments. For mouse peritoneal macrophages, C57BL/6 mice (6–8 weeks old) were intraperitoneally injected with thioglycollate (Sigma). Three days later, abdominal cells were collected and cultured in RPMI-1640 medium with 10% FBS, then adhered peritoneal macrophages were subjected for successive experiments. Mice were housed in pathogen-free conditions. All animal experiments were approved by the Animal Review Committee of Zhejiang University School of Medicine and were in compliance with institutional guidelines.

Primary macrophages were infected with RSV (kindly provided by Dr. Qingqing Wang, Zhejiang University School of Medicine, MOI = 10), VSV (MOI = 1), and herpes simplex virus (HSV) (MOI = 10) (kindly provided by Dr. Xiaojian Wang, Zhejiang University School of Medicine). HEK293T cells were infected with VSV (MOI = 0.1). MOIs were selected as described previously (19). The cells or supernatants were harvested for immunoblotting assays or ELISA. All experiments using viruses were conducted in a biosecurity level 2 laboratory approved by School of Basic Medical Sciences, Zhejiang University.

Plasmids, Transfection, and RNA Interference

Plasmids expressing PINK1 (RC206970), Parkin (RC221147), and TRAF3 (RC201106) were purchased from Origene Technologies (Rockville, MD, USA). The vector of these plasmids is pCMV6 Entry with C-terminal Myc/DDK (Flag) tags. Mutants PINK1ΔKD and PINK1 L347P were amplified by PCR from full-length PINK1 cDNA using a MutanBest kit (TaKaRa). Plasmids expressing HA-IRF3, GFP-TRAF3, HA-Ub and Flag-YAP1 were provided by Dr. Huazhang An (Second Military Medical University, Shanghai). The plasmids were transfected into RAW264.7 and HEK293T cells using jetPEI (Polyplus, Illkirch, France). PINK1- specific siRNA was transfected into primary macrophages using Lipofectamine RNAiMAX (Thermo Fisher Scientific, Waltham, MA, USA) according to the standard protocol. PINK1 siRNA (5′- CCA GGC GGU AAU UGA CUA TT-3′, 5′- UAG UCA AUU ACC GCA CUG GTT-3′) was from GenePharma (Shanghai, China).

Generation of PINK1 Knockout Cells

CRISP/Cas9 guide RNA targeting sequence for mouse Pink1 was designed using the MIT online tool (http://crisp.mit.edu). The CRISPR plasmid pEP-330x (kindly provided by Dr. Xiaojian Wang, Zhejiang University School of Medicine) contains expression cassettes of Cas9 and puromycin resistant gene. gRNA targeting the exons of PINK1 was GAGGTCACTGCTCCAGCGAG and inserted into the pEP-330x vector, and then co-transfected into RAW264.7 cells using jetPEI for 48 h. Then puromycin (8 μg/ml) (Sigma-Aldrich) was used for selection in RAW264.7 cells. Individual clones were isolated by limiting dilution cloning, and knockout of PINK1 was confirmed via western blotting.

Antibodies

Antibodies against phosphorylated and total IRF3, IKKε, TBK1, NF-κB p65, ERK, JNK, and p38 were purchased from Cell Signaling Technology (Danvers, MA, USA). Anti-TRAF3, anti-β-actin, and HRP-conjugated secondary antibodies were from Santa Cruz. Anti-Myc, anti-Flag, anti-HA, and anti-GFP were from Origene. Anti-PINK1, anti-Parkin, and anti-YAP1 were from Abcam Biotechnology (Cambridge, UK). Anti-K48-ubiquitin and anti-K63-ubiquitin were from Millipore (Kenilworth, USA).

RNA Isolation and Real-Time Quantitative PCR (Q-PCR)

Total RNA was isolated from cells with TRIzol reagent (Takara) following the manufacturer's directions. cDNA was generated from total RNA using reverse transcriptase (Takara). SYBR RT-PCR kits (Takara) were used for quantitative real-time PCR analysis as described (20). The primers used for mRNA analysis are listed in **Table 1**. Gapdh and β-actin were used as housekeeping genes for human and mouse samples, respectively. Quantitative normalization of target mRNA expression was performed for each sample using housekeeping gene expression as an internal control.

ELISA

Cell supernatants were collected and mouse Il-6 (eBioscience, Thermo Fisher Scientific) and IFN-β (Biolegend, San Diego, CA) levels were determined according to manufacturer's instructions. The ELISA plates were read on a microplate reader. The results were calculated as the difference between the absorbance at 570 nm and the absorbance at 450 nm. Quantification was performed according to the standard curve as described in the manufacturer's instructions.

Immunoblotting and Immunoprecipitation

Cells were lysed using cell lysis buffer containing protease inhibitor "cocktail" (Cell Signaling Technology). The protein concentrations in the extracts were measured using the BCA assay (Thermo Fisher Scientific). For immunoblotting, equal amounts of extracts were separated by SDS-PAGE, transferred onto polyvinylidene fluoride membranes (Millipore), and then probed with the indicated antibodies. For immunoprecipitation, the supernatants were incubated overnight with specific antibodies at 4°C overnight, then incubated with protein A/G Sepharose (sc-2003, Santa Cruz) for another 2 h. The beads were washed four times with cold PBS containing 0.05% Tween-20, and immunoprecipitates were eluted with loading buffer. β-actin levels in total cell lysates were measured to show equal protein loading.

TABLE 1 | Primers for Real-time quantitative PCR.

Human pink1 forward primer	5′- CAAGAGAGGTCCCAAGCAAC−3′
Human pink1 reverse primer	5′- GGCAGCACATCAGGGTAGTC−3′
Human gapdh forward primer	5′-ATTCCACCCATGGCAAATTC-3′
Human gapdh reverse primer	5′-GGATCTCGCTCCTGCAAGATG-3′
Mouse pink1 forward primer	5′- GAGCAGACTCCCAGTTCTCG−3′
Mouse pink1 reverse primer	5′-GTCCCACTCCACAAGGATGT−3′
Mouse actin forward primer	5′- AGTGTGACGTTGACATCCGT-3′
Mouse actin reverse primer	5′-GCAGCTCAGTAACAGTCCGC-3′
Mouse il-6 forward primer	5′-TAGTCCTTCCTACCCCAATTTCC-3′
Mouse il-6 reverse primer	5′-TTGGTCCTTAGCCACTCCTTC-3′
Mouse IFN-β forward primer	5′- ATGAGTGGTGGTTGCAGGC−3′
Mouse IFN-β reverse primer	5′- TGACCTTTCAAATGCAGTAGATTCA−3′
VSV-G forward primer	5′- ACGGCGTACTTCCAGATGG-3′
VSV-G reverse primer	5′- CTCGGTTCAAGATCCAGGT-3′

Immunofluorescence Staining

HEK293T cells grown on coverslips were infected or uninfected with VSV at 4 h. To label mitochondria, 100 nM MitoTracker™ Red CMXRos (Invitrogen) was added to the medium for 25 min at 37°C. Cells were washed with PBS and fixed with 2% paraformaldehyde, permeabilized with 0.1% Triton X-100, blocked with 5% BSA, and stained with mouse anti-PINK1 and rabbit anti-TRAF3, anti-YAP1 antibody, followed stained with Alexa Fluor 488 anti-mouse and Alexa Fluor 594 anti-rabbit secondary antibody, to detect co-localization of PINK1 with TRAF3, YAP1, or Mitochondria. The co-localization was detected with Zeiss LSM 880 with AiryScan.

Human Peripheral Blood Samples

A total of 38 peripheral blood samples of bronchiolitis with RSV infection were collected from Children's Hospital, Zhejiang University School of Medicine, China. An additional 21 control blood samples were obtained from healthy children. RSV infection was confirmed by RSV antigen tests of nasopharyngeal aspirates. Other antigens (influenza virus, parainfluenza virus, metapneumovirus, and adenovirus antigens) or microbiological tests, including blood cultures, protein-purified derivative test, and serology for Chlamydia pneumonia, Mycoplasma pneumonia, and Legionella pneumophila, were performed to exclude other common respiratory tract infection and tuberculosis. Detailed patient information is shown in **Tables 2**, **3**. The ethics committee of Children's Hospital, Zhejiang University School of Medicine approved the study. Written informed consent was obtained from at least one guardian for each patient before enrollment.

Peripheral blood mononuclear cells (PBMCs) were isolated by Ficoll density gradient centrifugation (Sigma) following the manufacturer's instructions, stored at −80°C as cell pellets until RNA isolation was performed. The data were analyzed anonymously.

Statistical Analysis

Statistical significance between groups was determined using two-tailed Student's *t*-test and two-way ANOVA. *P*-values of <0.05 were considered statistically significant.

TABLE 2 | Basic information of human peripheral blood samples about healthy control and pediatric patients with RSV infection from Children's Hospital.

	Normal control $n = 21$	RSV patients $n = 38$
AGE(MONTHS)		
≤3	10	26
3–6	6	7
≥6	5	5
GENDER		
Male	14	28
Female	7	10

Twenty-one control blood samples were obtained from healthy children. A total of 38 peripheral blood samples of bronchiolitis with RSV infection were collected from Children's Hospital.

TABLE 3 | The detailed information of RSV-infected patients.

Number	Gender	Age	Grade of infection	RSV antigen test	Clinical symptom		
					Cough	Short of breath	Fever
1	Male	1M24D	Mild	+	+	+	−
2	Female	2M10D	Mild	+	+	+	−
3	Female	6M13D	Mild	+	+	+	−
4	Female	2M26D	Mild	+	+	+	−
5	Female	3M19D	Mild	+	+	+	−
6	Male	6M8D	Mild	+	+	+	+
7	Female	3M5D	Mild	+	+	-	−
8	Male	1M11D	Mild	+	+	+	−
9	Male	4M18D	Mild	+	+	+	−
10	Male	3M3D	Mild	+	+	+	−
11	Male	2M3D	Mild	+	+	+	−
12	Male	8M17D	Mild	+	+	+	−
13	Male	9M9D	Mild	+	+	+	−
14	Male	2M11D	Mild	+	+	+	−
15	Male	9M8D	Mild	+	+	+	−
16	Male	2M8D	Mild	+	+	+	−
17	Male	2M21D	Mild	+	+	+	−
18	Male	1M4D	Mild	+	+	+	−
19	Female	1M8D	Mild	+	+	-	−
20	Male	4M2D	Mild	+	+	+	−
21	Female	1M28D	Moderate	+	+	+	−
22	Male	2M20D	Moderate	+	+	+	−
23	Male	2M2D	Moderate	+	+	+	+
24	Male	2M5D	Moderate	+	+	+	−
25	Male	2M7D	Moderate	+	+	+	−
26	Male	2M29D	Moderate	+	+	+	−
27	Male	1M4D	Moderate	+	+	+	−
28	Male	4M4D	Moderate	+	+	+	−
29	Female	4M21D	Moderate	+	+	+	−
30	Male	2M29D	Moderate	+	+	+	−
31	Male	1M10D	Moderate	+	+	+	−
32	Male	1M20D	Moderate	+	+	+	−
33	Female	1M23D	Moderate	+	+	+	−
34	Male	1M14D	Moderate	+	+	+	−
35	Male	1M14D	Moderate	+	+	+	−
36	Male	1M4D	Severe	+	+	+	−
37	Male	2M24D	Severe	+	+	+	+
38	Female	1M21D	Severe	+	+	+	+

Additional information for all patients:
In the age group, "Y" is year, "M" is month, "D" is day.
The tests for other viral antigens are negative, including influenza virus, parainfluenza virus, metapneumovirus, and adenovirus.
The tests for other respiratory tract infection, including tuberculosis, Chlamydia pneumoniae, Mycoplasma pneumonia, and Legionella pneumophila are negative.

RESULTS

RNA and DNA Viral Infection Down Regulates PINK1 Expression in Macrophages

To investigate whether PINK1 is involved in host antiviral innate immune response, we detected PINK1 expression in primary mouse peritoneal macrophages (PMs) infected with RNA viruses, including VSV and RSV, and DNA virus, HSV. As shown in **Figure 1A**, PINK1 mRNA expression was down-regulated after VSV, RSV, or HSV infection in PMs. Consistent with the mRNA result, Western blotting showed that PINK1 protein expression was attenuated upon VSV infection (**Figure 1B**). Moreover, PINK1 expression was decreased in RAW264.7 macrophage cell line (**Figure 1C**). We further recruited a cohort of peripheral blood samples from 38 pediatric patients with RSV infection and

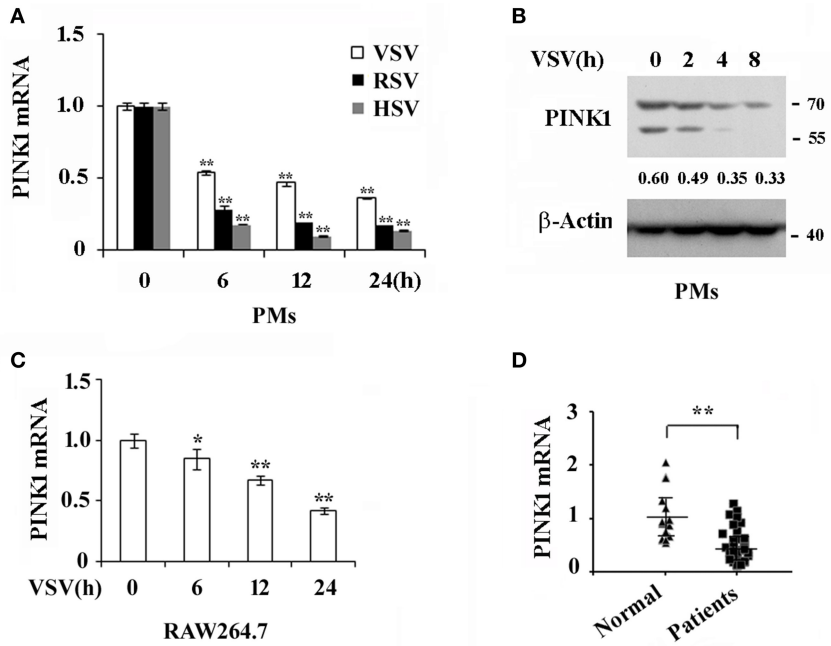

FIGURE 1 | Virus infection down regulates PINK1 expression in macrophages. **(A)** Q-PCR analysis of PINK1 mRNA expression in mouse peritoneal macrophages (PMs) (3×10^5) infected with VSV (MOI = 1), RSV (MOI = 10), or HSV (MOI = 10), respectively, for indicated hours. **(B)** Immunoblot analysis of PINK1 protein expression in mouse peritoneal macrophages (3×10^6) infected with VSV for indicated hours. Numbers below lanes (top) indicate densitometry of the presented protein relative to β-Actin expression in that same lane (below). **(C)** Q-PCR analysis of PINK1 mRNA expression in RAW264.7 cells (1×10^5) infected with VSV for indicated hours. **(D)** Q-PCR analysis of PINK1 mRNA expression in peripheral blood mononuclear cells (PBMCs) of 38 pediatric patients with RSV infection and 21 healthy children. Data are mean ± SD. Similar results were obtained in three independent experiments.*$p < 0.05$, **$p < 0.01$, compared with control.

21 healthy control children from Children's Hospital of Zhejiang University School of Medicine. Downregulated PINK1 mRNA expression was also observed in peripheral blood mononuclear cells (PBMCs) from patients compared with that in the healthy group (**Figure 1D**). Taken together, these data indicated that PINK1 expression might be correlated with the host antiviral immune response.

PINK1 Knockdown Inhibits Virus-Triggered Cytokines Production in Macrophages

To investigate the role and functional significance of PINK1 in the host antiviral innate immune response, we silenced PINK1 expression with small interfering RNA in mouse peritoneal macrophages, followed by infecting with different viruses. Western blotting confirmed that PINK1 expression was significantly downregulated in macrophages transfected with PINK1-specific siRNA (**Figure 2A**). QPCR and ELISA analysis revealed that IFN-β expression was significantly decreased after VSV infection. Proinflammatory cytokine IL-6 expression was also downregulated in PINK1-knockdown macrophages infected with VSV (**Figure 2B**). Infection with different VSV (MOI) doses in macrophages induced similar decreases in IFN-β expression (**Figure 2C**). In addition, downregulation of IFN-β and IL-6 expression in PINK1-silenced macrophages was validated by QPCR and ELISA analysis in macrophages infected with another RNA virus, RSV, and a DNA virus, HSV (**Figures 2D,E**). Furthermore, infection with VSV in PINK1 knockout macrophages showed similar statistically significant decreases in IFN-β and IL-6 expression (**Figure 2F**). These data demonstrated that PINK1 knockdown suppressed virus-induced type I interferon and proinflammatory cytokine production. We therefore focused on the regulatory role of PINK1 in RNA virus-induced innate immune response.

PINK1 Promotes RLR-Triggered IRF3 and NF-κB Activation

Upon RNA virus infection, transcription factors such as IRF3, NF-κB, and ATF2-c-Jun are activated and recruited to initiate type I interferon and proinflammatory cytokine transcription (21, 22). To elucidate the underlying mechanism by which PINK1 mediates RNA virus-induced cytokines production, we observed the effect of PINK1 knockdown and overexpression on IRF3 and NF-κB activation in macrophages. PINK1-specific siRNA significantly inhibited VSV-induced phosphorylation of IRF3, NF-κB subunit p65, and upstream IKKε in peritoneal macrophages. TBK1 phosphorylation was not affected by PINK1 knockdown. However, downregulation of p65 and IKKε might partly result from decreased p65 and IKKε total protein expression (**Figure 3A**). Consistent with these results, IRF3, p65, and IKKε phosphorylation was enhanced in PINK1-overexpressing RAW264.7 cells compared with control cells (**Figure 3B**). The

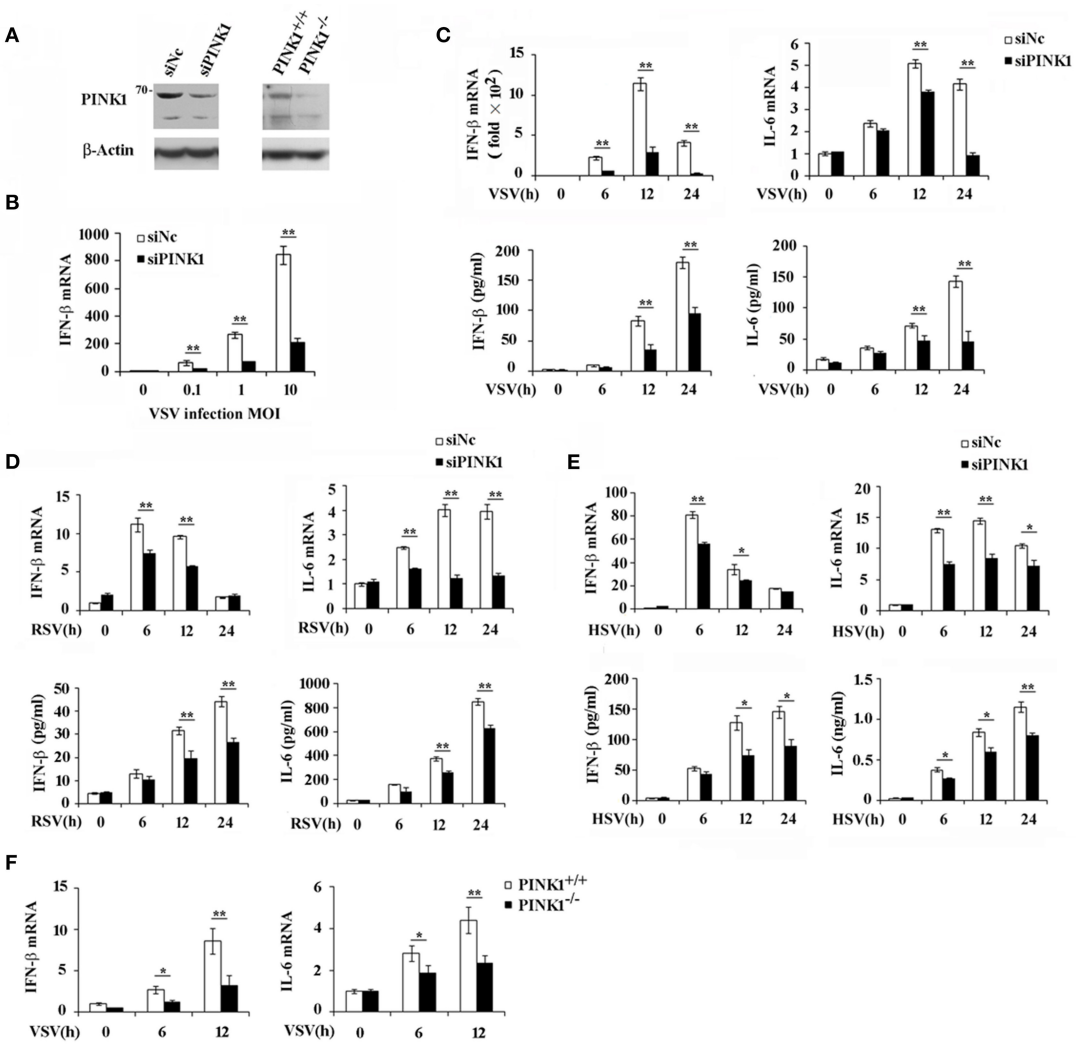

FIGURE 2 | PINK1 knockdown or knockout suppresses virus-induced type I interferon and proinflammatory cytokine production. Mouse peritoneal macrophages (PMs) were transfected with 30 nM scrambled negative control siRNA (siNC) or PINK1 siRNA (siPINK1) for 48 h. PINK1 knockout RAW264.7 macrophages (PINK1$^{-/-}$) were generated using CRISPR/Cas9 gene-editing system. **(A)** Immunoblot analysis of PINK1 expression level in PMs with PINK1 knockdown, or RAW264.7 cells with PINK1 knockout. **(B)** qPCR analysis of IFN-β mRNA expression in PMs infected for indicated MOIs with VSV for 6 h. **(C–E)** qPCR and ELISA analysis of IFN-β and IL-6 levels of in PMs infected with VSV, RSV, or HSV, respectively, for indicated hours. **(F)** qPCR analysis of IFN-β and IL-6 levels in wild type (PINK1$^{+/+}$) and PINK1 knockout cells (PINK1$^{-/-}$) RAW264.7 cells infected with VSV for indicated hours. Data are mean ± SD and are representative of three independent results. *$p < 0.05$, **$p < 0.01$, compared with control.

mitogen-activated protein kinases JNK and p38 mediate activation of the ATF2-c-Jun heteodimer in the virus-induced cytokines response (21). Pink1 knockdown slightly inhibited the VSV-induced MAPK activation. However, MAPK phosphorylation except ERK was not significantly affected by PINK1 overexpression in macrophages (**Figures 3A,B**). These data demonstrated that PINK1 might mediate RLR-triggered immune response by regulating molecules upstream of IRF3 and NF-κB.

PINK1 Associates With TRAF3 and IRF3 After RLR Activation

To further investigate the underlying mechanisms by which PINK1 positively regulates RIG-I triggered signaling, we investigated potential PINK1 target proteins in the RIG-I signaling pathway in mouse peritoneal macrophages. The primary upstream signal adaptors of RIG-I signaling, such as RIG-I, MAVS, TRAF3, TBK1, IRF3, were detected in immune complexes precipitated with an anti-PINK1 antibody. PINK1 physically interacted with endogenous TRAF3 in resting primary mouse peritoneal macrophages, and this interaction was enhanced upon VSV infection, whereas the interaction between PINK1 and IRF3 was only detected after VSV infection. In addition, the association of PINK1 with Parkin, an E3 ubiquitin-ligase, was detected in both resting and stimulating macrophages. However, PINK1 did not detectably associate with RIG-I, MAVS, or TBK1 (**Figure 4A**). We further detected the interaction between PINK1 and TRAF3 or IRF3

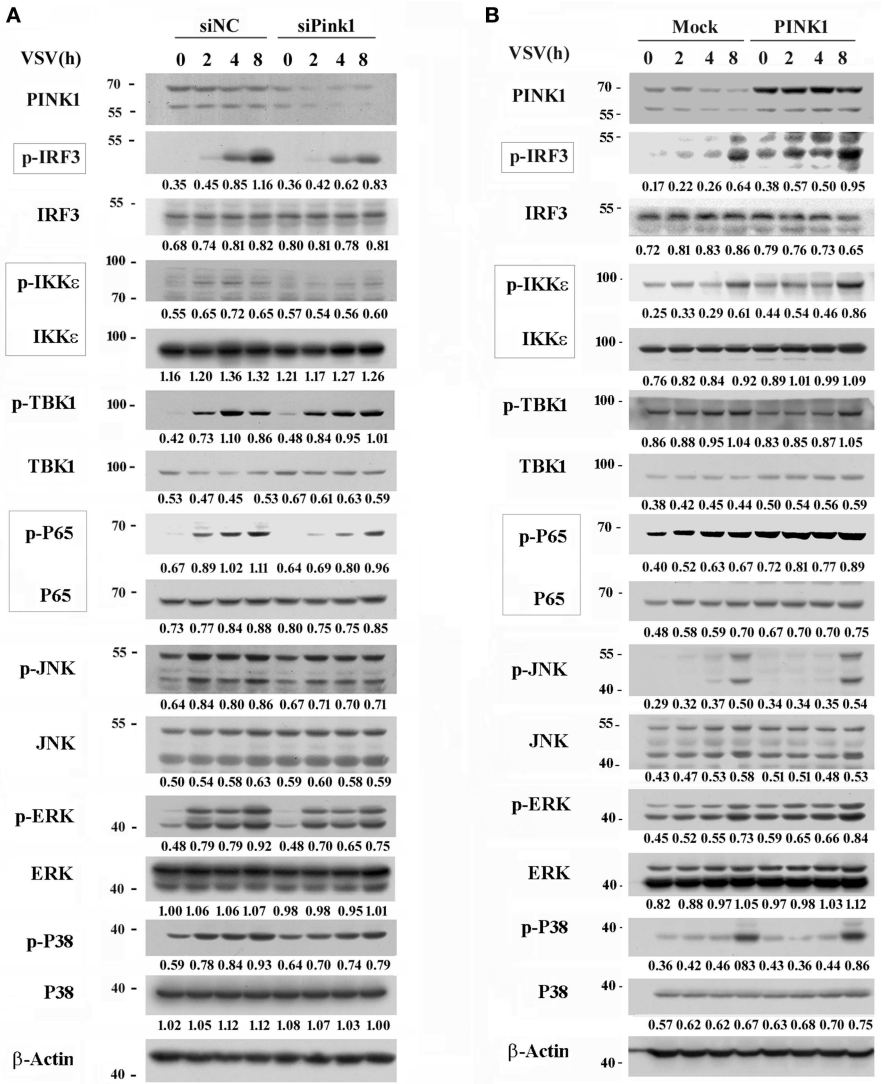

FIGURE 3 | PINK1 promotes RLR-triggered IRF3 and NF-κB activation in macrophages. Mouse peritoneal macrophages transfected with 30 nM scrambled negative control siRNA (siNC) or PINK1 siRNA **(A)**, or RAW264.7 cells transfected with plasmids encoding Myc-PINK1 **(B)**, were infected with VSV for indicated hours. Phosphorylated or total proteins in lysates were detected by western blot. Numbers below lanes (top) indicate densitometry of the presented protein relative to β-Actin expression in that same lane (below). Data are representative of three independent experiments.

in HEK293 cells. Consistent with the result in macrophages, exogenously expressed Myc-PINK1 efficiently interacted with Flag-TRAF3 or HA-IRF3 (**Figures 4B,C**). The co-localization of PINK1 and TRAF3 was observed in the cytosol in both VSV uninfected or infected HEK293T cells. Furthermore, subcellular co-localization analysis showed that PINK1 colocalized with the motichondrial marker (MitoTracker). Additionally, viral infection had no significant effect on the co-localization of PINK1 and mitochondria (**Figure 4D**). Collectively, these results indicated that PINK1 regulated RLR-triggered IRF3 and NF-κB activation possibly by targeting TRAF3 and IRF3, and PINK1 colocalized with TARF3 in the cytosol mitochondria.

PINK1 Promotes RLR-Triggered Immune Response via Kinase Domain Dependent Manner

PINK1 contains an N-terminal mitochondrial targeting sequence (MTS), a transmembrane domain (TMD), and a central highly conserved serine-threonine kinase domain (KD). To determine whether PINK1 interacts with TRAF3 and promotes RLR-triggered immune response via its kinase domain, we constructed two mutations: PINK1ΔKD, which lacks kinase domain and PINK1 L347P, which is reported to exhibit low protein stability and reduced kinase activity in cells (23, 24). Binding analysis revealed that both PINK1 wild type (WT) and PINK1 L347P interacted with TRAF3

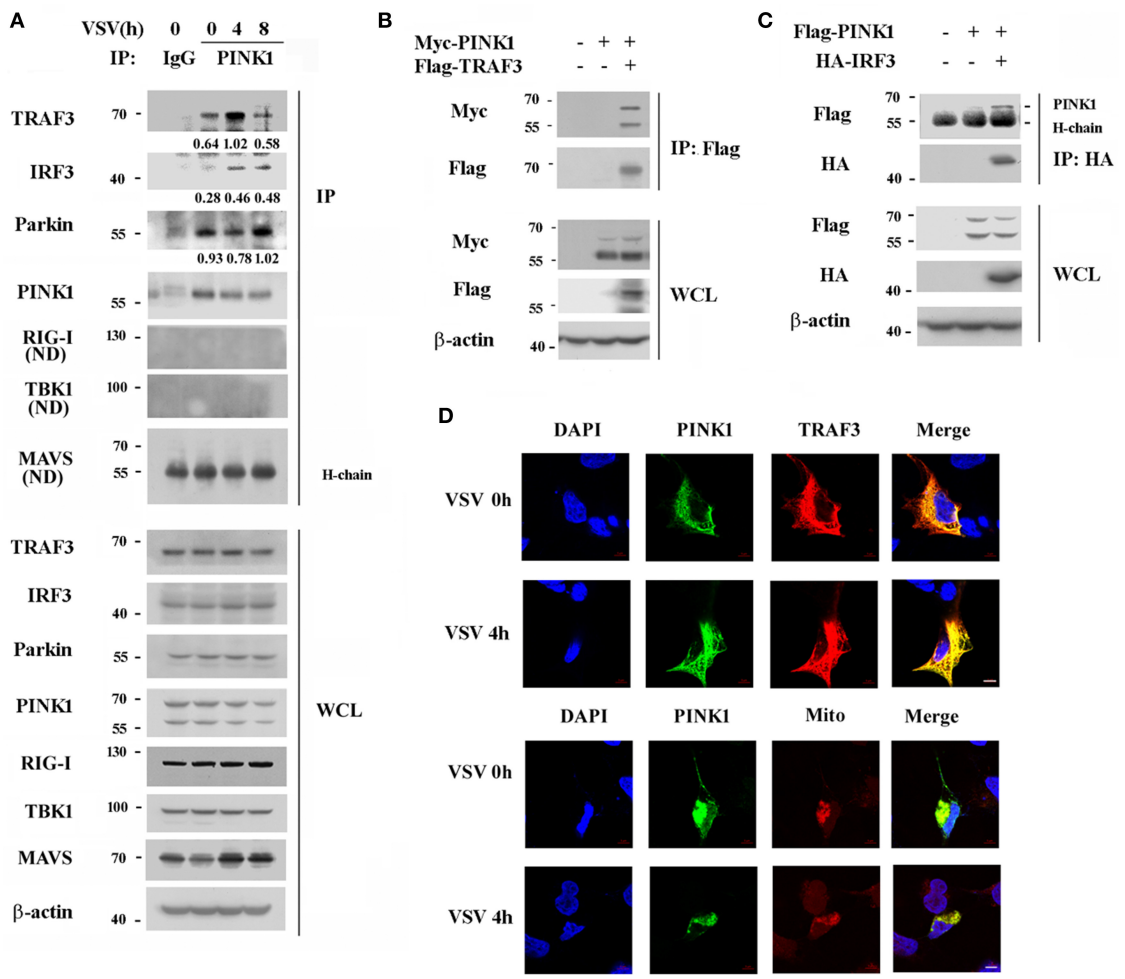

FIGURE 4 | PINK1 interacts with TRAF3 and IRF3 upon VSV infection. **(A)** Mouse peritoneal macrophages were infected with VSV for indicated hours. Immunoblot analysis of endogenous TRAF3, IRF3, Parkin, RIG-I, TBK1, and MAVS immunoprecipitated with antibody to PINK1. IgG was as control. Numbers between two blots indicate densitometry of TRAF3, IRF3, or Parkin relative to that of PINK1 in immunoprecipitates. **(B,C)** HEK293T cells were transfected with PINK1 expressing plasmid together with Flag-TRAF3 or HA-IRF3 plasmid. Cells were lysated 24 h after transfection for immunoblot analysis of indicated proteins immunoprecipitated with antibody to Flag **(B)** or HA **(C)** tag. **(D)** Confocal microscopy of HEK293T co-transfected with Myc-PINK1 and Flag-TRAF3 plasmids followed by VSV infection for 4 h. MitoTracker (Mito) was used to probe the mitochondrion (red). DAPI served as a marker of nuclei (blue). Scale bar, 5 μm. Data are representative of three independent experiments.

in HEK293T cells in a VSV-infection independent manner, whereas the kinase domain-deleted PINK1ΔKD mutant did not (**Figure 5A**). PINK1(c-tagged) WT plasmid shows an intact band of full length protein at about 70 kDa and a major degradation product at about 60 kDa. L347P mutation mainly shows degradation band (23). PINK1 WT stable RAW264.7 cells mainly express 70 kDa band, whereas L347P mutation stable cells express much more 60 kDa degradation band (**Figure 5B**). Furthermore, the antiviral function dependent on the induced expression of type I interferon and proinflammatory cytokine by PINK1 was abolished in both PINK1-mutated cells (**Figures 5B,C**).Taken together, these data suggested that PINK1 promoted RLR-triggered immune response in a kinase domain-dependent manner.

PINK1 Inhibits Parkin-Mediated K48-Linked TRAF3 Ubiquitination

Ubiquitination is a versatile posttranslational modification that plays important roles in antiviral immune response. TRAF3 is reported to be modified with a poly-ubiquitin chain to provide a scaffold for adaptor complex formation in RIG-I signaling (25, 26). PINK1 plays neuroprotective roles against dysfunctional mitochondria by recruiting Parkin, a cytosolic E3 ubiquitin ligase (27). Based on the interaction of PINK1 with TRAF3 and Parkin, we analyzed the effect of PINK1 on TRAF3 expression and ubiquitination. We detected the effect of PINK1 expression on TRAF3 protein expression in response to VSV infection. PINK1 knockdown resulted in lower TRAF3 expression in mouse peritoneal macrophages following VSV infection (**Figure 6A**). Consistent with the knockdown results, PINK1 overexpression

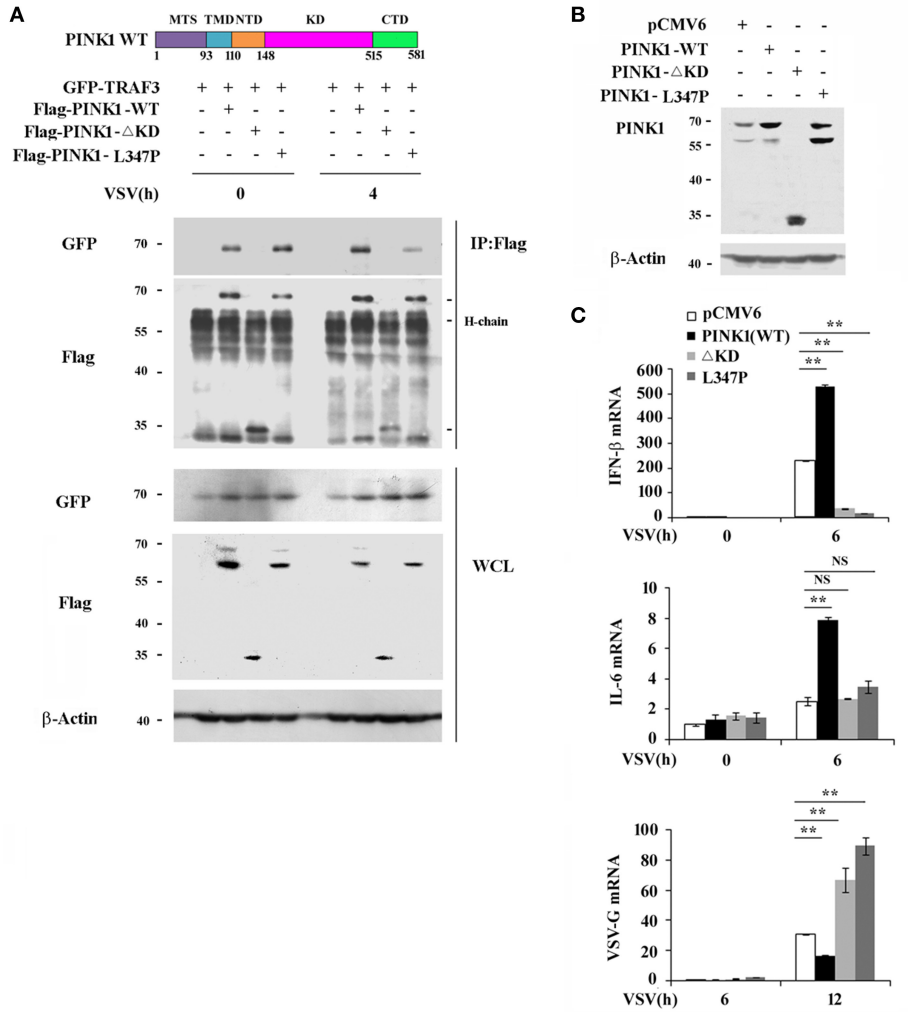

FIGURE 5 | PINK1 promotes RLR-triggered immune response via kinase domain dependent manner. **(A)** Immunoblot analysis of HEK293T cells that cotransfected with GFP-TRAF3 plus Flag-PINK1, Flag-PINK1 mutants vectors followed by VSV infection for 4 h, then immunoprecipitated with antibody to Flag tag. **(B)** Immunoblot analysis of RAW264.7 cells stably overexpressed with empty vector or vector encoding PINK1 and its mutants. **(C)** qPCR analysis of IFN-β, IL-6, and VSV-G mRNA in stably transfected RAW264.7 cells expression of PINK1 variants, infected with VSV for indicated times. Data are representative of three independent experiments. $^{**}p < 0.01$.

yielded higher basal TRAF3 expression levels and increased TRAF3 protein expression in RAW264.7 macrophages after VSV infection (**Figure 6B**). Considering that PINK1 interacts with Parkin in a VSV infection-independent manner in macrophages (**Figure 4A**), we investigated whether PINK1 regulates TRAF3 expression via ubiquitination. Compared with transfection using empty vector, Parkin overexpression increased the K48-linked ubiquitination of TRAF3 in both resting and VSV-infected HEK293 cells. However, PINK1 overexpression caused substantial loss of K48 ubiquitination in a dose-dependent manner. Parkin did not affect K63-linked ubiquitination (**Figure 6C**). At the same time, the presence of PINK1 downregulated Parkin expression (**Figure 6C**). These results suggested that PINK1 regulated TRAF3 protein levels through K48-linked proteasomal degradation, likely due to reduced Parkin expression.

PINK1 Inhibits the Interaction of YAP1 With IRF3

PINK1 is reported to be a positive regulator of cell cycle progression (28), while YAP1 is a transcriptional activator of the Hippo signaling pathway, which promotes cell growth and inhibits apoptosis (29). Recently, YAP1 was identified as a negative regulator of innate immunity by interacting with IRF3 to impair dimmer formation and nuclear translocation after viral infection (30). This finding led us to investigate whether PINK1 regulates the RIG-I pathway via YAP1 upon RNA virus infection. PINK1 interacted with endogenous YAP1 in resting macrophage, and the association was significantly increased by VSV infection for 4 h (**Figure 7A**). Immunoflurescence analysis showed that PINK1 colocalized with YAP1 in both resting and VSV infected HEK293T cells (**Figure 7B**). Further study revealed that PINK1 did not interfere with the interaction between YAP1 and IRF3

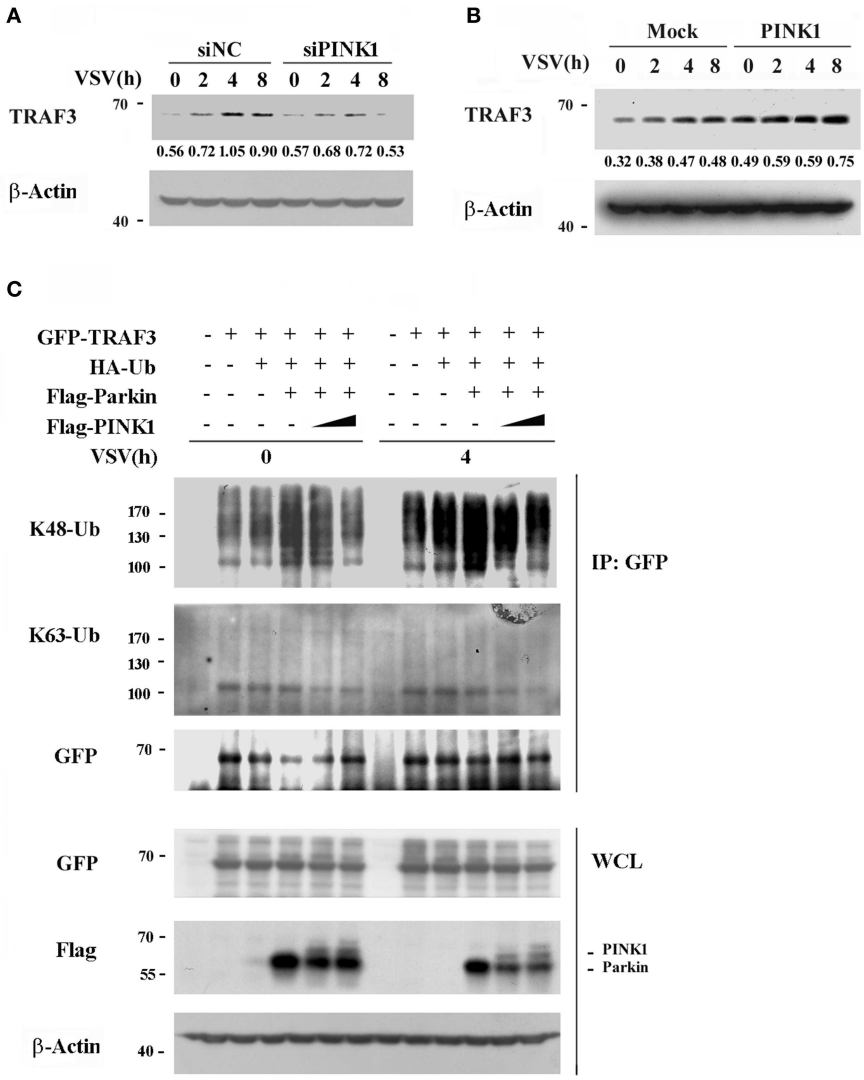

FIGURE 6 | PINK1 inhibits TRAF3 degradation. Mouse peritoneal macrophages transfected with scrambled negative control siRNA (siNC) or PINK1 specific siRNA (30 nM) **(A)**, or RAW264.7 cells transfected with PINK1 plasmid **(B)**, were infected with VSV for indicated hours. TRAF3 proteins in lysates were detected by western blot. Numbers below lanes (top) indicate densitometry of the presented protein relative to β-Actin expression in that same lane (below). **(C)** HEK293T cells were transfected with GFP-TRAF3, HA-Ub, Flag-Parkin, and varying doses of Flag-PINK1 (0, 0.5, and 1 μg) and infected with VSV for 4 h. Cells were treated with MG132 (10 uM) and harvested for immunoblot analysis of K48-Ub and K63-Ub immunoprecipitated with antibody to GFP tag. Data are representative of three independent experiments.

in resting HEK293 cells. The exogenous YAP1/IRF3 complex was more easily detected in HEK293 cells 6 h after infection with VSV. However, the association was almost undetectable in cells overexpressing PINK1 (**Figure 7C**). In addition, PINK1 knockdown only affected YAP1 phosphorylation at Ser127 after VSV infection for 8 h (**Figure 7D**). These findings demonstrated that PINK1 positively regulated RIG-I signaling at least partly by impairing the interaction of YAP1 with IRF3 and liberating IRF3 from YAP1-mediated inhibition.

DISCUSSION

Mutations in PINK1 and Parkin are the two most common causes of early-onset, recessively inherited PD (8, 31). Immune dysregulation, including the upregulation of inflammatory gene expression, has long been considered a hallmark of PD. Numerous viruses can enter the nervous system and induce a variety of encephalopathies, including parkinsonism (16). However, the precise role of PINK1 in antiviral innate immune responses, as well as its crosstalk with the TLR, RLR signaling pathway is poorly understood. In the present study, we have shown that PINK1 positively regulates the RLR-triggered antiviral immune response by inhibiting TRAF3 degradation and YAP1/IRF3 complex formation (**Figure 8**). To our knowledge, this is the first report to link PINK1 and RLR signaling.

Viruses use different strategies to escape host antiviral immunity and support persistent viral infection and spread (32). Some IAV (Influenza A virus) strains control innate antiviral

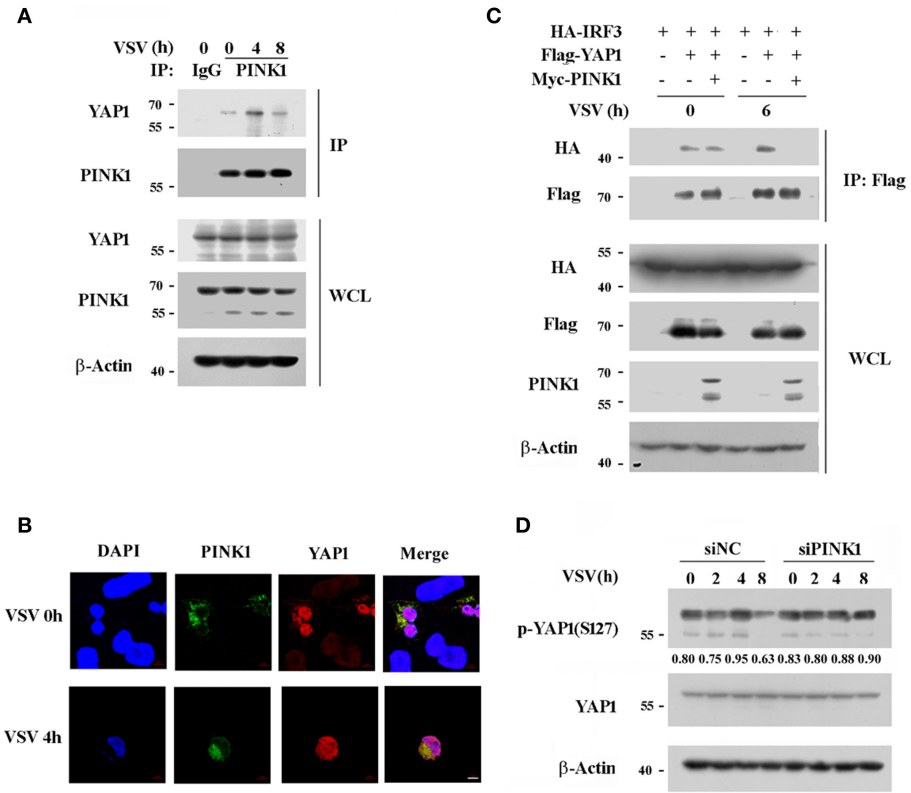

FIGURE 7 | PINK1 associates with YAP1 and inhibits the interaction of YAP1 with IRF3. **(A)** Mouse peritoneal macrophages were infected with VSV for indicated hours. Immunoblot analysis of endogenous YAP1 immunoprecipitated with antibody to PINK1. IgG was as control. **(B)** Confocal microscopy of HEK293T cells that co-transfected with Myc-PINK1 and Flag-YAP1 plasmids followed by VSV infection for 4 h. Scale bar, 5 μm. **(C)** HEK293T cells were transfected for 24 h with plasmids encoding HA-IRF3, Flag-YAP1, and Myc-PINK1. Immunoblot analysis of indicated proteins immunoprecipitated with antibody to Flag tag. **(D)** Mouse peritoneal macrophages transfected with scrambled negative control siRNA (siNC) or PINK1 specific siRNA (30 nM) were infected with VSV for indicated hours. Phosphorylated or total proteins of YAP1 in lysates were detected by western blot. Similar results were obtained in three independent experiments.

defense by binding to Riplet and inhibiting Lys63-linked RIG-I polyubiquitylation by NS1 protein (33). An epidemic strain of DENV (Dengue virus) isolated in Puerto Rico has been shown to sustain RIG-I signaling by binding to TRIM25 in a sequence-specific manner and inhibiting its deubiquitylation (34). Here we observed decreased PINK1 expression in PBMCs from pediatric patients infected with RSV compared with those from healthy children. PINK1 expression was also downregulated in primary macrophages infected with DNA and RNA viruses. These data suggest that PINK1 expression might be correlated with the host antiviral immune response.

TRAF3 plays a pivotal role in RLR-triggered IRF3 activation and subsequent type I interferon and proinflammatory cytokine production (35). PINK1 positively regulates the antiviral immune response through enhanced association with TRAF3 and IRF3 upon virus infection, which promotes IRF3 phosphorylation and results in increased IFN-β and IL-6 transcription. Furthermore, PINK1 associates with TRAF3 and promotes RIG-I triggered cytokine transcription in a kinase domain-dependent manner. However, macrophages overexpressing the ΔKD and L347P PINK1 variants displayed much lower IFN-β expression and subsequently much higher VSV-G mRNA compared with control cells. PINK1 mutants might reduce E3 ligase activity, leading to increased susceptibility to stress and accumulation of un/misfolded proteins in cells, eventually leading to cell death (36). Thus, the lower IFN-β expression in PINK1 mutant-overexpressing cells upon VSV infection might be associated with un/misfolded proteins such as Parkin recruitment and cell death. Further studies are therefore needed to examine the cell viability of macrophages overexpressing PINK1 mutants.

Ubiquitination of adaptor proteins is one of the most versatile posttranslational regulations and is widely involved in the precise modulation of antiviral response activity (26, 37). E3 ubiquitin ligases, such as TRIM23, TRIM29, were involved in posttranslational modification of NEMO or MAVS by ubiquitination to regulate antiviral immune response (38–40). TRAF3 maintains its activity in a suitable state by undergoing K48- and K63-linked ubiquitination after viral stimulation (41, 42). We detected an association between PINK1 and TRAF3 in resting macrophages, which was enhanced upon VSV infection. However, PINK1 does not belong to any known ubiquitin ligase families. In the mitophagy pathway, the ubiquitin-like

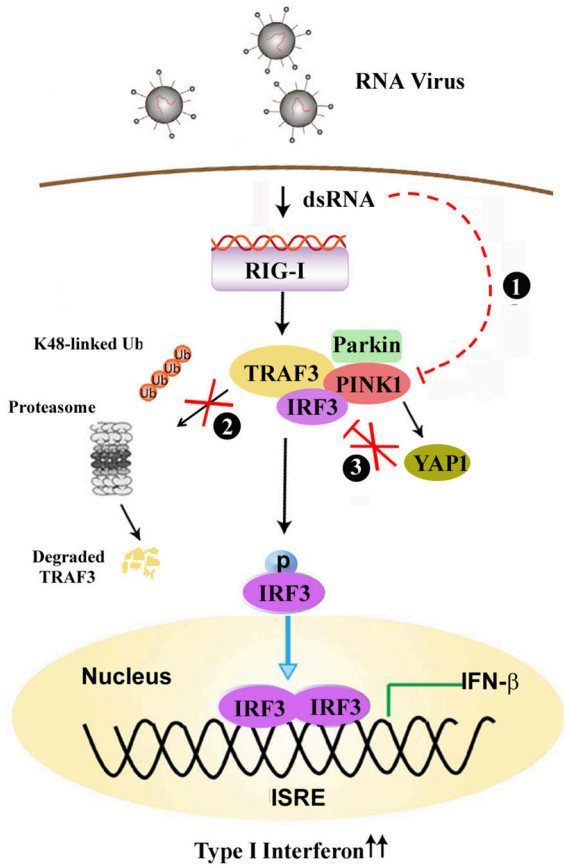

FIGURE 8 | PINK1 positively regulates the RLR-triggered antiviral immune response by inhibiting TRAF3 degradation and relieving YAP-mediated inhibition of the cellular antiviral response. (1) Virus infection down-regulates PINK1 expression in macrophages. (2) PINK1 promotes RLR-triggered IRF3 activation via inhibiting Parkin-mediated K48-linked ubiquitination of TRAF3, (3) and PINK1 inhibits YAP1/IRF3 complex formation, which ultimately promotes RIG-I triggered antiviral immune response.

domain (UBL) of Parkin is a crucial substrate of PINK1 that is phosphorylated at Ser65 (43, 44). Recently, Parkin was reported to be a negative regulator of antiviral signaling pathway by targeting TRAF3 for degradation (45). Xiong et al. reported that PINK1 expression not only regulates Parkin E3 ligase activity but also promotes the degradation of Parkin substrates, including Parkin itself (36). Our results showed that PINK1 promoted TRAF3 expression upon viral infection, likely due to PINK1-mediated Parkin degradation and repressed Parkin-mediated TRAF3 K48-linked ubiquitination, leading to decreased TRAF3 degradation. Our data suggest that PINK1 regulate TRAF3 degradation in response to viral stimulus, possibly by promoting Parkin degradation, to precisely modulate the immune response.

YAP functions as a transcriptional regulator of organ-size control and tissue homeostasis (46). Park2 (Parkin) was identified as a YAP target gene and was upregulated in SalvCKO TRAP-seq (47). Hippo deficient cardiomyocytes showed increased expression of stress response genes including the quality control gene of mitochondria, Park2 (Parkin) (48). Wang et al. reported that YAP can negatively regulate antiviral innate immunity by interacting with IRF3 and impairing IRF3 dimer formation and subsequent nuclear translocation (30). Considering that PINK1 binds IRF3 after viral infection in macrophages, we speculate that YAP1 might be involved in the PINK1-mediated antiviral innate immune response. In this study, we found that PINK1 disrupted the binding between YAP1 and IRF3 following VSV infection. PINK1 knockdown only affect the phosphorylation of YAP at Ser127 at 8 h upon VSV infection (**Figure 3C**). YAP phosphorylation at Ser403 is critical for IKKε-mediated YAP lysosomal degradation and dissociation of YAP from IRF3 (30). Whether PINK1 affect YAP1 phosphorylation at Ser403 and thus impair the interaction between YAP1 and IRF3 is worthy of further study. Our data suggest that PINK1 promotes VSV-triggered RLR signaling at least partly by inhibiting the association of YAP1 and IRF3.

In conclusion, our data offer insights into PINK1 and Parkin function in antiviral innate immune response. In addition to mitochondrial quality control, PINK1 positively regulates the RIG-I triggered innate immune response by inhibiting TRAF3 degradation and relieving YAP-mediated inhibition of the cellular antiviral response.

ETHICS STATEMENT

Human subjects: This study was carried out in accordance with the recommendations of institutional guidelines, the ethics committee of Children's Hospital, Zhejiang University School of Medicine with written informed consent from guardians of all subjects. At least one guardian for each subject gave written informed consent in accordance with the Declaration of Helsinki. The protocol was approved by the ethics committee of Children's Hospital, Zhejiang University School of Medicine.

Animal subjects: This study was carried out in accordance with the recommendations of institutional guidelines, the Animal Review Committee of Zhejiang University School of Medicine. The protocol was approved by the Animal Review Committee of Zhejiang University School of Medicine.

AUTHOR CONTRIBUTIONS

JZ and HY designed and supervised the research. JZ, RY, and ZZ conducted the experiments. QL, YZ, and QW analyzed the data. JZ wrote the manuscript.

FUNDING

This work was supported by grants from the National Natural Science Foundation of China (31870865), and Zhejiang Provincial Natural Science Foundation (LY18H100001, LY15H100001), and the Double First-rate project initiatives.

REFERENCES

1. Broz P, Monack DM. Newly described pattern recognition receptors team up against intracellular pathogens. *Nat Rew Immunol.* (2013) 13:551–65. doi: 10.1038/nri3479
2. Wu J, Chen ZJ. Innate immune sensing and signaling of cytosolic nucleic acids. *Annu Rev Immunol.* (2014) 32:461–88. doi: 10.1146/annurev-immunol-032713-120156
3. Kato H, Takahasi K, Fujita T. RIG-I-like receptors: cytoplasmic sensors for non-self RNA. *Immunol Rev.* (2011) 243:91–8. doi: 10.1111/j.1600-065X.2011.01052.x
4. Sun L, Wu J, Du F, Chen X, Chen ZJ. Cyclic GMP-AMP synthase is a cytosolic DNA sensor that activates the type I interferon pathway. *Science.* (2013) 339:786–91. doi: 10.1126/science.1232458
5. Kowalinski E, Lunardi T, McCarthy AA, Louber J, Brunel J, Grigorov B, et al. Structural basis for the activation of innate immune pattern-recognition receptor RIG-I by viral RNA. *Cell.* (2011) 147:423–35. doi: 10.1016/j.cell.2011.09.039
6. Loo YM, Gale M Jr. Immune signaling by RIG-I-like receptors. *Immunity.* (2011) 34:680–92. doi: 10.1016/j.immuni.2011.05.003
7. Zhang Q, Wan H, Huang S, Zhang Y, Wang Y, Guo X, et al. Critical role of RIG-I-like receptors in inflammation in chronic obstructive pulmonary disease. *Clin Respir J.* (2016) 10:22–31. doi: 10.1111/crj.12177
8. Valente EM, Abou-Sleiman PM, Caputo V, Muqit MM, Harvey K, Gispert S, et al. Hereditary early-onset Parkinson's disease caused by mutations in PINK1. *Science.* (2004) 304:1158–60. doi: 10.1126/science.1096284
9. Voigt A, Berlemann LA, Winklhofer KF. The mitochondrial kinase PINK1: functions beyond mitophagy. *J Neurochem.* (2016) 139(Suppl. 1): 232–9. doi: 10.1111/jnc.13655
10. Arena G, Valente EM. PINK1 in the limelight: multiple functions of an eclectic protein in human health and disease. *J Pathol.* (2017) 241:251–63. doi: 10.1002/path.4815
11. Cang X, Wang X, Liu P, Wu X, Yan J, Chen J, et al. PINK1 alleviates palmitate induced insulin resistance in HepG2 cells by suppressing ROS mediated MAPK pathways. *Biochem Biophys Res Commun.* (2016) 478:431–8. doi: 10.1016/j.bbrc.2016.07.004
12. Matheoud D, Sugiura A, Bellemare-Pelletier A, Laplante A, Rondeau C, Chemali M, et al. Parkinson's disease-related proteins PINK1 and parkin repress mitochondrial antigen presentation. *Cell.* (2016) 166:314–27. doi: 10.1016/j.cell.2016.05.039
13. Stanaway JD, Flaxman AD, Naghavi M, Fitzmaurice C, Vos T, Abubakar I, et al. The global burden of viral hepatitis from 1990 to 2013: findings from the Global Burden of Disease Study 2013. *Lancet.* (2016) 388:1081–8. doi: 10.1016/S0140-6736(16)30579-7
14. Kim SJ, Khan M, Quan J, Till A, Subramani S, Siddiqui A. Hepatitis B virus disrupts mitochondrial dynamics: induces fission and mitophagy to attenuate apoptosis. *PLoS Pathog.* (2013) 9:e1003722. doi: 10.1371/journal.ppat.1003722
15. Kim SJ, Syed GH, Siddiqui A. Hepatitis C virus induces the mitochondrial translocation of Parkin and subsequent mitophagy. *PLoS Pathog.* (2013) 9:e1003285. doi: 10.1371/journal.ppat.1003285
16. Jang H, Boltz DA, Webster RG, Smeyne RJ. Viral parkinsonism. *Biochim Biophys Acta.* (2009) 1792:714–21. doi: 10.1016/j.bbadis.2008.08.001
17. Wijarnpreecha K, Chesdachai S, Jaruvongvanich V, Ungprasert P. Hepatitis C virus infection and risk of Parkinson's disease: a systematic review and meta-analysis. *Eur J Gastroenterol Hepatol.* (2018) 30:9–13. doi: 10.1097/MEG.0000000000000991
18. Tsai HH, Liou HH, Muo CH, Lee CZ, Yen RF, Kao CH. Hepatitis C virus infection as a risk factor for Parkinson disease: a nationwide cohort study. *Neurology.* (2016) 86:840–6. doi: 10.1212/WNL.0000000000002307
19. Song Y, Lai L, Chong Z, He J, Zhang Y, Xue Y, et al. E3 ligase FBXW7 is critical for RIG-I stabilization during antiviral responses. *Nat Commun.* (2017) 8:14654. doi: 10.1038/ncomms14654
20. Zhang Z, Tang Z, Ma X, Sun K, Fan L, Fang J, et al. TAOK1 negatively regulates IL-17-mediated signaling and inflammation. *Cell Mol Immunol.* (2018) 15:794–802. doi: 10.1038/cmi.2017.158
21. Falvo JV, Parekh BS, Lin CH, Fraenkel E, Maniatis T. Assembly of a functional beta interferon enhanceosome is dependent on ATF-2-c-jun heterodimer orientation. *Mol Cell Biol.* (2000) 20:4814–25. doi: 10.1128/MCB.20.13.4814-4825.2000
22. Wathelet MG, Lin CH, Parekh BS, Ronco LV, Howley PM, Maniatis T. Virus infection induces the assembly of coordinately activated transcription factors on the IFN-beta enhancer *in vivo*. *Mol Cell.* (1998) 1:507–18. doi: 10.1016/S1097-2765 (00) 80051-9
23. Beilina A, Van Der Brug M, Ahmad R, Kesavapany S, Miller DW, Petsko GA, et al. Mutations in PTEN-induced putative kinase 1 associated with recessive parkinsonism have differential effects on protein stability. *Proc Natl Acad Sci USA.* (2005) 102:5703–8. doi: 10.1073/pnas.0500617102
24. Moriwaki Y, Kim YJ, Ido Y, Misawa H, Kawashima K, Endo S, et al. L347P PINK1 mutant that fails to bind to Hsp90/Cdc37 chaperones is rapidly degraded in a proteasome-dependent manner. *Neurosci Res.* (2008) 61:43–8. doi: 10.1016 /j.neures.2008.01.006
25. Hacker H, Tseng PH, Karin M. Expanding TRAF function: TRAF3 as a tri-faced immune regulator. *Nat Rev Immunol.* (2011) 11:457–68. doi: 10.1038/nri2998
26. Tseng PH, Matsuzawa A, Zhang W, Mino T, Vignali DA, Karin M. Different modes of ubiquitination of the adaptor TRAF3 selectively activate the expression of type I interferons and proinflammatory cytokines. *Nat Immunol.* (2010) 11:70–5. doi: 10.1038/ni.1819
27. Triplett JC, Zhang Z, Sultana R, Cai J, Klein JB, Bueler H, Butterfield DA. Quantitative expression proteomics and phosphoproteomics profile of brain from PINK1 knockout mice: insights into mechanisms of familial Parkinson's disease. *J Neurochem.* (2015) 133:750–65. doi: 10.1111/jnc.13039
28. O'Flanagan CH, Morais VA, Wurst W, De Strooper B, O'Neill C. The Parkinson's gene PINK1 regulates cell cycle progression and promotes cancer-associated phenotypes. *Oncogene.* (2015) 34:1363–74. doi: 10.1038/onc.2014.81
29. Huang J, Wu S, Barrera J, Matthews K, Pan D. The Hippo signaling pathway coordinately regulates cell proliferation and apoptosis by inactivating Yorkie, the Drosophila Homolog of YAP. *Cell.* (2005) 122:421–34. doi: 10.1016/j.cell.2005.06.007
30. Wang S, Xie F, Chu F, Zhang Z, Yang B, Dai T, et al. YAP antagonizes innate antiviral immunity and is targeted for lysosomal degradation through IKKepsilon-mediated phosphorylation. *Nat Immunol.* (2017) 18:733–43. doi: 10.1038/ni.3744
31. Kitada T, Asakawa S, Hattori N, Matsumine H, Yamamura Y, Minoshima S, et al. Mutations in the parkin gene cause autosomal recessive juvenile parkinsonism. *Nature.* (1998) 392:605–8. doi: 10.1038/33416
32. Chan YK, Gack MU. Viral evasion of intracellular DNA and RNA sensing. *Nat Rev Microbiol.* (2016) 14:360–73. doi: 10.1038/nrmicro.2016.45
33. Rajsbaum R, Albrecht RA, Wang MK, Maharaj NP, Versteeg GA, Nistal-Villan E, et al. Species-specific inhibition of RIG-I ubiquitination and IFN induction by the influenza A virus NS1 protein. *PLoS Pathog.* (2012) 8:e1003059. doi: 10.1371 /journal.ppat.1003059
34. Manokaran G, Finol E, Wang C, Gunaratne J, Bahl J, Ong EZ, et al. Dengue subgenomic RNA binds TRIM25 to inhibit interferon expression for epidemiological fitness. *Science.* (2015) 350:217–21. doi: 10.1126/science.aab3369
35. Saha SK, Cheng G. TRAF3: a new regulator of type I interferons. *Cell Cycle.* (2006) 5:804–7. doi: 10.4161/cc.5.8.2637
36. Xiong H, Wang D, Chen L, Choo YS, Ma H, Tang C, et al. Parkin, PINK1, and DJ-1 form a ubiquitin E3 ligase complex promoting unfolded protein degradation. *J Clin Invest.* (2009) 119:650–60. doi: 10.1172/JCI37617
37. Malynn BA, Ma A. Ubiquitin makes its mark on immune regulation. *Immunity.* (2010) 33:843–52. doi: 10.1016/j.immuni.2010.12.007
38. Arimoto K, Funami K, Saeki Y, Tanaka K, Okawa K, Takeuchi O, et al. Polyubiquitin conjugation to NEMO by triparite motif protein 23 (TRIM23) is critical in antiviral defense. *Proc Natl Acad Sci USA.* (2010) 107:15856–61. doi: 10.1073/pnas.1004621107
39. Xing J, Weng L, Yuan B, Wang Z, Jia L, Jin R, et al. Identification of a role for TRIM29 in the control of innate immunity in the respiratory tract. *Nat Immunol.* (2016) 17:1373–80. doi: 10.1038/ni.3580

40. Xing J, Zhang A, Minze LJ, Li XC, Zhang Z. TRIM29 negatively regulates the type I IFN production in response to RNA virus. *J Immunol.* (2018) 201:183–92. doi: 10.4049/jimmunol.1701569
41. Li S, Zheng H, Mao AP, Zhong B, Li Y, Liu Y, et al. Regulation of virus-triggered signaling by OTUB1- and OTUB2-mediated deubiquitination of TRAF3 and TRAF6. *J Biol Chem.* (2010) 285:4291–7. doi: 10.1074/jbc.M109.074971
42. Wang C, Huang Y, Sheng J, Huang H, Zhou J. Estrogen receptor alpha inhibits RLR-mediated immune response via ubiquitinating TRAF3. *Cell Signal.* (2015) 27:1977–83. doi: 10.1016/j.cellsig.2015.07.008
43. Kane LA, Lazarou M, Fogel AI, Li Y, Yamano K, Sarraf SA, et al. PINK1 phosphorylates ubiquitin to activate Parkin E3 ubiquitin ligase activity. *J Cell Biol.* (2014) 205:143–53. doi: 10.1083/jcb.201402104
44. Wauer T, Simicek M, Schubert A, Komander D. Mechanism of phospho-ubiquitin-induced PARKIN activation. *Nature.* (2015) 524:370–4. doi: 10.1038/nature14879
45. Xin D, Gu H, Liu E, Sun Q. Parkin negatively regulates the antiviral signaling pathway by targeting TRAF3 for degradation. *J Biol Chem.* (2018) 293:11996–2010. doi: 10.1074/ jbc.RA117.001201
46. Yu FX, Meng Z, Plouffe SW, Guan KL. Hippo pathway regulation of gastrointestinal tissues. *Annu Rev Physiol.* (2015) 77:201–27. doi: 10.1146/annurev-physiol-021014-071733
47. Morikawa Y, Zhang M, Heallen T, Leach J, Tao G, Xiao Y, et al. Actin cytoskeletal remodeling with protrusion formation is essential for heart regeneration in Hippo-deficient mice. *Sci Signal.* (2015) 8:ra41. doi: 10.1126/scisignal.2005781
48. Leach JP, Heallen T, Zhang M, Rahmani M, Morikawa Y, Hill MC, et al. Hippo pathway deficiency reverses systolic heart failure after infarction. *Nature.* (2017) 550:260–4. doi: 10.1038/nature24045

Conflict of Interest Statement: The authors declare that the research was conducted in the absence of any commercial or financial relationships that could be construed as a potential conflict of interest.

frontiers in Immunology

ORIGINAL RESEARCH
published: 31 May 2019
doi: 10.3389/fimmu.2019.01209

Human Toll-like Receptor 8 (TLR8) Is an Important Sensor of Pyogenic Bacteria, and Is Attenuated by Cell Surface TLR Signaling

Siv H. Moen[1,2], *Birgitta Ehrnström*[1,2,3], *June F. Kojen*[1,2], *Mariia Yurchenko*[1,2], *Kai S. Beckwith*[1,2], *Jan E. Afset*[2,4], *Jan K. Damås*[1,2,3], *Zhenyi Hu*[5], *Hang Yin*[6], *Terje Espevik*[1,2] *and Jørgen Stenvik*[1,2,3]*

[1] Centre of Molecular Inflammation Research, Norwegian University of Science and Technology, Trondheim, Norway, [2] Department of Clinical and Molecular Medicine, Norwegian University of Science and Technology, Trondheim, Norway, [3] Department of Infectious Diseases, Clinic of Medicine, St. Olavs Hospital HF, Trondheim University Hospital, Trondheim, Norway, [4] Clinic of Laboratory Medicine, St. Olavs Hospital HF, Trondheim University Hospital, Trondheim, Norway, [5] Department of Chemistry and Biochemistry and BioFrontiers Institute, University of Colorado Boulder, Boulder, CO, United States, [6] School of Pharmaceutical Sciences, Tsinghua University-Peking University Joint Center for Life Sciences, Beijing Advanced Innovation Center for Structural Biology, Tsinghua University, Beijing, China

OPEN ACCESS

Edited by:
Thai Tran, National University of Singapore, Singapore

Reviewed by:
Jean-Marc Cavaillon, Institut Pasteur, France
Nicola Tamassia, University of Verona, Italy

***Correspondence:**
Jørgen Stenvik
jorgen.stenvik@ntnu.no

Specialty section:
This article was submitted to Molecular Innate Immunity, a section of the journal Frontiers in Immunology

Received: *28 February 2019*
Accepted: *13 May 2019*
Published: *31 May 2019*

Citation:
Moen SH, Ehrnström B, Kojen JF, Yurchenko M, Beckwith KS, Afset JE, Damås JK, Hu Z, Yin H, Espevik T and Stenvik J (2019) Human Toll-like Receptor 8 (TLR8) Is an Important Sensor of Pyogenic Bacteria, and Is Attenuated by Cell Surface TLR Signaling. Front. Immunol. 10:1209. doi: 10.3389/fimmu.2019.01209

TLR8 is an endosomal sensor of RNA degradation products in human phagocytes, and is involved in the recognition of viral and bacterial pathogens. We previously showed that in human primary monocytes and monocyte derived macrophages, TLR8 senses entire *Staphylococcus aureus* and *Streptococcus agalactiae* (group B *streptococcus*, GBS), resulting in the activation of IRF5 and production of IFNβ, IL-12p70, and TNF. However, the quantitative and qualitative impact of TLR8 for the sensing of bacteria have remained unclear because selective inhibitors have been unavailable. Moreover, while we have shown that TLR2 activation attenuates TLR8-IRF5 signaling, the molecular mechanism of this crosstalk is unknown. We here used a recently developed chemical antagonist of TLR8 to determine its role in human primary monocytes challenged with *S. aureus,* GBS, *Streptococcus pneumonia, Pseudomonas aeruginosa,* and *E. coli*. The inhibitor completely blocked cytokine production in monocytes stimulated with TLR8-agonists, but not TLR2-, and TLR4-agonists. Upon challenge with *S. aureus*, GBS, and *S. pneumonia*, the TLR8 inhibitor almost eliminated the production of IL-1β and IL-12p70, and it strongly reduced the release of IL-6, TNF, and IL-10. With *P. aeruginosa* infection, the TLR8 inhibitor impaired the production of IL-12p70 and IL-1β, while with *E. coli* infection the inhibitor had less effect that varied depending on the strain and conditions. Signaling via TLR2, TLR4, or TLR5, but not TLR8, rapidly eliminated IRAK-1 detection by immunoblotting due to IRAK-1 modifications during activation. Silencing of IRAK-1 reduced the induction of IFNβ and TNF by TLR8 activation, suggesting that IRAK-1 is required for TLR8-IRF5 signaling. The TLR-induced modifications of IRAK-1 also correlated closely with attenuation of TLR8-IRF5 activation, suggesting that sequestration and/or modification of Myddosome components by cell surface TLRs limit the function of TLR8. Accordingly, inhibition of CD14- and TLR4-activation during *E. coli* challenge increased the activation of IRF5 and the production of IL-1β and IL-12p70. We

conclude that TLR8 is a dominating sensor of several species of pyogenic bacteria in human monocytes, while some bacteria attenuate TLR8-signaling via cell surface TLR- activation. Taken together, TLR8 appears as a more important sensor in the antibacterial defense system than previously known.

Keywords: human TLR8, bacteria, monocytes, cytokines, IRAK-1

INTRODUCTION

Toll-like receptors (TLR) sense distinct pathogen associated molecular patterns (PAMPs) and initiate inflammatory reactions important for innate and adaptive defense. Humans with genetic defects in the central TLR/IL-1R signaling adaptors MyD88- or IRAK-4 have increased susceptibility to pyogenic bacterial infections, but only during infancy and early childhood (1, 2). On the other hand, excessive inflammation via uncontrolled TLR signaling can initiate sepsis, a syndrome defined as a dysregulated host response resulting in life-threatening organ failure (3). Inhibition of pro-inflammatory sensors and mediators of the host is protective in several animal models of sepsis, yet multiple clinical trials have failed (4). Therefore, there is a need to improve our understanding of the cell host-pathogen interactions, and to clarify which host responses that are protective and which that have adverse effects. This can aid in the identification of new targets and strategies for prevention or treatment of sepsis.

Human TLR8 is highly expressed as a functional cleavage product in endosomes of monocytes and macrophages (5). Mechanistically, the RNA degradation products uridine and short oligomers bind cooperatively at two distinct sites in the N-terminal domain. This induce a conformational change of the pre-formed TLR8-dimer leading to MyD88 recruitment and signaling. Small-molecule agonists such as CL075 have high affinity to the uridine binding site, and is capable in activating TLR8 without RNA oligomers (6). Rodent TLR8 differs structurally and is not activated by these ligands (7), but can be activated in neurons by endogenous microRNA which regulate neuropathic pain (8).

The impact of TLR8 during infection is unclear because neither small animal models nor selective and efficient inhibitors have been available. We previously showed that TLR8 senses entire *S. aureus* and GBS in primary monocytes and macrophages, resulting in the activation of IRF5 and production of IFNβ, IL-12p70, and TNF (9, 10). RNA is likely the bacterial structure required for TLR8 activation, as enzymatic degradation of RNA in *S. aureus* lysates (9) or in GBS upon heat-inactivation strongly attenuate cytokine induction (10). Bacterial RNA is also considered a vita PAMP, a marker of microbial viability (11). Others have shown that TLR8 also contributes in IL-6 production during infection with *Streptococcus pyogenes* (group A *streptococcus,* GAS) (12) and *Escherichia coli* (11, 13) in human myeloid cells. A weakness of these studies is the reliance on molecular tools with limited efficacy and specificity (e.g., siRNA and non-selective inhibitors), and model systems using cell lines do not accurately reflect the role of TLR8 in human primary cells. Thus, the quantitative and qualitative role of TLR8 for the sensing of bacteria needs further clarification. We also revealed that activation of TLR2 negatively regulates TLR8-IRF5 signaling (9). Consequently, bacteria that express high levels of TLR2-agonistic lipoproteins can avoid detection via TLR8, but the molecular mechanism behind this negative TLR-TLR crosstalk is still unknown.

A chemical antagonist of human TLR8 (CU-CPT9a) with high selectivity and efficiency was recently developed (14). CU-CPT9a binds close to the uridine/CL075 binding site in the N-terminal domain and locks TLR8 in the resting state. We here used CU-CPT9a to clarify the role of human TLR8 during bacterial challenge of primary monocytes. Our data show that TLR8 is the dominating sensor of Gram-positive pyogenic bacteria that are major human pathogens. TLR8 also participates in the sensing of the pyogenic Gram-negative species *P. aeruginosa* and *E. coli*. We further show that TLR8 signaling requires IRAK-1 expression, and that cell surface TLR activation attenuates TLR8 signaling, likely via a mechanism involving IRAK-1 and/or other Myddosome components.

MATERIALS AND METHODS

Materials

The TLR8 antagonist CU-CPT9a is previously described (14) and was provided by The Regents of the University of Colorado, a body corporate for and on behalf of the University of Colorado Boulder. The TLR-agonists FSL-1 (TLR2/6), CL075 and polyuridylic acid (polyU; TLR8), ultrapure LPS O111:B4 (TLR4), and purified flagellin from *P. aeruginosa* (TLR5) were purchased from Invivogen. Poly-L-arginine (pLA), the IRAK-4 inhibitor (PF-06426779), and the proteasome inhibitor MG132 were from Sigma-Aldrich (Merck). Humanized anti-CD14 and IgG2/4 control were generously provided by prof. Tom Eirik Mollnes (University of Oslo, Oslo, Norway). BioPlex cytokine assays were from Bio-Rad, and the cytokine levels were determined as per the manufacturer's instructions using Bio-Plex Pro™ Reagent Kit III and the Bio-Plex™ 200 System.

Bacteria

The bacterial strains GBS NEM316, *S. aureus* 113/113Δ*lgt*, and *S. aureus* Cowan were generously provided by professors Philipp Henneke (University of Freiburg, Germany), Friedrich Göetz (University of Tübingen, Tübingen, Germany), and Timothy Foster (Trinity College, Dublin, Ireland), respectively. The *E. coli* Seattle 1946 strain was obtained from the American Type Culture Collection (ATCC 25922), while *E. coli* and ClearColi® BL21 (DE3) strains were from Lucigen Corporation (USA). Anonymized clinical isolates of GBS, *S. aureus*, *S. pneumoniae*, *P. aeruginosa,* and *E. coli* were from a diagnostic collection by the Department of Medical Microbiology, St. Olavs Hospital,

Trondheim, Norway. The bacteria were grown on Tryptic soy agar (TSA) or blood agar. For challenge experiments, colonies of *E. coli, S. aureus* and *P. aeruginosa* were grown in Tryptic Soy Broth, while GBS were grown in Todd-Hewitt Broth during vigorously shaking at 37°C. *S. pneumoniae* were grown in Brain-Heart Infusion broth at 37°C and 5% CO_2. Overnight cultures were diluted 1:100 in fresh broth and grown to exponential phase (∼4 h). Bacteria were quantified by optical density, as previously described (10), and the MOI was calculated according to the corresponding CFU counts.

Monocyte Isolation and Challenge

Human buffycoats and serum were from the Blood bank at St. Olavs Hospital (Trondheim, Norway), with approval by the Regional Committee for Medical and Health Research Ethics (REC Central, Norway, no. 2009/2245). PBMC were isolated using Lymphoprep as described by the manufacturer (Axis Shield Diagnostics, Scotland). Monocytes were purified by adherence in culture plates and maintained in RPMI 1640 (Life Technologies) supplemented with 10% pooled human serum. The cells were pre-incubated with the TLR8 antagonist CU-CPT9a and the control reagent for 2 h, and with the other inhibitors for 30 min. Subsequently, the cells were challenged with bacteria or TLR-agonists, and Gentamicin (100 μg/ml) was added 1 h after the initiation of the challenge to kill extracellular bacteria. Supernatants were stored at −20°C until analyses. THP-1 cells overexpressing recombinant TLR8 was used as previously described (10).

Immunofluorescence and scanR Analysis

Immunofluorescence labeling and analyses with scanR high-content screening system (Olympus) was done as previously described (9, 10). Primary antibodies used were mouse anti-human IRF5 mAb (Abcam, 10T1, ab33478), rabbit anti-human p65/RelA XP-mAb Cell Signaling Technologies (CST # 8242), and rabbit anti-human p65A (Santa Cruz Biotechnology, #sc-109).

Western Blotting

Cells were collected and lysed in buffer [1% IGEPAL CA-630, 150 mM NaCl, 50 mM Tris-HCl, pH 7,5, 10% glycerol, 1 mM NaF, 2 mM Na_3VO_4, and a protease-phosphatase inhibitor (Complete Mini tablets, Basel, Switzerland)]. Cell lysates were mixed with NuPage LDS sample buffer (Invitrogen) supplemented with 25 mM DTT and denatured at 70°C for 10 min. The samples were separated on 10% Bis-Tris polyacrylamide gels and transferred to nitrocellulose membranes using the iBlot Dry Blotting System (Invitrogen). The membranes were blocked with 5% bovine serum albumin diluted in Tris-buffered saline containing 0.05% Tween-20. Antibodies used were anti-IRAK-1 (CST D51G7, #4504), anti-IRAK-2 (CST #4367) and anti-IRAK-4 (CST #4363), anti-P-Ser396-IRF3 (CST, 4D4G, #4947), and anti-IkBα (CST, 44D4, #4812). Monoclonal anti-GAPDH (Abcam #8245) or anti-beta-tubulin (Abcam, ab6046) were used as loading controls. After incubation with horseradish peroxidase-conjugated secondary antibodies (DAKO), the images were developed using Super Signal West Femto Maximum Sensitivity Substrate (Thermo Scientific) and Odyssey FC Imaging System (LI-COR). Quantification was done using the Image Studio software.

Gene Silencing and Quantitative PCR

Monocytes were differentiated to macrophages (MDMs) for 5 to 6 days in RPMI 1,640 with 30% pooled human serum. Medium was replaced with RPMI 1640 containing 10% serum before siRNA treatment. A pool of four individual ON-TARGETplus siRNAs (Dharmacon) was transfected using siLentFect (Bio-Rad), yielding a final concentration of 5 nM siRNA. The transfection was repeated after 3 days, and the silenced MDMs were challenged with TLR8 ligand. RNA was isolated with RNeasy including DNAse treatment (Qiagen), cDNA was transcribed with the Maxima cDNA synthesis kit (Thermo Fisher Scientific), and quantitative PCR was done with StepOnePlus using TaqMan probes (Life Technologies) and Perfecta qPCR FastMix (Quanta). The probes used were Hs01077958_s1 (IFNβ), Hs00174128_m1 (TNF), Hs01018347_m1 (IRAK-1). TBP (Hs00427620_m1) served as endogenous mRNA control, and relative expression was calculated using the ΔΔCt method, and plotted as fold induction by stimulation.

Statistics

Data from independent experiments with monocytes from different donors was used for the statistical calculations, indicated as N (number of experiments). Data was log-transformed to increase the likelihood of a Gaussian data distribution, as this is required for parametrical tests. Data sets with one factor were analyzed by one-way repeated-measures (RM) analysis of variance (ANOVA) and Dunette's multiple comparison test, while data sets with two factors were analyzed by two-way RM ANOVA and Bonferroni's multiple comparison test. For data sets with missing values a mixed model analysis was used. For some samples the cytokine levels were below the limit of detectionand these conditions were excluded from the analysis as indicated with the symbol "v." Significance levels are indicated as: $^{*}p < 0.05$, $^{**}p < 0.01$, and $^{***}p < 0.001$. Graphs and analyses were generated with GraphPad Prism (v8.01).

RESULTS

The Role of TLR8 in the Sensing of *S. aureus*, GBS, and *E. coli* by Human Primary Monocytes

We here examined the role of TLR8 in the sensing of live bacteria by human primary monocytes using CU-CPT9a, a recently developed small-molecule inhibitor of TLR8 which does not affect the activation of other human TLRs (14). To determine the optimal dose of the inhibitor, we pre-treated monocytes with serial dilutions of CU-CPT9a and challenged the cells with the TLR8 ligands pU/pLA (polyuridylicacid/poly-L-arginine) and CL075. CU-CPT9a completely blocked the cytokine production at 2.5–5 μM while the control compound (Ctrl) had no effect (**Figure S1**). Cell viability analysis of monocytes revealed that 5 μM CU-CPT9a did not induce cell death (data not shown). To determine the impact of TLR8 in the sensing of live bacteria, we

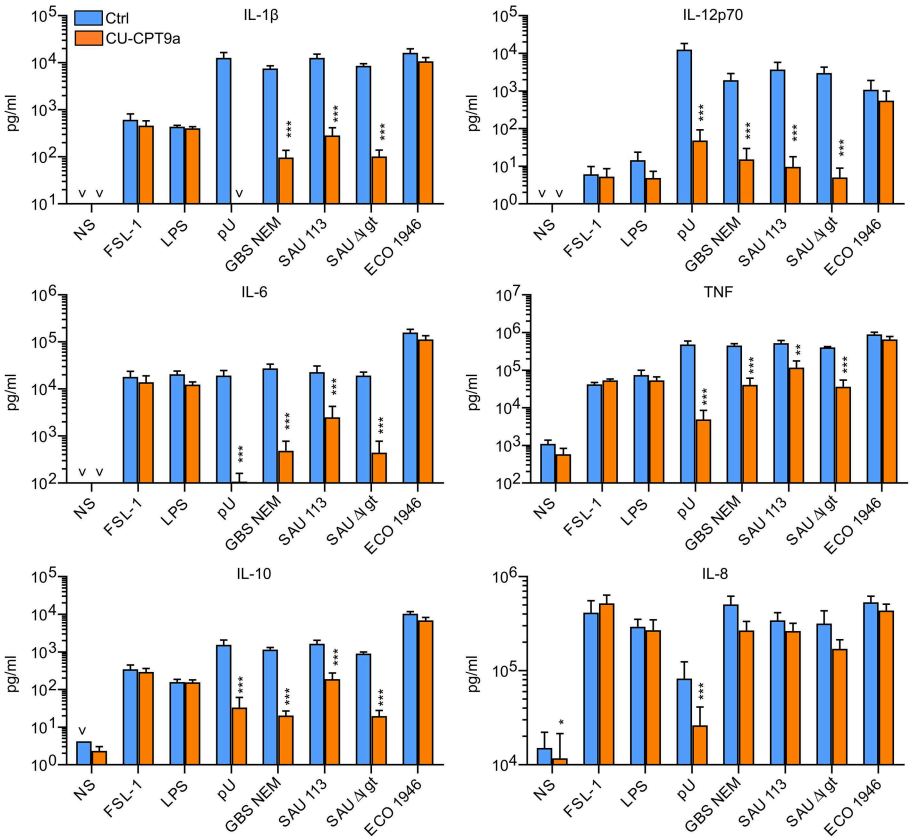

FIGURE 1 | TLR8 inhibition strongly attenuates cytokine production from human primary monocytes challenged with Group B streptococcus (GBS) and *S. aureus*, but not a strain of *E. coli*. Monocytes were pre-treated with control reagent (Ctrl, 5 μM) or TLR8 antagonist (CU-CPT9a, 5 μM) and challenged with TLR8-ligand pU (polyU/poly-L-arginine, 1 μg/ml), TLR2-ligand FSL-1 (100 ng/ml), TLR4-ligand LPS (O111:B4, 100 ng/ml), or live GBS (NEM316), *S. aureus* wild-type (SAU 113) and *lgt*-deficient (SAU 113Δ*lgt*), or *E. coli* Seattle 1946 (ECO1946) for 22 h. Bacterial doses were 1 × 10^6/ml for GBS and *S. aureus* (MOI 0.1 for GBS, 0.2 for SAU), and 2 × 10^5/ml for *E. coli* (MOI 0.2). Graphs show mean + SEM ($N = 4$). NS, no stimuli. *$p < 0.05$, **$p < 0.01$, and ***$p < 0.001$.

blocked TLR8 activation using 5 μM CU-CPT9a and challenged monocytes with GBS (GBS NEM316) and *S. aureus* 113 (SAU 113) at two doses for 6 and 22 h. We also included an isogenic *lgt*-deficient strain of *S. aureus* which lacks TLR2-stimulatory lipoproteins (SAU 113Δ*lgt*) (15), and an *E. coli* reference strain (Seattle 1946, ECO 1946). TLR2-, TLR4-, and TLR8-ligands were included as controls of specificity and efficiency. CU-CPT9a inhibited the cytokine induction by pU/pLA stimulation completely, but had no effect on cytokine induction by LPS and FSL-1 stimulation (**Figure 1**),demonstrating the high efficacy and selectivity of this inhibitor also for these experimental conditions. With live bacteria challenge, CU-CPT9a strongly attenuated the cytokine induction by GBS and *S. aureus*, for both time points and bacterial doses examined (**Figure 1**, **Figure S2**). Production of IL-1β and IL-12p70 induced by these bacteria was almost eliminated (**Table 1A**). TLR8 inhibition also strongly reduced TNF and IL-6 induction by GBS and *S. aureus*, and reduced IL-10 production at the late time point, while TLR8-inhibition increased the level of IL-8 after 22 h of infection with the highest dose of bacteria (**Table 1A**). In contrast, cytokine induction by ECO 1946 was not much affected by TLR8 inhibition. This is in accordance with previous findings using this particular strain, where TLR8 silencing failed to attenuate cytokine production in monocyte-derived macrophages (MDMs) (10). CU-CPT9a reduced the induction of TNF, IL-6, and IL-10 by the SAU 113-Δ*lgt* strain slightly more than with the SAU 113 wild-type strain (**Table 1A**). This suggest that TLR2 only plays a minor role in the sensing of *S. aureus* by monocytes compared to TLR8 for these experimental settings.

The Role of TLR8 During Challenge of Monocytes With Clinical Bacteria Isolates

We further examined the role of TLR8 in bacterial sensing using clinical isolates of GBS, *S. aureus*, *S. pneumonia*, *E. coli*, and *P. aeruginosa*. Cytokine production was determined 18 h after initiating the challenge, with two doses and two isolates per species. CU-CPT9a strongly reduced (70–100%) the production of IL-12p70 and IL-1β after challenging the monocytes with the Gram-positive species GBS, *S. aureus*, and *S. pneumonia* (**Figure 2** and **Table 1B**). The inhibitor also clearly antagonized TNF, IL-6, and IL-10 production during Gram-positive infections, whereas the IL-8 levels increased by TLR8-inhibition for the highest bacterial dose. The limited effect of TLR8-inhibitor on the induction of IL-8 release by

TABLE 1 | Percentage reduction in cytokine release by TLR8 inhibition during bacterial challenge of monocytes.

(**A**) Infection with high/low dose of bacteria strains for 6- and 22 h ($N = 4$). The doses were $5 \times 10^6/1 \times 10^6$ per ml for GBS and *S. aureus*, and $1 \times 10^6/2 \times 10^5$ per ml for *E. coli*.

Strain (6 h)	IL-12p70	IL-1β	IL-6	TNF	IL-10	IL-8
GBS NEM316	**100**/**100**	**98**/**99**	**86**/**96**	**78**/**88**	5/**48**	−5/**48**
SAU 113-wt	**100**/**100**	**96**/**97**	**60**/**83**	**48**/**69**	−81/−42	−40/33
SAU 113-*dlgt*	**100**/**100**	**99**/**99**	**91**/**95**	**78**/**86**	−80/−11	−35/**43**
ECO 1946	54/28	29/27	−17/25	−10/20	−30/−27	−56/2
(22 h) GBS NEM316	**100**/**99**	**98**/**99**	**85**/**98**	**75**/**91**	**96**/**98**	–**200**/47
SAU 113-wt	**100**/**100**	**95**/**98**	**61**/**89**	53/**78**	59/**89**	–**215**/23
SAU 113-*dlgt*	**100**/**100**	**99**/**99**	**90**/**98**	**81**/**91**	**97**/**98**	–**242**/46
ECO 1946	77/49	37/35	−14/29	−5/27	−11/33	–**120**/18

(**B**) Infection with high/low dose of clinical bacteria isolates for 18 h ($N = 5$). The doses were $5 \times 10^6/1 \times 10^6$ per ml for the Gram positive bacteria, and $1 \times 10^6/2 \times 10^5$ per ml for the Gram negative species.

Isolate (18 h)	IL-12p70	IL-1β	IL-6	TNF	IL-10	IL-8
GBS 248	**99**/**99**	**98**/**99**	**90**/**96**	**90**/**97**	**93**/**97**	−51/56
GBS 250	**99**/**99**	**99**/**98**	**85**/**91**	**89**/**97**	**92**/**92**	–**134**/36
SAU 17-2	**95**/**100**	**93**/**98**	42/**89**	62/**93**	**81**/**92**	–**324**/−6
SAU 17-3	**93**/**98**	**95**/**97**	48/**86**	65/**89**	**82**/**87**	–**289**/−19
SPN 18-1	**92**/**97**	**70**/**78**	44/**66**	72/**87**	46/**64**	−44/**32**
SPN 38	**98**/**99**	**93**/**91**	67/**69**	**89**/**89**	**75**/**72**	−56/35
ECO 17-1	55/32	35/23	−1/20	−2/46	27/−26	−44/66
ECO 18-1	**81**/58	58/36	−19/24	12/32	−20/−21	−55/32
PSA 17-1	**92**/**93**	**81**/**78**	−5/29	52/60	32/28	–**147**/28
PSA 17-2	**86**/**88**	72/63	−10/20	54/50	39/14	−126/29

(**C**) Infection with *E. coli* isolates (1×10^7-1×10^6-1×10^5 per ml) for 5 h ($N = 8$–10).

Isolate (5 h)	IL-12p70	IL-1β	IL-6	TNF	IL-8
ECO 17-1	81/75/37	**48**/**37**/**34**	**39**/**47**/**42**	**44**/**40**/**34**	**20**/**31**/**25**
ECO 18-1	**87**/**89**/62	**62**/**56**/**42**	**50**/**41**/**48**	**46**/31/21	1/-7/-1

*The values correspond to the data in **Figures 1**, **2**, and **Figures S2**, **S3**, and the effects that are statistical significant ($p < 0.05$) are shown in bold.*

the bacteria reflects the relative weak induction of IL-8 by TLR8 agonist relative to TLR2 or TLR4 agonists (**Figure 1**, **S2**). In addition, IL-8 release is also efficiently released by cell stimulation with complement activation products (16). For the Gram-negative isolates, TLR8 blockade strongly reduced the IL-12p70 (86–93%) and IL-1β production (63–78%) during *P. aeruginosa* challenge. In comparison, CU-CPT9a reduced the cytokine levels less clearly upon challenge with clinical isolates of *E. coli*. Still, the production of IL-12p70 was reduced by up to 81% using CU-CPT9a and the highest dose of ECO 18-1 (**Table 1B**). We also examined the effects of CU-CPT9a during challenge with the *E. coli* isolates for 5 h. This revealed significant and non-redundant contribution of TLR8 to cytokine production during *E. coli* infection. Still, the percentage reduction in cytokine release by blocking TLR8 signaling is less for *E. coli* than for the other bacteria examined, and varies significantly among different strains and isolates of *E. coli*, as well as by the conditions examined (**Table 1C** and **Figure S3**). In conclusion, TLR8 appears as a dominant sensor of the Gram-positive isolates in monocytes, and it also plays a significant role for the detection of the Gram-negative isolates tested here.

Cell Surface TLR Activation Limits TLR8-IRF5 Signaling and Induces a Rapid Loss of IRAK-1 Detection by Immunoblotting

We previously revealed that activation of TLR2 negatively regulates TLR8-TAK-1-IKKβ-IRF5 signaling in monocytes (9). Because *E. coli* is a weak activator of TLR8, we questioned if *E. coli* also can attenuate TLR8. To examine possible interference with TLR8-IRF5 signaling, we stimulated monocytes with CL075, and used *E. coli*, TLR4-, or TLR5- agonist as co-stimuli. CL075 activated TLR8-IRF5 signaling, but LPS and Flagellin did not. With ECO 17-1 infection there was a tendency for increased levels of nuclear IRF5 (**Figure 3A**), which might

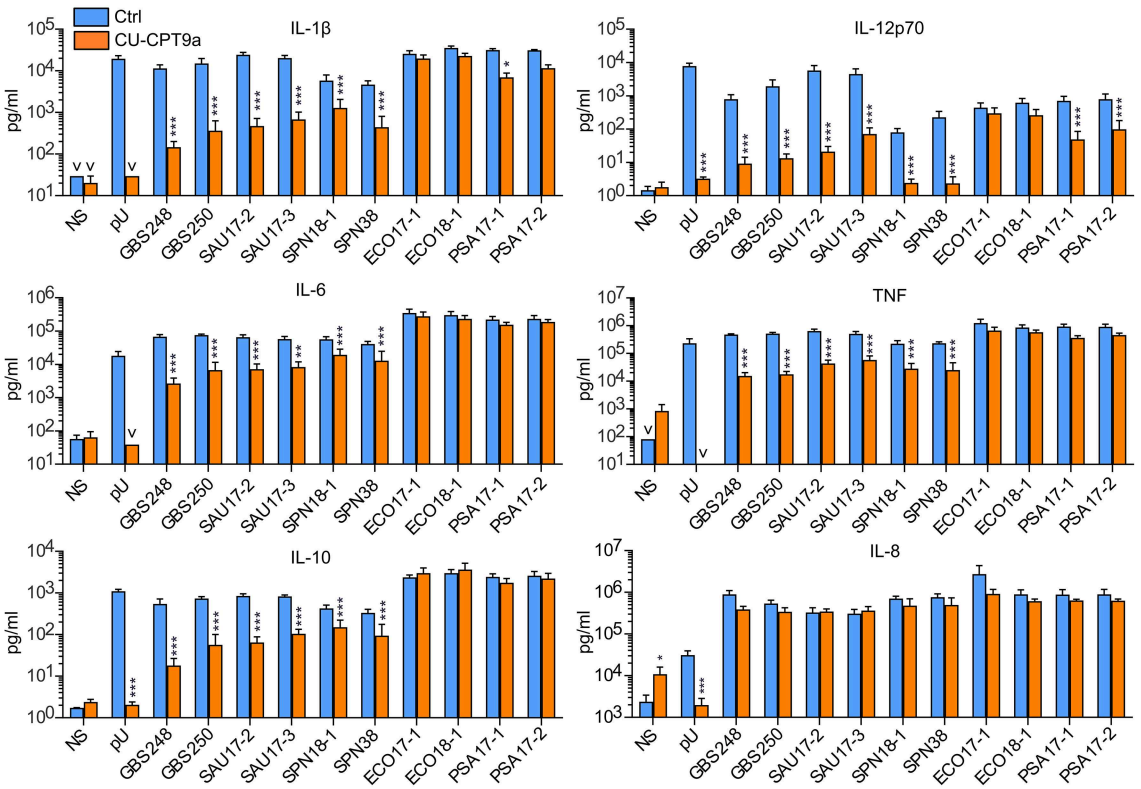

FIGURE 2 | TLR8 inhibition strongly attenuates cytokine production from human primary monocytes challenged with clinical isolates of Gram-positive bacteria, while for the Gram-negative species *P. aeruginosa* (PSA) and *E. coli* this has less effects. Monocytes were pre-treated with control reagent (Ctrl, 5 μM) or TLR8 antagonist (CU-CPT9a, 5 μM) and challenged with TLR8-ligand pU or two clinical isolates of GBS, SAU, *S. pneumonia* (SPN), *E. coli* (ECO), and PSA for 18 h. The dose of Gram-positive bacteria was 1×10^6/ml (MOI 0.1 for GBS, 0.2 for SAU, and 0.5 for SPN). The dose of Gram-negative bacteria was 2×10^5/ml (MOI 0.2). Graphs show mean + SEM ($N = 5$). NS, no stimuli. $^*p < 0.05$, $^{**}p < 0.01$, and $^{***}p < 0.001$.

reflect a low TLR8-agonistic activity of this isolate. In co-stimulation with CL075, all three treatments (LPS, ECO 17-1, and Flagellin) significantly reduced the IRF5 nuclear accumulation (**Figure 3A**). Thus, similar to TLR2 activation (9, 10), signaling by TLR4 and TLR5 in human primary monocytes suppress TLR8-IRF5 signaling. Because *E. coli* expresses ligands for all three TLRs, this could impair TLR8-dependent recognition of this bacterium.

We next questioned if inhibition of TLR8 occurs at the level of proximal TLR signaling, at the Myddosome. Activation of IRF5 by TLR8 is dependent on the catalytic activity of IRAK-4 (17), and we were able to reproduced this finding using a specific IRAK-4 inhibitor (data now shown). We further examined the expression of total IRAK-1, IRAK-2, and IRAK-4 by immunoblotting after treatment with ECO 17-1, GBS or TLR ligands for 30 min. Challenge with ECO 17-1 or LPS triggered a loss of the IRAK-1 protein band that was detected in resting cells, while CL075 apparently had no effect, whether given alone or in combination with LPS or ECO 17-1 (**Figure 3B**). Still, quantification of IRAK-1 revealed a tendency for reduced IRAK-1 levels with CL075, while the levels of total IRAK-2 and IRAK-4 did not change during these conditions (**Figure S4A**). Both LPS and ECO 17-1 triggered phosphorylation of IRF3 at Ser396 (IRF3-P), thus correlating with the loss of the IRAK-1 band (**Figure 3B**). Stimulation with FSL-1 also induced loss of IRAK-1 detection, similar to LPS and ECO 17-1 (**Figure 3C**), even though FSL-1 does not induce IRF3 phosphorylation (10). In contrast to *E. coli*, GBS did not trigger the loss of IRAK-1 detection, and neither GBS nor CL075 influenced the TLR2-effect on IRAK-1. Again, the levels of IRAK-2 and IRAK-4 remained stable for all conditions (**Figure 3C**), while CL075 stimulation gave a tendency toward reduced IRAK-1 signal (**Figure S4B**). We next examined the early time kinetics of surface-TLR-mediated inhibition of TLR8-IRF5 signaling. IRF5 started to accumulate in the monocytes nuclei approximately 15 min after CL075 addition (**Figure 3D**). Co-stimulation with FSL-1 blocked the TLR8-IRF5 signaling already at this early stage. This indicates that TLR2 activation attenuates TLR8-signaling directly, and not via regulation of gene expression, translation, or autocrine/paracrine factors. In comparison to IRF5, CL075 stimulation increased the nuclear level of p65/RelA within 5 min, and co-stimulation with FSL-1 did not reduce but rather increased p65/RelA translocation (**Figure 3D**). Inhibition of TLR8-IRF5 signaling correlated with the rapid loss of IRAK-1 detection, which was observed 15 min after addition of FSL-1 and Flagellin, and 30 min after LPS (**Figure 3E**). We conclude that early signaling by surface TLRs

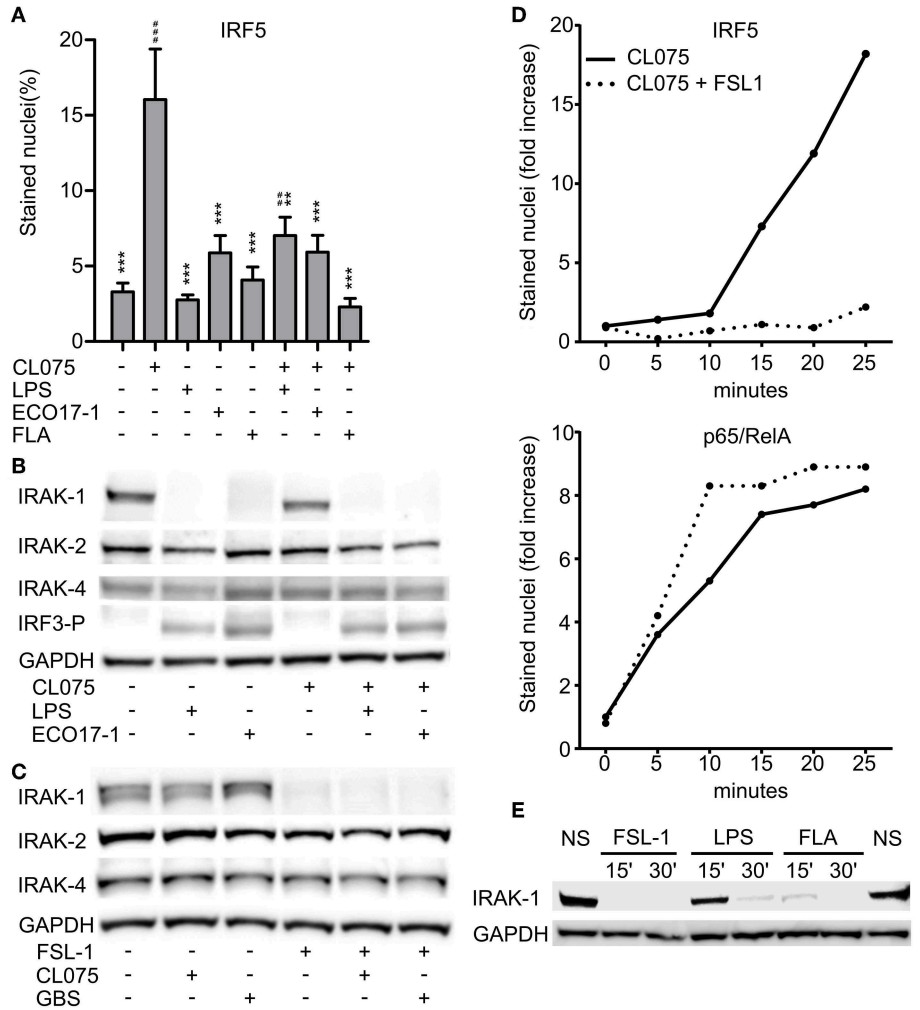

FIGURE 3 | Surface TLR activation antagonize TLR8-IRF5 signaling and triggers a rapid loss of IRAK-1 detection on Western blot. **(A)** Levels of nuclear IRF5 in monocytes stimulated for 2 h with TLR8-agonist CL075 (1 μg/ml), TLR4-agonist LPS (1 μg/ml), ECO 17-1 (1×10^6/ml), or TLR5-agonist Flagellin (FLA, 1 μg/ml) or combinations of these. Quantification of nuclear IRF5 was done by IF and scanR analysis (mean + SEM, $N = 4$).*indicate significant difference from CL075, while #indicate significant difference from no stimuli. $^{\#\#}p < 0.01$, $^{\#\#\#}p < 0.001$, $^{**}p < 0.01$, and $^{***}p < 0.001$. **(B)** Immunoblots of total IRAK-1, IRAK-2, IRAK-4, and IRF3-P after 30 min of treatment with CL075 (1 μg/ml), LPS (1 μg/ml), or ECO 17-1 (1×10^6/ml) alone and in combinations. GAPDH served as a loading control, and a representative of four independent experiments is shown. **(C)** Immunoblots of total IRAK-1, IRAK-2, and IRAK-4 after 30 min of treatment with FLS-1 (100 ng/ml), CL075 (1 μg/ml), or live GBS (5×10^6/ml) alone and in combinations. A representative of four independent experiments is shown. **(D)** Kinetics of IRF5 and p65/RelA nuclear accumulation in monocytes after treatment with CL075 (1 μg/ml) alone or combined with FLS-1 (100 ng/ml). Quantification of IRF5 and p65/RelA positively stained nuclei was done by IF and scanR analysis. A representative of four independent experiments is shown. **(E)** Effects of TLR stimulation for 15 and 30 min on IRAK-1 detection on immunoblot. Cells were untreated (NS) or stimulated with FSL-1 (100 ng/ml), LPS (1 μg/ml), and FLA (1 μg/ml). A representative experiment out of three independent experiments is shown.

differs from TLR8 at the level of IRAK-1, and the close correlation between the loss of IRAK-1 detection and the loss of TLR8-IRF5 activation indicates that the inhibitory crosstalk occurs at the Myddosome level.

IRAK-1 Is Involved in Early TLR8-IRF5 Signaling, but Is Not Strongly and Rapidly Modified as in Surface TLR Signaling

TLR- and IL-1R-signaling can induce depletion of IRAK-1 via proteasomal degradation (18). On the other hand, detection of IRAK-1 on western blots may be lost because hyperphosphorylation and ubiquiylation of IRAK-1 during activation can slow down the migration of IRAK-1 and/or mask the antibody-binding epitopes (19). To clarify if IRAK-1 was degraded in our experimental model, we added the proteasome inhibitor MG132 and challenged the cells with *E. coli* for 60 min. The inhibitor efficiently blocked the degradation of IkBα, but the IRAK-1 band still disappeared (**Figure 4A**). This suggest that IRAK-1 detection is lost from the immunoblots after surface TLR activation due to covalent modifications such as phosphorylation and/or ubiquitination. Higher levels of

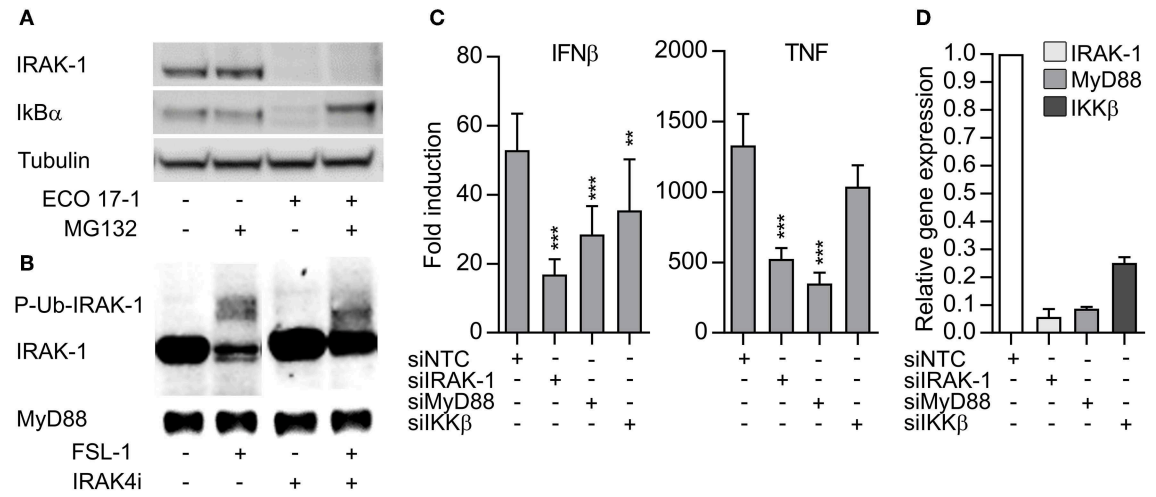

FIGURE 4 | The loss IRAK-1 detection on immunoblot after *E. coli* infection is not caused by proteosomal degradation, and TLR8 signaling is dependent on IRAK-1. **(A)** Monocytes were treated with a proteasome inhibitor (MG132, 20 μM) for 30 min and then infected with ECO 17-1 ($1 \times 10e^6$ bacteria/ml) for 1 h. Total IRAK-1 and IkBα in cell lysates were examined by immunoblotting. Tubulin served as a loading control, and a representative of four independent experiments is shown. **(B)** THP-1 cells were differentiated, pre-incubated with IRAK-4 inhibitor (1 μM) or vehicle control, and stimulated with FSL-1 (100 ng/ml) for 30 min. Immunoblots of total IRAK-1 and MyD88 in lysates are shown in a representative of three independent experiments. **(C)** Human monocyte-derived macrophages (MDMs) were transfected with non-targeting control siRNA (NTC) or siRNA against IRAK1 (siIRAK-1), MyD88 (siMyD88), and IKKβ (siIKKβ). After 6 days, the cells were treated with TLR8 agonist CL075 (1 μg/ml) for 4 h. IFNβ and TNF expression were determined by quantitative PCR. $N = 14$. $^{**}p < 0.01$ and $^{***}p < 0.001$. **(D)** Efficiency of gene silencing in MDMs. The experiment was performed as described above, without agonist treatment ($N = 3$). Graphs show mean + SEM.

IRAK-1 was found in lysates of THP-1 macrophages, and FSL-1 stimulation of these cells for 30 min induced changes in IRAK-1 migration, resulting in the detection of a number of larger IRAK-1 species on the western blots. Moreover, inhibition of the IRAK-4 catalytic activity partially reversed the changes in IRAK-1 migration (**Figure 4B**). These findings support the model of Vollmer et al. (19), where TLR/IL-1R-signaling results in rapid hyperphosphorylation and ubiquitlyation of IRAK-1, resulting in the loss of IRAK-1 detection by immunoblotting with some antibodies. The non-modified IRAK-1 band remained detectable 30 min after CL075 stimulation (**Figures 3B,C**), although there was a tendency toward a decrease (**Figure S4**). This questions whether IRAK-1 is involved or not in the early TLR8 signaling in primary myeloid cells. To clarify this, we silenced IRAK-1 in MDMs using siRNA and examined the effect on TLR8 signaling. Silencing of MyD88 and IKKβ were included as controls. Knockdown of IRAK-1 and MyD88 significantly reduced the induction of IFNβ and TNF after CL075 stimulation for 4 h (**Figure 4C**). IKKβ appeared less efficiently silenced (**Figure 4D**), but the partial silencing still reduced the induction of IFNβ by the TLR8-agonist, in agreement with an essential function of IKKβ in TLR8-IRF5 signaling (9).

E. coli-Induced CD14/TLR4 Signaling Triggers IRAK-1 Modification and Limits TLR8-Dependent Sensing

We next questioned whether *E. coli* evades TLR8 dependent sensing via surface-TLR-signaling that involves IRAK-1 modifications. To clarify the role of TLR4 in this process, we challenged monocytes with an LPS-deficient *E. coli* strain (Clear-Coli, CCO BL21) which does not activate TLR4. CCO BL21 did not activate IRF3 phosphorylation (**Figure 5A**), which confirms that it is an inefficient activator of TLR4. The mutant bacteria did not trigger loss of IRAK-1 detection at the lower doses (1×10^5 and 10^6/ml), while at the higher concentration (1×10^7/ml) it did (**Figure 5A**). Hence, while TLR4 is central for the *E. coli*-induced modification of IRAK-1 at low concentrations of the bacteria, other sensors such as TLR2 and TLR5 might contribute, depending on the strain and conditions.

P. aeruginosa can also be sensed via TLR2, TLR4, and TLR5. Strains from the environment or adapted to laboratory, as well as clinical isolates from bloodstream or urinary tract infections, typically express penta-acylated LPS with low TLR4 agonist activity. In contrast, strains isolated from the airways of cystic fibrosis patients express hexa-acylated LPS that potently activates human TLR4 (20). For most *P. aeruginosa* strains, combined sensing via TLR4 and TLR2 might be important (21, 22). The *P. aeruginosa* isolates used here were from bloodstream- and wound- infections, suggesting that they express penta-acylated LPS. As they also seem to activate TLR8 more efficiently than *E. coli* (**Figure 2**), we questioned if this difference is due to less efficient activation of TLR4-MyD88-IRAK-1 signaling. Indeed, PSA 17-1 (blood culture isolate) did not induce phosphorylation of IRF3, and only triggered IRAK-1 modifications at the highest bacterial dose (**Figure 5B**). Therefore, the relatively strong activation of TLR8 by this bacterium correlates with less efficient signaling via TLR4-TRIF-IRF3 and TLR4-MyD88-IRAK-1.

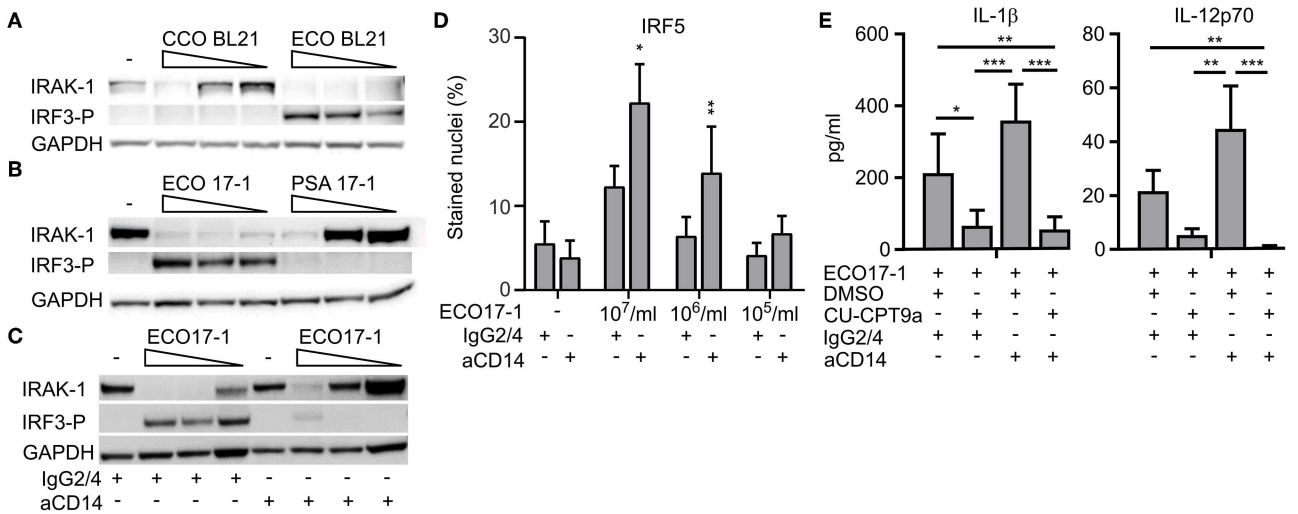

FIGURE 5 | *E. coli* induced loss of IRAK-1 detection by immunoblotting is caused mainly by CD14- and TLR4-activation, and this limits TLR8-dependent sensing of *E. coli*. **(A)** The role of TLR4 in the loss of IRAK-1 detection during infection with *E. coli* was examined using the *E. coli* strain BL21 and its isogenic mutant Clear-Coli (CCO BL21), which does not activate TLR4. Monocytes were infected for 1 h with 1×10^7-1×10^6-1×10^5 bacteria/ml, and the levels of total IRAK-1 and IRF3-P were determined by immunoblotting using GAPDH as loading control. A representative of three independent experiments is shown. **(B)** *E. coli* (ECO 17-1) induces loss of IRAK-1 detection more efficiently than *P. aerugionosa* (PSA 17-1), and correlates with less efficient TLR4-IRF3 activation and more efficient TLR8 activation by the latter species. Infection and immunoblotting were done as described above, and a representative of three independent experiments is shown. **(C)** Effect of a CD14 blocking antibody on *E. coli*-mediated loss of IRAK-1 detection. Monocytes were treated with anti-human CD14 (15 μg/ml) or its isotype control (IgG2/4) 30 min prior to infection. Infection with ECO17-1 and immunoblotting were done as described above, and a representative of three independent experiments is shown. **(D)** Effect of CD14-blocking antibody on ECO 17-1 mediated IRF5-activation. After 30 min of pre-treatment of monocytes with anti-CD14 and control IgG2/4, cells were infected with ECO 17-1 for 2 h. The level of nuclear IRF5 was quantified by IF and scanR imaging. Graphs show mean + SEM ($N = 4$). **(E)** Effect of combined CD14/TLR8 blocking on ECO 17-1-induced production of IL-1β and IL-12p70. Monocytes were pre-treated with anti-CD14, CU-CPT9a, appropriate controls, or combinations thereof for 2 h. Infection with ECO 17-1 (1×10^6/ml) was done for 5 h, and the levels of IL-1β and IL-12p70 produced were determined with BioPlex. Graphs show mean + SEM ($N = 6$). $^*p < 0.05$, $^{**}p < 0.01$, and $^{***}p < 0.001$.

We further examined the role of CD14 in *E. coli*-induced IRAK-1 modification, because CD14 is an important cofactor for both TLR2 and TLR4 (23). After 60 min of challenge with ECO 17-1, the CD14 blocking antibody attenuated the phosphorylation of IRF3 and increased the amount of non-modified IRAK-1 (**Figure 5C**), thus resembling the findings with PSA 17-1 (**Figure 5B**). Anti-CD14 further increased the activation of IRF5 during 2 h of challenge with ECO 17-1 (**Figure 5D**). This indicates that TLR8-dependent sensing of *E. coli* is suppressed by CD14/TLR4-MyD88-IRAK-1 signaling. Finally, anti-CD14 treatment enhanced the release of IL-1β and IL-12p70 during challenge with ECO 17-1 for 5 h, and the production of cytokines were largely TLR8-dependent in this condition, as demonstrated using the TLR8 inhibitor (**Figure 5E**). We conclude that sensing of *E. coli* via CD14/TLR4-IRAK-1 limits its sensing via TLR8.

DISCUSSION

We previously showed a role of TLR8 in the sensing of *S. aureus* (9) and GBS (10) in primary human monocytes and monocyte-derived macrophages, while TLR8 was not involved in the recognition of the *E. coli* strain Seattle 1946 (10). We here confirm and significantly extend these findings using a newly developed TLR8 antagonist with high selectivity and efficiency (14). We show that TLR8 is a dominant sensor of the Gram-positive species *S. aureus*, GBS, and *S. pneumonia* in human primary monocytes. TLR8 also contributes to non-redundant cytokine induction by clinical isolates of *P. aeruginosa* and *E. coli*, although it does not recognize the *E. coli* strain Seattle 1946.

While the impact of TLR8 in bacterial infections *in vivo* still is unclear, we find these new data interesting in the context of human MyD88- and IRAK-4 deficiency, where signaling by most TLRs and IL-1Rs is lost (24). During infancy and early childhood, but not in adulthood, these patients suffer from a strikingly narrow range of pyogenic infections caused by *S. aureus*, *P. aeruginosa*, and *S. pneumonia* (1, 2, 24). Hence, because TLR8 is central in the recognition of these bacteria by monocytes, the loss of TLR8 signaling may explain the increased susceptibility of these patients. Still, we do not know how important TLR8 is in the skin and the airway mucosa, the sites where these infections typically arise. Sensing via TLR2- and IL-1R-dependent mechanisms, may also be important here. Also, the loss of a single TLR is expected to result in incomplete penetrance of the clinical phenotype due to high redundancy and compensatory mechanisms (25). Besides TLRs, peptidoglycan fragments of both Gram positive and Gram negative bacteria can be sensed via the cytosolic sensors NOD1 and NOD2 (26, 27), and numerous studies have revealed that

NOD- and MyD88-dependent signaling typically give synergistic responses (28). Moreover, the release of high levels of IL-1β by monocytes suggests that the bacteria may activate the NLPR3 inflammasome (29). In support of this, it was recently shown that the archaeon *Methanosphaera stadtmanae* is sensed via a TLR8-NLRP3 pathway in human myeloid cells (30). Taken together, we hypothesize that bacterial sensing via TLR8 and TLR2, in combination with IL-1R- and NOD/NLR-signaling, is critical in the defense against pyogenic infections in infants and children. The specific impact of TLR8 for the outcome of the complex host-pathogen interactions will likely vary, depending on genetic- and non-genetic factors of both the host and the pathogen.

We have earlier shown that TLR2 signaling inhibits TLR8-IRF5 activation, but the mechanism is not known (9). We here demonstrate that TLR2 co-stimulation blocks TLR8-IRF5 nuclear accumulation within 15 min. TLR4- and TLR5-agonists have a similar inhibitory effect, resulting in the attenuation of TLR8-IRF5-dependent cytokines release from monocytes, such as IL-12p70. In contrast, stimulation of human monocyte-derived DCs with LPS and R848 for 48 h gave synergistic IL-12p70 production (31). This may imply that the negative TLR4-TLR8-crosstalk in monocytes is overcome during the differentiation to DCs, while the mechanism behind is unknown.

Inhibition of TLR8-IRF5 signaling by surface TLRs correlates with their recruitment and activation of IRAK-1, as revealed by a rapid decline in the amounts of non-modified IRAK-1 with simultaneous appearance of hyperphosphorylated and ubiquitylated IRAK-1 species on western blot (19). In human cells, IRAK-4 is constitutively active and is autophosphorylated during the Myddosome assembly, while IRAK-1 is recruited by IRAK-4 and becomes activated upon dimerization (19). TLR8 does not trigger such rapid and extensive modifications of IRAK-1 as the cell surface TLRs, even though IRAK-1 is involved in TLR8-IRF5 signaling and IFNβ and TNF induction. We find that the IRAK-4 catalytic activity also is critical for TLR8-IRF5 signaling, in agreement with a previous study (17). Hence, IRAK-4-mediated phosphorylation of IRAK-1 may be essential in IRF5 activation. In contrast, inhibition of IRAK-4 catalytic activity only partially reduces NF-kB- and MAPK-signaling in human monocytes and murine macrophages, suggesting that these responses mainly require the structural function of IRAK-4 (17, 32).

The roles of IRAK-1 and IRAK-2 in MyD88-signaling are less clear than IRAK-4, and variable degrees of redundancy have been described in different cells and experimental conditions (19, 33–36). In murine dendritic cells, the catalytic activity of IRAK-1 was needed for TLR7- and TLR9-induced IFNα production (35, 36), while IRAK-2 mainly has a role in sustaining the response (35). In human MDMs and THP-1 cells, TLR-induced TNF release was dependent on IRAK-1 but not IRAK-2 (34). On the other hand, cells from an IRAK-1 deficient patient indicates that IRAK-1 and IRAK-2 are mainly redundant in TLR-induced pro-inflammatory cytokine induction in PBMCs, while IRAK-1 is non-redundant in TLR signaling in fibroblast (33). These results are partly conflicting with our data, which may be due to the different cellular contexts, experimental conditions and readouts. The IRAK-1 deficient PBMCs were stimulated for 36 h with R848 that also activates TLR7. Because pDCs and B-lymphocytes express TLR7 (37), activation of these cells within the PBMC population may have obscured the role of IRAK-1 in TLR8-signaling in monocytes. Also, we earlier showed that TLR7-induced IFNβ production in human monocytes is not affected by TLR2 co-stimulation (9), indicating that TLR7- and TLR8-signaling in monocytes differ. Our results suggest that IRAK-1 is particularly important in the early activation of TLR8-IRF5 signaling and IRF5-dependent cytokine induction, such as induction of IL-12p70 and IFNβ. We therefore propose a model of signaling where cell surface TLRs rapidly recruit and modify most of the IRAK-1 pool in the monocytes, and this may also include the sequestration of MyD88 and/or IRAK-4. This results in attenuation of TLR8-IRF5 signaling and IRF5-dependent cytokine induction (**Figure S5**). Similar to this model, TLR2-signaling suppressed TLR7-, and TLR9-induced IFNα production in murine BMDCs, which also correlated with loss of IRAK-1 detection on western blotting (38).

E. coli activates TLR8 less efficiently compared to the other bacterial species examined, including *P. aeruginosa*. CD14/TLR4-mediated detection of *E. coli* limits TLR8-IRF5 signaling according to the suggested model. In comparison, most *P. aeruginosa* strains activate TLR4 less efficiently, resulting in a more important role of TLR8 in detecting this bacterium. The Gram-positive species examined appear as even weaker activators of surface TLR signaling, and TLR8-dependent sensing is thus dominating. In addition to antagonizing TLR8-IRF5 signaling, cell surface TLRs trigger redundant cytokine production that also reduces the impact of TLR8-mediated bacterial sensing. Still, TLR8 contributed to increased cytokine production in response to the *E. coli* isolates, as most clearly seen for IL-12p70 and IL-1β. Production of these cytokines was also highly TLR8-dependent during infection with the other bacteria. In mice, IL-1β is critical for the resistance against experimental GBS and *S. aureus* infection, likely via IL-1R-mediated chemokine production which recruits neutrophils to the site of infection (39–41). TLR8-induced IL-12 production may be a critical signal for differentiation of follicular Th-cells and for efficient production of antibodies against invading bacteria such as *E. coli*, *Salmonella typhimurium*, and *Mycobacterium tuberculosis* (11). Even so, the functional impact of TLR8 in adaptive immunity in humans *in vivo* is still unclear, and patients with MyD88- or IRAK-4-deficiency appear not to be strongly impaired in antigen-specific T- and B-cell responses (1). Hence, further studies are required to clarify the different aspects of TLR8-mediated immunity and the functional consequences of the TLR-TLR negative crosstalk.

In conclusion, TLR8 is a major bacterial sensor in monocytes, and probably plays a more important role in the defense against bacteria than previously known. TLR8 seems dominant in the sensing of bacteria that avoid efficient activation of TLRs at the cell surface, such as staphylococci and streptococci. On the other hand, strong activation of cell surface TLRs by bacteria such as *E. coli*, limits TLR8 signaling, possibly via competition for Myddosome components. Nevertheless, TLR8

also contributes in the sensing of Gram-negative infections by monocytes.

DATA AVAILABILITY

The datasets generated for this study are available on request to the corresponding author.

ETHICS STATEMENT

Human buffycoats and serum were from the Blood bank at St. Olavs Hospital (Trondheim, Norway), with approval by the Regional Committee for Medical and Health Research Ethics (REC Central, Norway, no. 2009/2245).

AUTHOR CONTRIBUTIONS

SM, BE, JK, and JS planned and performed the experimental work, including cell isolation and cultivation, bacteria preparation and infection experiments. JS initiated the study, performed experiments with the TLR8-inhibitor, the scanR experiments, produced the final figures, and wrote the manuscript with help from SM and BE. SM did the silencing experiments and the immunoblotting. BE performed the experiments with the clinical isolates. JK did the bioplex analyses and contributed in the gene silencing experiments. MY assisted in the work on the signaling mechanisms and the discussion. KB contributed with discussion and interpretation of the work. JA provided the clinical isolates with recommendations for bacterial growth. ZH and HY provided the TLR8-inhibitor and control reagent and recommendations for their use. JD and TE contributed to the conception and interpretation of the work. All authors have read and approved the final version of the manuscript.

FUNDING

This work was funded by The Liaison Committee for education, research and innovation in Central Norway by Grant 90162400 (to JS) and the Research Council of Norway Grant 223255/F50 through its Centers of Excellence funding scheme. In addition, it was funded by the National Natural Science Foundation of China (No. 21825702) (to HY).

ACKNOWLEDGMENTS

The imaging and analyses using the scanR system was carried out at the Cellular and Molecular Imaging Core Facility (CMIC) at the Norwegian University of Science and Technology.

SUPPLEMENTARY MATERIAL

The Supplementary Material for this article can be found online at: https://www.frontiersin.org/articles/10.3389/fimmu.2019.01209/full#supplementary-material

Figure S1 | Efficiency of the TLR8 inhibitor CU-CPT9a in human primary monocytes. **(A)** Monocytes were pre-treated for 2 h with the control compound (Ctrl) or the TLR8 antagonist (CU-CPT9a) at different concentrations. Subsequently, the cells were stimulated with the TLR8-ligands pU/pLA (polyU/poly-L-arginine, 1 μg/ml) and CL075 (1 μg/ml). Supernatant was collected after 6.5 h and cytokine levels were determined with BioPlex. $N = 2$. **(B)** Chemical structure of CU-CPT9a and the control compound.

Figure S2 | TLR8 inhibition strongly attenuates cytokine production from human primary monocytes challenged with Group B streptococcus (GBS) and *S. aureus*, but not a strain of *E. coli*. Cytokine levels were determined after 6 h of bacterial challenge. Bacterial doses were 5×10^6/ml and 1×10^6/ml for GBS and *S. aureus* (MOI 0.5/0.1 for GBS, 1.0/0.2 for SAU), and 1×10^6/ml and 2×10^5/ml for *E. coli* (MOI 1.0/0.2). Graphs show mean + SEM ($N = 4$). NS, no stimuli. $^*p < 0.05$, $^{**}p < 0.01$, and $^{***}p < 0.001$. For additional experimental details, see the **Figure 1** legend.

Figure S3 | TLR8 inhibition significantly reduces cytokine release from human primary monocytes challenged with *E. coli* isolates for 5 h. Cytokine release by monocytes pre-treated with control reagent (DMSO) or TLR8 antagonist (CU-CPT9a, 5 μM) and challenged with three doses of *E. coli* (ECO 17-1 and ECO 18-1): 1×10^7/ml, 1×10^6/ml, and 1×10^5/ml (MOI 10.0, 1.0, and 0.10). Graphs show mean + SEM ($N = 8$–10). NS, no stimuli. $^*p < 0.05$, $^{**}p < 0.01$, and $^{***}p < 0.001$.

Figure S4 | Quantification of the levels of IRAK-1, IRAK-2, IRAK-4, and P-IRF3 on western blot analysis after activation of TLR2, TLR4, or TLR8, *E. coli*, and GBS for 30 min, as indicated. $N = 4$ **(A)** or $N = 3$ **(B)**, and the data correspond to **Figures 3B,C**. $^*p < 0.05$ and $^{**}p < 0.01$.

Figure S5 | Model of TLR-mediated sensing of Gram negative and Gram positive bacteria and negative crosstalk of TLR-signaling. TLR8 is a major sensor of Gram positive bacteria, while cell surface TLRs, in particular TLR4, is most important for sensing of Gram negative species. TLR8-IKKβ-IRF5 signaling in monocytes depends on IRAK-4 kinase activity and IRAK-1. TLR8-IRF5 activation is important for production of IFNβ, IL-12p70, IL-1β, and TNF. Cell surface TLR signaling results in recruitment and modification of IRAK-1 within minutes, and it closely correlates with rapid attenuation of TLR8-IRF5 activation. A possible explanation for this negative crosstalk is the sequestration of the Myddosome-components by the cell surface TLRs.

REFERENCES

1. Picard C, von Bernuth H, Ghandil P, Chrabieh M, Levy O, Arkwright PD, et al. Clinical features and outcome of patients with IRAK-4 and MyD88 deficiency. *Medicine.* (2010) 89:403–25. doi: 10.1097/MD.0b013e3181fd8ec3
2. Picard C, Casanova J-L, Puel A. Infectious diseases in patients with IRAK-4, MyD88, NEMO, or IκBα deficiency. *Clin Microbiol Rev.* (2011) 24:490–7. doi: 10.1128/CMR.00001-11
3. Singer M, Deutschman CSS, Seymour CW, Shankar-Hari M, Annane D, Bauer M, , et al. The third international consensus definitions for sepsis and septic shock (Sepsis-3). *JAMA.* (2016) 315:801–10. doi: 10.1001/jama.2016.0287
4. Marshall JC. Why have clinical trials in sepsis failed? *Trends Mol Med.* (2014) 20:195–203. doi: 10.1016/j.molmed.2014.01.007
5. Ishii N, Funami K, Tatematsu M, Seya T, Matsumoto M. Endosomal localization of TLR8 confers distinctive proteolytic processing on human myeloid cells. *J Immunol.* (2014) 193:5118–28. doi: 10.4049/jimmunol.1401375
6. Tanji H, Ohto U, Shibata T, Taoka M, Yamauchi Y, Isobe T, et al. Toll-like receptor 8 senses degradation products of single-stranded RNA. *Nat Struct Mol Biol.* (2015) 22:109–15. doi: 10.1038/nsmb.2943
7. Liu J, Xu C, Hsu L-C, Luo Y, Xiang R, Chuang T-H. A five-amino-acid motif in the undefined region of the TLR8 ectodomain is required for species-specific ligand recognition. *Mol Immunol.* (2010) 47:1083–90. doi: 10.1016/j.molimm.2009.11.003

8. Zhang ZJ, Guo JS, Li SS, Wu XB, Cao DL, Jiang BC, et al. TLR8 and its endogenous ligand miR-21 contribute to neuropathic pain in murine DRG. *J Exp Med.* (2018) 215:jem.20180800. doi: 10.1084/jem.20180800
9. Bergstrøm B, Aune MHH, Awuh JAA, Kojen JFF, Blix KJJ, Ryan L, et al. TLR8 Senses *Staphylococcus aureus* RNA in human primary monocytes and macrophages and induces IFN-β production via a TAK1-IKKβ-IRF5 signaling pathway. *J Immunol.* (2015) 195:1100–11. doi: 10.4049/jimmunol.1403176
10. Ehrnström B, Beckwith KS, Yurchenko M, Moen SH, Kojen JF, Lentini G, et al. Toll-Like receptor 8 is a major sensor of group b streptococcus but not *Escherichia coli* in human primary monocytes and macrophages. *Front Immunol.* (2017) 8:01243. doi: 10.3389/fimmu.2017.01243
11. Ugolini M, Gerhard J, Burkert S, Jensen KJ, Georg P, Ebner F, et al. Recognition of microbial viability via TLR8 promotes T follicular helper cell differentiation and vaccine responses. *Nat Immunol.* (2018) 19:386–96. doi: 10.1038/s41590-018-0068-4
12. Eigenbrod T, Pelka K, Latz E, Kreikemeyer B, Dalpke AHH. TLR8 senses bacterial RNA in human monocytes and plays a nonredundant role for recognition of *Streptococcus pyogenes*. *J Immunol.* (2015) 195:1092–99. doi: 10.4049/jimmunol.1403173
13. Krüger A, Oldenburg M, Chebrolu C, Beisser D, Kolter J, Sigmund AM, et al. Human TLR 8 senses UR/URR motifs in bacterial and mitochondrial RNA. *EMBO Rep.* (2015) 16:1656–63. doi: 10.15252/embr.201540861
14. Zhang S, Hu Z, Tanji H, Jiang S, Das N, Li J, et al. Small-molecule inhibition of TLR8 through stabilization of its resting state. *Nat Chem Biol.* (2017) 14:58–64. doi: 10.1038/nchembio.2518
15. Stoll H, Dengjel J, Nerz C, Gotz F. *Staphylococcus aureus* deficient in lipidation of prelipoproteins is attenuated in growth and immune activation. *Infect Immun.* (2005) 73:2411–23. doi: 10.1128/Iai.73.4.2411-2423.2005
16. Lappegård TK, Christiansen D, Pharo A, Billmann E, Christian B, Lindstad J, et al. Human genetic deficiencies reveal the roles of complement in the inflammatory network: lessons from nature. *Proc Natl Acad Sci USA.* (2009) 106:15861–6. doi: 10.1073/pnas.0903613106
17. Cushing L, Winkler A, Jelinsky SA, Lee K, Korver W, Hawtin R, et al. IRAK4 kinase activity controls Toll-like receptor induced inflammation through the transcription factor IRF5 in primary human monocytes. *J Biol Chem.* (2017) 292:18689–98. doi: 10.1074/jbc.M117.796912
18. Yamin TT, Miller DK. The interleukin-1 receptor-associated kinase is degraded by proteasomes following its phosphorylation. *J Biol Chem.* (1997) 272:21540–7. doi: 10.1074/jbc.272.34.21540
19. Vollmer S, Strickson S, Zhang T, Gray N, Lee KL, Rao VR, et al. The mechanism of activation of IRAK1 and IRAK4 by interleukin-1 and Toll-like receptor agonists. *Biochem J.* (2017) 474:2027–38. doi: 10.1042/BCJ20170097
20. Hajjar AM, Tsai JH, Wilson CB, Miller SI. Human Toll-like receptor 4 recognizes host-specific LPS modifications. *Nat Immunol.* (2002) 3:354–9. doi: 10.1038/ni777
21. Elson G, Dunn-Siegrist I, Daubeuf B, Pugin J. Contribution of Toll-like receptors to the innate immune response to Gram-negative and Gram-positive bacteria. *Blood.* (2007) 109:1574–83. doi: 10.1182/blood-2006-06-032961
22. Xaplanteri P, Lagoumintzis G, Dimitracopoulos G, Paliogianni F. Synergistic regulation of Pseudomonas aeruginosa-induced cytokine production in human monocytes by mannose receptor and TLR2. *Eur J Immunol.* (2009) 39:730–40. doi: 10.1002/eji.200838872
23. Christiansen D, Brekke OL, Stenvik J, Lambris JD, Espevik T, Mollnes TE. Differential effect of inhibiting MD-2 and CD14 on LPS- Versus whole e. coli bacteria-induced cytokine responses in human blood. *Adv Exp Med Biol.* (2012) 946:237–51. doi: 10.1007/978-1-4614-0106-3_14
24. von Bernuth H, Picard C, Puel A, Casanova J-L. Experimental and natural infections in MyD88- and IRAK-4-deficient mice and humans. *Eur J Immunol.* (2012) 42:3126–35. doi: 10.1002/eji.201242683
25. Casanova JL, Abel L. Human genetics of infectious diseases: unique insights into immunological redundancy. *Semin Immunol.* (2018) 36:1–12. doi: 10.1016/j.smim.2017.12.008
26. Kapetanovic R, Parlato M, Fitting C, Quesniaux V, Cavaillon JM, Adib-Conquy M. Mechanism of TNF induction by heat-killled *Staphylococcus aureus* differ upon the origin of mononuclear phagocytes. *Am J Physiol Cell Physiol.* (2011) 300:C850–9. doi: 10.1152/ajpcell.00187.2010
27. Kim YG, Park JH, Shaw MH, Franchi L, Inohara N, Núñez G. The cytosolic sensors Nod1 and Nod2 are critical for bacterial recognition and host defense after exposure to toll-like receptor ligands. *Immunity.* (2008) 28:246–57. doi: 10.1016/j.immuni.2007.12.012
28. Pashenkov MV, Murugina NE, Budikhina AS, Pinegin BV. Synergistic interactions between NOD receptors and TLRs: mechanisms and clinical implications. *J Leukoc Biol.* (2018) 105:1–12. doi: 10.1002/JLB.2RU0718-290R
29. Man SM, Kanneganti T-D. Regulation of inflammasome activation. *Immunol Rev.* (2015) 265:6–21. doi: 10.1111/imr.12296
30. Vierbuchen T, Bang C, Rosigkeit H, Schmitz RA, Heine H. The human-associated archaeon Methanosphaera stadtmanae is recognized through its RNA and induces TLR8-dependent NLRP3 inflammasome activation. *Front Immunol.* (2017) 8:01535. doi: 10.3389/fimmu.2017.01535
31. Napolitani G, Rinaldi A, Bertoni F, Sallusto F, Lanzavecchia A. Selected toll-like receptor agonist combinations synergistically trigger a T helper type 1 -polarizing program in dendritic cells. *Nat Immunol.* (2005) 6:769–76. doi: 10.1038/ni1223
32. De Nardo D, Balka KR, Gloria YC, Rao VR, Latz E, Masters SL. Interleukin-1 receptor-associated kinase 4 (IRAK4) plays a dual role in myddosome formation and Toll-like receptor signaling. *J Biol Chem.* (2018) 293:15195–207. doi: 10.1074/jbc.RA118.003314
33. Della Mina E, Borghesi A, Zhou H, Bougarn S, Boughorbel S, Israel L, et al. Inherited human IRAK-1 deficiency selectively impairs TLR signaling in fibroblasts. *Proc Natl Acad Sci USA.* (2017) 114:E514–23. doi: 10.1073/pnas.1620139114
34. Sun J, Li N, Oh K, Dutta B, Vayttaden SJ, Lin B, et al. Comprehensive RNAi-based screening of human and mouse TLR pathways identifies species-specific preferences in signaling protein use. *Sci Signal.* (2016) 9:aab2191. doi: 10.1126/scisignal.aab2191
35. Pauls E, Nanda SK, Smith H, Toth R, Arthur JSC, Cohen P. Two phases of inflammatory mediator production defined by the study of IRAK2 and IRAK1 knock-in mice. *J Immunol.* (2013) 191:2717–30. doi: 10.4049/jimmunol.1203268
36. Uematsu S, Sato S, Yamamoto M, Hirotani T, Kato H, Takeshita F, et al. Interleukin-1 receptor-associated kinase-1 plays an essential role for Toll-like receptor (TLR)7- and TLR9-mediated interferon-α induction. *J Exp Med.* (2005) 201:915–23. doi: 10.1084/jem.20042372
37. Hornung V, Rothenfusser S, Britsch S, Krug A, Jahrsdörfer B, Giese T, et al. Quantitative expression of toll-like receptor 1-10 mRNA in cellular subsets of human peripheral blood mononuclear cells and sensitivity to CpG oligodeoxynucleotides. *J Immunol.* (2002) 168:4531–7. doi: 10.4049/jimmunol.168.9.4531
38. Liu YC, Simmons DP, Li X, Abbott DW, Boom WH, Harding C V. TLR2 signaling depletes IRAK1 and inhibits induction of type I IFN by TLR7/9. *J Immunol.* (2012) 188:1019–26. doi: 10.4049/jimmunol.1102181
39. Biondo C, Mancuso G, Midiri A, Signorino G, Domina M, Lanza Cariccio V, et al. Essential role of interleukin-1 signaling in host defenses against group B streptococcus. *MBio.* (2014) 5:1–11. doi: 10.1128/mBio.01428-14
40. Biondo C, Mancuso G, Midiri A, Signorino G, Domina M, Lanza Cariccio V, et al. The interleukin-1β/CXCL1/2/neutrophil axis mediates host protection against group B streptococcal infection. *Infect Immun.* (2014) 82:4508–17. doi: 10.1128/IAI.02104-14
41. Miller LS, O'Connell RM, Gutierrez MA, Pietras EM, Shahangian A, Gross CE, et al. MyD88 mediates neutrophil recruitment initiated by IL-1R but not TLR2 activation in immunity against *Staphylococcus aureus*. *Immunity.* (2006) 24:79–91. doi: 10.1016/j.immuni.2005.11.011

Conflict of Interest Statement: The authors declare that the research was conducted in the absence of any commercial or financial relationships that could be construed as a potential conflict of interest.

frontiers in Immunology

REVIEW
published: 25 June 2019
doi: 10.3389/fimmu.2019.01449

The Role of Adaptor Proteins in the Biology of Natural Killer T (NKT) Cells

*Evelyn Gerth and Jochen Mattner**

Mikrobiologisches Institut - Klinische Mikrobiologie, Immunologie und Hygiene, Universitätsklinikum Erlangen, Friedrich-Alexander Universität (FAU) Erlangen-Nürnberg, Erlangen, Germany

Adaptor proteins contribute to the selection, differentiation and activation of natural killer T (NKT) cells, an innate(-like) lymphocyte population endowed with powerful immunomodulatory properties. Distinct from conventional T lymphocytes NKT cells preferentially home to the liver, undergo a thymic maturation and differentiation process and recognize glycolipid antigens presented by the MHC class I-like molecule CD1d on antigen presenting cells. NKT cells express a semi-invariant T cell receptor (TCR), which combines the Vα14-Jα18 chain with a Vβ2, Vβ7, or Vβ8 chain in mice and the Vα24 chain with the Vβ11 chain in humans. The avidity of interactions between their TCR, the presented glycolipid antigen and CD1d govern the selection and differentiation of NKT cells. Compared to TCR ligation on conventional T cells engagement of the NKT cell TCR delivers substantially stronger signals, which trigger the unique NKT cell developmental program. Furthermore, NKT cells express a panoply of primarily inhibitory NK cell receptors (NKRs) that control their self-reactivity and avoid autoimmune activation. Adaptor proteins influence NKT cell biology through the integration of TCR, NKR and/or SLAM (signaling lymphocyte-activation molecule) receptor signals or the variation of CD1d-restricted antigen presentation. TCR and NKR ligation engage the SH2 domain-containing leukocyte protein of 76kDa slp-76 whereas the SLAM associated protein SAP serves as adaptor for the SLAM receptor family. Indeed, the selection and differentiation of NKT cells selectively requires co-stimulation via SLAM receptors. Furthermore, SAP deficiency causes X-linked lymphoproliferative disease with multiple immune defects including a lack of circulating NKT cells. While a deletion of slp-76 leads to a complete loss of all peripheral T cell populations, mutations in the SH2 domain of slp-76 selectively affect NKT cell biology. Furthermore, adaptor proteins influence the expression and trafficking of CD1d in antigen presenting cells and subsequently selection and activation of NKT cells. Adaptor protein complex 3 (AP-3), for example, is required for the efficient presentation of glycolipid antigens which require internalization and processing. Thus, our review will focus on the complex contribution of adaptor proteins to the delivery of TCR, NKR and SLAM receptor signals in the unique biology of NKT cells and CD1d-restricted antigen presentation.

Keywords: NKT cells, CD1d, adaptor proteins, T cell receptor, NK cell receptor, differentiation, polarization

OPEN ACCESS

Edited by:
Navin Kumar Verma, Nanyang Technological University, Singapore

Reviewed by:
Luc Van Kaer, Vanderbilt University, United States
Paolo Dellabona, San Raffaele Scientific Institute (IRCCS), Italy
Mariolina Salio, University of Oxford, United Kingdom

***Correspondence:**
Jochen Mattner
jochen.mattner@uk-erlangen.de

Specialty section:
This article was submitted to T Cell Biology, a section of the journal Frontiers in Immunology

Received: *16 April 2019*
Accepted: *10 June 2019*
Published: *25 June 2019*

Citation:
Gerth E and Mattner J (2019) The Role of Adaptor Proteins in the Biology of Natural Killer T (NKT) Cells. Front. Immunol. 10:1449. doi: 10.3389/fimmu.2019.01449

INTRODUCTION

Specific and appropriate intercellular interactions or the communication of cells with their environment requires the integration and coordination of multiple signaling pathways. Adaptor proteins contain a series of protein-binding sites that link respective interaction partners to each other and facilitate the generation of larger signaling complexes (1). This is, for example, pivotal for the delivery of signals from the T cell receptor (TCR) which plays a critical role in T cell biology (2).

There exist several T cell populations with distinct functions (3). Alpha beta (αβ) T cells, for example, termed conventional (αβ) T cells, are predominantly part of the adaptive immune system and display a large TCR diversity. TCR ligation by self-peptides embedded in major histocompatibility complex (MHC) molecules on antigen-presenting cells (APCs) in the thymus determines the fate of developing conventional T cells. Weak TCR signals perpetuate positive selection whereas strong, agonist, signals support the removal of potentially self-reactive TCRs through negative selection (4). The resulting diverse TCR repertoire endows conventional T cells to respond to foreign antigens in the periphery upon exit from the thymus. NKT cells can be divided into two distinct subpopulations.

In contrast, mucosa-associated semi-invariant T (MAIT) cells, gamma delta (γδ) T cells and natural killer T (NKT) cells express semi-invariant TCRs with limited diversity and react rapidly to conserved self and/or microbial ligands. Most of these cells acquire memory cell features during thymic maturation and exhibit unique patterns of migration into peripheral, frequently non-lymphoid tissues where they become resident, regulate tissue homeostasis and/or fight infection (5). These innate(-like) T lymphocytes display also several other innate-like characteristics and are therefore considered to be mainly part of the innate immune system. Distinct from conventional T cells, innate(-like) lymphocytes recognize higher affinity and avidity antigens through their TCR, which has been suggested to deliver substantially stronger signals (4, 6). Thus, the TCR signal threshold for negative selection is higher. However, it is not completely understood how unconventional T cell precursors escape negative selection despite agonist signaling. Thus, adaptor proteins might play a pivotal role in the tight control of TCR signals as they tie multiple and complex intracellular pathways. Indeed, some adaptor proteins are specifically important for innate(-like) lymphocytes, and a lack of specific adaptor proteins impairs or even selectively inhibits the selection of these frequently autoreactive cell subsets. In detail, we will discuss here the impact of adaptor proteins on the biology of natural killer T (NKT) cells. We will focus thereby on type 1 or invariant NKT cells, which we will refer to as iNKT cells hereinafter.

NATURAL KILLER T (NKT) CELLS AND CD1D-MEDIATED ANTIGEN PRESENTATION

Natural killer T (NKT) cells belong to the group of innate(-like) unconventional T cells. They explosively release various cytokines and chemokines upon TCR engagement and thus, exhibit powerful immunomodulatory properties. NKT cells can be divided into two distinct lineages, namely type 1 or invariant NKT cells and type 2 NKT cells. Type 2 NKT cells exhibit a more diverse TCR repertoire. In contrast, type 1 or invariant NKT cells—hereinafter referred to as iNKT cells—express a semi-invariant canonical T cell receptor (TCR), which combines the Vα14-Jα18 chain with the Vbeta2, Vbeta7, or Vbeta8 chain in mice and the Vα24-Jα18 chain with the Vβ11 chain in humans. Simultaneously, they carry a wide range of activating and inhibitory NK cell receptors (NKRs) on their surface (7). The inhibitory NKRs presumably control the self-reactivity of iNKT cells and avoid autoimmune activation (8, 9). Vice versa, the NKT cell TCR shapes the pattern of NKR expression, as exemplified for Ly49 receptors (10). Furthermore, balanced signaling through activating and inhibitory NKRs might influence the developmental program of iNKT cells (11). As NKR signaling engages also adaptor proteins, the propagation of signal transduction through adaptor molecules is in particular critical for diverse ranges of cellular processes in iNKT cells.

In contrast to conventional T cells, iNKT cells respond to glycolipid antigens and home predominantly to the liver (12). Unlike the development of conventional T cell, the selection of iNKT cells requires antigen presentation by double-positive thymocytes rather than thymic epithelial cells (13–17). iNKT cells are selected on high-affinity self-glycolipid ligands presented by the MHC class I-like molecule CD1d (18) which triggers their unique developmental program (19). Their selection uniquely requires co-stimulation via SLAM (signaling lymphocyte-activation molecule) family members and the tyrosine kinase Fyn (20–32) as discussed below. Once selected in stage 0, iNKT cells pass through complex activation, expansion, maturation and differentiation processes, termed stages 1–3 (**Figure 1**). These include the induction and regulation of promyelocytic leukemia zinc finger PLZF, the iNKT cell lineage transcription factor, multiple rounds of intrathymic cell divisions, the acquisition of a memory phenotype, the activation of cytokine gene loci, and the expression of multiple NKRs over the course of several weeks (7, 33). Although associated with their development (33, 34), PLZF is not unique to iNKT cells and also expressed in innate lymphoid cells (ILCs), mucosa-associated semi-invariant T (MAIT) cells and subsets of γδ T cells (35–37).

Furthermore, iNKT cells differentiate into three polarized subsets, NKT1, NKT2, and NKT17 cells (38) before egress into the periphery (**Figure 1**). Although TCR signal strength has been implicated in the polarization of the three iNKT cell sublineages and the regulation of PLZF expression (39), the intrathymic branching traits and cellular and molecular mechanisms of sublineage diversification are still under investigation. TCR-specific signals contribute also to the tissue distribution and phenotypic presentation of iNKT cells (40, 41). Although the signal delivered through the iNKT cell TCR is stronger than for the conventional T cell TCR (6, 42–44), the role of the TCR signal strength in iNKT cell lineage commitment and differentiation is still under investigation.

Next to α/β-TCR$^+$ iNKT cells CD1d-restricted γ/δ T cells also respond to (glycol-)lipid antigens (45). These γ/δ NKT cells

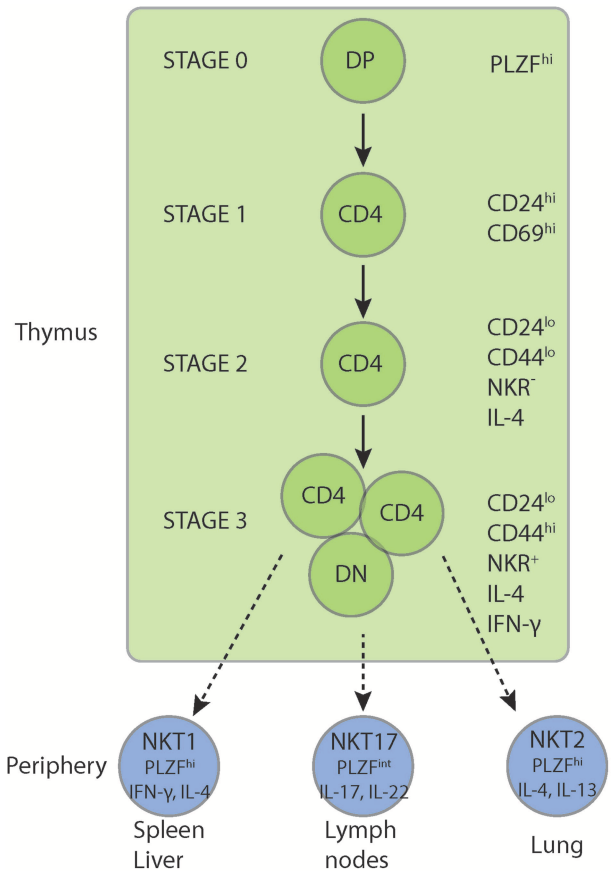

FIGURE 1 | iNKT cell development. iNKT cells express PLZF upon positive selection and undergo a unique intrathymic maturation, expansion, and differentiation program. This includes multiple rounds of intrathymic cell divisions, the acquisition of a memory phenotype, the activation of Th1, Th2 and Th17 cytokine genes and the expression of a panoply of NKRs**.** Furthermore, iNKT cells branch into three polarized subsets, NKT1, NKT2, and NKT17 cells before egress into the periphery. In the periphery NKT1 cells home preferentially to the spleen and liver while NKT2 and NKT17 cells mainly populate the lung and peripheral lymph nodes, respectively. Although TCR signal strength has been implicated in the polarization of the three iNKT cell sublineages and the regulation of PLZF expression, the intrathymic branching traits and cellular and molecular mechanisms of sublineage diversification are still under investigation. NKR, NK lineage receptors including NK1.1, Ly49, NKG2D, CD94, DX5; PLZF, promyelocytic leukemia zinc finger.

express γ1.1 and δ6.3 chains and the promyelocytic leukemia zinc finger *(*PLZF*),* the lineage transcription factor of NKT cells. Further comparisons of γ/δ- with α/β-TCR expressing NKT cells revealed also converging patterns of cytokine, gene and cell surface marker expression implying similar differentiation programs in both NKT cell subsets (33, 34, 37, 46–48). Thus, several observations obtained with α/β-TCR$^+$ iNKT cells, might be reflected in the biology of CD1d-restricted γ/δ T cells.

Another feature of iNKT cells distinct from conventional T cells is the recognition of glycolipid antigens presented by CD1d. CD1d molecules are assembled in the endoplasmatic reticulum (ER) as non-covalently linked heterodimers of an isotype-specific heavy chain and β-2-microglobulin (β2m). During its assembly in the ER, CD1d incorporates endogenous lipids and traffics to the plasma membrane. While certain lipids can load onto CD1d directly at the cell surface, CD1d with its hydrophobic binding groove of intermediate size usually has to recycle into late endosomal and lysosomal compartments for efficient antigen exchange and loading (49, 50). Upon trafficking back to the cell surface, antigens are presented by CD1d to NKT cells (51, 52).

ADAPTOR PROTEINS IN INKT CELL BIOLOGY

Adaptor molecules are multi-domain proteins lacking intrinsic catalytic activity, functioning instead by nucleating molecular complexes during signal transduction (53). Several adaptor proteins influence iNKT cell selection, differentiation and activation, either intrinsically or indirectly through interference with CD1d-mediated antigen presentation. For example, one of the pivotal molecules engaged upon TCR ligation is the intracellular adaptor protein slp-76. While the complete absence of slp-76 (54–56) or of its N-terminal region (57) leads to a lack of all peripheral T cell populations, selective mutations in the SH2 domain of slp-76 affect in particular iNKT cells (58). Most importantly and in strict contrast to conventional T cells, the selection of iNKT cells requires co-stimulation via SLAM (signaling lymphocyte-activation molecule) family members (20–24). Thus, the SLAM-associated adaptor protein (SAP) signaling pathway is selectively required for iNKT cell development. Adaptor proteins, however, can also influence CD1d expression by antigen presenting cells (APCs) and subsequently affect iNKT cell biology in an extrinsic manner. Adaptor protein complex 3 (AP-3), for example, is required for the efficient presentation of glycolipid antigens that require internalization and processing (59).

The slp-76 Family of Adaptor Proteins

The slp-76 family of adaptors includes the SH2 domain-containing leukocyte phosphoprotein of 76 kDa (slp-76), the B cell linker protein (BLNK), and the cytokine-dependent hematopoietic cell linker (Clnk) (53). All three proteins interact with similar but not identical signaling molecules and are critical for the integration of multitudinous signal cascades downstream of immunotyrosine-based activation motif (ITAM)-bearing receptors and integrins in various hematopoietic cell populations (60). Slp-76 is expressed in T cells, monocytes/macrophages, NK cells, mast cells and platelets (61, 62). BLNK reflects the slp-76 homolog in B cells. It shares about a 33% amino acid identity, but some of its structural domains are similar to those of slp-76 (60, 63, 64). BLNK is primarily responsible for the transmission of signals through the B cell receptor (BCR). CLNK is selectively expressed in various hematopoietic cells following cytokine stimulation (65).

The SH2 Domain-Containing Leukocyte Phosphoprotein of 76 kDa, Slp-76

Of these three family members primarily slp-76 is pivotal for T cell development and TCR signaling (61, 62). Due to impaired signals from the pre-TCR, double negative 3 (DN3) T cells

cannot transform into the double negative 4 (DN4) stage (54, 55, 57). Consequently, slp-76$^{-/-}$ mice lack all peripheral mature T cells (57).

The divergent functions of slp-76 are mediated by its distinct signaling domains (**Figure 2**). The N-terminal acidic domain contains three tyrosine residues (66) which become phosphorylated by the protein tyrosine kinase ZAP-70 upon TCR ligation (67, 68) and subsequently bind the SH2 domains of the guanine nucleotide exchange factor Vav (68–70), the adaptor protein Nck (71, 72) and the Tec-family kinase Itk (73, 74). The deletion of this N-terminal region (57) leads to a lack of all peripheral T cell populations, similar as the complete knockout of slp-76 protein (54, 55, 57). Of these three binding partners in particular Itk affects the development, maturation, cytokine production and survival of NKT cells (75–79). Itk-deficiency affected thereby not only α/β-TCR-, but also γ/δ-TCR-expressing NKT cells which in particular affect the control of Th2 responses and IgE production (80).

The central proline-rich domain of slp-76 interacts with the phospholipase PLCγ-1 (81) and the adaptor molecule GADS (Grb2-related adaptor downstream of Shc) (82). For none of these two molecules a role in NKT cell biology has been established so far.

The C-terminal SH2 domain of slp-76 binds to the serine-threonine kinase HPK-1 (hematopoietic progenitor kinase 1) (83) and to the adhesion and degranulation-promoting adaptor protein (ADAP) (84, 85). ADAP is required for thymocyte selection and TCR-mediated integrin activation (86–88). Thus, slp-76 interferes with inside-out and outside-in signaling cascades and integrin-expression (89) due to its multipoint binding with ADAP (90).

A missense mutation within the SH2-domain of slp-76 led to an accumulation of iNKT cells in the thymus and in peripheral lymph nodes. In contrast, iNKT cells were selectively reduced in the spleens and livers of mice with the same mutation, along with a reduced cytokine response, decreased levels of ADAP protein and altered integrin and NKR expression patterns (58). Although TCR signals were affected by these mutations, NKRs might contribute to the observed phenotype as this mutation affected also synapse formation and elimination of missing-self targets by natural killer (NK) cells (91). In this context, it is important to note that the tyrosine protein phosphatase SHP-1 dephosphorylates its direct substrate slp-76 (92), which reflects an important mechanism for the negative regulation of immune cell activation by inhibitory NKRs. Further studies need to delineate the mechanisms underlying the altered pattern of NKR expression in mice with this slp-76 mutation and the role of TCR signals in these processes. In addition, the specificity of this mutation for iNKT cells needs to be characterized in further detail by assessing the alterations in subsequent signaling pathways and by screening additional slp-76 mutations. Interestingly, despite exhibiting an NKR distribution that has been associated with enhanced Th1 polarization (7, 38), a simultaneous reduction of both IL-4- and IFN-γ-expression along with a reduced TCR-reactivity was observed in iNKT cells carrying this missense mutation within the SH2-domain of slp-76 (58). Thus, variations in the tissue distribution rather than the cytokine polarization are to be considered in patients with allelic mutations in TCR signaling molecules before pursuing vaccination strategies involving α-GalCer, the prototypical iNKT cell ligand as an adjuvant.

The Cytokine-Dependent Hematopoietic Cell Linker (clnk)

Next to cytokine driven expression clnk plays a role in Fc-epsilon R1-mediated mast cell degranulation, B cell receptor (BCR) and TCR signaling (60, 65). While not found in resting T cells, clnk is abundantly expressed in previously activated T cells (65). Similar to slp-76, clnk consists of a tyrosine- and proline-rich amino-terminal basic domain, an SH2 domain and a carboxy-terminal tail (60). While the SH2 domains of slp-76 and clnk exhibit the highest degree of homology within their SH2 domains the sequence variations outside this region suggest that clnk might not be phosphorylated by ZAP-70 and does not associate with Vav, Nck, or GADS. Clnk can rescue TCR signals in slp-76-deficient T cells (65), but clnk itself is dispensable for T cell function and differentiation (93). Clnk might contribute to the coordination of antigen-receptor signaling and cytokine stimulation. Interestingly, clnk might mediate diverse or even opposite signals by TCRs and NKRs as it promotes iNKT cell responses, but impairs NK cell function (94). Thus, clnk might function as a molecular switch, which controls diverse immune responses in different cell populations.

Signaling Lymphocytic Activation Molecule (SLAM) and Signaling Lymphocytic Activation Molecule-Associated Protein (SAP)

The signaling lymphocytic activation molecule (SLAM) family of cell surface receptors comprises six members named 2B4 (CD244), Ly9 (CD229), CRACCSLAM (CD150), CD84, and Ly108 (95, 96) which are exclusively expressed on hematopoietic cells. They represent homophilic receptors with the exception of 2B4, which recognizes CD48. SLAM family receptors possess an extracellular segment with two or four immunoglobulin-like domains responsible for ligand recognition, a single transmembrane region and a cytoplasmic domain. This cytoplasmic domain bears one to three inhibitory or activating immunoreceptor tyrosine-based switch motifs (ITSMs) (97).

Signaling lymphocytic activation molecule (SLAM)-associated proteins (SAPs) are adaptor molecules which contain Src homology 2 (SH2) domains. SAPs are expressed in T cells, NK cells, and iNKT cells. The SAP family of adaptors includes three members most commonly known as SAP (also named SH2D1A), Ewing's sarcoma-associated transcript-2 (EAT-2; also named SH2D1B1) and EAT-2-related transducer (ERT; also named SH2D1B2) (98). Mutations in the SAP (SH2D1A) gene located on chromosome X are responsible for X-linked lymphoproliferative disease (XLP), characterized by higher susceptibility to Epstein-Barr virus (EBV) infection, B cell lymphomas, severe immune dysregulation, a nearly complete loss of iNKT cells and an impaired humoral immunity (22, 23, 99–102). The correlation of an augmented susceptibility to EBV infections with the lack of

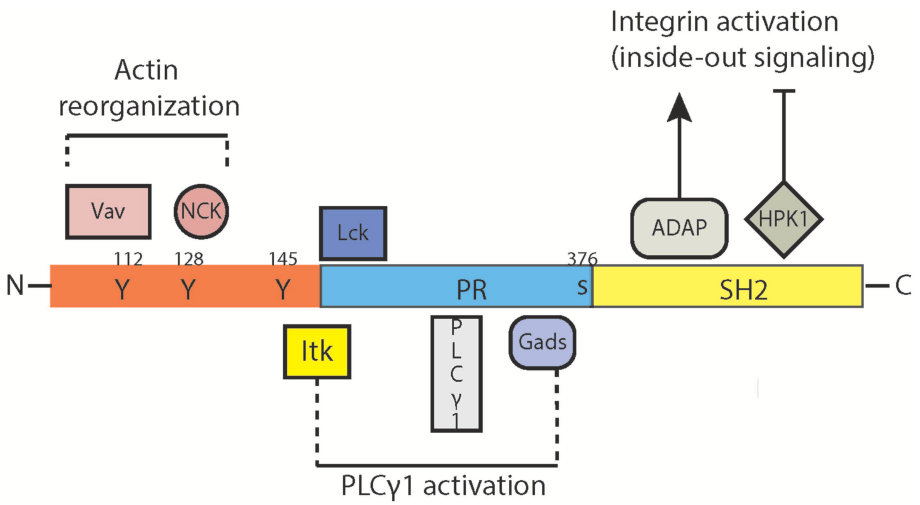

FIGURE 2 | Signaling domains of slp-76. SLP76 (SRC homology 2 (SH2)-domain-containing leukocyte protein of 76 kDa) contains inducibly phosphorylated tyrosines in the amino (N) terminus, a central proline-rich (PR-) domain and a carboxy (C)-terminal SH2 domain. The N-terminal acidic domain binds to the SH2 domains of the guanine nucleotide exchange factor Vav, the adaptor protein Nck and the Tec-family kinase Itk. The subsequent signaling pathways influence predominantly the reorganization of actin. This domain of slp-76 interacts also with the phosphatidylinositol 3-kinases (PI3K) which interfere with multiple cellular functions such as proliferation, differentiation and survival. The central proline-rich domain of slp-76 interacts with the phospholipase PLCγ-1 and the adaptor molecule GADS (Grb2-related adaptor downstream of Shc). The C-terminal SH2 domain of slp-76 binds to the serine-threonine kinase HPK-1 (hematopoietic progenitor kinase 1) and to the adhesion and degranulation-promoting adaptor protein (ADAP), two molecule associated with the formation of the immunological synapse, integrin activation/expression and inside-out and outside-in signaling cascades. ADAP, adhesion- and degranulation-promoting adaptor protein; GADS, GRB2-related adaptor protein; GRB2, growth-factor-receptor-bound protein 2; HPK1, hematopoietic progenitor kinase 1; ITK, interleukin-2-inducible T-cell kinase; Lck, lymphocyte-specific protein tyrosine kinase; NCK, non-catalytic region of tyrosine kinase; PLCγ1, phospholipase Cgamma1; PI3K, phosphatidylinositol 3-kinase; PR, proline-rich; Vav, guanine nucleotide exchange factor.

iNKT cells together with the observation that the SLAM family receptor 2B4 exhibits defect signaling function in SAP-deficiency (103–105) suggest a key role for iNKT cells and SLAM family receptors in the immune response to EBV.

SAP family adaptor proteins respond through their SH2 domains to the cytoplasmic domains of SLAM family receptors by recruiting and activating the downstream tyrosine kinase Fyn (**Figure 3**) (106). However, SLAM family receptors can also signal through other SH2 domain–containing molecules such as the protein tyrosine phosphatases SHP-1 and SHP-2 or the SH2 domain inositol phosphatase 1 (SHIP-1), particularly in SAP deficiency (25, 97, 101, 107–111). While SAP-dependent SLAM family receptor signaling is pivotal for the selection of iNKT cells, these receptors inhibit SAP-independently follicular helper T cells and humoral immune responses (25).

iNKT cells are known to use unique signaling pathways (26). Fyn, for example, is required for iNKT cell development, but not for the differentiation of conventional T lymphocytes or NK cells (20, 21). The loss of SAP resulted in a complete absence of iNKT cells from both mice and humans. SAP-transmitted signaling events were uniquely required for the development of iNKT cells, as conventional T cells and NK cells developed normally in the absence of SAP (22, 23). The selection of iNKT cells also strictly requires co-stimulation via SLAM (signaling lymphocyte-activation molecule) family members (20–24). Homotypic interactions involving the SLAM family receptors 1 and 6 are required for iNKT cell differentiation (24). While SAP deficiency blocks positive selection at stage 0, the most immature stage of iNKT cell development (22, 23), mice lacking SLAM receptors exhibit less pronounced iNKT cell defects that appear to spare stage 0 iNKT cells (24, 25). Indeed, unlike SAP, SLAM family receptors promoted iNKT cell development and intrathymic maturation due to the restriction of TCR signal strength following positive selection and the limitation of activation induced cell death (27). This process involves the adaptor SAP-kinase Fyn complex and the protein tyrosine phosphatases SHP-1. Thus, this study uncovers important differences in SAP and SLAM signaling and highlights the complex processes underlying iNKT cell maturation and survival (112) as auto-reactive iNKT cell activation during thymic selection is thought to induce a substantially stronger TCR stimulus in comparison to that during the development of conventional T cells (6, 113). As a consequence the expression of the transcription factors Egr1 and Egr2 is strongly increased (113), which in turn directly induce PLZF, the key transcription factor controlling iNKT cell differentiation, migration, and functions (113). SAP regulates also cytokine production, expression of transcription factors, the polarization of iNKT cells favoring the development of NKT2 cells and the formation of the immunologic synapse (28, 114, 115). Furthermore, SAP expression in iNKT cells promotes cognate help to B cells (116, 117). Thus, the SLAM-associated adaptor protein (SAP) signaling pathway is selectively required for iNKT cell development and the loss of iNKT cells has been suggested

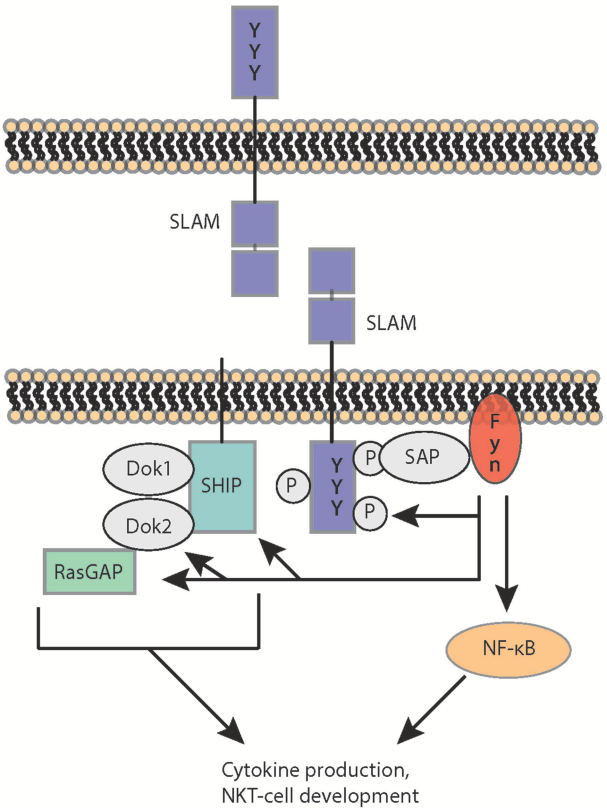

FIGURE 3 | SLAM receptor signaling. SLAM receptor ligation recruits and activates via SAP the protein tyrosine kinase FYN, which phosphorylates SLAM and subsequently generates docking sites for SRC homology 2 (SH2)-domain-containing downstream adaptor proteins and enzymes. SLAM engagement also cooperates with TCR-mediated signals leading to nuclear factor-κB (NF-κB) activation, cytokine production and NKT cell development. DOK1 and 2, docking proteins 1 and 2; RasGAP, RAS–GTPase-activating protein; SAP, Signaling lymphocytic activation molecule (SLAM)-associated proteins; SLAM, signaling lymphocytic activation molecule; SHIP, SH2-domain-containing inositol−5′ phosphatase.

to contribute to the genesis of the lethal immunodeficiency syndrome. The need for SAP-mediated signals may reflect the unique requirements for the positive selection of iNKT cells in the thymus. However, several questions remain unresolved. For example, the role of individual SLAM family receptors in cytokine polarization and iNKT cell differentiation needs to be characterized in more detail as well as the impact of subsequent signaling cascades and their interference with NKRs and TCRs. In addition, it is still unknown, whether and how TCR and SLAM family receptors interfere on a cellular and molecular level and why this is specific for iNKT cells.

Adaptor Protein-3 (AP-3)

The hetero-tetrameric AP (adaptor protein) complexes are involved in the sorting of cargo proteins into transport vesicles that traffic between the different organelles of the cell. They are known to bind to the tyrosine or dileucine-containing sequence motifs in transmembrane proteins in order to direct their selective localization to subsets of endosomal and lysosomal compartments (118, 119). Five members, AP-1 to AP-5 and their isoforms have been characterized in this family of cytosolic complexes (118–120). In contrast to AP-4 and-5, AP-1,-2, and-3 are clathrin-associated complexes (121). AP-1 and AP-2 direct proteins from the trans-Golgi network to endosomes and recycling compartments, respectively (122, 123). AP-3 localizes membrane proteins to lysosomes, platelet-dense granules, and melanosomes (124). AP-3-deficient mice as well as Hermansky-Pudlak syndrome type 2 (HPS-2) patients with mutations in the *AP-3* gene exhibited hypopigmentation and platelet dysfunction (125–129). AP-4 mediates vesicle trafficking from the *trans*-Golgi network to endosomes or the basolateral plasma membrane. The function of AP-5 localized in late endosomes is largely unknown (121). To date, there have been no interactions between AP-1, AP4, and AP-5 with CD1d described. However, CD1d directly interacts with AP-2, which targets the endosomal compartment, and AP-3, which targets the lysosomal compartment (59, 130). Indeed, AP-2 restrains iNKT cell activation due to the regulation of CD1d internalization (131), and a connection of AP-2 with autophagy as a regulator of iNKT cell activation, development and survival is currently under investigation. In this context, a deletion of the essential autophagy gene *Atg7* abrogated thymic iNKT cell development and peripheral iNKT cell functions in a cell-intrinsic manner (132, 133). Unexpectedly, however, *Atg7*-deficient thymocytes and bone marrow-derived DCs exhibited no defect in the presentation of glycolipid antigens, implying distinct differences in the mechanisms how AP-2 and autophagy genes affect iNKT cell development and activation that need to be dissected in the future.

In contrast, numerous studies have investigated the interaction of AP-3 and CD1d. Since CD1d recycles between the cell membrane and the lysosome back and forth, AP-3 interferes with glycolipid metabolism and CD1d-mediated (glyco-)lipid antigen presentation (134). Indeed, it was shown that AP-3 is required for the efficient presentation of glycolipid antigens that require internalization and processing (59, 135). AP-3 interacts with CD1d, but does not affect MHC II presentation (59, 135–137). Cells from AP-3-deficient mice show increased cell surface expression of CD1d but decreased expression in late endosomes. Consequently, AP-3-deficient splenocytes present glycolipids to iNKT cells less efficiently. Furthermore, AP-3–deficient mice exhibit significantly reduced iNKT cell numbers. The simultaneous analysis of CD1d mutants with alterations in the cytoplasmic tail to AP-3-knockout mice proved also that CD1d molecules in lysosomes are functional in antigen presentation (59, 130). iNKT cell numbers are reduced in patients with Hermansky-Pudlak syndrome type 2 (HPS-2) (138) and iNKT cell defects have been also associated with the susceptibility to infections and lymphoma in patients with this homozygous genomic AP-3 deletion (139). Thus, in summary these studies showed that the localization of CD1d to late endosomes or lysosomes is required for both (glycol-)lipid antigen presentation and the subsequent development of iNKT cells. These reports also demonstrated that different pathways mediate the intracellular trafficking of MHC II and CD1 molecules, which both scavenge late endosomes or lysosomes.

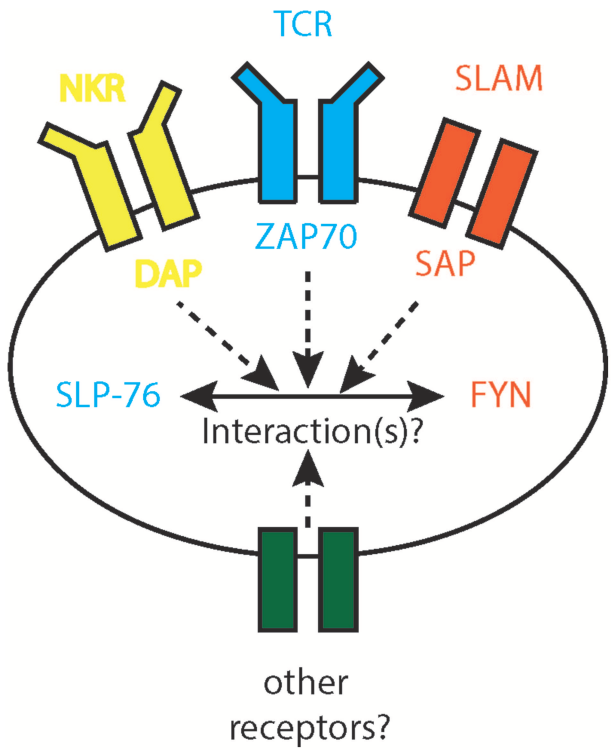

FIGURE 4 | Interactions of SAP and slp-76. SLAM receptor signaling cooperates with TCR and NKR signals. While TCR and NKR signal through slp-76, SLAM receptors utilize SAP and Fyn. It is unknown to date whether slp-76 and SAP interact, whether these three receptor classes combine slp-76 and SAP signals and whether other receptors share similar signaling pathways. DAP, DNAX activation adaptor protein; Fyn, SRC family tyrosine kinase; NKR, NK cell receptor; SAP, Signaling lymphocytic activation molecule (SLAM)-associated proteins; SLAM, signaling lymphocytic activation molecule; slp-76, SRC homology 2 (SH2)-domain-containing leukocyte protein of 76 kDa; TCR, T cell receptor; ZAP-70, zeta-chain associated protein kinase 70.

CONCLUSION

Adaptor proteins play a pivotal role in the biology of CD1d-restricted iNKT cells. SAP transfers SLAM receptor signals, propagates the thymic selection of iNKT cells and induces the iNKT cell effector program (33). The SH2 domain of slp-76 influences the tissue distribution and phenotype of iNKT cells in the periphery (58). AP-3 interferes with the presentation of glycolipid antigens by CD1d (59). Thus, these three adaptor proteins engage unique functions in iNKT cells biology distinct from conventional T lymphocytes. Particularly the expression of SAP and slp-76 in iNKT cells raises the question whether these two molecules interact (**Figure 4**). As SLAM receptors, NKRs and TCRs share adaptor proteins for signal transmission (140, 141), it will be interesting to define the contribution of the respective receptors to the observed phenotypes. Another interesting candidate to investigate in this context is the protein tyrosine kinase SHP-1 since it also interferes with all three receptor classes (111, 116, 142–144) and localizes with slp-76 and fyn in lipid rafts (145–147), even though evidence of physical interactions of these three molecules in iNKT cells is missing. As the strength of the TCR signals influences the polarization of iNKT cell subsets (39), the role of adaptor proteins in fine-tuning intracellular signal transduction is to characterize. In addition, as SLAM receptors are pivotal for the induction of the iNKT cell lineage transcription factor PLZF (33) and PLZF expression negatively correlates with the glycolytic potential of iNKT cells (148) potential connections between adaptor proteins and iNKT cell metabolism need to be identified.

AUTHOR CONTRIBUTIONS

EG prepared the figures and added comments to the manuscript. JM wrote the manuscript.

FUNDING

This study was supported by the Staedtler Stiftung (to JM), the German Research Foundation DFG (grant MA 2621/4-1 to JM and DFG-CRC1181—project number C04 to JM).

ACKNOWLEDGMENTS

We thank all the present members of our lab for their support and their contributions.

REFERENCES

1. Flynn DC. Adaptor proteins. *Oncogene*. (2001) 20:6270–2. doi: 10.1038/sj.onc.1204769
2. Peterson EJ, Clements JL, Fang N, Koretzky GA. Adaptor proteins in lymphocyte antigen-receptor signaling. *Curr Opin Immunol*. (1998) 10:337–44. doi: 10.1016/S0952-7915(98)80173-8
3. Edholm ES, Banach M, Robert J. Evolution of innate-like T cells and their selection by MHC class I-like molecules. *Immunogenetics*. (2016) 68:525–36. doi: 10.1007/s00251-016-0929-7
4. Moran AE, Hogquist KA. T-cell receptor affinity in thymic development. *Immunology*. (2012) 135:261–7. doi: 10.1111/j.1365-2567.2011.03547.x
5. Legoux F, Salou M, Lantz O. Unconventional or preset alphabeta T cells: evolutionarily conserved tissue-resident T cells recognizing nonpeptidic ligands. *Annu Rev Cell Dev Biol*. (2017) 33:511–35. doi: 10.1146/annurev-cellbio-100616-060725
6. Moran AE, Holzapfel KL, Xing Y, Cunningham NR, Maltzman JS, Punt J, et al. T cell receptor signal strength in Treg and iNKT cell development demonstrated by a novel fluorescent reporter mouse. *J Exp Med*. (2011) 208:1279–89. doi: 10.1084/jem.20110308
7. Bendelac A, Savage PB, Teyton L. The biology of NKT cells. *Annu Rev Immunol*. (2007) 25:297–336. doi: 10.1146/annurev.immunol.25.022106.141711
8. Bendelac A, Bonneville M, Kearney JF. Autoreactivity by design: innate B and T lymphocytes. *Nat Rev Immunol*. (2001) 1:177–86. doi: 10.1038/35105052
9. Kronenberg M, Rudensky A. Regulation of immunity by self-reactive T cells. *Nature*. (2005) 435:598–604. doi: 10.1038/nature03725

10. Skold M, Stenstrom M, Sidobre S, Hoglund P, Kronenberg M, Cardell S. MHC-dependent and -independent modulation of endogenous Ly49 receptors on NK1.1+ T lymphocytes directed by T-cell receptor type. *Immunology*. (2003) 110:313–21. doi: 10.1046/j.1365-2567.2003.01741.x
11. Voyle RB, Beermann F, Lees RK, Schumann J, Zimmer J, Held W, et al. Ligand-dependent inhibition of CD1d-restricted NKT cell development in mice transgenic for the activating receptor Ly49D. *J Exp Med*. (2003) 197:919–25. doi: 10.1084/jem.20021615
12. Mattner J. Natural killer T (NKT) cells in autoimmune hepatitis. *Curr Opin Immunol*. (2013) 25:697–703. doi: 10.1016/j.coi.2013.09.008
13. Bix M, Coles M, Raulet D. Positive selection of V beta 8+ CD4-8- thymocytes by class I molecules expressed by hematopoietic cells. *J Exp Med*. (1993) 178:901–8. doi: 10.1084/jem.178.3.901
14. Bendelac A, Killeen N, Littman DR, Schwartz RH. A subset of CD4+ thymocytes selected by MHC class I molecules. *Science*. (1994) 263:1774–8. doi: 10.1126/science.7907820
15. Ohteki T, MacDonald HR. Major histocompatibility complex class I related molecules control the development of CD4+8- and CD4-8- subsets of natural killer 1.1+ T cell receptor-alpha/beta+ cells in the liver of mice. *J Exp Med*. (1994) 180:699–704. doi: 10.1084/jem.180.2.699
16. Bendelac A. Positive selection of mouse NK1+ T cells by CD1-expressing cortical thymocytes. *J Exp Med*. (1995) 182:2091–6. doi: 10.1084/jem.182.6.2091
17. Coles MC, Raulet DH. NK1.1+ T cells in the liver arise in the thymus and are selected by interactions with class I molecules on CD4+CD8+ cells. *J Immunol*. (2000) 164:2412–8. doi: 10.4049/jimmunol.164.5.2412
18. Gapin L, Godfrey DI, Rossjohn J. Natural Killer T cell obsession with self-antigens. *Curr Opin Immunol*. (2013) 25:168–73. doi: 10.1016/j.coi.2013.01.002
19. Constantinides MG, Bendelac A. Transcriptional regulation of the NKT cell lineage. *Curr Opin Immunol*. (2013) 25:161–7. doi: 10.1016/j.coi.2013.01.003
20. Eberl G, Lowin-Kropf B, MacDonald HR. Cutting edge: NKT cell development is selectively impaired in Fyn- deficient mice. *J Immunol*. (1999) 163:4091–4.
21. Gadue P, Morton N, Stein PL. The Src family tyrosine kinase Fyn regulates natural killer T cell development. *J Exp Med*. (1999) 190:1189–96. doi: 10.1084/jem.190.8.1189
22. Nichols KE, Hom J, Gong SY, Ganguly A, Ma CS, Cannons JL, et al. Regulation of NKT cell development by SAP, the protein defective in XLP. *Nat Med*. (2005) 11:340–5. doi: 10.1038/nm1189
23. Pasquier B, Yin L, Fondaneche MC, Relouzat F, Bloch-Queyrat C, Lambert N, et al. Defective NKT cell development in mice and humans lacking the adapter SAP, the X-linked lymphoproliferative syndrome gene product. *J Exp Med*. (2005) 201:695–701. doi: 10.1084/jem.20042432
24. Griewank K, Borowski C, Rietdijk S, Wang N, Julien A, Wei DG, et al. Homotypic interactions mediated by Slamf1 and Slamf6 receptors control NKT cell lineage development. *Immunity*. (2007) 27:751–62. doi: 10.1016/j.immuni.2007.08.020
25. Chen S, Cai C, Li Z, Liu G, Wang Y, Blonska M, et al. Dissection of SAP-dependent and SAP-independent SLAM family signaling in NKT cell development and humoral immunity. *J Exp Med*. (2017) 214:475–89. doi: 10.1084/jem.20161312
26. Kronenberg M, Gapin L. The unconventional lifestyle of NKT cells. *Nat Rev Immunol*. (2002) 2:557–68. doi: 10.1038/nri854
27. Lu Y, Zhong MC, Qian J, Calderon V, Cruz Tleugabulova M, Mallevaey T, et al. SLAM receptors foster iNKT cell development by reducing TCR signal strength after positive selection. *Nat Immunol*. (2019) 20:447–57. doi: 10.1038/s41590-019-0334-0
28. Michel ML, Lenoir C, Massot B, Diem S, Pasquier B, Sawa S, et al. SLAM-associated protein favors the development of iNKT2 over iNKT17 cells. *Eur J Immunol*. (2016) 46:2162–74. doi: 10.1002/eji.201646313
29. De Calisto J, Wang N, Wang G, Yigit B, Engel P, Terhorst C. SAP-dependent and -independent regulation of innate T cell development involving SLAMF receptors. *Front Immunol*. (2014) 5:186. doi: 10.3389/fimmu.2014.00186
30. Huang B, Gomez-Rodriguez J, Preite S, Garrett LJ, Harper UL, Schwartzberg PL. CRISPR-mediated triple knockout of SLAMF1, SLAMF5 and SLAMF6 supports positive signaling roles in NKT cell development. *PLoS ONE*. (2016) 11:e0156072. doi: 10.1371/journal.pone.0156072
31. Baglaenko Y, Cruz Tleugabulova M, Gracey E, Talaei N, Manion KP, Chang NH, et al. Invariant NKT cell activation is potentiated by homotypic trans-Ly108 interactions. *J Immunol*. (2017) 198:3949–62. doi: 10.4049/jimmunol.1601369
32. Cuenca M, Punet-Ortiz J, Ruart M, Terhorst C, Engel P. Ly9 (SLAMF3) receptor differentially regulates iNKT cell development and activation in mice. *Eur J Immunol*. (2018) 48:99–105. doi: 10.1002/eji.201746925
33. Savage AK, Constantinides MG, Han J, Picard D, Martin E, Li B, et al. The transcription factor PLZF directs the effector program of the NKT cell lineage. *Immunity*. (2008) 29:391–403. doi: 10.1016/j.immuni.2008.07.011
34. Kovalovsky D, Uche OU, Eladad S, Hobbs RM, Yi W, Alonzo E, et al. The BTB-zinc finger transcriptional regulator PLZF controls the development of invariant natural killer T cell effector functions. *Nat Immunol*. (2008) 9:1055–64. doi: 10.1038/ni.1641
35. Constantinides MG, McDonald BD, Verhoef PA, Bendelac A. A committed precursor to innate lymphoid cells. *Nature*. (2014) 508:397–401. doi: 10.1038/nature13047
36. Koay HF, Gherardin NA, Enders A, Loh L, Mackay LK, Almeida CF, et al. A three-stage intrathymic development pathway for the mucosal-associated invariant T cell lineage. *Nat Immunol*. (2016) 17:1300–11. doi: 10.1038/ni.3565
37. Kreslavsky T, Savage AK, Hobbs R, Gounari F, Bronson R, Pereira P, et al. TCR-inducible PLZF transcription factor required for innate phenotype of a subset of gammadelta T cells with restricted TCR diversity. *Proc Natl Acad Sci USA*. (2009) 106:12453–8. doi: 10.1073/pnas.0903895106
38. Lee YJ, Holzapfel KL, Zhu J, Jameson SC, Hogquist KA. Steady-state production of IL-4 modulates immunity in mouse strains and is determined by lineage diversity of iNKT cells. *Nat Immunol*. (2013) 14:1146–54. doi: 10.1038/ni.2731
39. Tuttle KD, Krovi SH, Zhang J, Bedel R, Harmacek L, Peterson LK, et al. TCR signal strength controls thymic differentiation of iNKT cell subsets. *Nat Commun*. (2018) 9:2650. doi: 10.1038/s41467-018-05026-6
40. Subleski JJ, Hall VL, Wolfe TB, Scarzello AJ, Weiss JM, Chan T, et al. TCR-dependent and -independent activation underlie liver-specific regulation of NKT cells. *J Immunol*. (2011) 186:838–47. doi: 10.4049/jimmunol.1001735
41. Lee YJ, Wang H, Starrett GJ, Phuong V, Jameson SC, Hogquist KA. Tissue-specific distribution of iNKT cells impacts their cytokine response. *Immunity*. (2015) 43:566–78. doi: 10.1016/j.immuni.2015.06.025
42. Stritesky GL, Jameson SC, Hogquist KA. Selection of self-reactive T cells in the thymus. *Annu Rev Immunol*. (2012) 30:95–114. doi: 10.1146/annurev-immunol-020711-075035
43. Hogquist KA, Jameson SC. The self-obsession of T cells: how TCR signaling thresholds affect fate 'decisions' and effector function. *Nat Immunol*. (2014) 15:815–23. doi: 10.1038/ni.2938
44. Gapin L. Development of invariant natural killer T cells. *Curr Opin Immunol*. (2016) 39:68–74. doi: 10.1016/j.coi.2016.01.001
45. Luoma AM, Castro CD, Adams EJ. gammadelta T cell surveillance via CD1 molecules. *Trends Immunol*. (2014) 35:613–21. doi: 10.1016/j.it.2014.09.003
46. Alonzo ES, Gottschalk RA, Das J, Egawa T, Hobbs RM, Pandolfi PP, et al. Development of promyelocytic zinc finger and ThPOK-expressing innate gamma delta T cells is controlled by strength of TCR signaling and Id3. *J Immunol*. (2010) 184:1268–79. doi: 10.4049/jimmunol.0903218
47. Verykokakis M, Boos MD, Bendelac A, Adams EJ, Pereira P, Kee BL. Inhibitor of DNA binding 3 limits development of murine slam-associated adaptor protein-dependent "innate" gammadelta T cells. *PLoS ONE*. (2010) 5:e9303. doi: 10.1371/journal.pone.0009303
48. Narayan K, Sylvia KE, Malhotra N, Yin CC, Martens G, Vallerskog T, et al. Immunological genome project, intrathymic programming of effector fates in three molecularly distinct gammadelta T cell subtypes. *Nat Immunol*. (2012) 13:511–8. doi: 10.1038/ni.2247
49. Koch M, Stronge VS, Shepherd D, Gadola SD, Mathew B, Ritter G, et al. The crystal structure of human CD1d with and without alpha-galactosylceramide. *Nat Immunol*. (2005) 6:819–26. doi: 10.1038/ni1225
50. Zajonc DM, Cantu C III, Mattner J, Zhou D, Savage PB, Bendelac A, et al. Structure and function of a potent agonist for the semi-invariant natural killer T cell receptor. *Nat Immunol*. (2005) 6:810–8. doi: 10.1038/ni1224

51. Hava, DL, Brigl M, van den Elzen P, Zajonc DM, Wilson IA, Brenner MB. CD1 assembly and the formation of CD1-antigen complexes. *Curr Opin Immunol.* (2005) 17:88–94. doi: 10.1016/j.coi.2004.12.003
52. Girardi E, Zajonc DM. Molecular basis of lipid antigen presentation by CD1d and recognition by natural killer T cells. *Immunol Rev*. (2012) 250:167–79. doi: 10.1111/j.1600-065X.2012.01166.x
53. Wu JN, Koretzky GA. The SLP-76 family of adapter proteins. *Semin Immunol*. (2004) 16:379–93. doi: 10.1016/j.smim.2004.08.018
54. Clements JL, Yang B, Ross-Barta SE, Eliason SL, Hrstka RF, Williamson RA, et al. Requirement for the leukocyte-specific adapter protein SLP-76 for normal T cell development. *Science*. (1998) 281:416–9. doi: 10.1126/science.281.5375.416
55. Pivniouk V, Tsitsikov E, Swinton P, Rathbun G, Alt FW, Geha RS. Impaired viability and profound block in thymocyte development in mice lacking the adaptor protein SLP-76. *Cell*. (1998) 94:229–38. doi: 10.1016/S0092-8674(00)81422-1
56. Yablonski D, Kuhne MR, Kadlecek T, Weiss A. Uncoupling of nonreceptor tyrosine kinases from PLC-gamma1 in an SLP-76-deficient T cell. *Science*. (1998) 281:413–6. doi: 10.1126/science.281.5375.413
57. Jordan MS, Smith JE, Burns JC, Austin JE, Nichols KE, Aschenbrenner AC, et al. Complementation in trans of altered thymocyte development in mice expressing mutant forms of the adaptor molecule SLP76. *Immunity*. (2008) 28:359–69. doi: 10.1016/j.immuni.2008.01.010
58. Danzer C, Koller A, Baier J, Arnold H, Giessler C, Opoka R, et al. A mutation within the SH2 domain of slp-76 regulates the tissue distribution and cytokine production of iNKT cells in mice. *Eur J Immunol*. (2016) 46:2121–36. doi: 10.1002/eji.201646331
59. Elewaut D, Lawton AP, Nagarajan NA, Maverakis E, Khurana A, Honing S, et al. The adaptor protein AP-3 is required for CD1d-mediated antigen presentation of glycosphingolipids and development of Valpha14i NKT cells. *J Exp Med*. (2003) 198:1133–46. doi: 10.1084/jem.20030143
60. Myung PS, Boerthe NJ, Koretzky GA. Adapter proteins in lymphocyte antigen-receptor signaling. *Curr Opin Immunol*. (2000) 12:256–66. doi: 10.1016/S0952-7915(00)00085-6
61. Jackman JK, Motto DG, Sun Q, Tanemoto M, Turck CW, Peltz GA, et al. Molecular cloning of SLP-76, a 76-kDa tyrosine phosphoprotein associated with Grb2 in T cells. *J Biol Chem*. (1995) 270:7029–32. doi: 10.1074/jbc.270.13.7029
62. Clements JL, Ross-Barta SE, Tygrett LT, Waldschmidt TJ, Koretzky GA. SLP-76 expression is restricted to hemopoietic cells of monocyte, granulocyte, and T lymphocyte lineage and is regulated during T cell maturation and activation. *J Immunol*. (1998) 161:3880–9.
63. Fu C, Turck CW, Kurosaki T, Chan AC. BLNK: a central linker protein in B cell activation. *Immunity*. (1998) 9:93–103. doi: 10.1016/S1074-7613(00)80591-9
64. Goitsuka R, Fujimura Y, Mamada H, Umeda A, Morimura T, Uetsuka K, et al. BASH, a novel signaling molecule preferentially expressed in B cells of the bursa of Fabricius. *J Immunol*. (1998) 161:5804–8.
65. Cao MY, Davidson D, Yu J, Latour S, Veillette A. Clnk, a novel SLP-76-related adaptor molecule expressed in cytokine-stimulated hemopoietic cells. *J Exp Med*. (1999) 190:1527–34. doi: 10.1084/jem.190.10.1527
66. Motto DG, Ross SE, Wu J, Hendricks-Taylor LR, Koretzky GA. Implication of the GRB2-associated phosphoprotein SLP-76 in T cell receptor-mediated interleukin 2 production. *J Exp Med*. (1996) 183:1937–43. doi: 10.1084/jem.183.4.1937
67. Bubeck Wardenburg J, Fu C, Jackman JK, Flotow H, Wilkinson SE, Williams DH, et al. Phosphorylation of SLP-76 by the ZAP-70 protein-tyrosine kinase is required for T-cell receptor function. *J Biol Chem*. (1996) 271:19641–4. doi: 10.1074/jbc.271.33.19641
68. Raab M, da Silva AJ, Findell PR, Rudd CE. Regulation of Vav-SLP-76 binding by ZAP-70 and its relevance to TCR zeta/CD3 induction of interleukin-2. *Immunity*. (1997) 6:155–64. doi: 10.1016/S1074-7613(00)80422-7
69. Tuosto L, Michel F, Acuto O. p95vav associates with tyrosine-phosphorylated SLP-76 in antigen-stimulated T cells. *J Exp Med*. (1996) 184:1161–6. doi: 10.1084/jem.184.3.1161
70. Wu J, Motto DG, Koretzky GA, Weiss A. Vav and SLP-76 interact and functionally cooperate in IL-2 gene activation. *Immunity*. (1996) 4:593–602. doi: 10.1016/S1074-7613(00)80485-9
71. Bubeck Wardenburg J, Pappu R, Bu JY, Mayer B, Chernoff J, Straus D, et al. Regulation of PAK activation and the T cell cytoskeleton by the linker protein SLP-76. *Immunity*. (1998) 9:607–16. doi: 10.1016/S1074-7613(00)80658-5
72. Wunderlich L, Farago A, Downward J, Buday L. Association of Nck with tyrosine-phosphorylated SLP-76 in activated T lymphocytes. *Eur J Immunol.* (1999) 29:1068–75. doi: 10.1002/(SICI)1521-4141(199904)29:04<1068::AID-IMMU1068>3.0.CO;2-P
73. Su YW, Zhang Y, Schweikert J, Koretzky GA, Reth M, Wienands J. Interaction of SLP adaptors with the SH2 domain of Tec family kinases. *Eur J Immunol.* (1999) 29:3702–11. doi: 10.1002/(SICI)1521-4141(199911)29:11<3702::AID-IMMU3702>3.0.CO;2-R
74. Bunnell SC, Diehn M, Yaffe MB, Findell PR, Cantley LC, Berg LJ. Biochemical interactions integrating Itk with the T cell receptor-initiated signaling cascade. *J Biol Chem*. (2000) 275:2219–30. doi: 10.1074/jbc.275.3.2219
75. Au-Yeung BB, Fowell DJ. A key role for Itk in both IFN gamma and IL-4 production by NKT cells. *J Immunol*. (2007) 179:111–9. doi: 10.4049/jimmunol.179.1.111
76. Felices M, Berg LJ. The Tec kinases Itk and Rlk regulate NKT cell maturation, cytokine production, and survival. *J Immunol*. (2008) 180:3007–18. doi: 10.4049/jimmunol.180.5.3007
77. Qi Q, Huang W, Bai Y, Balmus G, Weiss RS, August A. A unique role for ITK in survival of invariant NKT cells associated with the p53-dependent pathway in mice. *J Immunol*. (2012) 188:3611–9. doi: 10.4049/jimmunol.1102475
78. Qi Q, Kannan AK, August A. Tec family kinases: Itk signaling and the development of NKT alphabeta and gammadelta T cells. *FEBS J*. (2011) 278:1970–9. doi: 10.1111/j.1742-4658.2011.08074.x
79. Yin CC, Cho OH, Sylvia KE, Narayan K, Prince AL, Evans JW, et al. The Tec kinase ITK regulates thymic expansion, emigration, and maturation of gammadelta NKT cells. *J Immunol*. (2013) 190:2659–69. doi: 10.4049/jimmunol.1202531
80. Felices M, Yin CC, Kosaka Y, Kang J, Berg LJ. Tec kinase Itk in gammadeltaT cells is pivotal for controlling IgE production in vivo. *Proc Natl Acad Sci USA*. (2009) 106:8308–13. doi: 10.1073/pnas.0808459106
81. Yablonski D, Kadlecek T, Weiss A. Identification of a phospholipase C-gamma1 (PLC-gamma1) SH3 domain-binding site in SLP-76 required for T-cell receptor-mediated activation of PLC-gamma1 and NFAT. *Mol Cell Biol*. (2001) 21:4208–18. doi: 10.1128/MCB.21.13.4208-4218.2001
82. Liu SK, Fang N, Koretzky GA, McGlade CJ. The hematopoietic-specific adaptor protein gads functions in T-cell signaling via interactions with the SLP-76 and LAT adaptors. *Curr Biol*. (1999) 9:67–75. doi: 10.1016/S0960-9822(99)80017-7
83. Sauer K, Liou J, Singh SB, Yablonski D, Weiss A, Perlmutter RM. Hematopoietic progenitor kinase 1 associates physically and functionally with the adaptor proteins B cell linker protein and SLP-76 in lymphocytes. *J Biol Chem*. (2001) 276:45207–16. doi: 10.1074/jbc.M106811200
84. da Silva AJ, Li Z, de Vera C, Canto E, Findell P, Rudd CE. Cloning of a novel T-cell protein FYB that binds FYN and SH2-domain-containing leukocyte protein 76 and modulates interleukin 2 production. *Proc Natl Acad Sci USA*. (1997) 94:7493–8. doi: 10.1073/pnas.94.14.7493
85. Musci MA, Hendricks-Taylor LR, Motto DG, Paskind M, Kamens J, Turck CW, et al. Molecular cloning of SLAP-130, an SLP-76-associated substrate of the T cell antigen receptor-stimulated protein tyrosine kinases. *J Biol Chem*. (1997) 272:11674–7. doi: 10.1074/jbc.272.18.11674
86. Wu JN, Gheith S, Bezman NA, Liu QH, Fostel LV, Swanson AM, et al. Adhesion- and degranulation-promoting adapter protein is required for efficient thymocyte development and selection. *J Immunol*. (2006) 176:6681–9. doi: 10.4049/jimmunol.176.11.6681
87. Griffiths EK, Krawczyk C, Kong YY, Raab M, Hyduk SJ, Bouchard D, et al. Positive regulation of T cell activation and integrin adhesion by the adapter Fyb/Slap. *Science*. (2001) 293:2260–3. doi: 10.1126/science.1063397
88. Peterson EJ, Woods ML, Dmowski SA, Derimanov G, Jordan MS, Wu JN, et al. Coupling of the TCR to integrin activation by Slap-130/Fyb. *Science*. (2001) 293:2263–5. doi: 10.1126/science.1063486
89. Griffiths EK, Penninger JM. Communication between the TCR and integrins: role of the molecular adapter ADAP/Fyb/Slap. *Curr Opin Immunol*. (2002) 14:317–22. doi: 10.1016/S0952-7915(02)00334-5

90. Coussens NP, Hayashi R, Brown PH, Balagopalan L, Balbo A, Akpan I, et al. Multipoint binding of the SLP-76 SH2 domain to ADAP is critical for oligomerization of SLP-76 signaling complexes in stimulated T cells. *Mol Cell Biol*. (2013) 33:4140–51. doi: 10.1128/MCB.00410-13
91. Lampe K, Endale M, Cashman S, Fang H, Mattner J, Hildeman D, et al. Slp-76 is a critical determinant of NK-cell mediated recognition of missing-self targets. *Eur J Immunol*. (2015) 45:2072–83. doi: 10.1002/eji.201445352
92. Binstadt BA, Billadeau DD, Jevremovic D, Williams BL, Fang N, Yi T, et al. SLP-76 is a direct substrate of SHP-1 recruited to killer cell inhibitory receptors. *J Biol Chem*. (1998) 273:27518–23. doi: 10.1074/jbc.273.42.27518
93. Utting O, Sedgmen BJ, Watts TH, Shi X, Rottapel R, Iulianella A, et al. Immune functions in mice lacking Clnk, an SLP-76-related adaptor expressed in a subset of immune cells. *Mol Cell Biol*. (2004) 24:6067–75. doi: 10.1128/MCB.24.13.6067-6075.2004
94. Sasanuma H, Tatsuno A, Hidano S, Ohshima K, Matsuzaki Y, Hayashi K, et al. Dual function for the adaptor MIST in IFN-gamma production by NK and CD4+NKT cells regulated by the Src kinase Fgr. *Blood*. (2006) 107:3647–55. doi: 10.1182/blood-2005-10-4102
95. Cannons JL, Tangye SG, Schwartzberg PL. SLAM family receptors and SAP adaptors in immunity. *Annu Rev Immunol*. (2011) 29:665–705. doi: 10.1146/annurev-immunol-030409-101302
96. Ma CS, Nichols KE, Tangye SG. Regulation of cellular and humoral immune responses by the SLAM and SAP families of molecules. *Annu Rev Immunol*. (2007) 25:337–79. doi: 10.1146/annurev.immunol.25.022106.141651
97. Dong Z, Veillette A. How do SAP family deficiencies compromise immunity? *Trends Immunol*. (2010) 31:295–302. doi: 10.1016/j.it.2010.05.008
98. Veillette A. SLAM-family receptors: immune regulators with or without SAP-family adaptors. *Cold Spring Harb Perspect Biol*. (2010) 2:a002469. doi: 10.1101/cshperspect.a002469
99. Coffey AJ, Brooksbank RA, Brandau O, Oohashi T, Howell GR, Bye JM, et al. Host response to EBV infection in X-linked lymphoproliferative disease results from mutations in an SH2-domain encoding gene. *Nat Genet*. (1998) 20:129–35. doi: 10.1038/2424
100. Nichols KE, Harkin DP, Levitz S, Krainer M, Kolquist KA, Genovese C, et al. Inactivating mutations in an SH2 domain-encoding gene in X-linked lymphoproliferative syndrome. *Proc Natl Acad Sci USA*. (1998) 95:13765–70. doi: 10.1073/pnas.95.23.13765
101. Sayos J, Wu C, Morra M, Wang N, Zhang X, Allen D, et al. The X-linked lymphoproliferative-disease gene product SAP regulates signals induced through the co-receptor SLAM. *Nature*. (1998) 395:462–9. doi: 10.1038/26683
102. Morra M, Howie D, Grande MS, Sayos J, Wang N, Wu C, et al. X-linked lymphoproliferative disease: a progressive immunodeficiency. *Annu Rev Immunol*. (2001) 19:657–82. doi: 10.1146/annurev.immunol.19.1.657
103. Bottino C, Falco M, Parolini S, Marcenaro E, Augugliaro R, Sivori S, et al. NTB-A [correction of GNTB-A], a novel SH2D1A-associated surface molecule contributing to the inability of natural killer cells to kill Epstein-Barr virus-infected B cells in X-linked lymphoproliferative disease. *J Exp Med*. (2001) 194:235–46. doi: 10.1084/jem.194.3.235
104. Parolini S, Bottino C, Falco M, Augugliaro R, Giliani S, Franceschini R, et al. X-linked lymphoproliferative disease. 2B4 molecules displaying inhibitory rather than activating function are responsible for the inability of natural killer cells to kill Epstein-Barr virus-infected cells. *J Exp Med*. (2000) 192:337–46. doi: 10.1084/jem.192.3.337
105. Sharifi R, Sinclair JC, Gilmour KC, Arkwright PD, Kinnon C, Thrasher AJ, et al. SAP mediates specific cytotoxic T-cell functions in X-linked lymphoproliferative disease. *Blood*. (2004) 103:3821–7. doi: 10.1182/blood-2003-09-3359
106. Borowski C, Bendelac A. Signaling for NKT cell development: the SAP-FynT connection. *J Exp Med*. (2005) 201:833–6. doi: 10.1084/jem.20050339
107. Eissmann P, Beauchamp L, Wooters J, Tilton JC, Long EO, Watzl C. Molecular basis for positive and negative signaling by the natural killer cell receptor 2B4 (CD244). *Blood*. (2005) 105:4722–9. doi: 10.1182/blood-2004-09-3796
108. Dong Z, Davidson D, Perez-Quintero LA, Kurosaki T, Swat W, Veillette A. The adaptor SAP controls NK cell activation by regulating the enzymes Vav-1 and SHIP-1 and by enhancing conjugates with target cells. *Immunity*. (2012) 36:974–85. doi: 10.1016/j.immuni.2012.03.023
109. Le Borgne M, Shaw AS. SAP signaling: a dual mechanism of action. *Immunity*. (2012) 36:899–901. doi: 10.1016/j.immuni.2012.06.002
110. Zhao F, Cannons JL, Dutta M, Griffiths GM, Schwartzberg PL. Positive and negative signaling through SLAM receptors regulate synapse organization and thresholds of cytolysis. *Immunity*. (2012) 36:1003–16. doi: 10.1016/j.immuni.2012.05.017
111. Wu N, Zhong MC, Roncagalli R, Perez-Quintero LA, Guo H, Zhang Z, et al. A hematopoietic cell-driven mechanism involving SLAMF6 receptor, SAP adaptors and SHP-1 phosphatase regulates NK cell education. *Nat Immunol*. (2016) 17:387–96. doi: 10.1038/ni.3369
112. Iyer SS, Huang YH, Blumberg RS. SLAM-ing the brakes on iNKT cell selection. *Nat Immunol*. (2019) 20:378–9. doi: 10.1038/s41590-019-0355-8
113. Seiler MP, Mathew R, Liszewski MK, Spooner CJ, Barr K, Meng F, et al. Elevated and sustained expression of the transcription factors Egr1 and Egr2 controls NKT lineage differentiation in response to TCR signaling. *Nat Immunol*. (2012) 13:264–71. doi: 10.1038/ni.2230
114. Cen O, Ueda A, Guzman L, Jain J, Bassiri H, Nichols KE, et al. The adaptor molecule signaling lymphocytic activation molecule-associated protein (SAP) regulates IFN-gamma and IL-4 production in V alpha 14 transgenic NKT cells via effects on GATA-3 and T-bet expression. *J Immunol*. (2009) 182:1370–8. doi: 10.4049/jimmunol.182.3.1370
115. Das R, Bassiri H, Guan P, Wiener S, Banerjee PP, Zhong MC, et al. The adaptor molecule SAP plays essential roles during invariant NKT cell cytotoxicity and lytic synapse formation. *Blood*. (2013) 121:3386–95. doi: 10.1182/blood-2012-11-468868
116. Kageyama R, Cannons JL, Zhao F, Yusuf I, Lao C, Locci M, et al. The receptor Ly108 functions as a SAP adaptor-dependent on-off switch for T cell help to B cells and NKT cell development. *Immunity*. (2012) 36:986–1002. doi: 10.1016/j.immuni.2012.05.016
117. Detre C, Keszei M, Garrido-Mesa N, Kis-Toth K, Castro W, Agyemang AF, et al. SAP expression in invariant NKT cells is required for cognate help to support B-cell responses. *Blood*. (2012) 120:122–9. doi: 10.1182/blood-2011-11-395913
118. Boehm M, Bonifacino JS. Adaptins: the final recount. *Mol Biol Cell*. (2001) 12:2907–20. doi: 10.1091/mbc.12.10.2907
119. Robinson MS, Bonifacino JS. Adaptor-related proteins. *Curr Opin Cell Biol*. (2001) 13:444–53. doi: 10.1016/S0955-0674(00)00235-0
120. Kirchhausen T. Adaptors for clathrin-mediated traffic. *Annu Rev Cell Dev Biol*. (1999) 15:705–32. doi: 10.1146/annurev.cellbio.15.1.705
121. Park SY, Guo X. Adaptor protein complexes and intracellular transport. *Biosci Rep*. (2014) 34:e00123. doi: 10.1042/BSR20140069
122. Huang F, Nesterov A, Carter RE, Sorkin A. Trafficking of yellow-fluorescent-protein-tagged mu1 subunit of clathrin adaptor AP-1 complex in living cells. *Traffic*. (2001) 2:345–57. doi: 10.1034/j.1600-0854.2001.25020506.x
123. Rapoport I, Miyazaki M, Boll W, Duckworth B, Cantley LC, Shoelson S, et al. Regulatory interactions in the recognition of endocytic sorting signals by AP-2 complexes. *EMBO J*. (1997) 16:2240–50. doi: 10.1093/emboj/16.9.2240
124. Daugherty BL, Straley KS, Sanders JM, Phillips JW, Disdier M, McEver RP, et al. AP-3 adaptor functions in targeting P-selectin to secretory granules in endothelial cells. *Traffic*. (2001) 2:406–13. doi: 10.1034/j.1600-0854.2001.002006406.x
125. Kantheti P, Qiao X, Diaz ME, Peden AA, Meyer GE, Carskadon SL, et al. Mutation in AP-3 delta in the mocha mouse links endosomal transport to storage deficiency in platelets, melanosomes, and synaptic vesicles. *Neuron*. (1998) 21:111–22. doi: 10.1016/S.0896-6273(00)80519-X
126. Dell'Angelica EC, Shotelersuk V, Aguilar RC, Gahl WA, Bonifacino JS. Altered trafficking of lysosomal proteins in Hermansky-Pudlak syndrome due to mutations in the beta 3A subunit of the AP-3 adaptor. *Mol Cell*. (1999) 3:11–21. doi: 10.1016/S1097-2765(00)80170-7
127. Feng L, Seymour AB, Jiang S, To A, Peden AA, Novak EK, et al. The beta3A subunit gene (Ap3b1) of the AP-3 adaptor complex is altered in the mouse hypopigmentation mutant pearl, a model for Hermansky-Pudlak syndrome and night blindness. *Hum Mol Genet*. (1999) 8:323–30. doi: 10.1093/hmg/8.2.323
128. Shotelersuk V, Dell'Angelica EC, Hartnell L, Bonifacino JS, Gahl WA. A new variant of Hermansky-Pudlak syndrome due to mutations in a

gene responsible for vesicle formation. *Am J Med.* (2000) 108:423–27. doi: 10.1016/S0002-9343(99)00436-2
129. Yang W, Li C, Ward DM, Kaplan J, Mansour SL. Defective organellar membrane protein trafficking in Ap3b1-deficient cells. *J Cell Sci.* (2000) 113:4077–86.
130. Lawton AP, Prigozy TI, Brossay L, Pei B, Khurana A, Martin D, et al. The mouse CD1d cytoplasmic tail mediates CD1d trafficking and antigen presentation by adaptor protein 3-dependent and -independent mechanisms. *J Immunol.* (2005) 174:3179–86. doi: 10.4049/jimmunol.174.6.3179
131. Keller CW, Loi M, Ewert S, Quast I, Theiler R, Gannage M, et al. The autophagy machinery restrains iNKT cell activation through CD1D1 internalization. *Autophagy.* (2017) 13:1025–36. doi: 10.1080/15548627.2017.1297907
132. Salio M, Puleston DJ, Mathan TS, Shepherd D, Stranks AJ, Adamopoulou E, et al. Essential role for autophagy during invariant NKT cell development. *Proc Natl Acad Sci USA.* (2014) 111:E5678–E5687. doi: 10.1073/pnas.1413935112
133. Pei B, Zhao M, Miller BC, Vela JL, Bruinsma MW, Virgin HW, et al. Invariant NKT cells require autophagy to coordinate proliferation and survival signals during differentiation. *J Immunol.* (2015) 194:5872–84. doi: 10.4049/jimmunol.1402154
134. Ververs FA, Kalkhoven E, Van't Land B, Boes M, Schipper HS. Immunometabolic activation of invariant natural killer T cells. *Front Immunol.* (2018) 9:1192. doi: 10.3389/fimmu.2018.01192
135. Sugita M, Cao X, Watts GF, Rogers RA, Bonifacino JS, Brenner MB. Failure of trafficking and antigen presentation by CD1 in AP-3-deficient cells. *Immunity.* (2002) 16:697–706. doi: 10.1016/S1074-7613(02)00311-4
136. Sevilla LM, Richter SS, Miller J. Intracellular transport of MHC class II and associated invariant chain in antigen presenting cells from AP-3-deficient mocha mice. *Cell Immunol.* (2001) 210:143–53. doi: 10.1006/cimm.2001.1817
137. Caplan S, Dell'Angelica EC, Gahl WA, Bonifacino JS. Trafficking of major histocompatibility complex class II molecules in human B-lymphoblasts deficient in the AP-3 adaptor complex. *Immunol Lett.* (2000) 72:113–7. doi: 10.1016/S0165-2478(00)00176-0
138. Jung J, Bohn G, Allroth A, Boztug K, Brandes G, Sandrock I, et al. Identification of a homozygous deletion in the AP3B1 gene causing Hermansky-Pudlak syndrome, type 2. *Blood.* (2006) 108:362–9. doi: 10.1182/blood-2005-11-4377
139. Lorenzi L, Tabellini G, Vermi W, Moratto D, Porta F, Notarangelo LD, et al. Occurrence of nodular lymphocyte-predominant hodgkin lymphoma in hermansky-pudlak type 2 syndrome is associated to natural killer and natural killer T cell defects. *PLoS ONE.* (2013) 8:e80131. doi: 10.1371/journal.pone.0080131
140. Yablonski D, Weiss A. Mechanisms of signaling by the hematopoietic-specific adaptor proteins, SLP-76 and LAT and their B cell counterpart, BLNK/SLP-65. *Adv Immunol.* (2001) 79:93–128. doi: 10.1016/S0065-2776(01)79003-7
141. Schwartzberg PL, Mueller KL, Qi H, Cannons JL. SLAM receptors and SAP influence lymphocyte interactions, development and function. *Nat Rev Immunol.* (2009) 9:39–46. doi: 10.1038/nri2456
142. Plas DR, Johnson R, Pingel JT, Matthews RJ, Dalton M, Roy G, et al. Direct regulation of ZAP-70 by SHP-1 in T cell antigen receptor signaling. *Science.* (1996) 272:1173–6. doi: 10.1126/science.272.5265.1173
143. Burshtyn DN, Scharenberg AM, Wagtmann N, Rajagopalan S, Berrada K, Yi T, et al. Recruitment of tyrosine phosphatase HCP by the killer cell inhibitor receptor. *Immunity.* (1996) 4:77–85. doi: 10.1016/S1074-7613(00)80300-3
144. Nakamura MC, Niemi EC, Fisher MJ, Shultz LD, Seaman WE, Ryan JC. Mouse Ly-49A interrupts early signaling events in natural killer cell cytotoxicity and functionally associates with the SHP-1 tyrosine phosphatase. *J Exp Med.* (1997) 185:673–84. doi: 10.1084/jem.185.4.673
145. Fawcett VC, Lorenz U. Localization of Src homology 2 domain-containing phosphatase 1 (SHP-1) to lipid rafts in T lymphocytes: functional implications and a role for the SHP-1 carboxyl terminus. *J Immunol.* (2005) 174:2849–59. doi: 10.4049/jimmunol.174.5.2849
146. Langlet C, Bernard AM, Drevot P, He HT. Membrane rafts and signaling by the multichain immune recognition receptors. *Curr Opin Immunol.* (2000) 12:250–5. doi: 10.1016/S0952-7915(00)00084-4
147. Boerth NJ, Sadler JJ, Bauer DE, Clements JL, Gheith SM, Koretzky GA. Recruitment of SLP-76 to the membrane and glycolipid-enriched membrane microdomains replaces the requirement for linker for activation of T cells in T cell receptor signaling. *J Exp Med.* (2000) 192:1047–58. doi: 10.1084/jem.192.7.1047
148. Kumar A, Pyaram K, Yarosz EL, Hong H, Lyssiotis CA, Giri S, et al. Enhanced oxidative phosphorylation in NKT cells is essential for their survival and function. *Proc Natl Acad Sci USA.* (2019) 116:7439–48. doi: 10.1073/pnas.1901376116

Conflict of Interest Statement: The authors declare that the research was conducted in the absence of any commercial or financial relationships that could be construed as a potential conflict of interest.

frontiers in Immunology

REVIEW
published: 25 July 2019
doi: 10.3389/fimmu.2019.01704

Bridging the Gap: Modulatory Roles of the Grb2-Family Adaptor, Gads, in Cellular and Allergic Immune Responses

*Deborah Yablonski**

The Immune Cell Signaling Lab, Department of Immunology, Ruth and Bruce Rappaport Faculty of Medicine, Technion—Israel Institute of Technology, Haifa, Israel

OPEN ACCESS

Edited by:
Navin Kumar Verma, Nanyang Technological University, Singapore

Reviewed by:
Bernard Malissen, INSERM U1104 Centre d'Immunologie de Marseille-Luminy, France
Anne Spurkland, University of Oslo, Norway
Petr Draber, Institute of Molecular Genetics (ASCR), Czechia
Cosima T. Baldari, University of Siena, Italy

***Correspondence:**
Deborah Yablonski
debya@technion.ac.il

Specialty section:
This article was submitted to T Cell Biology, a section of the journal Frontiers in Immunology

Received: *07 May 2019*
Accepted: *08 July 2019*
Published: *25 July 2019*

Citation:
Yablonski D (2019) Bridging the Gap: Modulatory Roles of the Grb2-Family Adaptor, Gads, in Cellular and Allergic Immune Responses. Front. Immunol. 10:1704. doi: 10.3389/fimmu.2019.01704

Antigen receptor signaling pathways are organized by adaptor proteins. Three adaptors, LAT, Gads, and SLP-76, form a heterotrimeric complex that mediates signaling by the T cell antigen receptor (TCR) and by the mast cell high affinity receptor for IgE (FcεRI). In both pathways, antigen recognition triggers tyrosine phosphorylation of LAT and SLP-76. The recruitment of SLP-76 to phospho-LAT is bridged by Gads, a Grb2 family adaptor composed of two SH3 domains flanking a central SH2 domain and an unstructured linker region. The LAT-Gads-SLP-76 complex is further incorporated into larger microclusters that mediate antigen receptor signaling. Gads is positively regulated by dimerization, which promotes its cooperative binding to LAT. Negative regulation occurs via phosphorylation or caspase-mediated cleavage of the linker region of Gads. FcεRI-mediated mast cell activation is profoundly impaired in LAT- Gads- or SLP-76-deficient mice. Unexpectedly, the thymic developmental phenotype of Gads-deficient mice is much milder than the phenotype of LAT- or SLP-76-deficient mice. This distinction suggests that Gads is not absolutely required for TCR signaling, but may modulate its sensitivity, or regulate a particular branch of the TCR signaling pathway; indeed, the phenotypic similarity of Gads- and Itk-deficient mice suggests a functional connection between Gads and Itk. Additional Gads binding partners include costimulatory proteins such as CD28 and CD6, adaptors such as Shc, ubiquitin regulatory proteins such as USP8 and AMSH, and kinases such as HPK1 and BCR-ABL, but the functional implications of these interactions are not yet fully understood. No interacting proteins or function have been ascribed to the evolutionarily conserved N-terminal SH3 of Gads. Here we explore the biochemical and functional properties of Gads, and its role in regulating allergy, T cell development and T-cell mediated immunity.

Keywords: Gads, SLP-76, LAT, TCR, FcεRI, signal transduction, thymocyte development

INTRODUCTION

Gads—A Grb2-Family Adaptor Specialized for Immune Cell Signaling

Gads is a hematopoietically-expressed adaptor protein that regulates T cell development, T cell-mediated immune responses and mast cell-mediated allergic responses. By virtue of its domain structure, Gads is a member of the Grb2 family of adaptors, which includes Grb2, Gads and Grap. This family is characterized by a central SH2 domain flanked by two SH3 domains, with Gads containing an additional glutamine- and proline-rich spacer between the SH2 and C-terminal SH3 domains (**Figure 1A**). Whereas Grb2 is ubiquitously expressed, Grap is primarily hematopoietic, and Gads is expressed exclusively in hematopoietic cell types, with particularly high expression in thymocytes, T cells, and mast cells, intermediate expression in monocytes, and no detectable expression in macrophages (1, 2). A low level of Gads expression has been detected in NK cells and in naïve murine and human B cells, where it is downregulated upon BCR stimulation (3, 4).

The signaling functions of Grb2-family adaptors are mediated by their conserved Src homology (SH) domains. SH2 is a structurally conserved modular domain, found in over 100 signaling proteins (5). Each SH2 domain contains a single binding cleft, which binds with moderate affinity to a characteristic phospho-tyrosine (pY) motif; in particular, Grb2-family SH2 domains bind to the pYxN motif (6).

The SH3 domain is another type of modular protein-protein interaction domain, found in hundreds of human proteins. SH3 domains typically bind with moderate affinity to canonical proline-rich motifs (7); however, the C-terminal SH3 of Gads binds with high affinity to a non-canonical RxxK motif (8–10).

In resting cells, Grb2 adaptors are found in the cytoplasm, where they bind constitutively to key signaling proteins via their SH3 domains. Grb2 utilizes both SH3 domains to bind to the Ras exchange factor, SOS (11). Gads does not bind to SOS (12, 13), but binds to a hematopoietic adaptor, SLP-76, via a high affinity interaction of its C-terminal SH3 with an RxxK motif in SLP-76 (9, 10, 14, 15).

One Adaptor With Many Names

Discovered in the late 1990s by six different groups, Gads was given six different names: Grb2-family adaptor downstream of Shc (Gads) (16), Grb2-related adaptor protein-2 (Grap2) (17), Monocyte Adaptor (Mona) (1), Grb2-related protein of the lymphoid system (GrpL) (12), Grb2 family member of 40 kD (Grf40) (18), and Grb2-related protein with insert domain (GRID) (19). Most of these groups cloned Gads by virtue of its ability to form stable protein-protein interactions via its SH2 or C-terminal SH3 domain. A number of groups identified Gads by screening cDNA expression libraries with pYxN-containing phosho-protein baits, such as Shc (16), Fms (1), RET (20), or the cytoplasmic tail of CD28 (19). In addition, Gads has been shown to bind via its SH2 to BCR-Abl and c-Kit (16), SHP-2 (12), and CD6 (21). Other groups identified Gads in the course of yeast two hybrid screens with bait proteins that contain an RxxK motif, such as Gab1 (17), AMSH (18), and, more recently, USP8 (also known as UBPY) (14, 22). In addition, the C-terminal SH3 of Gads can bind to RxxK motifs in HPK1 (23–25) and Gab3 (1). The known Gads-binding partners are summarized in **Figure 1B**.

The Bridging Function of Gads—Two Cell Types, One Signalosome

Soon after the identification of Gads, it became apparent that its main function is to serve as an antigen receptor-induced bridge between two other hematopoietic adaptors, LAT and SLP-76 (12, 13, 18) (**Figure 1B**). Gads performs this bridging function in two cell types: T cells and mast cells. These cell types have distinct developmental pathways, and use structurally distinct receptors to recognize different types of antigens; nevertheless, the signaling pathways triggered upon antigen recognition are remarkably similar.

Recognition of antigen by the T cell antigen receptor (TCR) or the mast cell FcεRI triggers multi-site tyrosine phosphorylation of a trans-membrane adaptor, known as LAT, to which Grb2 and Gads bind via their SH2 domain. In this way, Grb2 recruits SOS to LAT, whereas Gads recruits SLP-76 to LAT. These events culminate in the antigen-induced assembly of a large, LAT-nucleated signaling complex, sometimes referred to as the LAT signalosome, which triggers downstream signaling events (**Figure 2**).

The superficially non-descript role of Gads as a bridge between two more famous adaptors, LAT and SLP-76 [reviewed in (26, 27)], may explain why Gads has not been reviewed in depth since 2001 (2), except in the context of the Grb2 family as a whole (28). Since this time, numerous studies have provided insight into the roles played by Gads and the regulatory inputs acting on Gads, which together warrant a closer look at this immune cell signaling molecule.

Proximal Signaling by the T Cell Antigen Receptor—A Quick Overview

Each T cell expresses a clonotypic antigen receptor (TCR), specific for a particular combination of antigenic peptide and cell surface MHC molecule (pMHC). Within the cell, TCR ligation triggers a cascade of tyrosine kinases (29, 30), initiated by the Src-family kinase, Lck, which phosphorylates ITAM motifs within the TCR complex. Dual-phosphorylated ITAMs bind the Syk-family kinase, ZAP-70. Active ZAP-70 then phosphorylates LAT at least four sites, including Tyr^{132}, Tyr^{171}, Tyr^{191}, and Tyr^{226} (31–34). Of these sites, PLC-γ1 binds directly to LAT $pTyr^{132}$, whereas the three C-terminal sites conform to the Grb2 family-specific motif, pYxN (**Figure 2**).

In parallel, ZAP-70 phosphorylates SLP-76 at three N-terminal tyrosines (35–37), which bind to the adaptor, Nck, the guanine nucleotide exchange factor, Vav, and the Tec-family tyrosine kinase, Itk. Vav and Nck are responsible for TCR-induced changes to the actin cytoskeleton, whereas Itk participates in a signaling pathway leading to the activation of phospholipase C-γ1 (PLC-γ1). Finally, the C-terminal SH2 of SLP-76 binds to additional signaling proteins, including the adaptor ADAP (previously known as SLAP130/Fyb) and the serine threonine kinase HPK1. HPK1 phosphorylates two

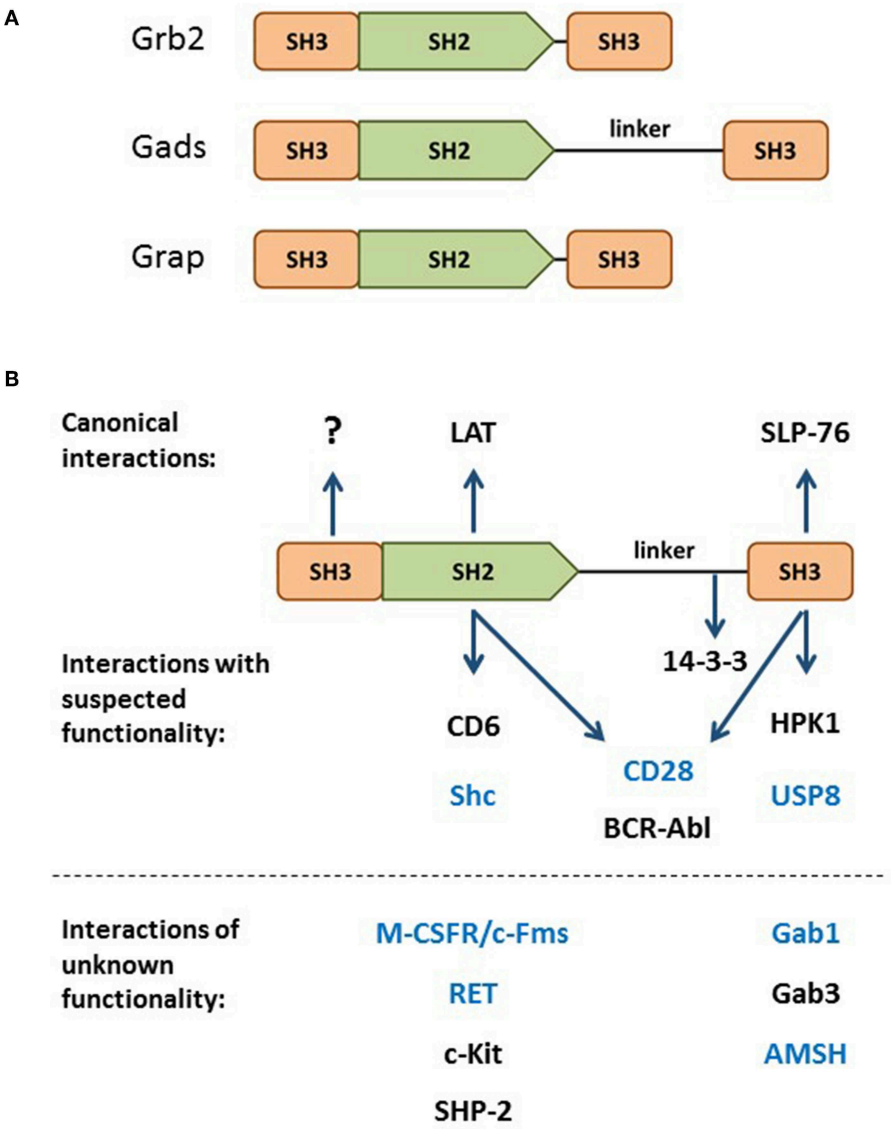

FIGURE 1 | The Grb2 family. **(A)** Domain structure of the Grb2 family members: Grb2, Gads, and Grap. **(B)** Through its SH2 and C-terminal SH3, Gads bridges the antigen receptor-induced recruitment of SLP-76 to LAT (shown at top). Additional binding partners are listed below their relevant binding domain, with interactions of unknown functional relevance listed below the dotted line. The N-terminal SH3 has no known binding partner or regulatory function. Bait proteins that were used to identify Gads are shown in blue. 14-3-3 binds to a threonine phosphorylation site within the linker region. CD28 and BCR-Abl may interact with two Gads domains.

defined sites on SLP-76 and Gads (indicated by purple arrows in **Figure 2**), which will be discussed below.

One of the most important functions of the LAT signalosome is to mediate the TCR-induced activation of PLC-γ1. PLC-γ1 binds to LAT Tyr^{132}, and is activated upon its phosphorylation on two tyrosine residues (38, 39). Itk-mediated phosphorylation of PLC-γ1 occurs by a sequential mechanism (indicated by pink arrows in **Figure 2**), in which Itk binds to and is activated by SLP-76 (40–42), then phosphorylates SLP-76 at Tyr^{173}, a conserved site that is required for the subsequent Itk-mediated phosphorylation of PLC-γ1 (36, 43). Activated PLC-γ1 generates second messengers that trigger calcium increase and the activation of Ras and PKC, with consequent activation of calcium- and Ras-dependent transcription factors that are required for TCR-induced transcriptional changes (44).

THE REGULATED ASSEMBLY AND DISASSEMBLY OF LAT-NUCLEATED SIGNALING COMPLEXES

Cooperative Assembly of the LAT Signalosome

The LAT signalosome is a complex structure composed of many different proteins, which is rapidly assembled upon TCR stimulation. All four distal tyrosines of LAT are required

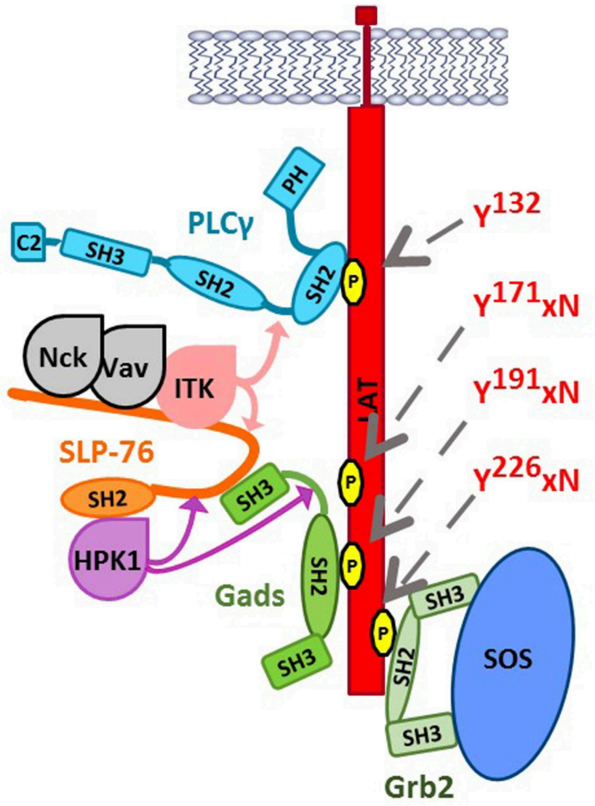

FIGURE 2 | The LAT-nucleated signaling complex. Upon TCR stimulation, LAT is phosphorylated by ZAP-70 at Tyr^{132}, Tyr^{171}, Tyr^{191}, and Tyr^{226} (indicated by gray arrows), triggering the SH2-mediated recruitment of key signaling proteins. PLC-γ1 binds directly to LAT at $pTyr^{132}$. Grb2 bridges the recruitment of SOS to LAT. Gads binds cooperatively to $pTyr^{171}$ and $pTyr^{191}$, bridging the recruitment of SLP-76 and its associated binding partners to LAT. Nck, Vav, and Itk bind to N-terminal tyrosine phosphorylation sites on SLP-76 (Tyr^{113}, Tyr^{128}, and Tyr^{145}), whereas HPK1 and ADAP (not shown) can bind to the C-terminal SH2 of SLP-76. Binding to SLP-76 is required for the catalytic activity of two SLP-76-associated kinases, Itk, and HPK1. Substrates of Itk within the signalosome are indicated by light pink arrows; Itk phosphorylates SLP-76 at Tyr^{173}, which is required for subsequent Itk-mediated phosphorylation of PLCγ1 at Tyr^{783}. HPK1 phosphorylates SLP-76 and Gads at negatively regulatory sites, indicated by purple arrows (SLP-76 Ser^{376} and Gads Thr^{262}).

for signalosome function (31–34), suggesting that a complete signalosome must be assembled. Biophysical measurements show that the three distal tyrosines can bind to Grb2 or Gads with comparable affinity (8); yet, in intact cells, at least two motifs are required for the stable recruitment of Grb2, and two particular motifs (Y171 and Y191) are specifically required for the stable recruitment of Gads into the signalosome (34). These observations suggest that signalosome assembly is promoted by cooperative binding events; however, the basis for cooperativity was not known.

Gads SH2-Mediated Dimerization Promotes Its Cooperative Binding to LAT

Recently, we discovered that the Gads protein undergoes spontaneous, reversible dimerization. Gads dimerization depends on its SH2 domain, and is further stabilized by additional domains found in full-length Gads (45). We used a structural model to identify the SH2 dimerization interface, and showed that it is distinct from the pTyr-binding pocket (45) (**Figure 3A**). This model suggests how paired binding of Gads to its dual binding sites on LAT may stabilize the dimeric configuration (**Figure 3B**). Consistent with this idea, competitive binding experiments revealed preferentially paired binding of Gads to a dual-phosphorylated LAT peptide, even in the presence of excess, competing single-phosphorylated LAT (45). Mutational inactivation of the dimerization interface reduced the preferentially paired binding of Gads to LAT, and impaired its ability to discriminate between single- and dual-phosphorylated LAT. In intact cells, disruption of the dimerization interface disrupted the antigen receptor-induced recruitment of Gads to phospho-LAT, moderately impaired TCR responsiveness in a model cell line, and profoundly impaired FcεRI-mediated activation of primary, bone marrow-derived mast cells (45).

Other Examples of Cooperativity at LAT

Assembly of the LAT signalosome appears to be driven by multiple cooperative binding events, including, but not limited to Gads dimerization. A recent study highlighted the cooperative assembly of LAT, Gads, SLP-76, and PLC-γ1 into a tetrameric complex centered around LAT Tyr^{132} and Tyr^{171} (46). Upon *in vitro* reconstitution of this binding complex, elimination of any one of the above components reduced the binding interactions between the other three. Further, cooperative interactions mediated by Grb2 are also likely to influence signalosome assembly. SH2-mediated dimerization of Grb2 can occur via a domain swapping mechanism, in which the C-terminal helix of the SH2 domain takes its place in a neighboring SH2 domain, thereby producing a stably intertwined dimeric form (47–49). It will be interesting to see whether Grb2 SH2 dimerization affects its binding to LAT, and how the competitive binding of Grb2 and Gads to overlapping sites on LAT eventually determines the overall structure and stoichiometry of the signalosome.

Why Are Cooperative Interactions at LAT so Important?

One insight may be seen in the recent observation that signaling through LFA-1 triggers phosphorylation of LAT at Tyr^{171} but not at Tyr^{191}, Tyr^{226}, or Tyr^{132}. This selective phosphorylation allows LAT to bind to a Grb2-SKAP1 complex, but not to Gads-SLP-76 (50). The absence of binding to Gads-SLP-76 is consistent with the requirement for two sites to mediate the cooperative binding of LAT to Gads (34, 45). This observation further suggests that Gads cooperativity may allow cells to identify productive TCR activation, which leads to ZAP-70-dependent phosphorylation of LAT at four tyrosines. In contrast, initial scanning of the APC would lead to LFA-1-dependent phosphorylation of LAT at Tyr^{171} alone. It remains to be shown whether Tyr^{171} is in fact phosphorylated in the context of a transient, non-cognate interaction between a T cell and an APC.

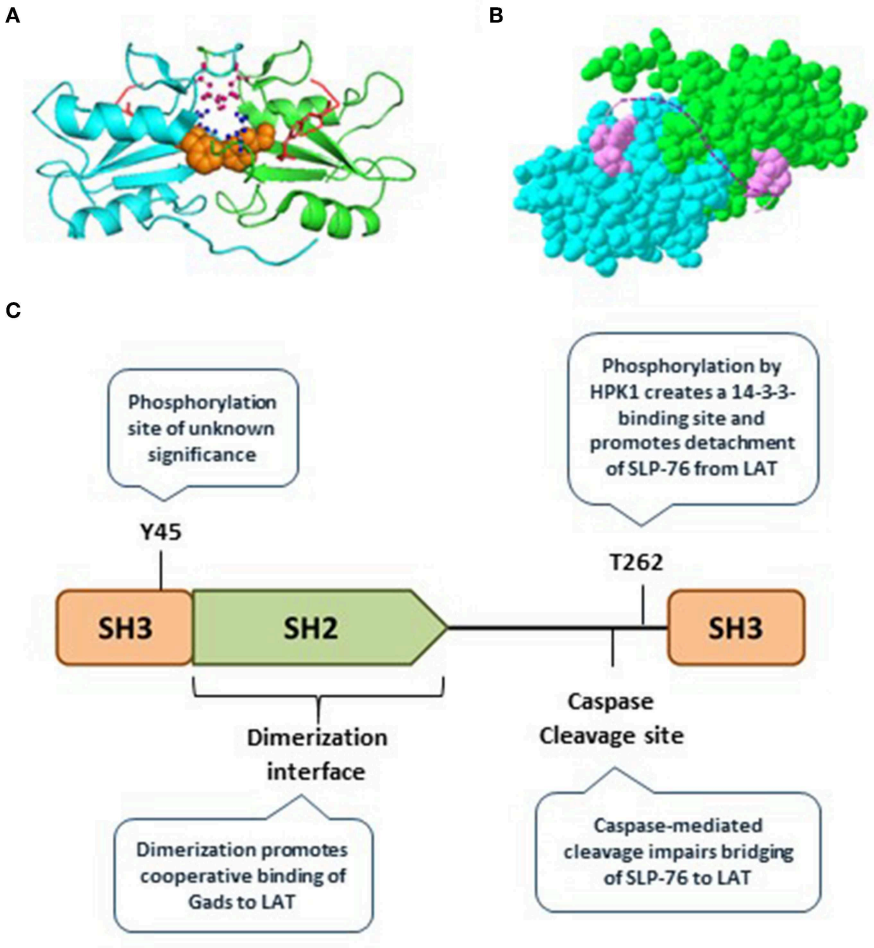

FIGURE 3 | Gads regulatory sites include an SH2 dimerization interface. **(A)** The SH2 domain of murine Gads, cocrystalized with a short LAT peptide encompassing LAT pTyr^{171} [(6); PDB file 1R1P]. The minimal asymmetric unit includes two pairs of closely associated Gads SH2 domains, each bound to a pLAT peptide. Shown is the structure of one pair of SH2 domains (cyan and green chains), each bound to the LAT peptide (red). Three amino acid side chains from the putative dimerization interface are shown, including F92 (orange), R109 (pink), and D91 (blue). **(B)** A space-filling representation of the structure shown in **A**, revealing an extensive dimerization interface measuring ~850 Å^2. The dotted pink line illustrates the possibility that the two bound pTyr peptides could represent dual binding sites on a single molecule of LAT, binding cooperatively to two molecules of Gads. **(C)** Summary of the currently known regulatory mechanisms converging on Gads, including Gads dimerization, HPK1-mediated phosphorylation of Gads, and caspase3-mediated cleavage of Gads. Tyr^{45} is a conserved TCR-inducible Gads phosphorylation site of unknown function, found within the N-terminal SH3 of Gads.

Signaling Microclusters Promote TCR Responsiveness

Upon TCR stimulation, LAT-nucleated signaling complexes (**Figure 2**) are incorporated into larger (micrometer or sub-micrometer) structures, referred to as microclusters (51) (**Figure 4**). Microclusters containing SLP-76, LAT, and Gads appear rapidly at the site of TCR stimulation, followed by their microtubule-mediated translocation toward the center of the stimulatory contact site (52, 53). Live cell imaging revealed that the appearance of the first microclusters coincides with the initiation of calcium flux, suggesting that microcluster formation may be required for downstream signaling events (52).

The Grb2-SOS complex is an important driver of microcluster formation (**Figure 4**, right). Each SOS molecule can bind to two molecules of Grb2, which may bind to pTyr sites on adjacent molecules of LAT, thereby recruiting multiple molecules of LAT into the microcluster (11, 54). Since each LAT molecule can bind up to three molecules of Grb2, the potential for cluster formation by this mechanism is quite large.

In addition to Grb2 and SOS, both SLP-76 and Gads are required to support the formation, persistence and translocation of TCR-induced microclusters (53). The recruitment of SLP-76 into microclusters depends on two of its protein-interaction sites: its Gads-binding motif, and its C-terminal SH2 domain. Surprisingly, SLP-76 itself is required for the recruitment of Gads into microclusters (53). These results demonstrate that the Gads-mediated recruitment of SLP-76 to LAT is necessary, but not sufficient for microcluster formation; in addition, a ligand of the SLP-76 SH2 domain is required to recruit SLP-76 and its associated Gads into the clusters.

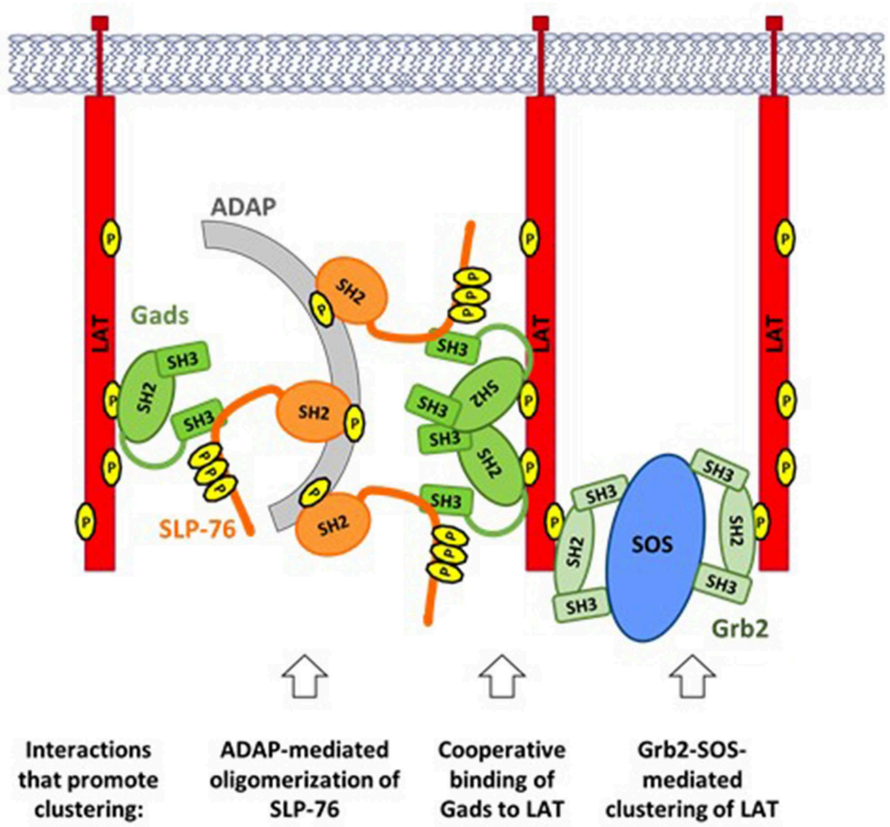

FIGURE 4 | TCR-induced clustering of LAT. A web of multipoint, SH2-mediated interactions promotes the formation of microclusters, containing LAT, Gads, and SLP-76. ADAP-mediated oligomerization of SLP-76: Upon TCR stimulation ADAP is phosphorylated at three tyrosines that bind to the SH2 of SLP-76, leading to oligomerization of SLP-76 and its associated Gads. Cooperative binding of Gads to LAT: Gads SH2 dimerization promotes its cooperative binding to two adjacent sites on LAT, thereby recruiting ADAP-oligomerized SLP-76 to one or more LAT molecules. Grb2-SOS-mediated clustering of LAT: Each molecule of SOS can bind to two molecules of Grb2, each of which may bind to a different molecule of LAT, thereby bringing them into the growing cluster. Each of the above interactions can occur repeatedly, creating a web of interacting proteins that together stabilize a large signaling cluster.

The SH2 domain of SLP-76 contributes to microcluster formation via its interaction with another adaptor protein known as ADAP (**Figure 4**, left). ADAP pre-localizes at TCR protrusions that may make contact with the APC (55). Upon TCR stimulation, ADAP is phosphorylated at three tyrosines that bind to SLP-76, resulting in the stable oligomerization of SLP-76 and its associated Gads (56). Oligomerized SLP-76 may then be recruited to LAT via the cooperatively paired binding of Gads to LAT $pTyr^{171}$ and $pTyr^{191}$ (45). In the context of ADAP-trimerized SLP-76, these Gads-mediated interactions may contribute to the cross-linking of two or more LAT molecules (**Figure 4**, center), similar to the cross-linking induced by Grb2-SOS. Consistent with this notion, all three ADAP tyrosines are required for the optimal assembly and stabilization of TCR-induced microclusters (56); whereas any microclusters that form in the absence of ADAP are immobile, smaller, and less persistent than those seen in wild-type cells (55, 57).

A common theme shared by all of the above mechanisms is that clustering is driven by the multipoint binding of individual signaling proteins to each other. Multipoint binding of Grb2 to SOS, Grb2 to LAT, SLP-76 to ADAP and Gads to LAT together create a web of interactions, linking individual signaling complexes into large microclusters that may amplify proximal signaling events to trigger profound downstream responsiveness.

Negative Regulatory Pathways Intersecting at Gads

The multiple cooperative interactions occurring at LAT result in the formation of highly stable signaling complexes and microclusters (54). This cooperative network likely contributes to the sensitivity of TCR signaling and supports the binary (fully on or off) nature of T cell responses. Yet, the high stability of the physical signaling network suggests that dedicated regulatory pathways must be required to disassemble the complexes and microclusters in order to terminate signaling.

Microcluster disassembly appears to be a regulated, stepwise process. Gads and SLP-76 are among the first signaling molecules to exit the LAT-nucleated signaling microclusters (58), suggesting that disassembly may be initiated and regulated by pathways acting on Gads. Here we discuss two types of negative regulatory pathways that

act on the linker region of Gads to promote signalosome disassembly and limit TCR responsiveness: HPK1-mediated phosphorylation of Gads, and caspase-mediated cleavage of Gads (**Figure 3C**).

HPK1 Mediates a Negative Feedback Loop, Activated by Gads and SLP-76

A member of the germinal center kinase (GCK) family, the serine/threonine kinase HPK1 (also known as MAP4K1) is expressed exclusively in hematopoietic cells and is activated upon TCR stimulation (59, 60). Lck, ZAP-70, LAT, and SLP-76 are all required for the TCR-induced activation of HPK1, suggesting that it forms part of the canonical TCR signaling pathway (60). Upon its activation, HPK1 appears to balance different downstream branches of the TCR response, by promoting the activation of JNK and NFκB, while simultaneously inhibiting the activation of Erk and AP1 (60–62).

Most importantly, HPK1 forms part of a negative feedback loop that limits signalosome activity. In the first part of the loop, SLP-76 acts within the LAT signalosome to mediate the activation of HPK1 (62). In the second part of the loop, HPK1 limits TCR responsiveness, by phosphorylating SLP-76 and Gads at negative regulatory sites, depicted by purple arrows in **Figure 2** (63–66).

The TCR-induced activation of HPK1 occurs by a multistep mechanism, involving SLP-76 and Grb2-family adaptors. Upon TCR stimulation, a proline-rich region of HPK1, which can bind to Grb2-family adaptors, mediates its recruitment to LAT (24, 25, 59, 60). It is not yet clear exactly how HPK1 is recruited LAT; however, Gads binds weakly to HPK1 (23), suggesting that it is probably not the primary mechanism of recruitment. Once recruited to LAT, HPK1 is phosphorylated by ZAP-70 on Tyr^{379}, which binds with high (∼8 nM) affinity to the SH2 of SLP-76, and this interaction is essential for the catalytic activation of HPK1 (56, 62). Activation of HPK1 also depends on the Gads-binding motif of SLP-76 (62), further supporting the notion that HPK1 activation occurs within the LAT signalosome. Taken together, the evidence suggests that HPK1 activation depends on its Grb2-dependent recruitment to LAT, where it is phosphorylated by ZAP-70, and then binds to and is activated by the SH2 of SLP-76.

Active HPK1 exerts negative feedback by phosphorylating SLP-76 at Ser^{376} and Gads at Thr^{262} (63, 64). Both HPK1-targeted sites bind in a phosphorylation-dependent manner to 14-3-3 proteins, which appear to promote the detachment of SLP-76 and Gads from LAT microclusters (63, 64). In addition, phosphorylation of SLP-76 at S^{376} may trigger its ubiquitin-mediated degradation (67). Consistent with its negative regulatory function, HPK1-deficient primary T cells exhibit increased TCR-induced phosphorylation of SLP-76 and proliferation (66). Moreover, mutational inactivation of SLP-76 Ser^{376} or Gads T^{262} in a T cell line model resulted in increased TCR-induced phosphorylation of PLC-γ1, as well as increased TCR+CD28-induced transcription of the IL-2 gene (63, 65). Thus, HPK1 appears to activate a negative regulatory feedback pathway, which is at least partially mediated by phosphorylation of 14-3-3-binding sites on SLP-76 and Gads.

Caspase-Mediated Cleavage of Gads May Limit Immune Responsiveness

At later time points in the process of T cell activation, Gads activity is limited by caspase3-mediated cleavage, which occurs at a conserved DIND cleavage site found within the linker region of Gads (68, 69). Cleavage at this site separates the LAT-binding SH2 domain of Gads from the SLP-76-binding C-terminal SH3, and thus cleavage of Gads can strongly impair the recruitment of SLP-76 to LAT. In T cell lines, caspase3-mediated cleavage of Gads occurs approximately 1 h after stimulation of CD95, also known as the Fas receptor (68, 69). It is interesting to note that *in vivo* caspase3-mediated cleavage of Gads has been observed upon the induction of oral tolerance, and also upon treatment of primary T cells with anergizing stimuli; indeed the expression of a caspase3-resistant allele of Gads rendered T cells partially resistant to anergy (70, 71). These observations suggest that caspase-mediated cleavage of Gads may be part of the mechanism by which T cell tolerance is maintained.

EVOLUTIONARY CONSERVATION OF GADS

Only two Gads domains, its central SH2 and C-terminal SH3, have been implicated in its role as a bridge between LAT and SLP-76. It is quite remarkable that Gads SH2 and C-SH3 have many potential binding partners (**Figure 1B**), whereas no interacting proteins or signaling functions have been ascribed to the N-terminal SH3 of Gads.

To gain insight into the relative importance of each Gads domain, we examined their evolutionary conservation, by aligning 66 vertebrate Gads orthologs (listed in **Supplementary Table 1**), representing a wide variety of taxonomical orders. A representative alignment of 14 Gads orthologs was color coded to indicate the extent of conservation among the 66 vertebrate species that we examined (**Supplementary Figure 1**). This analysis revealed remarkable conservation of all three SH domains of Gads. Fifty one percent of the N-SH3 residues, 60% of the SH2, and 48% of the C-SH3 residues were identical in over 95% of species examined (**Supplementary Figure 1**, yellow residues). When considering only 23 avian and 27 mammalian orthologs (excluding 3 marsupial orthologs), we found that 81% of N-SH3 residues, 77% of SH2 residues and 73% of C-SH3 residues were identical in over 92% of the species (**Supplementary Figure 1**, yellow and green residues). The remarkable evolutionary conservation of the N-terminal SH3 suggests that it performs an evolutionarily conserved, albeit currently unknown function, which may be mechanistically linked, or unrelated to the role of Gads as a bridge between SLP-76 and LAT.

The linker region varied between vertebrate classes, both in its sequence and in length. It was longest in mammalian orthologs (107–129 residues), due to the presence of a central proline-and glutamine-rich region of variable sequence, which was shorter or absent in the other vertebrate classes. The highest conservation within the linker sequence was observed among avian orthologs, in which it was of intermediate length (94–96

residues), and featured a central glutamine-rich motif, but no proline-rich motifs. No linker motifs were conserved among all vertebrate classes, but a motif encompassing the caspase cleavage site (RxGGSLDxxD) (68, 69) and another encompassing the threonine phosphorylation site (RRHTDP) (64) were conserved among mammalian and avian species (**Supplementary Figure 1**). Taken together these observations suggest that the linker region may serve a class-specific regulatory role that is not part of the core signaling function of Gads.

Overall, the high evolutionary conservation of Gads provides evidence for its important biological functions. To better understand its functions, it is instructive to compare the phenotypes of mice lacking Gads, to mice lacking LAT or SLP-76. As detailed below, the mast cell phenotypes of these mice are closely matched, consistent with the notion that the main role of Gads in mast cells is to serve as a bridge between LAT and SLP-76. In contrast, the T cell phenotypes are quite divergent, suggesting that Gads may play additional regulatory roles in T cells.

REGULATORY ROLES OF GADS *IN VIVO*

The Mast Cell High-Affinity Receptor for IgE (FcεRI) Signals Through a LAT-Gads-SLP-76 Complex

Type I hypersensitivity is a common type of allergic response that occurs when sensitized mast cells respond to environmental antigens (also known as allergens) via their high affinity receptor for IgE (the FcεRI). Sensitization occurs upon the binding of allergen-specific IgE to the FcεRI, which thereby functions as an indirect antigen receptor. Subsequent exposure to allergen activates the FcεRI, triggering a cascade of events that is highly analogous to the TCR signaling pathway [reviewed in (72, 73)]. In brief, phosphorylated receptor ITAM motifs activate a Syk-family kinase that phosphorylates LAT and SLP-76, leading to the formation of a LAT-nucleated signalosome, bridged by Gads. These proximal events result in the activation of PLC-γ, with a consequent increase in intracellular calcium that triggers the release of preformed granules containing a variety of allergic mediators. Over a longer time scale, the FcεRI triggers the transcription, translation and release of inflammatory cytokines, including IL-6 and others.

Neither LAT, SLP-76, nor Gads are required for mast cell development. LAT-deficient mice had normal numbers of mast cells in the skin (74), SLP-76-deficient mice had normal numbers of mast cells in the skin and bronchi (75), and Gads-deficient mice had normal numbers of mast cells in the skin, stomach and peritoneal cavity (76). Mast cells can also be derived *ex vivo* by prolonged culture of bone marrow precursors in the presence of IL-3. Such bone marrow-derived mast cells (BMMCs) were readily obtained in the absence of LAT, SLP-76, or Gads (74–76), suggesting that all three adaptors are dispensable for mast cell differentiation and proliferation. Nevertheless, all three adaptors were required for FcεRI responsiveness, both *in vivo* and *ex vivo*.

To assess FcεRI responsiveness *in vivo*, endogenous mast cells are sensitized by treating mice with monoclonal IgE (anti-DNP), followed by intravenous administration of a DNPylated protein antigen. When assayed in this manner, SLP-76-deficient and LAT-deficient mice exhibited no sign of passive systemic anaphylaxis as measured by systemic release of histamine (74, 75). The response of SLP-76 deficient mice was limited to a mild and transient tachycardia whereas wild-type mice exhibited profound tachycardia that was lethal in 50% of the mice (75). Gads-deficient mice were similarly non-responsive when sensitized locally in the ear and assessed for passive cutaneous anaphylaxis in response to DNPylated antigen (76).

For in depth examination of FcεRI-induced signaling events, LAT-, SLP-76-, and Gads-deficient primary bone marrow-derived mast cell lines (BMMCs) were sensitized with monoclonal IgE (anti-DNP) and stimulated with a DNPylated protein antigen. FcεRI-induced phosphorylation of PLCγ was reduced in both LAT- and SLP-76-deficient BMMCs (74, 75), but to our knowledge was not assessed in Gads-deficient BMMCs. Downstream of PLCγ, calcium flux was markedly impaired in LAT-, SLP-76- and Gads-deficient BMMCs (74–76). Further downstream, the rapid FcεRI-induced release of preformed mediators was abrogated in SLP-76-deficient BMMC (75), and markedly decreased in LAT-deficient (74) and in Gads-deficient BMMC (76). The slower FcεRI-induced release of cytokines was virtually absent in SLP-76-deficient (75) and in Gads-deficient BMMC (76) and was markedly reduced in LAT-deficient BMMC (74).

Overall, the phenotypic similarity of LAT- Gads- and SLP-76-deficient BMMC suggests that the three adaptors function together to mediate FcεRI responsiveness. This conclusion is further supported by mutational analysis. Substitution of the four distal LAT tyrosines with phenylalanine (4YF) produced a mast cell phenotype equivalent to the loss of LAT (77), suggesting that FcεRI responsiveness depends on a LAT-nucleated signalosome. Further, the bridging function of Gads can be specifically ablated by a 20 amino acid deletion in SLP-76 (Δ224–244), which disrupts its interaction with Gads (13). This deletion precisely phenocopied a lack of SLP-76 in all mast cell assays (78–80), providing strong evidence that the BMMC-specific signaling functions of SLP-76 absolutely depend on its association with Gads. Finally, mutational inactivation of the Gads dimerization interface phenocopied a loss of Gads (45), suggesting that FcεRI responsiveness depends on the ability of Gads to bind cooperatively to the LAT signalosome. Taken together, these results strongly suggest that the most important signaling function of Gads in mast cells is to bridge the FcεRI-induced formation of the LAT signalosome, which is required for all downstream responses.

A possible caveat to the above conclusion relates to subtle differences in the phenotypes reported for LAT- Gads- and SLP-76-deficient BMMC. In particular, the impairment of FcεRI responsiveness appears to be most severe in SLP-76-deficient BMMC and somewhat milder in LAT-deficient BMMC. This difference may reflect the presence of LAT2, which can bind to Gads, and thereby partially compensate for the absence of LAT1 (81). Alternatively, the phenotypic differences may reflect subtle differences in experimental protocols, such as the strength of antigenic stimulation that was applied, and/or the method of data analysis. It is important to note that BMMC responses are often

binary, such that the frequency of responding cells depends on the concentration of antigen applied, and strong stimulation can partially compensate for the lack of Gads (45). Similarly, SLP-76-deficient BMMCs exhibited barely detectable calcium flux when stimulated with a low dose of DNPylated antigen, whereas calcium flux was detectable in a small fraction of SLP-76-deficient cells upon stimulation with a 100-fold higher dose (75). It is therefore possible that the partial responsiveness of LAT-deficient BMMCs may reflect a binary response of a small population of cells upon stimulation with a relatively high concentration of antigen.

The Essential Role of SLP-76 and LAT in the T Cell Lineage

A Quick Overview of Thymic Development

All T cell lineages develop in the thymus, from which a number of developmentally and functionally distinguishable subtypes emerge to the periphery. The two main subtypes are αβ and γδ T cells, which differ in the genetic loci that undergo rearrangement to produce the clonotypic TCR. αβ thymocytes cells further differentiate into the CD4 and CD8 lineages, including various subtypes of each. In all thymocyte lineages, signaling by the newly rearranged TCR drives thymocyte selection and maturation. Thus, mutations that impair TCR signaling necessarily impair thymocyte development.

The development of conventional αβ T cells proceeds through three main stages: the double negative (DN: $CD4^-CD8^-$), double positive (DP: $CD4^+CD8^+$) and single positive (SP: $CD4^+$ or $CD8^+$) stages (**Figure 5A**). These broad phases can be further subdivided, based on additional cell surface markers (**Figure 5B**). DN thymocytes pass through four sub-stages (DN1-DN4, also known as proT1-proT4) that are distinguished by their expression of CD25 and CD44. As thymocytes enter DN3 ($CD25^+CD44^-$), they begin to rearrange the TCR β, γ and δ loci. Rearrangement of the γ and δ loci triggers progression to the γδ lineage; however, the vast majority of DN3 thymocytes rearrange the TCR β locus, resulting in expression of the pre-TCR, composed of the TCRβ, pre-Tα, and CD3 subunits. At the β-selection checkpoint, signaling pathways emanating from the pre-TCR trigger rapid thymocyte proliferation followed by transition through DN4 ($CD25^-CD44^-$) and on to the DP stage (82–84). DP thymocytes then rearrange the TCRα locus, resulting in the expression of a mature clonotypic αβ TCR. Recognition of self pMHC by the αβ TCR triggers intracellular signaling events that determine the cell fate (85–87). Moderate affinity interactions trigger positive selection, accompanied by changes in cell surface markers (**Figure 5C**), including increased expression of the TCR and passage to the SP compartment, whereas high affinity interactions trigger negative selection, leading to cell death and the removal of self-reactive T cell clones.

The Essential Role of LAT and SLP-76 in T Cell Development and Function

Consistent with their prominent role in TCR signaling, both LAT and SLP-76 are absolutely required for thymocyte maturation (88–90). Mice lacking LAT or SLP-76 are characterized by a small thymus, with cellularity reduced by 10-fold or more compared to wild-type. TCR β rearrangement proceeds normally, but the β-selection checkpoint is blocked due to impaired pre-TCR signal transduction, resulting in an accumulation of DN3 thymocytes, and a complete absence of all developmental stages beyond DN3. Consistent with these developmental defects, no mature αβ or γδ T cells can be detected in the periphery (88–90). Further supporting the severity of the signaling defect, treatment of LAT- or SLP-76-deficient mice with anti-CD3 did not trigger developmental progression beyond the DN stage (89, 90).

Conditional deletion of LAT or SLP-76 was used to characterize their role at later developmental stages. Deletion of either adaptor at the DP stage markedly impaired positive selection of thymocytes, as revealed by a profound block at the DP to SP transition. Further supporting this interpretation, LAT- or SLP-76-deficient thymocytes lacked the $CD24^{lo}TCR\beta^{hi}$ and $CD5^{hi}$ surface marker phenotypes, which characterize cells that have undergone positive selection. The impairment of positive selection was directly related to a lack of TCR signaling, as no calcium flux was observed upon TCR stimulation of SLP-76- or LAT-deficient DP thymocytes (91, 92). Similar results were observed upon conditional deletion of SLP-76 or LAT in mature, naïve T cells (93, 94). Absence of either adaptor abrogated short-term TCR responsiveness in all assays, including TCR-induced phosphorylation of PLC-γ and Erk, calcium flux, upregulation of activation markers, and TCR-induced proliferation, and also impaired homeostatic proliferation *in vivo* (93, 94). Consistent with these results, TCR signaling is profoundly blocked in LAT- and SLP-76-deficient T cell lines (95, 96). Taken together these phenotypes establish the necessity of SLP-76 and LAT for TCR responsiveness at all stages of T cell development, from earliest expression of the pre-TCR to the activation of peripheral T cells.

The Puzzling Role of Gads in the T Cell Lineage

The severe phenotypes of LAT- or SLP-76-deficient mice (74, 75, 88–94), raise the question of whether these two adaptors function as part of an obligate signaling complex bridged by Gads, or whether they may exert some of their signaling functions independently of each other.

The answer to this question may depend on the cell type. As described above, Gads-deficient mast cells phenocopy LAT- or SLP-deficient mast cells (74–76); moreover, mutational analyses of the adaptors (45, 77–80) provide strong evidence that LAT, Gads and SLP-76 function as an obligate complex in the FcεRI signaling pathway.

The role of Gads in the T cell lineage is more complex. Gads is expressed in all T cells, beginning from the earliest stages of thymic development (97), yet T cell development and function appear to be partially independent of the bridging activity of Gads, as detailed below.

Mutational Studies Reveal TCR Signaling Pathways and Thymocyte Development Are Partially Independent of Gads

The partial dependence of TCR signaling on Gads was first noted upon stable reconstitution of a SLP-76-deficient, Jurkat-derived

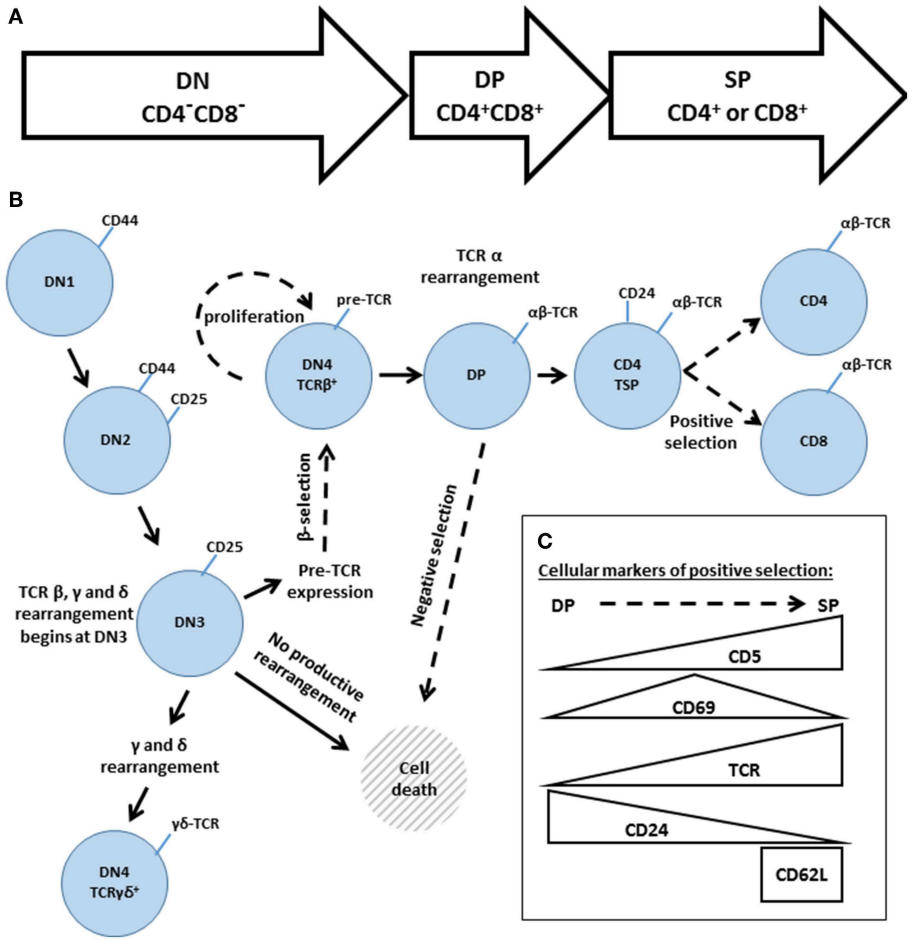

FIGURE 5 | An overview of thymic development. **(A)** The three phases of thymocyte development, known as double negative (DN, $CD4^{-}CD8^{-}$) double positive (DP, $CD4^{+}CD8^{+}$) and single positive (SP, $CD4^{+}$, or $CD8^{+}$). **(B)** A higher resolution depiction, based on additional cell surface markers. Transitions regulated by Gads are indicated by dashed arrows. The DN phase can be subdivided into DN1 ($CD44^{hi}CD25^{-}$), DN2 ($CD44^{hi}CD25^{+}$), DN3 ($CD44^{lo}CD25^{+}$), and DN4 ($CD44^{lo}CD25^{-}$). TCR rearrangement begins during DN3. Successful rearrangement of TCRβ results in expression of the pre-TCR, composed of TCRβ, pre-Tα and CD3. At the β-selection checkpoint, pre-TCR signaling triggers cellular proliferation and transition through DN4 and on to the DP stage. DP cells rearrange TCRα, and the resulting mature αβ TCR may recognize self-pMHC ligands. High affinity recognition of pMHC triggers cell death through negative selection. Moderate affinity recognition triggers positive selection, accompanied by increased expression of CD5, CD69, and the TCR. Positively selected cells pass through a CD4 transitional single positive stage (TSP), characterized by high expression of CD24, and then transition into the mature SP compartment ($CD4^{+}$ or $CD8^{+}$ and $TCR^{hi}CD24^{lo}CD62L^{hi}$). **(C)** Schematic summary of the markers of positive selection.

T cell line (J14) with wild-type or mutant alleles of SLP-76. Deletion of a 20 amino acid Gads-binding motif (Δ224–244) abrogated the binding of SLP-76 to Gads; nevertheless, TCR-induced tyrosine phosphorylation of SLP-76 was intact, and TCR responsiveness was markedly, but incompletely impaired (98). Complete impairment was observed upon substitution of the three N-terminal tyrosines of SLP-76 with phenylalanine (Y3F) (98). As another approach to reduce Gads-mediated signaling, overexpression of the Gads-binding motif (GBF) of SLP-76 competitively blocked the binding of Gads to SLP-76, resulting in impaired TCR-induced membrane recruitment of SLP-76, calcium flux, and upregulation of the CD69 activation marker (99). The role of Gads in mediating membrane recruitment of SLP-76 was directly addressed by fusing mutated SLP-76 to the transmembrane domain of LAT, thereby anchoring it to the membrane. Whereas signaling was disrupted by targeted point mutations that inactivate the Gads-binding motif of SLP-76, signaling was substantially rescued upon anchoring the mutated SLP-76 to the membrane, via its fusion to LAT (99).

Taken together, the T cell line-based experiments suggest that the interactions of SLP-76 with its N-terminal binding partners (Itk, Vav, and Nck) are absolutely required for TCR responsiveness. This SLP-76-nucleated complex appears to function best when recruited to LAT; nevertheless, SLP-76-dependent TCR signaling can proceed, albeit at reduced efficiency, in the absence of Gads-mediated recruitment. Consistent with this interpretation, upon deletion of Gads from the Jurkat T cell line, TCR-induced phosphorylation of SLP-76 remained intact, and TCR-induced PLC-γ phosphorylation,

calcium flux and activation of NFAT were substantially reduced, but not eliminated (65). An important caveat to these conclusions is that cell line-based experiments involve strong stimulation of the TCR using an anti-TCR antibody, which may partially bypass the need for the bridging function of Gads.

Mouse models were used to explore the importance of Gads-mediated signalosome assembly under the strength of TCR stimulation that naturally occurs during thymic development. *In vivo* signalosome assembly can be disrupted in many different ways: by mutating the Gads-binding sites on LAT, by deletion or competitive inhibition of the Gads-binding site on SLP-76, or by deletion of Gads itself. Since LAT and SLP-76 are absolutely required for passage through the β-selection checkpoint, a reasonable estimation of TCR signaling competence can be based on the ability of thymocytes to develop beyond the DN3 stage.

LAT contains 10 conserved tyrosine residues, of which the four distal tyrosines (labeled in **Figure 2**) appear to be necessary and sufficient for signalosome assembly (31–34). Substitution of all four with phenylalanine phenocopied the absence of LAT in thymic development (100), as did substitution of only the three most-distal tyrosines (34, 101). In retroviral reconstitution experiments, a LAT construct containing only the four distal tyrosines supported TCR-induced binding of LAT to Gads, Grb2 and PLC-γ, and supported thymic development *in vivo* (34). Surprisingly, upon mutation of either of the Gads binding sites (Y171 or Y191), binding to Gads was lost, but thymic development was largely intact, resulting in the production of DP and SP thymocytes as well as peripheral CD4 and CD8 T cells (34). Given the inherent variability of retroviral reconstitution, it is impossible to estimate the degree to which this LAT mutant phenocopies wild-type LAT; however, this experiment certainly suggests that the LAT-Gads interaction is not absolutely required for thymic development.

To more precisely address the contribution of Gads bridging activity to T cell development and function, SLP-76-deficient mice were stably reconstituted with wild type or mutant alleles of SLP-76 (102, 103). Whereas wild-type SLP-76 fully supported thymic development, deletion of the Gads binding site (Δ224–244) resulted in an incomplete block at the DN3 to DN4 transition with ∼75% reduction in thymic cellularity; nevertheless, DP and SP thymocytes were present, as well as peripheral CD4 and CD8 T cells (102, 103). In addition to affecting T cell development, the Δ224–244 mutation markedly impaired TCR-induced phosphorylation of PLC-γ1 (103) but only moderately reduced consequent downstream responses, including TCR-induced calcium flux, expression of the CD69 and CD5 activation markers, and proliferation (102, 103).

The above mutational analyses demonstrate that the TCR signaling functions of SLP-76 and LAT are only partially dependent on the bridging activity of Gads. Multiple lines of genetic evidence demonstrate that assembly of the LAT-Gads-SLP-76 signalosome promotes TCR responsiveness, but is not absolutely required for TCR signaling nor for thymic development.

Modulatory Role of Gads in T Cell Development and Function

Consistent with the above mutational analyses, Gads-deficient mice exhibit substantial, but incomplete defects in thymic development. Whereas LAT- or SLP-76-deficient mice arrest thymic development the DN3 to DN4 transition (88–90), Gads-deficient mice exhibit a partial block at this transition (97, 104), as well as defects in positive and negative selection (105, 106). Overall, thymic cellularity is reduced by 4-fold or more, including marked reductions in the total number of DP and SP thymocytes and a reduced ratio of CD4 to CD8 SP cells in the thymus and in the periphery (97, 106). Thus, Gads regulates multiple stages of thymic development, indicated by dashed arrows in **Figure 5B**, and detailed below.

Role of Gads at the β-selection checkpoint

The earliest steps of thymic development appear to be largely independent of Gads. As thymocytes enter DN3, they begin to rearrange the TCR β, γ, and δ genes (107, 108). Gads-deficient mice show no reduction in the absolute number of $TCR\beta^+$ or $TCR\gamma\delta^+$ DN3 thymocytes, demonstrating that Gads is not required for TCR gene rearrangement (104). Subsequently, $TCR\beta^+$ and $TCR\gamma\delta^+$ DN3 thymocytes differ markedly in their requirement for Gads at the DN3 to DN4 transition. Within the αβ lineage, the β-selection checkpoint is markedly impaired in the absence of Gads, resulting in a ∼20-fold reduction in the number of $TCR\beta^+$ DN4 thymocytes compared to wild-type mice (104). In contrast, Gads-deficient $TCR\gamma\delta^+$ DN3 thymocytes progress efficiently to DN4, and the number of $TCR\gamma\delta^+$ DN4 thymocytes is reduced by <2-fold compared to wild-type mice (104). The incomplete developmental block of Gads-deficient mice at the DN3 to DN4 transition may therefore be partly explained by Gads-independent progression of $TCR\gamma\delta^+$ thymocytes, which ultimately constitute 50% of the DN4 compartment in Gads-deficient mice, but only 10% in wild type mice (104).

The β-selection checkpoint depends on signals emanating from the pre-TCR, which trigger rapid proliferation and passage through DN4 and into the DP compartment (83). This developmental transition can be accelerated by *in vivo* administration of anti-CD3, which induced the advancement of virtually all wild-type DN3 thymocytes into the DN4 compartment; in contrast, <5% of Gads-deficient DN3 thymocytes advanced to DN4 upon anti-CD3 treatment (106). To better assess pre-TCR responsiveness under physiologic levels of signaling, Zeng et al. (104) measured cell cycling in $TCR\beta^+$ DN thymocytes. Upon the appearance of TCRβ, wild-type and Gads-deficient DN3 thymocytes exhibited a comparable increase in cell cycling, possibly indicating some degree of Gads-independent pre-TCR responsiveness. Subsequently, as thymocytes reduce expression of CD25 and transit to the DN4 compartment, wild-type cells continued cycling, whereas Gads-deficient cells exhibited decreased cycling and increased apoptosis. Taken together, the results suggest that Gads is required for sustained pre-TCR-induced proliferation and/or survival upon transition to DN4.

Role of Gads in positive and negative selection

Despite the marked impairment of β-selection, roughly three quarters of Gads-deficient thymocytes can be found in the DP compartment (97, 106). This unexpected observation suggests a bottleneck. Cells may be slow to enter the DP compartment due to impaired β-selection, but are also slow to exit this compartment, due to impaired positive and negative selection (**Figure 5B**, dashed arrows).

Positive and negative selection depend on signals emanating from the mature αβ TCR as it recognizes self pMHC ligands (109, 110). The TCR responsiveness of Gads-deficient thymocytes was examined upon *ex vivo* stimulation with anti-CD3. Whereas CD3-induced phosphorylation of SLP-76 was largely intact, the phosphorylation of PLC-γ and subsequent calcium flux were undetectable (106). When administered *in vivo,* anti-CD3 can mimic negative selection by persistently activating the TCR, triggering the deletion of DP thymocytes; however, no such deletion was observed in Gads-deficient mice (106). Mice carrying the HY TCR transgene, specific for the male-expressed H-Y antigen, are commonly used to assess positive and negative selection in a more physiologic setting. Whereas HY^+ thymocytes are deleted by negative selection in wild-type male mice, they were not deleted in Gads-deficient male mice; moreover, positive selection was profoundly impaired in HY^+ female mice (106). Together, the results suggest that in the absence of Gads, positive and negative selection are profoundly impaired due to impaired SLP-76-mediated signaling.

Closer examination of positive selection revealed that Gads-deficient DP thymocytes can advance as far as the $CD4^+$ transitional SP (TSP) compartment ($CD4^+CD8^-CD24^{hi}$) (105). The vast majority of Gads deficient TSP thymocytes retain an unactivated phenotype ($TCR\beta^{lo}CD69^{lo}$), suggesting that have not yet undergone positive selection (105). Further advancement to the mature ($CD24^{lo}TCR\beta^{hi}CD62L^{hi}$) CD4 SP compartment is profoundly impaired, whereas advancement to the mature CD8 compartment is only moderately impaired (105). The defect in positive selection was confirmed using additional transgenic TCR models, including the MHC type II-restricted OT-II model and the MHC type I-restricted OT-I and P14 transgenic TCR models. Gads-deficient OT-II thymocytes arrested in the CD4 TSP compartment, reflecting a severe defect in positive selection (105). In contrast, Gads-deficient OT-I and P14 thymocytes were profoundly, but incomplete arrested in the CD4 TSP compartment, with the development of mature CD8 SP thymocytes and peripheral naïve CD8 T cells bearing the transgenic TCR (105). Taken together the results suggest that MHC class II-mediated positive selection is strongly dependent on Gads, possibly explaining the reduced ratio of CD4 to CD8 SP thymocytes observed in Gads-deficient mice.

Surprising peripheral T cell phenotypes of Gads-deficient mice

Consistent with their thymic defects, Gads-deficient mice have reduced numbers of peripheral CD4 and CD8 T cells, which exhibit moderately reduced expression of the TCR (97, 106). The ratio of peripheral CD4 to CD8 T cells is markedly reduced, reflecting the reduced production of mature CD4 SP cells in the thymus. Moreover, Gads-deficient peripheral CD4 T cells exhibit increased homeostatic proliferation accompanied by increased cell death, which together result in their reduced persistence in the periphery (97). This defect was not observed in peripheral CD8 T cells, which gradually increase in number as the mice age (97).

It is important to note that most of the peripheral T cells found in Gads-deficient mice have a non-naïve phenotype. Gads-deficient CD4 T cells tend to have an activated phenotype ($CD44^{hi}CD62L^{lo}CD69^{hi}$), whereas virtually all of the CD8 T cells have a memory phenotype ($CD44^{hi}CD62L^{hi}CD69^{lo}$) (97). Consistent with their non-nave phenotype, Gads-deficient CD4 and CD8 T cells exhibited an enhanced ability to produce IFNγ upon *ex vivo* stimulation with PMA and ionomycin (97). These observations clearly suggest that Gads-deficient peripheral T cells represent an altered developmental pathway, and may not be directly comparable in their subset composition or function to wild-type peripheral T cells.

Despite the multiple developmental defects within the T cell lineage, Gads-deficient peripheral T cells appear to be capable of supporting a degree of immune responsiveness. Seconds after TCR stimulation, TCR-induced calcium flux was profoundly impaired in Gads deficient CD4 and CD8 T cells; nevertheless a clearly detectable minority of cells responded when the concentration of stimulant was increased (97). Consistent with this observation, Gads-deficient OT-I T cells proliferated upon stimulation with their cognate peptide antigen (SIINFEKL); however, the threshold concentration of antigen required to induce multiple rounds of proliferation was increased by ∼100-fold (111). Most surprisingly, Gads-deficient mice respond to immunization, producing antigen-specific IgM and IgG at levels comparable to wild-type mice (76). This result suggests that T cell helper activity may remain intact in the absence of Gads; however, it is not yet clear whether the helper activity is provided by conventional or innate-like T cell subsets. Taken together, it appears that Gads-deficient T cells can support immune responsiveness, provided that the dose of stimulating antigen is sufficiently high.

CAN WE SOLVE THE PUZZLE OF GADS?

The complex thymic and peripheral T cell phenotypes observed in Gads deficient mice are substantially milder than the arrested thymic development of LAT- and SLP-76 deficient mice. Whereas SLP-76 and LAT-deficient-mice completely lack peripheral T cells, Gads-deficient mice retain peripheral T cells that are capable of mediating a degree of immune responsiveness. Given that Gads serves as a TCR-inducible bridge between SLP-76 and LAT, how can we explain this marked divergence of phenotypes?

Here we shall discuss evidence supporting four possible explanations, which are not mutually exclusive. (1) Partially redundant mechanisms may allow for Gads-independent recruitment of SLP-76 to LAT; (2) Certain signaling functions of LAT and SLP-76 may be independent of their association; (3) A Gads-dependent branch of the TCR signaling pathway may

selectively regulate the development of particular T cell subsets; and (4) Gads may perform regulatory functions outside of the LAT signalosome.

Explanation #1: Partially Redundant Mechanisms May Allow for Gads-Independent Recruitment of SLP-76 to LAT

Without a doubt, Gads provides the most efficient and sensitive mechanism for recruiting SLP-76 to LAT, due to the high-affinity, constitutive binding of SLP-76 to Gads (18), coupled with the cooperatively stabilized binding of Gads to phospho-LAT (45). Nevertheless, a weak, TCR-inducible interaction of SLP-76 with phospho-LAT can be detected in the absence of Gads (65, 112). This barely detectable interaction suggests that compensatory mechanisms for recruiting SLP-76 to LAT may account for the residual TCR signaling activity observed in Gads-deficient cells.

Can Other Grb2 Family Members Compensate for the Lack of Gads?

One possible compensatory mechanism is the Gads-independent recruitment of SLP-76 to LAT by other Grb2-family members, Grb2 or Grap. Both Gads and Grb2 can bind via their C-terminal SH3 domains to a non-canonical RxxK motif found in SLP-76; however, Gads binds this motif with high affinity, measured at 9-20 nM (8, 10, 46), whereas Grb2 binds with ∼500-fold lower affinity (10, 14, 15). Due to its low affinity, Grb2 cannot interact with SLP-76 in the presence of competing Gads (18); however, the absence of Gads may permit weak, Grb2-mediated recruitment of SLP-76 to LAT. A third family member, Grap, co-purifies with both SLP-76 and LAT (113); albeit the affinity of these interactions have not been reported. Any such compensatory recruitment may be cooperatively stabilized by additional interactions occurring within the LAT-nucleated signalosome. For example, binding of the SH3 domain of LAT-bound PLC-γ1 to a proline-rich motif in SLP-76 can substantially stabilize the recruitment of SLP-76 to LAT (46, 98). While consistent with previously reported protein-protein interactions, neither Grb2- nor Grap-mediated recruitment of SLP-76 to LAT has been directly demonstrated.

Can SH2-Mediated Clustering of SLP-76 Compensate for the Lack of Gads?

The Grb2-based mechanism of recruitment cannot explain the substantial signaling activity exhibited by SLP-76Δ224-244 (98, 102, 103), a mutant allele that lacks the RxxK motif, and therefore cannot bind to Gads or to Grb2. SLP-76Δ224-244 supports a degree of thymic development that is roughly comparable to mice lacking the SH2 domain of SLP-76 (102, 103). One possible interpretation of these results is that the SH2 domain and RxxK motifs of SLP-76 may mediate partially redundant mechanisms for recruiting SLP-76 to LAT.

ADAP is an adaptor that mediates clustering of SLP-76 via its multipoint binding to the SH2 domain of SLP-76 (**Figure 4**). We suggest that ADAP-mediated oligomerization of SLP-76 may partially compensate for the absence of Gads. We further note that ADAP binds to SKAP1, which may be recruited to LAT via its interaction with Grb2 (50). This speculative chain of interactions (SLP-76-ADAP-SKAP1-Grb2-LAT) is built on known protein-protein interactions, but its ability to recruit SLP-76 to LAT has not been directly demonstrated.

Explanation #2: Certain Signaling Functions of LAT and SLP-76 May Be Independent of Their Association

While intriguing, the above-described compensatory mechanisms are not sufficient to explain the puzzle of Gads. The proposed mechanisms are quite weak, as the TCR-induced recruitment of SLP-76 to LAT is barely detectable in the absence of Gads. How then can we explain the relatively mild thymic phenotypes of Gads-deficient mice?

We suggest that separate SLP-76- and LAT-nucleated signaling complexes can form in the absence of Gads, and may mediate a degree of TCR responsiveness in the absence of their stable association. Indeed, the TCR-induced phosphorylation of SLP-76 and LAT are intact in Gads-deficient thymocytes (106) and T cell lines (65, 112). Further, some SLP-76 dependent signaling events are intact in Gads-deficient T cell line. Gads was not required for TCR-induced activation of AKT, nor was it required for TCR-induced actin polymerization or adhesion to the APC (112). SLP-76-dependent activation of Itk was likewise intact in Gads-deficient T cells, as evidenced by the intact TCR-induced phosphorylation of SLP-76 at its Itk-targeted site, Tyr^{173} (36, 40, 65).

Nevertheless, certain functions of LAT and SLP-76 are clearly dependent on Gads. Most importantly, Itk-mediated phosphorylation of PLC-γ1 was markedly reduced, and consequent downstream responses, including TCR-induced calcium flux, activation of the NFAT transcription factor, secretion of IL-2 and expression of the CD69 activation marker were substantially reduced in the absence of Gads (65).

These results provide evidence that one of the most important biochemical functions of Gads is to facilitate the interaction of SLP-76-bound Itk with its substrate, LAT-bound PLC-γ1 (40, 65). Gads accomplishes this by recruiting SLP-76 to LAT, thereby bringing Itk into close proximity with its substrate. Under conditions of high-intensity TCR stimulation, large numbers of SLP-76- and LAT-nucleated signaling complexes may accumulate and interact transiently via random diffusion, thereby bypassing the need for Gads. Consistent with this notion, Gads appears to be most important under conditions of low-intensity TCR stimulation, where Gads expression increases the frequency of responding cells (65, 111).

Explanation #3: A Gads-Dependent Branch of the TCR Signaling Pathway May Selectively Regulate the Development of Particular T Cell Subsets

Any functional description of Gads must account for the non-naïve, $CD44^{hi}$ phenotype exhibited by Gads-deficient peripheral T cells (97). This phenotype presents something of a paradox, as it suggests that the cells are antigen-experienced, and therefore

TCR responsive; yet Gads-deficient thymocytes and peripheral T cells exhibit profoundly impaired TCR responsiveness (97, 106).

A similar non-naïve peripheral phenotype has been observed in mice lacking the Tec-family kinase Itk (114–116), and also in mice bearing a mutation at SLP-76 Tyr^{145} (117), a site that is implicated in the binding and activation of Itk. As described above, one of the most important biochemical functions of Gads is to facilitate the interaction of SLP-76-bound Itk with its substrate, LAT-bound PLC-γ1 (40, 65). Studies of Itk-deficient mice suggest a number of ways in which reduced signaling through the Gads-SLP-76-Itk branch of the TCR signaling pathway may result in the accumulation of non-naïve peripheral T cells.

Reduced Signaling Through Gads-SLP-76-Itk May Result in a Skewed TCR Repertoire

One potential source of a non-naïve phenotype may be the presence of self-reactive T cell clones in the periphery. Whereas self-reactive thymocytes are normally eliminated by negative selection, partial impairment of TCR signaling in the DP compartment may shift the boundary between positive and negative selection (109, 118), thereby allowing the maturation of self-reactive SP thymocytes.

This type of repertoire shift was observed in mice lacking the Tec-family tyrosine kinases, Itk and Rlk, and expressing the HY transgenic TCR (119). Whereas HY^{+} TCR-transgenic thymocytes are negatively selected by their cognate antigen in male wild-type mice, they were positively selected in $Itk^{-/-}Rlk^{-/-}$ male mice, suggesting that partially impaired TCR signaling resulted in the conversion of a negatively-selecting self-antigen into a positively-selecting TCR ligand (119). An analogous shift in the selection boundary may occur in Gads-deficient thymocytes; however, this has not been directly demonstrated.

Once in the periphery, constitutive exposure of self-reactive Gads-deficient T cells to their cognate self-antigen may result in a non-naïve phenotype. Consistent with this explanation, OT-I mice, in which the TCR repertoire is fixed, produce peripheral CD8 T cells with a naïve phenotype, even in mice lacking Itk or Gads (105, 114). Taken together, these results suggest that impairment of the Gads-SLP-76-Itk branch of the TCR signaling pathway results in a non-naïve phenotype that is at least partially due to an altered TCR repertoire.

Reduced Signaling Through Gads-SLP-76-Itk May Skew Additional Thymic Developmental Decisions

In addition to influencing the TCR repertoire, the impaired positive selection observed in Gads- or Itk-deficient mice may impede the development of conventional αβ T cells, while favoring the development of specialized T cell sub-populations with innate-like phenotypes. Mice lacking Itk exhibit altered thymic selection which results in the maturation of CD4 and CD8 T cells with an innate-like phenotype (114–116, 120, 121). Innate-like T cells are characterized by the constitutive expression of activation markers such as CD44 and may bear additional markers including CD122, NK1.1, and others. The peripheral T cells found in Gads-deficient mice bear certain characteristics of innate-like T cells, including relatively low expression of the TCR, an activated phenotype found on most Gads-deficient CD4 T cells ($CD44^{hi}CD62L^{lo}CD69^{hi}$), a memory phenotype exhibited by virtually all Gads-deficient CD8 T cells ($CD44^{hi}CD62L^{hi}CD69^{lo}$), and an enhanced ability to produce IFNγ upon *ex vivo* stimulation with PMA and ionomycin (97). Further characterization of additional cell surface markers, transcription factors and functional responses that characterize different innate-like T cell subsets (122) will be required to determine whether the peripheral T cells found in Gads-deficient mice are in fact innate-like, or merely activated conventional T cells. Finally, an inducible deletion of Gads will be required to determine the point of origin of the innate-like phenotype, which may be generated by altered selection in the thymus, or by increased homeostatic proliferation in the periphery.

Explanation #4: Gads May Perform Additional Regulatory Functions Outside of the LAT Signalosome

Until now, we have viewed Gads exclusively as a component of the LAT-nucleated signalosome. Here, we consider the possibility that Gads may perform additional regulatory functions via its SH2-mediated interactions with other types of signaling complexes. The SH2 of Gads is specific for pYxN motifs, which are found in a variety of signaling proteins. Whereas many molecules of Gads are recruited to LAT, others may bind to costimulatory receptors such as CD28 and CD6, or to cytoplasmic signaling complexes nucleated by Shc (**Figure 1B**). Each of these Gads-binding partners plays a role in modulating T cell development and activation, and it is possible that some of their activity is mediated through Gads. According to this notion, the complex phenotype of Gads-deficient mice is the result of partial impairment of LAT-mediated signaling, combined with the impairment of additional Gads-dependent signaling pathways.

Does CD28 Costimulatory Activity Depend on Gads?

It has been known for some time that Gads can bind to a membrane-proximal pYMNM motif found in the cytoplasmic tail of the T cell costimulatory receptor, CD28 (19). The functional significance of this interaction is not clearly established, as the same pYMNM motif binds to PI3K and to Grb2 (123). To our knowledge, no study has addressed the CD28 signaling competence of a Gads-deficient T cell line or mouse, and so the contribution of Gads to CD28 signaling remains speculative.

The evidence implicating Gads in CD28 signaling is mixed. The cytoplasmic tail of CD28 includes two PxxP motifs, which are required to support the binding of CD28 to Gads in intact cells, and are likewise required for CD28 activity in some assay systems (124). This mutational evidence suggested an involvement of Gads in mediating CD28 costimulation; however, a subsequent binding study failed to confirm a direct dependence of Gads binding on the PxxP motifs (125). Indeed,

a more recent study suggests that CD28 signaling depends specifically on its interaction with Grb2 (126). Based on current knowledge its seems unlikely that any aspect of the Gads-deficient phenotype can be directly attributed to reduced signaling through CD28.

What Is the Role of Gads in CD6 Costimulation?

CD6 is a T cell surface glycoprotein that binds to CD166 on antigen presenting cells. CD6 appears to combine costimulatory and inhibitory activities, which together may set the threshold for T cell activation (127, 128). Upon TCR stimulation, the long cytoplasmic tail of CD6 is tyrosine phosphorylated at multiple sites, two of which bind to the SH2 domains of SLP-76 and Gads (21, 113, 127). Direct binding studies confirmed that CD6 Tyr^{662} binds to the SH2 of SLP-76, whereas Tyr^{629} binds to the SH2 of Gads (21). Within intact cells, the high affinity constitutive association of SLP-76 and Gads promotes their cooperative, bivalent binding to CD6. Thus, the binding of Gads to CD6 depends on SLP-76, whereas mutation of CD6 at either Tyr^{662} or Tyr^{629} abrogates its binding to both SLP-76 and Gads (21).

The costimulatory activity of CD6 is revealed by experiments in which co-ligation of CD6 with CD3 augments TCR-induced production of IL-2. This costimulatory activity depends on the SLP-76 binding site, Tyr^{662} and the Gads binding site, Tyr^{629} (21). To further test the importance of these interactions, a C-terminal fragment of CD6 encompassing the binding sites for SLP-76 and Gads was fused to a CD19-specific chimeric antigen receptor (CD19-CAR). Inclusion of the CD6 fragment in the CAR construct increased CAR-induced production of IFN-γ as well as CAR-mediated killing of CD19-expressing cells (129). While intriguing, the role of SLP-76 and Gads in mediating increased potency of the CAR construct remains to be determined. More importantly, to date, no study has assessed CD6-mediated costimulatory activity in Gads-deficient mice or T cells; therefore, the possible contribution of Gads to CD6-mediated signaling remains to be definitively demonstrated.

What About Gads Binding to Shc?

Over 20 years ago, Shc-derived pTyr peptide baits were used to clone Gads from a cDNA expression library; indeed, the name of Gads (Grb2-family adaptor downstream of Shc) denotes its SH2-mediated binding to Shc (16). Soon thereafter, it became apparent that Gads SH2 domain binds to LAT (13, 18), and the implications of its interaction with Shc were not further explored. Given the marked phenotypic divergence between LAT- and Gads-deficient mice, it may be worthwhile to re-explore the mechanistic connections between Gads and Shc.

The Shc family of adaptor proteins has three members, but only ShcA is expressed in T cells, where it has two isoforms, p45 and p52. ShcA is a ubiquitously expressed protein, characterized by an N-terminal PTB domain, a C-terminal SH2 domain and a central region containing three tyrosine phosphorylation sites, two of which can bind to Grb2-family adaptors (130). ShcA is required for fetal development past embryonic day 11.5 (131); however, it may also have specific functions in the T cell lineage.

Some evidence implicates ShcA in the activation of T cell lines, as both isoforms are rapidly tyrosine-phosphorylated in response to TCR stimulation (132) and in response to incubation with IL-2 (133). Moreover, a Shc-deficient Jurkat-derived T cell line exhibits impaired TCR-induced activation of C-Rel, resulting in impaired TCR-induced production of IL-2 (134).

The specific role of ShcA in T cell development was studied by T-cell specific impairment of its function *in vivo*. In one approach, a mutant ShcA transgene lacking three tyrosine phosphorylation sites (ShcFFF) was conditionally expressed in the T cell lineage (135). ShcFFF may serve as a dominant negative allele, as it can interact with specific binding partners via its PTB and SH2 domains, but cannot recruit Grb2-family adaptors into the signaling complex. When expressed from the earliest stages of thymocyte development, the ShcFFF transgene essentially phenocopied Gads-deficient mice. Like-Gads-deficient mice, ShcFFF-expressing mice have a thymus that is 3 to 10-fold smaller than wild-type due to a partial block at the DN3 to DN4 (β-selection) checkpoint; further, this block is associated with reduced proliferation of DN3 and DN4 cells, and cannot be overcome by the *in vivo* administration of anti-CD3 (97, 104, 106, 135). A similar phenotype was observed upon conditional deletion of Shc in the DN compartment (135). Based on these results, we must consider the possibility that the phenotype of Gads-deficient mice is at least partially due to reduced signaling through Shc.

FUTURE DIRECTIONS

Further research will be required to solve the puzzle of Gads. Whereas Gads is clearly required for FcεRI-mediated allergic responses, its role in T cell-mediated immunity is complex, and not easily characterized. This difficulty arises from the marked developmental defects of Gads-deficient thymocytes, which confound the interpretation of its function in peripheral T cells. Mice bearing an inducible-deletion of Gads, currently under development in our lab, will be a valuable tool for resolving this issue. A second difficulty concerns the multiple regulatory pathways intersecting at Gads. Gads-deficient mice lack both its positive and negative regulatory inputs, which may partly explain their mild phenotype. Third, we must consider the evidence that some functions of LAT and SLP-76 appear to be Gads-independent, whereas some functions of Gads may occur outside of the LAT-nucleated complex. It remains to be seen whether the Gads-like phenotypes exhibited by some mouse strains can be seen as defining a new regulatory pathway, dependent on Gads, Itk and possibly Shc, or whether their shared phenotypes merely reflect the expected outcome of partial impairment of TCR signaling. Finally, it is intriguing to consider the N-terminal SH3 of Gads, a domain that plays no role in bridging SLP-76 to LAT, and has no identified binding partners or biological functions, but is nevertheless strongly conserved throughout evolution. The study of this region may uncover new signaling functions that will help to illuminate the puzzle of Gads.

AUTHOR CONTRIBUTIONS

DY researched and wrote this article and designed all of the figures therein.

FUNDING

This work was supported by a grant from the Israel Science Foundation (1288/17), by the United States-Israel Binational Science Foundation (2017195) and by the Colleck Research Fund.

ACKNOWLEDGMENTS

I thank all of the members of my research group for thoughtful discussions regarding this review.

SUPPLEMENTARY MATERIAL

The Supplementary Material for this article can be found online at: https://www.frontiersin.org/articles/10.3389/fimmu.2019.01704/full#supplementary-material

REFERENCES

1. Bourette RP, Arnaud S, Myles GM, Blanchet JP, Rohrschneider LR, Mouchiroud G. Mona, a novel hematopoietic-specific adaptor interacting with the macrophage colony-stimulating factor receptor, is implicated in monocyte/macrophage development. *EMBO J.* (1998) 17:7273–81. doi: 10.1093/emboj/17.24.7273
2. Liu SK, Berry DM, McGlade CJ. The role of Gads in hematopoietic cell signalling. *Oncogene.* (2001) 20:6284–90. doi: 10.1038/sj.onc.1204771
3. Yankee TM, Draves KE, Clark EA. Expression and function of the adaptor protein Gads in murine B cells. *Eur J Immunol.* (2005) 35:1184–92. doi: 10.1002/eji.200425507
4. Yankee TM, Solow SA, Draves KD, Clark EA. Expression of the Grb2-related protein of the lymphoid system in B cell subsets enhances B cell antigen receptor signaling through mitogen-activated protein kinase pathways. *J Immunol.* (2003) 170:349–55. doi: 10.4049/jimmunol.170.1.349
5. Pawson T. Specificity in signal transduction: from phosphotyrosine-SH2 domain interactions to complex cellular systems. *Cell.* (2004) 116:191–203. doi: 10.1016/S0092-8674(03)01077-8
6. Cho S, Velikovsky CA, Swaminathan CP, Houtman JC, Samelson LE, Mariuzza RA. Structural basis for differential recognition of tyrosine-phosphorylated sites in the linker for activation of T cells (LAT) by the adaptor Gads. *EMBO J.* (2004) 23:1441–51. doi: 10.1038/sj.emboj.7600168
7. Zarrinpar A, Bhattacharyya RP, Lim WA. The Structure and Function of Proline Recognition Domains. *Sci STKE.* (2003) 2003:re8. doi: 10.1126/stke.2003.179.re8
8. Houtman JC, Higashimoto Y, Dimasi N, Cho S, Yamaguchi H, Bowden B, et al. Binding specificity of multiprotein signaling complexes is determined by both cooperative interactions and affinity preferences. *Biochemistry.* (2004) 43:4170–8. doi: 10.1021/bi0357311
9. Liu Q, Berry D, Nash P, Pawson T, McGlade CJ, Li SS. Structural basis for specific binding of the Gads SH3 domain to an RxxK motif-containing SLP-76 peptide: a novel mode of peptide recognition. *Mol Cell.* (2003) 11:471–81. doi: 10.1016/S1097-2765(03)00046-7
10. Seet BT, Berry DM, Maltzman JS, Shabason J, Raina M, Koretzky GA, et al. Efficient T-cell receptor signaling requires a high-affinity interaction between the Gads C-SH3 domain and the SLP-76 RxxK motif. *EMBO J.* (2007) 26:678–89. doi: 10.1038/sj.emboj.7601535
11. Houtman JCD, Yamaguchi H, Barda-Saad M, Braiman A, Bowden B, Appella E, et al. Oligomerization of signaling complexes by the multipoint binding of GRB2 to both LAT and SOS1. *Nat Struct Mol Biol.* (2006) 13:798–805. doi: 10.1038/nsmb1133
12. Law C-L, Ewings MK, Chaudhary PM, Solow SA, Yun TJ, Marshall AJ, et al. GrpL, a Grb2-related adaptor protein, interacts with SLP-76 to regulate nuclear factor of activated T cell activation. *J Exp Med.* (1999) 189:1243–53. doi: 10.1084/jem.189.8.1243
13. Liu SK, Fang N, Koretzky GA, McGlade CJ. The hematopoietic-specific adaptor protein Gads functions in T-cell signaling via interactions with the SLP-76 and LAT adaptors. *Curr Biol.* (1999) 9:67–75. doi: 10.1016/S0960-9822(99)80017-7
14. Berry DM, Nash P, Liu SK, Pawson T, McGlade CJ. A high-affinity Arg-X-X-Lys SH3 binding motif confers specificity for the interaction between Gads and SLP-76 in T cell signaling. *Curr Biol.* (2002) 12:1336–41. doi: 10.1016/S0960-9822(02)01038-2
15. Harkiolaki M, Lewitzky M, Gilbert RJ, Jones EY, Bourette RP, Mouchiroud G, et al. Structural basis for SH3 domain-mediated high-affinity binding between Mona/Gads and SLP-76. *EMBO J.* (2003) 22:2571–82. doi: 10.1093/emboj/cdg258
16. Liu SK, McGlade CJ. Gads is a novel SH2 and SH3 domain-containing adaptor protein that binds to tyrosine-phosphorylated Shc. *Oncogene.* (1998) 17:3073–82. doi: 10.1038/sj.onc.1202337
17. Qiu M, Hua S, Agrawal M, Li G, Cai J, Chan E, et al. Molecular cloning and expression of human Grap-2, a novel leukocyte-specific SH2- and SH3-containing adaptor-like protein that binds to Gab-1. *Biochem Biophys Res Comm.* (1998) 253:443–7. doi: 10.1006/bbrc.1998.9795
18. Asada H, Ishii N, Sasaki Y, Endo K, Kasai H, Tanaka N, et al. Grf40, a novel Grb2 family member, is involved in T cell signaling through interactions with SLP-76 and LAT. *J Exp Med.* (1999) 189:1383–90. doi: 10.1084/jem.189.9.1383
19. Ellis JH, Ashman C, Burden MN, Kilpatrick KE, Morse MA, Hamblin PA. GRID, a novel Grb-2-related adapter protein that interacts with the activated T cell costimulatory receptor CD28. *J Immunol.* (2000) 164:5805–14. doi: 10.4049/jimmunol.164.11.5805
20. Ludwig L, Kessler H, Hoang-Vu C, Dralle H, Adler G, Boehm BO, et al. Grap-2, a novel RET binding protein, is involved in RET mitogenic signaling. *Oncogene.* (2003) 22:5362. doi: 10.1038/sj.onc.1206517
21. Breuning J, Brown MH. T cell costimulation by CD6 is dependent on bivalent binding of a GADS/SLP-76 complex. *Mol Cell Biol.* (2017) 37:e00071–17. doi: 10.1128/MCB.00071-17
22. Dufner A, Kisser A, Niendorf S, Basters A, Reissig S, Schonle A, et al. The ubiquitin-specific protease USP8 is critical for the development and homeostasis of T cells. *Nat Immunol.* (2015) 16:950–60. doi: 10.1038/ni.3230
23. Lewitzky M, Harkiolaki M, Domart MC, Jones EY, Feller SM. Mona/Gads SH3C binding to hematopoietic progenitor kinase 1 (HPK1) combines an atypical SH3 binding motif, R/KXXK, with a classical PXXP motif embedded in a polyproline type II (PPII) helix. *J Biol Chem.* (2004) 279:28724–32. doi: 10.1074/jbc.M402745200
24. Liu SK, Smith CA, Arnold R, Kiefer F, McGlade CJ. The adaptor protein Gads (Grb2-related adaptor downstream of Shc) is implicated in coupling hemopoietic progenitor kinase-1 to the activated TCR. *J Immunol.* (2000) 165:1417–26. doi: 10.4049/jimmunol.165.3.1417
25. Ma W, Xia C, Ling P, Qiu M, Luo Y, Tan TH, et al. Leukocyte-specific adaptor protein Grap2 interacts with hematopoietic progenitor kinase 1 (HPK1) to activate JNK signaling pathway in T lymphocytes. *Oncogene.* (2001) 20:1703–14. doi: 10.1038/sj.onc.1204224
26. Balagopalan L, Coussens NP, Sherman E, Samelson LE, Sommers CL. The LAT story: a tale of cooperativity, coordination, and choreography. *Cold Spring Harbor Perspect Biol.* (2010) 2:a005512. doi: 10.1101/cshperspect.a005512
27. Jordan MS, Koretzky GA. Coordination of receptor signaling in multiple hematopoietic cell lineages by the adaptor protein SLP-76. *Cold Spring Harb Perspect Biol.* (2010) 2:a002501. doi: 10.1101/cshperspect.a002501
28. Bilal MY, Houtman JCD. Transmission of T cell receptor-mediated signaling via the GRB2 family of adaptor proteins. *Signal Mech Regulat T Cell Divers Funct.* (2018) 72:147–76. doi: 10.1201/9781315371689-9

29. Brownlie RJ, Zamoyska R. T cell receptor signalling networks: branched, diversified and bounded. *Nat Rev Immunol.* (2013) 13:257–69. doi: 10.1038/nri3403
30. Chakraborty AK, Weiss A. Insights into the initiation of TCR signaling. *Nat Immunol.* (2014) 15:798–807. doi: 10.1038/ni.2940
31. Lin J, Weiss A. Identification of the minimal tyrosine residues required for linker for activation of T cell function. *J Biol Chem.* (2001) 276:29588–95. doi: 10.1074/jbc.M102221200
32. Paz PE, Wang S, Clarke H, Lu X, Stokoe D, Abo A. Mapping the Zap-70 phosphorylation sites on LAT (linker for activation of T cells) required for recruitment and activation of signalling proteins in T cells. *Biochem J.* (2001) 356:461–71. doi: 10.1042/bj3560461
33. Zhang W, Trible RP, Zhu M, Liu SK, McGlade CJ, Samelson LE. Association of Grb2, Gads and Phospholipase C-γ1 with phosphorylated LAT tyrosine residues. *J Biol Chem.* (2000) 275:23355–61. doi: 10.1074/jbc.M000404200
34. Zhu M, Janssen E, Zhang W. Minimal requirement of tyrosine residues of linker for activation of T cells in TCR signaling and thymocyte development. *J Immunol.* (2003) 170:325–33. doi: 10.4049/jimmunol.170.1.325
35. Fang N, Motto DG, Ross SE, Koretzky GA. Tyrosines 113, 128, and 145 of SLP-76 are required for optimal augmentation of NFAT promoter activity. *J Immunol.* (1996) 157:3769–73.
36. Sela M, Bogin Y, Beach D, Oellerich T, Lehne J, Smith-Garvin JE, et al. Sequential phosphorylation of SLP-76 at tyrosine 173 is required for activation of T and mast cells. *EMBO J.* (2011) 30:3160–72. doi: 10.1038/emboj.2011.213
37. Wardenburg JB, Fu C, Jackman JK, Flotow H, Wilkinson SE, Williams DH, et al. Phosphorylation of SLP-76 by the ZAP-70 protein-tyrosine kinase is required for T-cell receptor function. *J Biol Chem.* (1996) 271:19641–4. doi: 10.1074/jbc.271.33.19641
38. Poulin B, Sekiya F, Rhee SG. Intramolecular interaction between phosphorylated tyrosine-783 and the C-terminal Src homology 2 domain activates phospholipase C-gamma1. *Proc Natl Acad Sci USA.* (2005) 102:4276–81. doi: 10.1073/pnas.0409590102
39. Sekiya F, Poulin B, Kim YJ, Rhee SG. Mechanism of tyrosine phosphorylation and activation of phospholipase C-gamma 1. Tyrosine 783 phosphorylation is not sufficient for lipase activation. *J Biol Chem.* (2004) 279:32181–90. doi: 10.1074/jbc.M405116200
40. Bogin Y, Ainey C, Beach D, Yablonski D. SLP-76 mediates and maintains activation of the Tec family kinase ITK via the T cell antigen receptor-induced association between SLP-76 and ITK. *Proc Natl Acad Sci USA.* (2007) 104:6638–43. doi: 10.1073/pnas.0609771104
41. Bunnell SC, Diehn M, Yaffe MB, Findell PR, Cantley LC, Berg LJ. biochemical interactions integrating itk with the T cell receptor-initiated signaling cascade. *J Biol Chem.* (2000) 275:2219–30. doi: 10.1074/jbc.275.3.2219
42. Su Y-W, Zhang Y, Schweikert J, Koretzky GA, Reth M, Wienands J. Interaction of SLP adaptors with the SH2 domain of Tec family kinases. *Eur J Immunol.* (1999) 29:3702–11. doi: 10.1002/(SICI)1521-4141(199911)29:11<3702::AID-IMMU3702>3.0.CO;2-R
43. Devkota S, Joseph RE, Min L, Bruce Fulton D, Andreotti AH. Scaffold Protein SLP-76 Primes PLCγ1 for Activation by ITK-Mediated Phosphorylation. *J Mol Biol.* (2015) 427:2734–47. doi: 10.1016/j.jmb.2015.04.012
44. Carpenter G, Ji Q-S. Phospholipase C-γ as a signal transducing element. *Exp Cell Res.* (1999) 253:15–24. doi: 10.1006/excr.1999.4671
45. Sukenik S, Frushicheva MP, Waknin-Lellouche C, Hallumi E, Ifrach T, Shalah R, et al. Dimerization of the adaptor Gads facilitates antigen receptor signaling by promoting the cooperative binding of Gads to the adaptor LAT. *Sci Signal.* (2017) 10:eaal1482. doi: 10.1126/scisignal.aal1482
46. Manna A, Zhao H, Wada J, Balagopalan L, Tagad HD, Appella E, et al. Cooperative assembly of a four-molecule signaling complex formed upon T cell antigen receptor activation. *Proc Natl Acad Sci USA.* (2018) 115:E11914–E11923. doi: 10.1073/pnas.1817142115
47. Benfield AP, Whiddon BB, Clements JH, Martin SF. Structural and energetic aspects of Grb2-SH2 domain-swapping. *Arch Biochem Biophys.* (2007) 462:47–53. doi: 10.1016/j.abb.2007.03.010
48. Hosoe Y, Numoto N, Inaba S, Ogawa S, Morii H, Abe R, et al. Structural and functional properties of Grb2 SH2 dimer in CD28 binding. *Biophys Physicobiol.* (2019) 16:80–8. doi: 10.2142/biophysico.16.0_80
49. Schiering N, Casale E, Caccia P, Giordano P, Battistini C. Dimer formation through domain swapping in the crystal structure of the Grb2-SH2–Ac-pYVNV complex. *Biochemistry.* (2000) 39:13376–82. doi: 10.1021/bi0012336
50. Raab M, Lu Y, Kohler K, Smith X, Strebhardt K, Rudd CE. LFA-1 activates focal adhesion kinases FAK1/PYK2 to generate LAT-GRB2-SKAP1 complexes that terminate T-cell conjugate formation. *Nat Commun.* (2017) 8:16001. doi: 10.1038/ncomms16001
51. Balagopalan L, Kortum RL, Coussens NP, Barr VA, Samelson LE. The linker for activation of T cells (LAT) signaling hub: from signaling complexes to microclusters. *J Biol Chem.* (2015) 290:26422–9. doi: 10.1074/jbc.R115.665869
52. Bunnell SC, Hong DI, Kardon JR, Yamazaki T, McGlade CJ, Barr VA, et al. T cell receptor ligation induces the formation of dynamically regulated signaling assemblies. *J Cell Biol.* (2002) 158:1263–75. doi: 10.1083/jcb.200203043
53. Bunnell SC, Singer AL, Hong DI, Jacque BH, Jordan MS, Seminario MC, et al. Persistence of cooperatively stabilized signaling clusters drives T-cell activation. *Mol Cell Biol.* (2006) 26:7155–66. doi: 10.1128/MCB.00507-06
54. Su X, Ditlev JA, Hui E, Xing W, Banjade S, Okrut J, et al. Phase separation of signaling molecules promotes T cell receptor signal transduction. *Science.* (2016) 352:595–9. doi: 10.1126/science.aad9964
55. Lewis JB, Scangarello FA, Murphy JM, Eidell KP, Sodipo MO, Ophir MJ, et al. ADAP is an upstream regulator that precedes SLP-76 at sites of TCR engagement and stabilizes signaling microclusters. *J Cell Sci.* (2018) 131:jcs215517. doi: 10.1242/jcs.215517
56. Coussens NP, Hayashi R, Brown PH, Balagopalan L, Balbo A, Akpan I, et al. Multipoint binding of the SLP-76 SH2 domain to ADAP is critical for oligomerization of SLP-76 signaling complexes in stimulated T cells. *Mol Cell Biol.* (2013) 33:4140–51. doi: 10.1128/MCB.00410-13
57. Pauker MH, Reicher B, Fried S, Perl O, Barda-Saad M. Functional cooperation between the proteins Nck and ADAP is fundamental for actin reorganization. *Mol Cell Biol.* (2011) 31:2653–66. doi: 10.1128/MCB.01358-10
58. Yi J, Balagopalan L, Nguyen T, McIntire KM, Samelson LE. TCR microclusters form spatially segregated domains and sequentially assemble in calcium-dependent kinetic steps. *Nat Commun.* (2019) 10:277. doi: 10.1038/s41467-018-08064-2
59. Ling P, Meyer CF, Redmond LP, Shui J-W, Davis B, Rich RR, et al. Involvement of hematopoietic progenitor kinase 1 in T cell receptor signaling. *J Biol Chem.* (2001) 276:18908–14. doi: 10.1074/jbc.M101485200
60. Liou J, Kiefer F, Dang A, Hashimoto A, Cobb MH, Kurosaki T, et al. HPK1 is activated by lymphocyte antigen receptors and negatively regulates AP-1. *Immunity.* (2000) 12:399–408. doi: 10.1016/S1074-7613(00)80192-2
61. Brenner D, Brechmann M, Rohling S, Tapernoux M, Mock T, Winter D, et al. Phosphorylation of CARMA1 by HPK1 is critical for NF-kappaB activation in T cells. *Proc Natl Acad Sci USA.* (2009) 106:14508–13. doi: 10.1073/pnas.0900457106
62. Sauer K, Liou J, Singh SB, Yablonski D, Weiss A, Perlmutter RM. Hematopoietic progenitor kinase 1 associates physically and functionally with the adaptor proteins B cell linker protein and SLP-76 in lymphocytes. *J Biol Chem.* (2001) 276:45207–16. doi: 10.1074/jbc.M106811200
63. Di Bartolo V, Montagne B, Salek M, Jungwirth B, Carrette F, Fourtane J, et al. A novel pathway down-modulating T cell activation involves HPK-1-dependent recruitment of 14-3-3 proteins on SLP-76. *J Exp Med.* (2007) 204:681–91. doi: 10.1084/jem.20062066
64. Lasserre R, Cuche C, Blecher-Gonen R, Libman E, Biquand E, Danckaert A, et al. Release of serine/threonine-phosphorylated adaptors from signaling microclusters downregulates T cell activation. *J Cell Biol.* (2011) 195:839–53. doi: 10.1083/jcb.201103105
65. Lugassy J, Corso J, Beach D, Petrik T, Oellerich T, Urlaub H, et al. Modulation of TCR responsiveness by the Grb2-family adaptor, Gads. *Cell Signal.* (2015) 27:125–34. doi: 10.1016/j.cellsig.2014.10.005
66. Shui JW, Boomer JS, Han J, Xu J, Dement GA, Zhou G, et al. Hematopoietic progenitor kinase 1 negatively regulates T cell receptor

signaling and T cell-mediated immune responses. *Nat Immunol.* (2007) 8:84–91. doi: 10.1038/ni1416
67. Wang X, Li J-P, Chiu L-L, Lan J-L, Chen D-Y, Boomer J, et al. Attenuation of T cell receptor signaling by serine phosphorylation-mediated lysine 30 ubiquitination of SLP-76 protein. *J Biol Chem.* (2012) 287:34091–100. doi: 10.1074/jbc.M112.371062
68. Berry DM, Benn SJ, Cheng AM, McGlade CJ. Caspase-dependent cleavage of the hematopoietic specific adaptor protein Gads alters signalling from the T cell receptor. *Oncogene.* (2001) 20:1203–11. doi: 10.1038/sj.onc.1204218
69. Yankee TM, Draves KE, Ewings MK, Clark EA, Graves JD. CD95/Fas induces cleavage of the GrpL/Gads adaptor and desensitization of antigen receptor signaling. *Proc Natl Acad Sci USA.* (2001) 98:6789–93. doi: 10.1073/pnas.111158598
70. Kaji T, Hachimura S, Ise W, Kaminogawa S. Proteome analysis reveals caspase activation in hyporesponsive CD4 T lymphocytes induced *in vivo* by the oral administration of antigen. *J Biol Chem.* (2003) 278:27836–43. doi: 10.1074/jbc.M212820200
71. Puga I, Rao A, Macian F. Targeted cleavage of signaling proteins by caspase 3 inhibits T cell receptor signaling in anergic T cells. *Immunity.* (2008) 29:193–204. doi: 10.1016/j.immuni.2008.06.010
72. Alvarez-Errico D, Lessmann E, Rivera J. Adapters in the organization of mast cell signaling. *Immunol Rev.* (2009) 232:195–217. doi: 10.1111/j.1600-065X.2009.00834.x
73. Kambayashi T, Koretzky GA. Proximal signaling events in FcεRI-mediated mast cell activation. *J Allergy Clin Immunol.* (2007) 119:544–52. doi: 10.1016/j.jaci.2007.01.017
74. Saitoh S, Arudchandran R, Manetz TS, Zhang W, Sommers CL, Love PE, et al. LAT is essential for FcεRI-mediated mast cell activation. *Immunity.* (2000) 12:525–35. doi: 10.1016/S1074-7613(00)80204-6
75. Pivniouk VI, Martin TR, Lu-Kuo JM, Katz HR, Oettgen HC, Geha RS. SLP-76 deficiency impairs signaling via the high-affinity IgE receptor in mast cells. *J Clin Invest.* (1999) 103:1737–43.
76. Yamasaki S, Takase-Utsugi M, Ishikawa E, Sakuma M, Nishida K, Saito T, et al. Selective impairment of FcepsilonRI-mediated allergic reaction in Gads-deficient mice. *Int Immunol.* (2008) 20:1289–97. doi: 10.1093/intimm/dxn085
77. Saitoh S-I, Odom S, Gomez G, Sommers CL, Young HA, Rivera J, et al. The four distal tyrosines are required for LAT-dependent signaling in FcεRI-mediated mast cell activation. *J Exp Med.* (2003) 198:831–43. doi: 10.1084/jem.20030574
78. Kettner A, Pivniouk V, Kumar L, Herve F, Lee J-S, Mulligan R, et al. Structural requirements of SLP-76 in siganaling via the high-affinity immunoglobulin E receptor (FcεRI) in mast cells. *Mol Cell Biol.* (2003) 23:2395–406. doi: 10.1128/MCB.23.7.2395-2406.2003
79. Silverman MA, Shoag J, Wu J, Koretzky GA. Disruption of SLP-76 interaction with Gads inhibits dynamic clustering of SLP-76 and FcεRI signaling in mast cells. *Mol Cell Biol.* (2006) 26:1826–38. doi: 10.1128/MCB.26.5.1826-1838.2006
80. Wu JN, Jordan MS, Silverman MA, Peterson EJ, Koretzky GA. Differential requirement for adapter proteins Src homology 2 domain-containing leukocyte phosphoprotein of 76 kDa and adhesion- and degranulation-promoting adapter protein in FcepsilonRI signaling and mast cell function. *J Immunol.* (2004) 172:6768–74. doi: 10.4049/jimmunol.172.11.6768
81. Kambayashi T, Okumura M, Baker RG, Hsu CJ, Baumgart T, Zhang W, et al. Independent and cooperative roles of adaptor molecules in proximal signaling during FcepsilonRI-mediated mast cell activation. *Mol Cell Biol.* (2010) 30:4188–96. doi: 10.1128/MCB.00305-10
82. Aifantis I, Gounari F, Scorrano L, Borowski C, von Boehmer H. Constitutive pre-TCR signaling promotes differentiation through Ca^{2+} mobilization and activation of NF-kappaB and NFAT. *Nat Immunol.* (2001) 2:403–9. doi: 10.1038/87704
83. Aifantis I, Mandal M, Sawai K, Ferrando A, Vilimas T. Regulation of T-cell progenitor survival and cell-cycle entry by the pre-T-cell receptor. *Immunol Rev.* (2006) 209:159–69. doi: 10.1111/j.0105-2896.2006.00343.x
84. Voll RE, Jimi E, Phillips RJ, Barber DF, Rincon M, Hayday AC, et al. NF-κB activation by the pre-T cell receptor serves as a selective survival signal in T lymphocyte development. *Immunity.* (2000) 13:677–89. doi: 10.1016/S1074-7613(00)00067-4
85. Fu G, Rybakin V, Brzostek J, Paster W, Acuto O, Gascoigne NRJ. Fine-tuning T cell receptor signaling to control T cell development. *Trends Immunol.* (2014) 35:311–8. doi: 10.1016/j.it.2014.05.003
86. Moran AE, Hogquist KA. T-cell receptor affinity in thymic development. *Immunology.* (2012) 135:261–7. doi: 10.1111/j.1365-2567.2011.03547.x
87. Morris GP, Allen PM. How the TCR balances sensitivity and specificity for the recognition of self and pathogens. *Nat Immunol.* (2012) 13:121–8. doi: 10.1038/ni.2190
88. Clements JL, Yang B, Ross-Barta SE, Eliason SL, Hrstka RF, Williamson RA, et al. Requirement for the leukocyte-specific adapter protein SLP-76 for normal T cell development. *Science.* (1998) 281:416–9. doi: 10.1126/science.281.5375.416
89. Pivniouk V, Tsitsikov E, Swinton P, Rathbun G, Alt FW, Geha RS. Impaired viability and profound block in thymocyte development in mice lacking the adaptor protein SLP-76. *Cell.* (1998) 94:229–38. doi: 10.1016/S0092-8674(00)81422-1
90. Zhang W, Sommers CL, Burshtyn DN, Stebbins CC, DeJarnette JB, Trible RP, et al. Essential role of LAT in T cell development. *Immunity.* (1999) 10:323–32. doi: 10.1016/S1074-7613(00)80032-1
91. Maltzman JS, Kovoor L, Clements JL, Koretzky GA. Conditional deletion reveals a cell-autonomous requirement of SLP-76 for thymocyte selection. *J Exp Med.* (2005) 202:893–900. doi: 10.1084/jem.20051128
92. Shen S, Zhu M, Lau J, Chuck M, Zhang W. The essential role of LAT in thymocyte development during transition from the double-positive to single-positive stage. *J Immunol.* (2009) 182:5596–604. doi: 10.4049/jimmunol.0803170
93. Shen S, Chuck MI, Zhu M, Fuller DM, Yang CW, Zhang W. The importance of LAT in the activation, homeostasis, and regulatory function of T cells. *J Biol Chem.* (2010) 285:35393–405. doi: 10.1074/jbc.M110.145052
94. Wu GF, Corbo E, Schmidt M, Smith-Garvin JE, Riese MJ, Jordan MS, et al. Conditional deletion of SLP-76 in mature T cells abrogates peripheral immune responses. *Eur J Immunol.* (2011) 41:2064–73. doi: 10.1002/eji.201040809
95. Finco TS, Kadlecek T, Zhang W, Samelson LE, Weiss A. LAT is required for TCR-mediated activation of PLCγ1 and the Ras pathway. *Immunity.* (1998) 9:617–26. doi: 10.1016/S1074-7613(00)80659-7
96. Yablonski D, Kuhne MR, Kadlecek T, Weiss A. Uncoupling of nonreceptor tyrosine kinases from PLC-γ1 in an SLP-76-deficient T cell. *Science.* (1998) 281:413–6. doi: 10.1126/science.281.5375.413
97. Yankee TM, Yun TJ, Draves KE, Ganesh K, Bevan MJ, Murali-Krishna K, et al. The Gads (GrpL) adaptor protein regulates T cell homeostasis. *J Immunol.* (2004) 173:1711–20. doi: 10.4049/jimmunol.173.3.1711
98. Yablonski D, Kadlecek T, Weiss A. Identification of a PLC-γ1 SH3 domain-binding site in SLP-76, required for TCR-mediated activation of PLC-γ1 and NFAT. *Mol Cell Biol.* (2001) 21:4208–18. doi: 10.1128/MCB.21.13.4208-4218.2001
99. Singer AL, Bunnell SC, Obstfeld AE, Jordan MS, Wu JN, Myung PS, et al. Roles of the proline-rich domain in SLP-76 subcellular localization and T cell function. *J Biol Chem.* (2004) 279:15481–90. doi: 10.1074/jbc.M313339200
100. Sommers CL, Menon RK, Grinberg A, Zhang W, Samelson LE, Love PE. Knock-in mutation of the distal four tyrosines of linker for activation of T cells blocks murine T cell development. *J Exp Med.* (2001) 194:135–42. doi: 10.1084/jem.194.2.135
101. Nunez-Cruz S, Aguado E, Richelme S, Chetaille B, Mura AM, Richelme M, et al. LAT regulates gammadelta T cell homeostasis and differentiation. *Nat Immunol.* (2003) 4:999–1008. doi: 10.1038/ni977
102. Kumar L, Pivniouk V, de la Fuente MA, Laouini D, Geha RS. Differential role of SLP-76 domains in T cell development and function. *Proc Natl Acad Sci USA.* (2002) 99:884–9. doi: 10.1073/pnas.022619199
103. Myung PS, Derimanov GS, Jordan MS, Punt JA, Liu Q-H, Judd BA, et al. Differential Requirement for SLP-76 domains in T cell development and function. *Immunity.* (2001) 15:1011–26. doi: 10.1016/S1074-7613(01)00253-9
104. Zeng L, Dalheimer SL, Yankee TM. $Gads^{-/-}$ mice reveal functionally distinct subsets of TCRbeta$^+$ CD4$^-$CD8$^-$ double-negative thymocytes. *J Immunol.* (2007) 179:1013–21. doi: 10.4049/jimmunol.179.2.1013

105. Dalheimer SL, Zeng L, Draves KE, Hassaballa A, Jiwa NN, Parrish TD, et al. Gads-deficient thymocytes are blocked at the transitional single positive $CD4^+$ stage. *Eur J Immunol.* (2009) 39:1395–404. doi: 10.1002/eji.200838692
106. Yoder J, Pham C, Iizuka Y-M, Kanagawa O, Liu SK, McGlade J, et al. Requirement for the SLP-76 adaptor GADS in T cell development. *Science.* (2001) 291:1987–91. doi: 10.1126/science.1057176
107. Kreslavsky T, Gleimer M, Garbe AI, von Boehmer H. alphabeta versus gammadelta fate choice: counting the T-cell lineages at the branch point. *Immunol Rev.* (2010) 238:169–81. doi: 10.1111/j.1600-065X.2010.00947.x
108. Narayan K, Kang J. Disorderly conduct in γδ versus αβ T cell lineage commitment. *Semin Immunol.* (2010) 22:222–7. doi: 10.1016/j.smim.2010.04.003
109. Gascoigne NRJ, Palmer E. Signaling in thymic selection. *Curr Opin Immunol.* (2011) 23:207–12. doi: 10.1016/j.coi.2010.12.017
110. Klein L, Kyewski B, Allen PM, Hogquist KA. Positive and negative selection of the T cell repertoire: what thymocytes see (and don't see). *Nat Rev Immunol.* (2014) 14:377. doi: 10.1038/nri3667
111. Zhang EY, Parker BL, Yankee TM. Gads Regulates the Expansion Phase of $CD8^+$ T Cell-Mediated Immunity. *J Immunol.* (2011) 186:4579–89. doi: 10.4049/jimmunol.1001604
112. Bilal MY, Zhang EY, Dinkel B, Hardy D, Yankee TM, Houtman JC. GADS is required for TCR-mediated calcium influx and cytokine release, but not cellular adhesion, in human T cells. *Cell Signal.* (2015) 27:841–50. doi: 10.1016/j.cellsig.2015.01.012
113. Roncagalli R, Hauri S, Fiore F, Liang Y, Chen Z, Sansoni A, et al. Quantitative proteomics analysis of signalosome dynamics in primary T cells identifies the surface receptor CD6 as a Lat adaptor-independent TCR signaling hub. *Nat Immunol.* (2014) 15:384–92. doi: 10.1038/ni.2843
114. Atherly LO, Brehm MA, Welsh RM, Berg LJ. Tec kinases Itk and Rlk are required for $CD8^+$ T cell responses to virus infection independent of their role in $CD4^+$ T cell help. *J Immunol.* (2006) 176:1571–81. doi: 10.4049/jimmunol.176.3.1571
115. Hu J, August A. Naïve and innate memory phenotype $CD4^+$ T cells have different requirements for active Itk for their development. *J Immunol.* (2008) 180:6544–52. doi: 10.4049/jimmunol.180.10.6544
116. Hu J, Sahu N, Walsh E, August A. Memory phenotype $CD8^+$ T cells with innate function selectively develop in the absence of active Itk. *Eur J Immunol.* (2007) 37:2892–9. doi: 10.1002/eji.200737311
117. Gordon SM, Carty SA, Kim JS, Zou T, Smith-Garvin J, Alonzo ES, et al. Requirements for eomesodermin and promyelocytic leukemia zinc finger in the development of innate-like $CD8^+$ T cells. *J Immunol.* (2011) 186:4573–8. doi: 10.4049/jimmunol.1100037
118. Stepanek O, Prabhakar Arvind S, Osswald C, King Carolyn G, Bulek A, Naeher D, et al. Coreceptor scanning by the T cell receptor provides a mechanism for T cell tolerance. *Cell.* (2014) 159:333–45. doi: 10.1016/j.cell.2014.08.042
119. Schaeffer EM, Broussard C, Debnath J, Anderson S, McVicar DW, Schwartzberg PL. Tec family kinases modulate thresholds for thymocyte development and selection. *J Exp Med.* (2000) 192:987–1000. doi: 10.1084/jem.192.7.987
120. Broussard C, Fleischacker C, Horai R, Chetana M, Venegas AM, Sharp LL, et al. Altered development of $CD8^+$ T cell lineages in mice deficient for the Tec kinases Itk and Rlk. *Immunity.* (2006) 25:93–104. doi: 10.1016/j.immuni.2006.05.011
121. Dubois S, Waldmann TA, Muller JR. ITK and IL-15 support two distinct subsets of $CD8^+$ T cells. *Proc Natl Acad Sci USA.* (2006) 103:12075–80. doi: 10.1073/pnas.0605212103
122. Prince AL, Yin CC, Enos ME, Felices M, Berg LJ. The Tec kinases Itk and Rlk regulate conventional versus innate T-cell development. *Immunol Rev.* (2009) 228:115–31. doi: 10.1111/j.1600-065X.2008.00746.x
123. Esensten Jonathan H, Helou Ynes A, Chopra G, Weiss A, Bluestone Jeffrey A. CD28 costimulation: from mechanism to therapy. *Immunity.* (2016) 44:973–88. doi: 10.1016/j.immuni.2016.04.020
124. Watanabe R, Harada Y, Takeda K, Takahashi J, Ohnuki K, Ogawa S, et al. Grb2 and Gads exhibit different interactions with CD28 and play distinct roles in CD28-mediated costimulation. *J Immunol.* (2006) 177:1085–91. doi: 10.4049/jimmunol.177.2.1085
125. Higo K, Oda M, Morii H, Takahashi J, Harada Y, Ogawa S, et al. Quantitative analysis by surface plasmon resonance of CD28 interaction with cytoplasmic adaptor molecules Grb2, Gads and p85 PI3K. *Immunol Invest.* (2014) 43:278–91. doi: 10.3109/08820139.2013.875039
126. Thaker YR, Schneider H, Rudd CE. TCR and CD28 activate the transcription factor NF-κB in T-cells via distinct adaptor signaling complexes. *Immunol Lett.* (2015) 163:113–9. doi: 10.1016/j.imlet.2014.10.020
127. Hassan NJ, Simmonds SJ, Clarkson NG, Hanrahan S, Puklavec MJ, Bomb M, et al. CD6 regulates T-cell responses through activation-dependent recruitment of the positive regulator SLP-76. *Mol Cell Biol.* (2006) 26:6727–38. doi: 10.1128/MCB.00688-06
128. Oliveira MI, Gonçalves CM, Pinto M, Fabre S, Santos AM, Lee SF, et al. CD6 attenuates early and late signaling events, setting thresholds for T-cell activation. *Eur J Immunol.* (2012) 42:195–205. doi: 10.1002/eji.201040528
129. Breuning J, Philip B, Brown MH. Addition of the C-terminus of CD6 to a chimeric antigen receptor enhances cytotoxicity and does not compromise expression. *Immunology.* (2019) 156:130–5. doi: 10.1111/imm.13009
130. Palmer E. Shc: a dominant player after ten seasons. *Nat Immunol.* (2002) 3:710. doi: 10.1038/ni0802-710
131. Lai KM, Pawson T. The ShcA phosphotyrosine docking protein sensitizes cardiovascular signaling in the mouse embryo. *Genes Dev.* (2000) 14:1132–45.
132. Ravichandran K, Lee K, Songyang Z, Cantley L, Burn P, Burakoff S. Interaction of Shc with the zeta chain of the T cell receptor upon T cell activation. *Science.* (1993) 262:902–5. doi: 10.1126/science.8235613
133. Zhu X, Suen KL, Barbacid M, Bolen JB, Fargnoli J. Interleukin-2-induced tyrosine phosphorylation of Shc proteins correlates with factor-dependent T cell proliferation. *J Biol Chem.* (1994) 269:5518–22.
134. Iwashima M, Takamatsu M, Yamagishi H, Hatanaka Y, Huang Y-Y, McGinty C, et al. Genetic evidence for Shc requirement in TCR-induced c-Rel nuclear translocation and IL-2 expression. *Proc Natl Acad Sci USA.* (2002) 99:4544–9. doi: 10.1073/pnas.082647499
135. Zhang L, Camerini V, Bender TP, Ravichandran KS. A nonredundant role for the adapter protein Shc in thymic T cell development. *Nat Immunol.* (2002) 3:749. doi: 10.1038/ni820

Conflict of Interest Statement: The author declares that the research was conducted in the absence of any commercial or financial relationships that could be construed as a potential conflict of interest.

frontiers in Immunology

ORIGINAL RESEARCH
published: 01 October 2019
doi: 10.3389/fimmu.2019.02343

Immune Cell-Type Specific Ablation of Adapter Protein ADAP Differentially Modulates EAE

Jochen Rudolph[1,2], *Clara Meinke*[1,2], *Martin Voss*[1,2], *Karina Guttek*[1,2], *Stefanie Kliche*[1,2], *Dirk Reinhold*[1,2], *Burkhart Schraven*[1,2] *and Annegret Reinhold*[1,2]*

[1] *Institute for Molecular and Clinical Immunology, Otto von Guericke University Magdeburg, Magdeburg, Germany,* [2] *Health Campus Immunology, Infectiology and Inflammation, Magdeburg, Germany*

The cytosolic adhesion and degranulation-promoting adapter protein ADAP is expressed in various hematopoietic cells including T cells, NK cells, myeloid cells, and platelets but absent in mature B cells. The role of ADAP in T cell activation, proliferation and integrin activation is well-accepted. We previously demonstrated that conventional ADAP knockout mice show a significantly attenuated course of experimental autoimmune encephalomyelitis (EAE). To dissect the impact of different ADAP expressing cell populations on the reduced EAE severity, here, we generated lineage-specific conditional knockout mice. ADAP was deleted in T cells, myeloid cells, NK cells and platelets, respectively. Specific loss of ADAP was confirmed on the protein level. Detailed immunophenotyping was performed to assess the consequence of deletion of ADAP with regard to the maturation and distribution of immune cells in primary and secondary lymphoid organs. The analysis showed equivalent results as for conventional ADAP knockout mice: impaired thymocyte development in $ADAP^{fl/fl}$ Lck-Cre mice, normal NK cell and myeloid cell distribution in $ADAP^{fl/fl}$ NKp46-Cre mice and $ADAP^{fl/fl}$ LysM-Cre mice, respectively as well as thrombocytopenia in $ADAP^{fl/fl}$ PF4-Cre mice. Active EAE was induced in these animals by immunization with the myelin oligodendrocyte $glycoprotein_{35-55}$ peptide. The clinical course of EAE was significantly milder in mice with loss of ADAP in T cells, myeloid cells and NK cells compared to ADAP-sufficient control littermates. Surprisingly, specific deletion of ADAP in platelets resulted in a more exacerbated disease. These data show that T cell-independent as well as T cell-dependent mechanisms are responsible for the complex phenotype observed in conventional ADAP knockout mice.

Keywords: adapter protein, ADAP, EAE, conditional knockout mice, T cell, NK cell, myeloid cell, platelet

OPEN ACCESS

Edited by:
Navin Kumar Verma, Nanyang Technological University, Singapore

Reviewed by:
Sven G. Meuth, University Hospital Münster, Germany
Brandon Burbach, University of Minnesota Twin Cities, United States

***Correspondence:**
Annegret Reinhold
annegret.reinhold@med.ovgu.de

Specialty section:
This article was submitted to Molecular Innate Immunity, a section of the journal Frontiers in Immunology

Received: *03 May 2019*
Accepted: *17 September 2019*
Published: *01 October 2019*

Citation:
Rudolph J, Meinke C, Voss M, Guttek K, Kliche S, Reinhold D, Schraven B and Reinhold A (2019) Immune Cell-Type Specific Ablation of Adapter Protein ADAP Differentially Modulates EAE. Front. Immunol. 10:2343. doi: 10.3389/fimmu.2019.02343

INTRODUCTION

Adapter proteins contain modular domains that mediate constitutive or inducible interactions between proteins or proteins and lipids. By definition, they exhibit no enzymatic or transcriptional activity. The adhesion and degranulation-promoting adapter protein ADAP belongs to the group of cytosolic adapter proteins. ADAP is expressed within the hematopoietic system in T cells, NK cells, myeloid cells and platelets, but not in mature B cells (1, 2).

The function of ADAP is well-described in T cells. ADAP was the first adapter protein identified that is involved in inside-out signaling linking the TCR-stimulation to integrin activation (3, 4). ADAP-deficient mice show impaired thymic development, reduced TCR-induced integrin-dependent adhesion, decreased proliferation as well as diminished NF-κB activation and cytokine production (5–7). Interestingly, the loss of ADAP showed strong impact on $CD4^+$ T cell activation, expansion and effector function, whereas $CD8^+$ T cells revealed only moderate effects of ADAP deficiency (8). At the same time, Fiege et al. (9) provided evidence for a negative regulatory role of ADAP in the conversion of naïve $CD8^+$ T cells into memory phenotype under steady state condition. Furthermore, ADAP is a positive regulator for resident $CD8^+$ T cell memory formation during an acute pathogen infection (10). These data suggest that ADAP fulfills different function in $CD4^+$ and $CD8^+$ T cells.

In NK cells, ADAP is exclusively responsible for cytokine and chemokine secretion but not for cytotoxicity (11, 12). Neutrophils from ADAP-deficient mice show defective E-selectin-mediated integrin activation and slow leukocyte rolling in the mouse kidney ischemia-reperfusion model (13). The role of ADAP in other myeloid cells like mast cells, monocytes and macrophages remains largely unknown. ADAP-deficiency in microglia, the CNS-resident macrophage population does not influence microglia function such as NO production and cytokine release (14). Limited data are available about the role of ADAP in dendritic cells (DC). Previous results revealed that ADAP is critically involved in CD11c integrin-mediated cytokine production and actin polymerization (15).

In addition to lymphoid and myeloid cells, ADAP is required for selected platelet functions. ADAP-deficient mice show mild thrombocytopenia, normal bleeding time but more frequent re-bleeding from tail wounds (16). Moreover, ADAP-deficient platelets form unstable thrombi after carotoid artery occlusion (17). It was clearly demonstrated that ADAP interacts with the integrin binding proteins talin and kindlin-3. ADAP-deficient platelets exhibit decreased association with talin and kindlin-3 leading to reduced activation of integrin αIIbβ3 and decreased fibrinogen binding (18). In addition, ADAP is also involved in the regulation of platelet integrin α2β1 (19).

Taken together, independent of the cell type, the adapter protein ADAP is implicated in cell functions associated with integrin activation, cytoskeletal rearrangement and adhesion. Therefore, it is tempting to speculate that the loss of ADAP has an impact on immune-mediated diseases. We previously investigated the clinical course of experimental autoimmune encephalomyelitis (EAE), the most commonly used mouse model of the human disease multiple sclerosis, in conventional ADAP knockout mice. Indeed, we found that ADAP-deficient mice show significantly milder EAE compared to ADAP-sufficient wildtype mice (20).

EAE is a CNS demyelinating disease caused by autoreactive T cells directed against myelin proteins like MOG (myelin oligodendrocyte glycoprotein). The disease can be induced in susceptible animals by immunization with myelin peptides in combination with strong immune adjuvants like complete Freund's adjuvant. In addition, most protocols for induction of EAE in rodents use pertussis toxin to block G-protein coupled receptors and to enhance immune response (21). The histopathology consists of meningeal and perivascular inflammation dominated by activated $CD4^+$ T cells and macrophages and enhanced microglia reactivity (22). This pathological process leads to axonal injury and the formation of demyelinated plaques. In C57BL/6 mice, the disease shows a monophasic chronic-progressive clinical profile. The typical symptoms of diseased mice vary from tail plegia followed by hind limb and forelimb paralysis (21).

It is well-accepted that EAE is primarily driven by encephalitogenic helper T cells (Th1 and Th17) and regulatory T cells (23). During the induction phase of the disease, myelin-specific $CD4^+$ T cells are activated and expand in the peripheral lymphoid tissue. These effector T cells cross the blood-brain barrier and enter the CNS. The inflammatory response leads to the recruitment of other immune cells including monocytes, macrophages, dendritic cells, B cells, and NK cells (24). The invading monocytes, macrophages and dendritic cells express high amounts of MHC-II molecules and are involved in antigen presentation and reactivation of T cells within the CNS. In addition, monocytes and macrophages secrete pro- as well as anti-inflammatory cytokines depending on their environment (25). Also $CD8^+$ T cells are involved in cytotoxicity, pro-inflammatory cytokine production and demyelination during disease induction as well as in regulatory function during down modulation of inflammation (26). The role of NK cells in EAE is still controversial. NK cells contribute to both effector function via their cytotoxic activity and to regulatory function via the production of pro- and anti-inflammatory cytokines. It has been reported that NK cell depletion results in more exacerbated disease (27). The importance of NK cell-derived IFN-γ for macrophage expansion during early phase of EAE was clearly demonstrated (28). Furthermore, it was shown that platelets contribute to the pathogenesis of EAE by promoting the inflammatory response in the CNS. Depletion of platelets during the effector phase of EAE significantly ameliorated the disease progression (29).

All above-mentioned hematopoietic cells—T cells, NK cells, myeloid cells, and platelets - express the adaptor protein ADAP. We have previously demonstrated that conventional ADAP knockout mice show strongly attenuated EAE. However, this approach cannot answer the question, which cells contribute to the lower EAE severity. To dissect the role of ADAP in different cell types during EAE, we generated conditional knockout mice. After characterization of the immune system of these mice, we induced active EAE by application of MOG_{35-55} peptide in complete Freund's adjuvant (CFA) and monitored the disease course.

MATERIALS AND METHODS

Mice

Mice containing the knockout first allele C57BL/6N-$Fyb^{tm1a(EUCOMM)Hmgu}$/Cnrm (30) were sourced from the

EUCOMM project and were purchased from the European Mouse Mutant Archive EMMA. The lacZ and neomycin-resistance cassettes were both removed by breeding with transgenic mice expressing an Flp recombinase resulting in floxed alleles (containing *loxP* sites) and restoring the wildtype. To generate mice with the deletion of ADAP in a specific cell lineage, mice with floxed alleles were crossed with mice carrying the Cre recombinase. To delete ADAP in the megakaryocytic lineage, the Cre recombinase was under control of the platelet factor-4 (PF4) promotor as previously described (31). To delete ADAP in thymocytes and T cells, the B6.Cg-$^{Tg(Lck-cre)548Jxm}$/J mouse strain expressing the Cre recombinase under control of the lymphocyte protein tyrosine kinase (Lck) promotor was provided by Prof. Ursula Bommhardt (Magdeburg). To generate mice with the deletion of ADAP in the NK cell lineage, the NKp46-iCre knock-in mice were provided by Prof. Eric Vivier (Paris) (32). To delete ADAP in the myeloid cell lineage, we used the LysM-Cre knock-in mice, where the Cre recombinase was inserted into the lysosome 2 gene (B6N.129P2(B6)-Lyz2 $^{tm1(cre)Ifo}$/J, provided by Prof. Peter Mertens, Magdeburg).

The general scheme of generation of conditional ADAP knockout mice is shown in **Figure S1**. The presence or absence of the *FRT* sites, the *loxP* sites, the gene of interest and the respective Cre transgene were checked routinely by PCR using genomic DNA isolated from ear tissue. The primer sequences are listed as **Table S1**.

Conventional ADAP-deficient mice (6) were backcrossed to C57BL/6JBom for at least ten generations. For all experiments, 8–14 week old animals were used. To investigate specific effects of ADAP deletion and to exclude off target effects of Cre recombinase, ADAP$^{wt/wt}$ Cre^{tg} (Cre control) and ADAP$^{fl/fl}$ Cre^{tg} (conditional k.o.) mice were always used as littermates.

Animals were bred and maintained under specific-pathogen-free conditions in the central animal facility of the medical faculty of the University of Magdeburg. All procedures were conducted according to protocols approved by the local authorities (Landesverwaltungsamt Sachsen-Anhalt; reference number: 42502-2-1273 UniMD).

EAE Induction

Induction of EAE was performed as described earlier (33). Briefly, active EAE was induced by immunization with 200 μg MOG_{35-55} peptide emulsified in complete Freund's adjuvant (CFA, Sigma-Aldrich) containing 800 μg of heat-killed *Mycobacterium tuberculosis* (Difco Laboratories). The emulsion was administered s.c. as four 50-μl injections into the flanks of each leg. In addition, 200 ng of pertussis toxin (List Biological Laboratories) dissolved in 200 μl PBS was injected i.p. on days 0 and 2 after immunization as described earlier (34). Mice were monitored daily for clinical signs of EAE and graded on a scale of increasing severity from 0 to 5 as follows: 0, no signs; 0.5, partial tail weakness; 1, limp tail or slight slowing of righting from supine position; 1.5, limp tail and slight slowing of righting; 2, partial hind limb weakness or marked slowing of righting; 2.5, dragging of hind limb(s) without complete paralysis; 3, complete paralysis of at least one hind limb; 3.5, hind limb paralysis and slight weakness of forelimbs; 4, severe forelimb weakness; 5, moribund or dead (35). For reasons of animal welfare, mice were killed when reaching a score of 3 or above. Mean clinical scores at each day were calculated by adding disease scores of individual mice divided by the number of mice in each group.

Flow Cytometry

To investigate the distribution of immune cells, cells isolated from thymus, bone marrow, spleen and peripheral blood were stained with the following antibodies: anti-CD3ε (clone 145-2C11), anti-CD4 (clone RM4-5), anti-CD8 (clone 53-6.7), anti-CD11b, anti-CD11c (clone N418), anti-NKp46 (clone 29A1.4), anti-NK1.1 (clone PK136), anti-B220 (clone RA3-6B2), anti-IgM (clone RMM-1), anti-IgD (clone 11-26c2a), and the respective isotype controls were purchased from BioLegend. Flow cytometric measurements were performed as 4-color analysis using FACSCalibur and Cellquest software (BD Biosciences).

For the detection of NK cell development in the bone marrow, cells were treated with Fc block (purified anti-CD32/CD16 monoclonal antibodies) and subsequently stained with anti-CD3ε-FITC, anti-CD4-FITC, anti-CD8-FITC, anti-CD19-FITC (clone 6D5), anti-Gr-1-FITC (clone RB6-8C5), anti-NKp46-BV450 (BD Biosciences), anti-NK1.1-PacificBlue, and anti-CD122-PE-Cy7 (clone T41-B1), anti-CD11b-APC/Cy7 (cloneM1/70). For detection of myeloid cell distribution, in addition anti-F4/80 (clone BM8), anti-CD11c (clone N418) and anti-Ly6G (clone 1A8) were used. Antibodies were purchased from BioLegend if not otherwise indicated. All steps were performed on ice and incubations at 4°C in the dark. After staining, cells were fixed with 2% PFA in PBS.

For intracellular ADAP staining, we used a polyclonal sheep anti-ADAP antiserum and the respective pre-immune serum kindly provided by G. Koretzky. The staining procedure was previously described (1) and works reliably to track ADAP protein expression. Briefly, the cells were first stained with the fixable viability dye eFluor® 506 (eBioscience) and then staining of cell surface molecules and fixation (2% paraformaldehyde) were performed. Fixed cells were permeabilized in Hank's Salt Solution (HSS) containing 2% FCS and 0.5% Saponin and intracellular staining with antisera and secondary donkey anti-sheep-FITC was performed in HSS/2% FCS/0.2% Saponin. These measurements were performed using a BD LSRFortessa and BD FACSDiva™ software (BD Biosciences) and analyzed with FlowJo® v10. Analyses were performed on viable and single cells.

For detection leukocytes in the brain, mice were euthanized by inhalation of CO_2. The abdominal cavity and thorax were opened immediately and transcardial perfusion was performed through the left ventricle using NaCl. The brain was carefully removed, cut into pieces and treated with collagenase (2.5 mg/ml, Roche Diagnostics) and DNAse I (1 mg/ml, SIGMA) for 45 min at 37°C. Tissue was ground through a cell strainer (70 μm), washed, resuspended in 37% Percoll, and layered onto 70% Percoll. After centrifugation (600 g, 25 min), cells were removed from the interphase, washed and stained for FACS analysis.

TGF-β1 Measurement

Platelet-poor plasma was obtained by double centrifugation (400 × g for 5 min and subsequently 6.000 × g for 15 min). Plasma concentrations of murine latent TGF-β1 were measured according to the instructions of the manufacturer using a specific ELISA kit (R&D Systems).

Statistical Analysis

Results are expressed as mean ± SEM. Unpaired Student's *t*-test was used to assess the statistical significance of the differences. Statistical comparison of EAE disease severity between different two groups of animals was accomplished by performing non-parametric Wilcoxon matched pairs test using GraphPad Prism software. $P < 0.05$ (*); $P < 0.01$ (**); $P < 0.001$ (***).

RESULTS

T Cell-Specific Conditional ADAP Knockout Shows Less Severe EAE

The phenotype of ADAP-deficient murine T cells is well-described (6). Therefore, we started to generate a T cell-specific ADAP knockout mouse using the commercially available C57BL/6N-Fyb$^{tm1a(EUCOMM)Hmgu}$/Cnrm (EUCOMM) mouse (**Figure S1**). The mouse strain containing the critical exon 2 of *fyb* gene flanked by 2 loxP sites was crossed to a transgenic mouse expressing Cre recombinase under control of the mouse Lck promotor. This promotor is active during embryonic stages of thymic development and in mature T cells (36). The T cell-specific knockout was confirmed by flow cytometry based on the intracellular ADAP staining with a specific polyclonal antiserum and the respective preimmune serum. As depicted in **Figure 1A**, CD4$^+$ CD8$^+$ double positive cells, representing the majority of thymocytes, showed a clear loss of ADAP expression in conditional knockout mice (ADAP$^{fl/fl}$ Lck-Cre^{tg}) compared to Cre control mice (ADAP$^{wt/wt}$ Lck-Cre^{tg}). This specific loss of ADAP expression was also seen in single positive CD4$^+$ or CD8$^+$ thymocytes of T cell-specific ADAP knockout mice (data not shown). In the spleen, the ADAP knockout was confirmed in mature T cells of ADAP$^{fl/fl}$ Lck-Cre^{tg} mice, whereas NK cells showed ADAP expression as strong as those derived from ADAP$^{wt/wt}$ Lck-Cre^{tg} mice. Since mature B cells are known to lack ADAP expression (1), ADAP was not detectable in splenic B cells (**Figure 1A**). Summarizing, these results indicated a specific loss of ADAP in thymocytes and T cells.

Next, we analyzed the constitution of primary lymphoid organs (thymus) and the peripheral blood of ADAP$^{wt/wt}$ Lck-Cre^{tg} (Cre control) and ADAP$^{fl/fl}$ Lck-Cre^{tg} (conditional k.o.) mice. Because of the known T-cell phenotype of conventional ADAP knockout mice, these animals and respective wildtype controls were included in the analysis. The distribution of double negative (CD4$^-$ CD8$^-$), double positive (CD4$^+$ CD8$^+$), CD4$^+$, and CD8$^+$ single positive thymocytes in conditional ADAP knockout mice reflected the distribution in conventional ADAP knockout mice: the percentage of double positive thymocytes was significantly increased and the percentage of CD4$^+$ thymocytes was significantly reduced (**Figure 1B**). The total numbers of cells in the thymus of were only slightly reduced in conditional k.o.mice compared to Cre control mice, whereas the conventional k.o.mice revealed significantly reduced cell numbers (**Figure 1C**). This observation indicates the possibility that other ADAP expressing cells influence thymic development. In the peripheral blood, conventional ADAP k.o. mice displayed reduced numbers of T cell subpopulations (CD3$^+$ CD4$^+$ and CD3$^+$ CD8$^+$). In contrast, in conditional k.o. mice (ADAP$^{fl/fl}$ Lck-Cre^{tg}) only the CD3$^+$ CD8$^+$ subpopulation showed significant reduction in the percentage of cells, whereas the CD3$^+$ CD4$^+$ T cell subpopulation was only slightly reduced (**Figure 1D**).

Thus, these data demonstrate that the T-cell specific conditional ADAP knockout (ADAP$^{fl/fl}$ Lck-Cre^{tg}) resembles the phenotype of the conventional ADAP knockout, namely the decreased portion of single positive thymocytes and mature T cells. However, this reduction is clearly less pronounced in the conditional knockout mice compared with conventional knockout mice.

Next, we investigated the clinical course of active experimental autoimmune encephalomyelitis (EAE) in the T-cell specific conditional ADAP knockout mice. EAE is a strongly T-cell dependent demyelinating disease of the central nervous system. We have previously shown that conventional ADAP knockout mice show less severe EAE compared to wildtype mice, however, most likely mainly due to T cell-independent mechanisms (20). Active EAE was induced by immunization of mice with MOG_{35-55} peptide. As shown in **Figure 1E**, we observed a statistically significant less severe clinical course of EAE in mice exclusively devoid of ADAP expression in T cells compared with Cre control mice. These results indicate that ADAP is involved in both, T-cell dependent and T-cell independent mechanisms of this autoimmune disease.

NK Cell-Specific Conditional ADAP Knockout Reveals Reduced EAE Severity

To delete ADAP specifically in NK cells, we made use of a "knock-in" mouse expressing the Cre recombinase under control of the NKp46 promotor. NKp46 is selectively expressed in NK cells with two exceptions reported: a minor T-cell subset and mucosal group-3 innate lymphoid cells (ILC3) (32). The NK-cell specific knockout was confirmed by intracellular ADAP staining as described. Bone marrow NK precursor cells of ADAP$^{wt/wt}$ NKp46-Cre^{het} (Cre control) mice show expression of ADAP, whereas cells from ADAP$^{fl/fl}$ NKp46-Cre^{het} (conditional k.o.) mice display loss of ADAP expression to the level of cells stained with preimmune serum (**Figure 2A**). The same holds true for the spleen: mature NK cells from Cre control mice express ADAP, whereas NK cells from conditional k.o. mice almost completely lost ADAP expression. In contrast, splenic T cells of ADAP$^{fl/fl}$ NKp46-Cre^{het} (conditional k.o.) mice showed ADAP expression as strong as those derived from ADAP$^{wt/wt}$ NKp46-Cre^{het} (Cre control) mice (**Figure 2A**).

We first investigated the different steps of NK cell maturation in the bone marrow (**Figure 2B**). NK cell differentiation is initiated at precursor stage (stage 1) that is characterized by the expression of CD122 (IL-2/IL-15 receptor ß chain) and

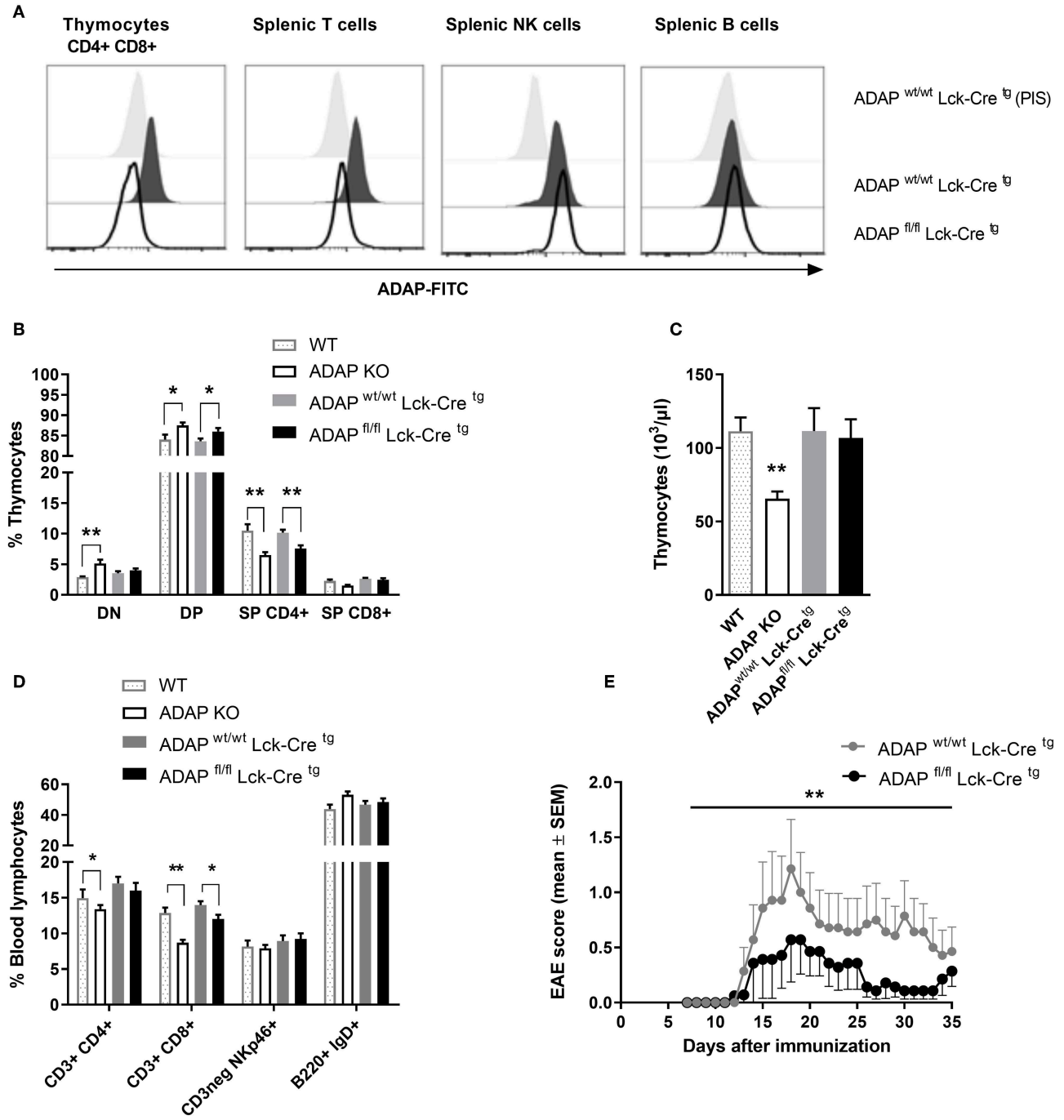

FIGURE 1 | Characterization of mice with specific deletion of ADAP in T cells. **(A)** Anti-ADAP serum or preimmune serum (PIS) were used to detect ADAP protein levels by flow cytometry in double positive $CD4^+$ $CD8^+$ thymocytes and in T cells ($CD3^+$), NK cells (CD3neg, $NK1.1^+$), and B cells ($CD19^+$) in the spleen from conditional knockout mice and Cre control mice. Representative histograms are results from three independent experiments. **(B)** Thymocytes were isolated from conditional knockout mice ($ADAP^{fl/fl}$ $Lck\text{-}Cre^{tg}$), Cre control mice ($ADAP^{wt/wt}$ $Lck\text{-}Cre^{tg}$), conventional ADAP knockout mice (ADAP KO), and respective wildtype control mice (WT). The frequencies of $CD4^-$ $CD8^-$ double negative thymocytes (DN), $CD4^+$ $CD8^+$ double positive thymocytes (DP), and single positive thymocytes (SP $CD4^+$, SP $CD8^+$) were analyzed by flow cytometry. **(C)** Absolute numbers of thymocytes per animal from conditional knockout mice, Cre control mice and conventional ADAP knockout mice are given. **(D)** The lymphocyte subpopulations in the peripheral blood were stained with the indicated antibodies. All results **(B–D)** are expressed as means + SEM of data from six independent experiments ($^*P < 0.05$; $^{**}P < 0.01$). **(E)** Active EAE was induced following immunization with MOG_{35-55} peptide in CFA at day 0 in combination with pertussis toxin at day 0 and day 2. The clinical score of active EAE was assessed for 35 days after immunization. Data are shown as means ± SEM [$n = 8$ animals per group; $^{**}P < 0.001$ (conditional ADAP knockout vs. Cre control)].

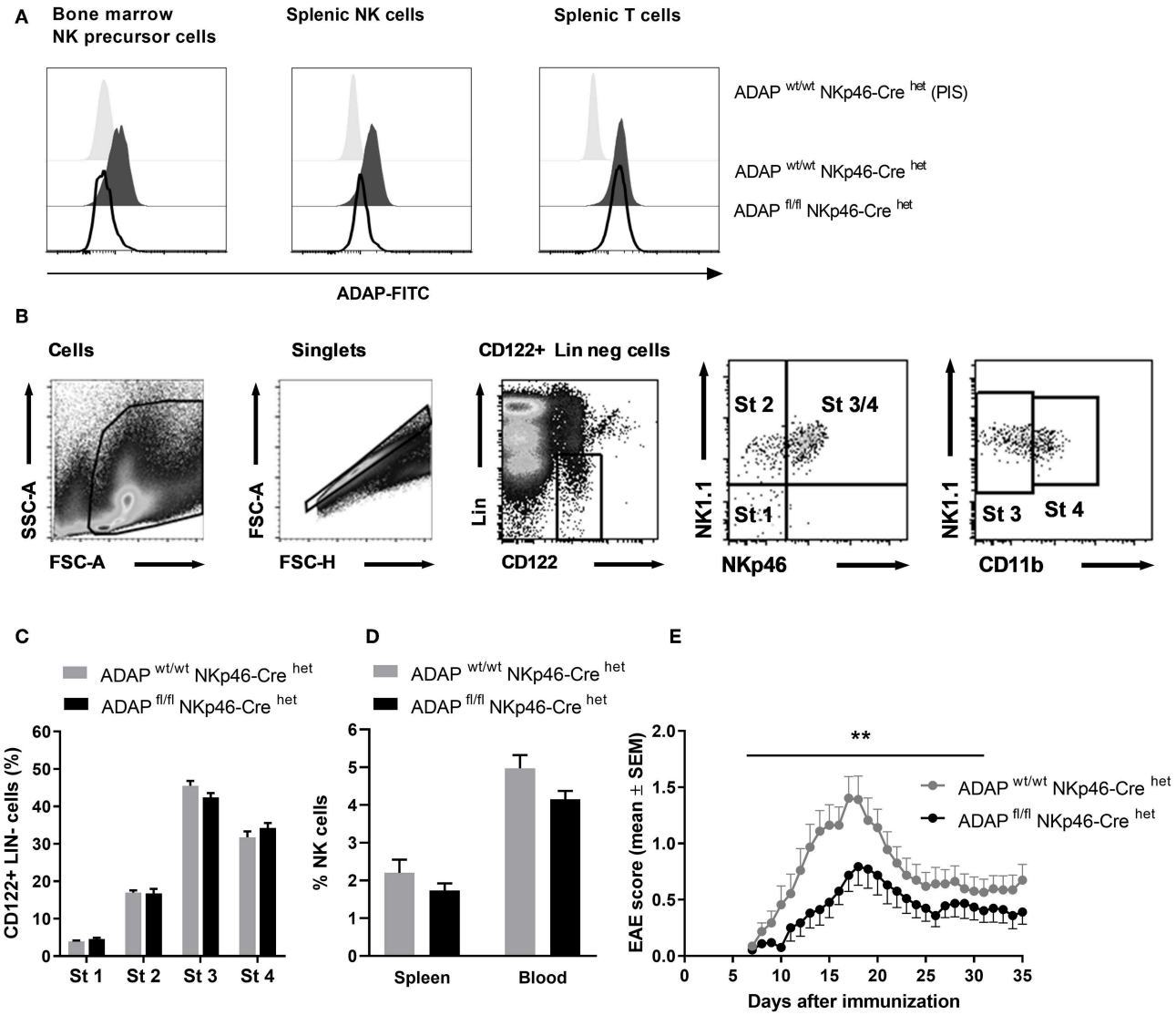

FIGURE 2 | Characterization of mice with specific deletion of ADAP in NK cells. **(A)** Anti-ADAP serum or preimmune serum (PIS) were used to detect ADAP expression by flow cytometry in bone marrow NK cell precursors (left), in splenic NK cells (middle) and in splenic T cells (right) from conditional knockout mice ($ADAP^{fl/fl}$ NKp46-Cre^{het}) and Cre control mice ($ADAP^{wt/wt}$ NKp46-Cre^{het}). Histograms show representative results from three independent experiments. **(B)** The gating strategy for the analysis of NK cell development in the bone marrow is shown. The lineage staining excludes T cells ($CD3^+$, $CD4^+$, $CD8^+$), B cells ($CD19^+$) and granulocytes ($Gr1^+$). The four different stages are depicted as dot plots according to their NK1.1, NKp46, and CD11b expression profile. **(C)** Quantification of the four different stages of NK cell development in the bone marrow is given as means + SEM of data from three independent experiments ($n = 6$ mice per group). **(D)** The graph shows frequencies of mature NK cells ($CD3^-$, $NK1.1^+$, $NKp46^+$) in the spleen and in the peripheral blood from conditional knockout mice ($ADAP^{fl/fl}$ NKp46-Cre^{het}) and Cre control mice ($ADAP^{wt/wt}$ NKp46-Cre^{het}); mean values + SEM ($n = 8$ animals per group). **(E)** Active EAE was induced by immunization with MOG_{35-55} peptide in CFA at day 0 in combination with pertussis toxin at day 0 and day 2. The disease severity was recorded as clinical score for 35 days after immunization. Data are shown as means ± SEM ($n = 23$ animals per group from three independent experiments). $^{**}P < 0.001$ conditional ADAP knockout vs. Cre control.

the absence of lineage markers CD3 and CD19 (**Figure 2B**). Immature NK cells are defined by the appearance of NK1.1 (stage 2) followed by the expression of NKp46 (stage 3). Fully mature NK cells additionally acquire the expression of CD11b (stage 4). We analyzed whether the loss of ADAP in NK cells is associated with modifications in the NK cell differentiation. As depicted in **Figure 2C**, the percentage of NK cells at the different developmental stages in the bone marrow was comparable in conditional knockout mice ($ADAP^{fl/fl}$ NKp46-Cre^{het}) and Cre control mice ($ADAP^{wt/wt}$ NKp46-Cre^{het}). Thus, ADAP expression has no influence on NK cell differentiation. We next analyzed the constitution of secondary (spleen) lymphoid organs and peripheral blood of $ADAP^{wt/wt}$ NKp46-Cre^{het} (Cre control) and $ADAP^{fl/fl}$ NKp46-Cre^{het} (conditional k.o.) mice. As expected, the percentages of mature NK cells in spleen and blood were similar in mice of both genotypes (**Figure 2D**).

Besides encephalitogenic T cells, also NK cells are involved in the development of EAE by providing an early source of IFN-γ (28). ADAP-deficient NK cells from conventional k.o. mice revealed reduced IFN-γ secretion *in vitro* (11). Based on these data, we were curious about the clinical course of EAE in the NK-cell specific conditional ADAP knockout mice. As expected, the loss of ADAP expression exclusively in NK cells ($ADAP^{fl/fl}$ NKp46-Cre^{het}) caused a significantly less severe course of the disease compared to controls (**Figure 2E**).

Deficiency of ADAP Restricted to Myeloid Cells Leads to Attenuated EAE Severity

The LysM-Cre knock-in mouse strain has a Cre recombinase inserted into the *lysozyme 2* gene. Cre-mediated recombination results in deletion of the floxed ADAP allele in the myeloid lineage including macrophages and neutrophils (37). Specific deletion was first monitored by PCR (**Figure S1**). On protein level, loss of ADAP in myeloid cells was confirmed by intracellular staining with the specific anti-ADAP antiserum. In bone marrow cell suspensions, granulocytes ($CD11b^+$ $Ly6G^+$) were discriminated from macrophages ($CD11b^+$ $F4/80^+$). Both cell types showed clear reduction of ADAP expression in conditional k.o. mice compared with Cre control mice (**Figure 3A**). This deletion was also seen in splenic granulocytes. In splenic macrophages of conditional k.o. mice, two populations were detected: one population with ADAP expression comparable to control mice and one population with reduced ADAP expression. This observation indicates that the LysM-Cre promotes good deletion of ADAP in neutrophils, whereas the deletion in the splenic macrophage population is less efficient (**Figure 3A**). Microglia are the brain-resident macrophages and originate from hematopoietic progenitors. Therefore, we started to explore recombination efficacy of LysM-Cre in microglia. Leukocytes were isolated from the brain adult mice and analyzed by flow cytometry as CD45 low $CD11b^+$ cell population (**Figure 3B**). Histograms depict ADAP expression in Cre control mice ($ADAP^{wt/wt}$ LysM-Cre^{het}) and reduction (but no loss) of ADAP expression in ADAP knockout mice ($ADAP^{fl/fl}$ LysM-Cre^{het}).

Next, we analyzed the frequency of granulocytes and macrophages in primary (bone marrow) and secondary lymphoid organs (spleen) of conditional k.o. mice and Cre control mice. The total numbers of cells in the bone marrow and the portion of macrophages and granulocytes in the bone marrow were identical in both genotypes (**Figure 3C**). The same result was achieved comparing the percentage of these myeloid cells in the spleen (macrophages and granulocytes) and in the peripheral blood (granulocytes; **Figure 3D**). DCs are not targeted by LysM-Cre mediated recombination (38). We did not observe differences in the proportion of CD11c+ cells between conditional k.o. mice and Cre control mice (**Figures 3C,D**).

CNS-resident microglia as well as invading macrophages and neutrophils contribute to the CNS autoimmune inflammation (39, 40). Based on our previous observation that conditional knockout mice with specific loss of ADAP in T cells and NK cells showed less severe EAE (**Figures 1E**, **2E**), we induced the disease by active immunization with MOG_{35-55} peptide in conditional knockout mice with reduction of ADAP expression in myeloid cells and monitored the disease progression by clinical assessment. Mice expressing the wildtype allele in the presence of Cre recombinase ($ADAP^{wt/wt}$ LysM-Cre^{het}) exhibited a typical disease course. In contrast, conditional ADAP knockout mice ($ADAP^{fl/fl}$ LysM-Cre^{het}) developed a significantly milder disease showing fewer clinical symptoms (**Figure 3E**). These results indicate that expression of ADAP in myeloid cells partially contributes to the pathogenesis of EAE.

Platelet-Specific Conditional ADAP Knockout Mice Develop Enhanced Active EAE

We generated platelet-specific ADAP knockout mice ($ADAP^{fl/fl}$ PF4-Cre^{tg}) and reported recently that these mice resemble the phenotype of conventional ADAP knockout mice showing thrombocytopenia and augmented re-bleeding from tail wounds. *In vitro,* ADAP-deficient platelets display impaired CLEC-2-mediated αIIbβ3 integrin activation, altered fibrinogen binding and reduced TGF-β1 and PF4 release (31). The role of platelets in EAE is controversially discussed (29, 41, 42). Furthermore, we could demonstrate that the loss of ADAP exclusively in platelets ($ADAP^{fl/fl}$ PF4-Cre^{tg}) caused a more severe disease course in the model of passive adoptive transfer EAE compared to that in Cre control mice (31). To allow a direct comparison of EAE course with the conditional ADAP knockout in T cells, NK cells and myeloid cells, here, we induced the active EAE by immunization of mice with MOG_{35-55} peptide also in the platelet-specific ADAP knockout mice. As shown in **Figure 4**, mice with the platelet-specific deletion of ADAP ($ADAP^{fl/fl}$ PF4-Cre^{tg}) developed a significantly more severe EAE compared to control animals ($ADAP^{wt/wt}$ PF4-Cre^{tg}). These data suggest a role of platelets in EAE that is at least partially controlled by ADAP.

We could previously show that systemic injection of TGF-β1 reduced the EAE severity in the passive adoptive transfer model in platelet-specific ADAP knockout mice (31). Based on this observation, we wanted to compare the plasma TGF-β1 concentrations of the different conditional ADAP knockout mice. To this end, we analyzed the level of circulating latent TGF-β1 at steady state and at day 35 of active EAE. As shown in **Figure 5A**, platelet-specific ADAP knockout mice revealed significantly reduced levels of circulating latent TGF-β1 at steady state and at day 35 of active EAE compared to the respective control animals. In contrast, the concentrations of latent TGF-β1 were similar in NK cell-specific as well as in myeloid cell-specific conditional knockout mice and their respective control mice. In addition, there was no difference in the TGF-β1 concentration between the physiological steady state and during the autoimmune disease (**Figures 5B,C**). This result points toward a specific effect of ADAP depletion in platelets.

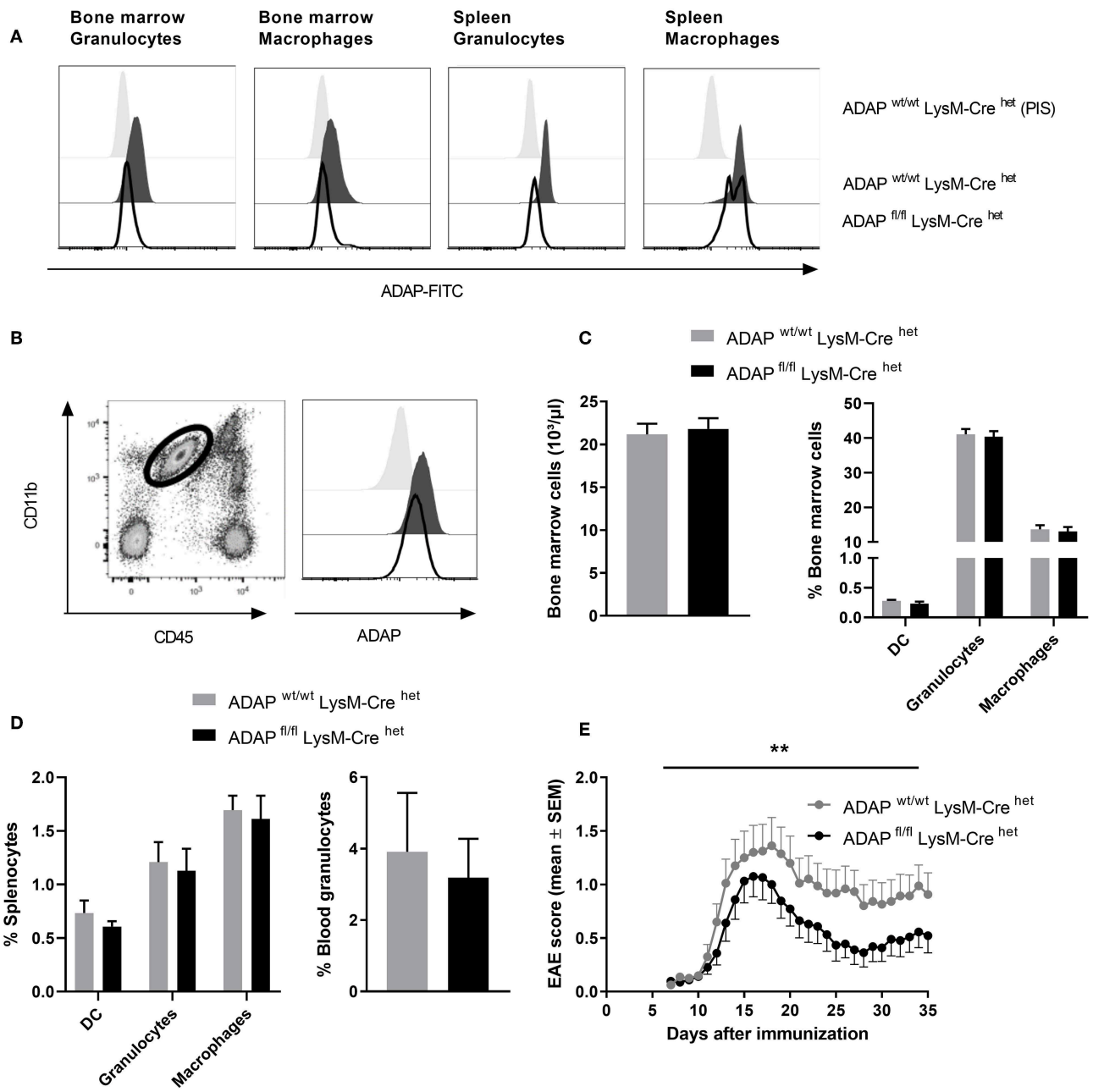

FIGURE 3 | Characterization of mice with specific deletion of ADAP in myeloid cells. **(A)** Anti-ADAP serum or preimmune serum (PIS) were used to detect ADAP expression by flow cytometry in bone marrow granulocytes ($CD11b^+$ $Ly6G^+$) and bone marrow macrophages ($CD11b^+$ $F4/80^+$) as well as in granulocytes and macrophages from the spleen of conditional knockout mice ($ADAP^{fl/fl}$ LysM-Cre^{het}) and Cre control mice ($ADAP^{wt/wt}$ LysM-Cre^{het}). Histograms show representative results from three independent experiments. **(B)** Leukocytes were isolated from the brain by Percoll gradient, stained with antibodies against CD11b and CD45 and analyzed by flow cytometry. The region indicates the CD45 low, CD11b high brain-resident microglia (dot plot). The histograms show ADAP expression level in microglia cells from conditional knockout mice ($ADAP^{fl/fl}$ LysM-Cre^{het}; black line) and Cre control mice ($ADAP^{wt/wt}$ LysM-Cre^{het}; dark gray, filled). Cells stained with preimmune serum (light gray, filled) were used as control. The plots show representative results out of three independent experiments. **(C)** Frequencies of precursors of dendritic cells ($CD11c^+$ DC), granulocytes ($CD11b^+$ $Ly6G^+$), and macrophages ($CD11b^+$ $F4/80^+$) in the bone marrow were determined using flow cytometry (left graph). The right graph illustrates the total number of bone marrow cells. **(D)** Distribution of mature dendritic cells, granulocytes and macrophages in the spleen (left graph) is shown together with the percentage of granulocytes in the peripheral blood (right graph). All results are expressed as means + SEM of data from minimum three independent experiments. **(E)** Active EAE was induced following immunization with MOG_{35-55} peptide in CFA. The clinical score of EAE was assessed for 35 days after immunization (means ± SEM; $n = 20$ animals per group from three independent experiments). $^{**}P < 0.01$ conditional knockout mice ($ADAP^{fl/fl}$ LysM-Cre^{het}) vs. Cre control mice ($ADAP^{wt/wt}$ LysM-Cre^{het}).

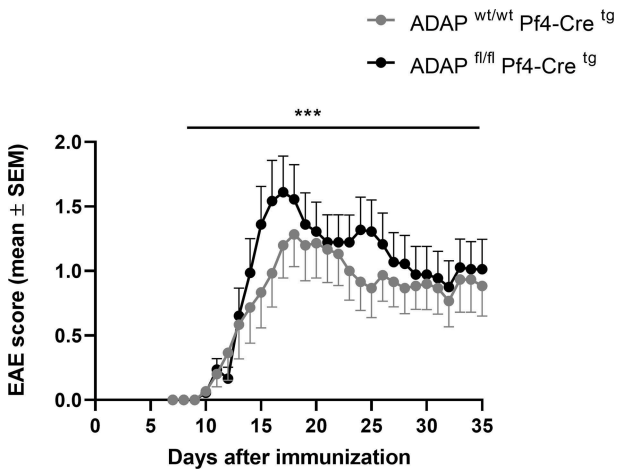

FIGURE 4 | Active EAE in platelet-specific conditional ADAP knockout mice. EAE was induced following immunization with MOG_{35-55} peptide in CFA. The clinical score of EAE was assessed for 35 days after immunization (mean ± SEM; $n = 15$ for Cre control ($ADAP^{wt/wt}$ PF4-Cre^{tg}) and $n = 18$ for conditional ADAP knockout ($ADAP^{fl/fl}$ PF4-Cre^{tg}); $^{***}P < 0.0001$ conditional ADAP knockout vs. Cre control).

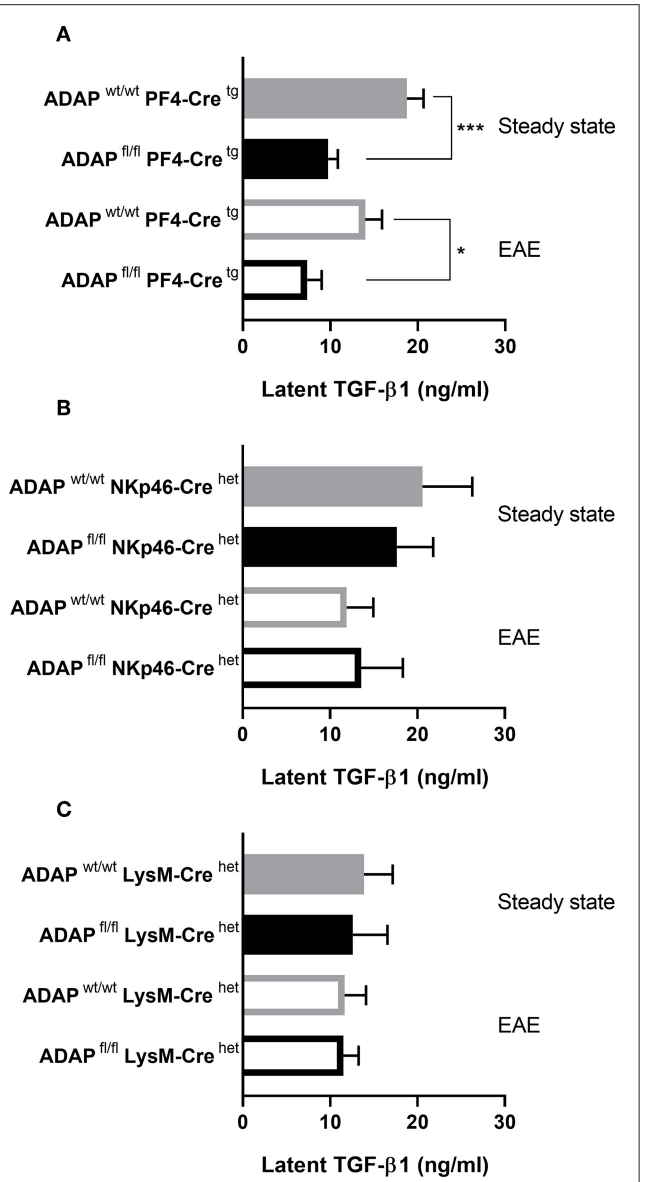

FIGURE 5 | Concentration of latent TGF-β1 in conditional ADAP knockout mice. Concentration of latent TGF-β1 was measured in platelet-free plasma of platelet-specific **(A)**, NK cell-specific **(B)**, and myeloid cell-specific **(C)** ADAP knockout mice under physiological steady state condition (filled columns) and at day 35 of active EAE (empty columns). Concentrations are given as mean + SEM of at least seven individual mice. $^{***}P < 0.001$; $^{*}P < 0.05$ conditional ADAP knockout vs. Cre control.

DISCUSSION

We have previously shown that conventional ADAP knockout mice develop a significantly milder clinical course of EAE by mainly T cell-independent mechanisms (20). To dissect the impact of different ADAP-expressing cell types on the ameliorated EAE severity, we generated conditional knockout mice. Our results show that the loss of ADAP in T cells, myeloid cells and NK cells resulted in less severe EAE whereas loss of ADAP in platelets leads to an exacerbated EAE compared to control animals.

Using Cre recombinase expressed as transgene under the control of the Lck promotor, we generated conditional knockout mice with deletion of ADAP in the T cell lineage. The major stages of T cell development in the thymus can be delineated by the expression of CD4 and CD8 which define the stages of double negative $CD4^-$ $CD8^-$ (DN), double positive $CD4^+$ $CD8^+$ (DP), and single positive $CD4^+$ or $CD8^+$ (SP) thymocytes. The Lck promotor is first expressed during early thymic development at the DN stage. DP thymocytes, the major population within the thymus, showed complete loss of ADAP protein in the $ADAP^{fl/fl}$ Lck-Cre^{tg} mice. Unlike in thymocytes, peripheral splenic T cells exhibited a reduction in ADAP expression. This lower recombination rate in splenic T cell was reported earlier. It was suggested that rare thymocytes with incomplete deletion mature, leave the thymus and undergo clonal expansion in the periphery (43).

The distribution of thymocytes revealed the known abnormalities shown by Wu et al. (44): the higher percentage of DP cells and the lower proportions of SP cells. Interestingly, the conditional knockout mice did not exhibit the overall decreased thymic cellularity reported earlier (5, 6, 44). The presence (in conditional knockout) or absence (in conventional knockout) of ADAP in dendritic cells and macrophages that are involved in selection processes during thymocyte development might be an explanation for this observation. In the spleen, conditional and conventional ADAP knockout mice show the same phenotype of significantly reduced relative numbers of T cells (6, 44).

The NKp46-Cre knock-in mouse is widely used to delete genes containing flanking loxP sites in NK cells. Using these mice, we could demonstrate that the loss of ADAP in bone marrow NK cells and in splenic NK cells is almost complete. Cre expression is induced under the control of the NKp46

promotor at stage 3 of NK cell development (32). Our results showing normal maturation of ADAP-deficient NK cells in the bone marrow are therefore consistent with earlier published data (45). Consequently, the distribution of mature NK cells in spleen and in peripheral blood revealed no significant differences between the conditional knockout mice and Cre control mice.

Besides conventional NK cells, the existence of distinct tissue-specific NK cell populations is accepted (46). In contrast to conventional NK cells that develop in the bone marrow, evidence is accumulating that these organ-specific NK cells develop at extramedullary sites in the thymus, gut, liver, and uterus (47). We are aware of the problem that these cells express NKp46 and Cre-mediated recombination might occur. However, we assume that the impact of these tissue–resident NK cells on the disease model of EAE can be neglected.

Myeloid cells represent a heterogeneous population including mononuclear and polymorphonuclear phagocytes. Abram et al. (38) performed a detailed analysis of specificity and efficiency of 13 different myeloid-Cre mouse strains crossed to ROSA26-EYFP reporter mice and assessed YFP expression using a standard protocol. LysM-Cre mice show up to 70% deletion in neutrophils. In addition, LysM-Cre promotes deletion with high efficiency in alveolar macrophages ($\approx$ 95%) and peritoneal macrophages ($\approx$ 90%) and with lower efficiency in splenic macrophages ($\approx$ 40%). For peripheral blood monocytes, the level of YFP^+ cells is approximately 40% (38). Our results show a clear reduction of ADAP expression in granulocytes and bone marrow macrophages. In spleen macrophages, we detected two populations with high and low ADAP expression, respectively. Our results closely match the reported data from Abram et al. (38). However, this direct comparison is hampered by the different methods used: quantification of a fluorescent marker vs. staining with a specific antibody. The LysM promotor also targets microglia and showed an average recombination rate of 45% (48). Brain microglia cells of the $ADAP^{fl/fl}$ LysM-Cre^{het} mice revealed a reduction of ADAP expression but no complete loss confirming the relatively low recombination efficiency. Our immunophenotyping data show that loss of ADAP expression in myeloid cells did not affect the frequency of these cells in the primary and secondary lymphoid organs of $ADAP^{fl/fl}$ LysM-Cre^{het} mice.

Only recently, we provided evidence that the PF4-Cre mediated deletion of ADAP is highly efficient and specific. The $ADAP^{fl/fl}$ PF4-Cre^{tg} mice resemble the phenotype of conventional ADAP knockout mice showing thrombocytopenia and augmented re-bleeding from tail wounds. The loss of ADAP in the megakaryocytic lineage had no impact on immune cell distribution in the lymphoid organs (31).

Overall, these mouse strains show deletion or reduction of ADAP expression in the specific target cell population. So far, no other reports using conditional ADAP knockout mice are available except for platelets (31, 49). The characterization of the conditional knockout mice revealed unaltered development and distribution of immune cells in the primary and secondary lymphoid organs when ADAP was deleted in myeloid cells, NK cells and platelets. Ablation of ADAP in T cells resembled the T cell phenotype of conventional ADAP knockout mouse. We are aware that inflammatory conditions like EAE could induce changes in Cre-mediated deletion efficiency and specificity compared to steady state. At least for PF4-Cre mediated recombination we could exclude this possibility during *in vitro* activation (31).

We used these characterized conditional knockout strains and performed comparative EAE experiments. To investigate the role of ADAP expressing immune cells during early and late stages of the autoimmune disease, we induced active EAE by immunization with the immunogenic MOG_{35-55} peptide in CFA.

In our previous study, we provided evidence that the resistance of conventional ADAP knockout mice to EAE is partially caused by T cell-independent mechanisms. Here, we show that mice with ADAP deficiency restricted to T cells developed less severe EAE. The results of these two studies seem contradictory. However, the impaired function of ADAP-deficient T cells (proliferation, IL-2 production, adhesion, NF-κB activation) had previously been characterized in detail (5–7). Thus, the reduced EAE severity in T cell-specific ADAP knockout mice is not surprising. In addition, induction of EAE after adoptive transfer of ADAP-deficient T cells into T cell-deficient mice caused a clear delay in disease onset compared to the adoptive transfer of ADAP-sufficient T cells (20). This observation indicates a partial T cell-dependent role of ADAP in EAE. Analysis of the different conditional ADAP-knockout strains allowed us to draw a more precise conclusion: T cell-dependent and T cell-independent mechanism are responsible for reduced EAE severity in conventional ADAP knockout mice. Concerning the T cell-dependent mechanism, two aspects have to be mentioned. First, the reduced numbers of mature T cells, especially $CD8^+$ T cells, in the periphery of conditional knockout mice. Second, the well-known impaired T cell function in the absence of ADAP. At present, we cannot discriminate between these two possibilities. We assume that both aspects contribute to the reduced EAE severity in the T cell-specific ADAP knockout mouse. Conditional ablation of ADAP separately in either $CD4^+$ or $CD8^+$ T cells would help to clarify this question.

In this study, we provide evidence that ADAP deficiency restricted to NK cells reduced EAE severity. We hypothesize that primarily the disturbed IFN-γ production by NK cells causes the better outcome of EAE in NK cell-specific conditional ADAP knockout mice. Rajasekaran et al. (11) demonstrated that cytokine production but not cytotoxicity of NK cells is regulated by ADAP. Therefore, we rule out the cytotoxic function of ADAP-deficient NK cells as a factor affecting reduced EAE severity. Besides, we suggest that potential adhesion and migration defects of ADAP-deficient NK cells should be taken into account.

Previous studies reported that the ILC3 population (innate lymphoid cells type 3) in the meninges is involved in the pathogenesis of EAE by sustaining the neuroinflammation (50). These cells express NKp46, the transcription factor RORγt, and produce the cytokines IL-17 and GM-CSF. We cannot exclude the possibility

that in this minor subpopulation in the meninges Cre-mediated deletion of ADAP occurs and therefore enhances the effect of milder EAE severity in ADAP$^{fl/fl}$ NKp46-Cre^{het} mice.

In conditional knockout mice with specific deletion of ADAP in myeloid cells, we observed an attenuated disease course compared to control mice. Neutrophils contribute to the pathogenesis of EAE by different mechanisms including release of cytokines, proteases, reactive oxygen species, phagocytosis and interaction with other immune cells [reviewed in (51)]. To access the CNS, circulating neutrophils have to leave the vasculature and to migrate to sites of neuroinflammation. Deficiency in ADAP attenuates E-selectin-mediated slow leukocyte rolling and adhesion of neutrophils and protects mice from acute kidney ischemia-reperfusion injury (13). This adhesion defect might explain our observation of lower EAE severity when ADAP is deleted in myeloid cells. It is difficult to estimate the impact of ADAP in monocytes and macrophages in the EAE model. The recombination efficiency is low and varies depending on the tissue localization of the macrophages. In our previous study, lethally irradiated ADAP knockout recipient mice reconstituted with wildtype bone marrow developed milder EAE compared with wildtype recipients (20). We concluded that radio-resistant cells could be partially responsible for the attenuated EAE severity. Based on experimental data of normal function in the absence of ADAP we excluded a role of microglia. Therefore, the possibility that other ADAP-deficient radio-resistant myeloid cells might be responsible for the attenuated EAE severity still exists. Mast cells are candidates that fulfill these criteria and will be in focus of our future research.

Recently, we reported the unexpected finding that mice with platelet-specific ablation of ADAP exhibited enhanced EAE severity in the passive EAE model where *ex vivo* activated myelin-specific TCR transgenic T cells (2D2 T cells) were adoptively transferred. In addition, we provided evidence that thrombocytopenia and reduced concentration of TGF-β1 are responsible for the more severe course of EAE. Within the present study, we induced active EAE. In active EAE, both the induction and effector phase of the disease take place *in vivo*. We confirmed our previous data (31) showing augmented disease severity in mice lacking ADAP specifically in platelets. The difference in the clinical course of EAE was especially pronounced during the early phase of the disease (at days 10–15). This result implicates a regulatory role of ADAP in platelets during induction of EAE. We hypothesize that also in active EAE the reduced level of TGF-β1 in the platelet-specific conditional knockout mouse is responsible for enhanced disease severity. *In vivo* administration of TGF-β1 improved EAE severity in the model of passive EAE in mice lacking ADAP in platelets. However, this effect was only achieved in a preventive but not in a therapeutic approach (31). This result indirectly supports our hypothesis that platelet-derived ADAP plays an important suppressive role during the induction phase of EAE. Platelets are the most important source of TGF-β1. As a potent anti-inflammatory cytokine, TGF-β1 is required to convert conventional CD4$^+$ T cells into induced regulatory T cells (52). The reduced TGF-β1 concentration thus might impair the development of regulatory T cells *in vivo*, leading to reduced immune suppression and enhanced EAE severity.

The question remains about the interplay between the described cell type-specific effects on the EAE course in conventional ADAP knockout mice. We believe that the impact of a single cell type is determined by the significance of this cell population for the pathogenesis of EAE. Most importantly, autoreactive T cells primed by (myeloid) antigen presenting cells are critical for this autoimmune disease. Infiltrating NK cells and platelets, although contributing, are less important. Since loss of ADAP in T cells, myeloid cells, and NK cells reduced EAE severity, the additive effects of these cells overbalances the EAE enhancing effect of ADAP-deficient platelets.

Summarizing, we can conclude that in conventional ADAP knockout mice T cell-dependent and T cell-independent mechanisms are involved in the resistance to EAE. Not a single cell type but different ADAP expressing myeloid cells as well as NK cells might exert synergistic effects contributing to significantly milder EAE. These investigations expand our knowledge about the complex role of the adapter protein ADAP in immune cells.

DATA AVAILABILITY STATEMENT

All datasets generated for this study are included in the manuscript/**Supplementary Files**.

ETHICS STATEMENT

This study was carried out in accordance with the recommendations of the German Tierschutzgesetz. The protocol was approved by Landesverwaltungsamt Sachsen-Anhalt, Referat 405 (42502-2-1273 Uni MD).

AUTHOR CONTRIBUTIONS

JR and AR designed and performed the research and analyzed data. KG, CM, and MV performed experiments and analyzed data. AR wrote the manuscript. SK, DR, and BS contributed to interpretation of data, critical writing, and revising the manuscript.

FUNDING

This work was funded by the Deutsche Forschungsgemeinschaft DFG (RE-2907/2-2) and by the SFB 854 (B12, B19).

ACKNOWLEDGMENTS

We thank Bernhard Nieswandt (Würzburg) for providing the PF4-Cre mouse line. The NKp46-iCre knock-in mice were kindly provided Eric Vivier (Paris). We thank Peter Mertens

(Magdeburg) who kindly provided the LysM-Cre knock-in mice and Ursula Bommhardt (Magdeburg) who kindly made available to us the Lck-Cre mice. The polyclonal anti-ADAP antiserum was a kind gift from Gary Koretzky (New York). We thank G. Weitz for the excellent technical assistance.

SUPPLEMENTARY MATERIAL

The Supplementary Material for this article can be found online at: https://www.frontiersin.org/articles/10.3389/fimmu.2019.02343/full#supplementary-material

REFERENCES

1. Dluzniewska J, Zou L, Harmon IR, Ellingson MT, Peterson EJ. Immature hematopoietic cells display selective requirements for adhesion- and degranulation-promoting adaptor protein in development and homeostatsis. *Eur J Immunol*. (2007) 37:3208–19. doi: 10.1002/eji.200737094
2. Witte A, Degen J, Baumgart K, Waldt N, Kuropka B, Freund C, et al. Emerging roles of ADAP, SKAP55, and SKAP-HOM for integrin and NF-kB signaling in T cells. *J Clin Cell Immunol*. (2012) S12:002. doi: 10.4172/2155-9899.S12-007
3. Griffiths EK, Penninger JM. Communication between the TCR and integrins: role of the molecular adapter ADAP/Fyb/Slap. *Curr Opin Immunol*. (2002) 14:317–22. doi: 10.1016/S0952-7915(02)00334-5
4. Peterson EJ. The TCR ADAPts to integrin-mediated cell adhesion. *Immunol Rev*. (2003) 192:113–21. doi: 10.1034/j.1600-065X.2003.00026.x
5. Griffiths EK, Krawczyk C, Kong YY, Raab M, Hyduk SJ, Bouchard D, et al. Positive regulation of T cell activation and integrin adhesion by the adapter Fyb/Slap. *Science*. (2001) 293:2260–3. doi: 10.1126/science.1063397
6. Peterson EJ, Woods ML, Dmowski SA, Derimanov G, Jordan MS, Wu JN, et al. Coupling of the TCR to integrin activation by Slap-130/Fyb. *Science*. (2001) 293:2263–5. doi: 10.1126/science.1063486
7. Medeiros RB, Burbach BJ, Mueller KL, Srivastava R, Moon JJ, Highfill S, et al. Regulation of NF-kappaB activation in T cells via association of the adapter proteins ADAP and CARMA1. *Science*. (2007) 316:754–8. doi: 10.1126/science.1137895
8. Parzmair GP, Gereke M, Haberkorn O, Annemann M, Podlasly L, Kliche S, et al. ADAP plays a pivotal role in $CD4^+$ T cell activation but is only marginally involved in $CD8^+$ T cell activation, differentiation, and immunity to pathogens. *J Leukoc Biol*. (2017) 101:407–19. doi: 10.1189/jlb.1A0216-090RR
9. Fiege JK, Burbach BJ, Shimizu Y. Negative regulation of memory phenotype CD8 T cell conversion by adhesion and degranulation-promoting adapter protein. *J Immunol*. (2015) 195:3119–28. doi: 10.4049/jimmunol.1402670
10. Fiege JK, Beura LK, Burbach BJ, Shimizu Y. Adhesion- and degranulation-promoting adapter protein promotes CD8 T cell differentiation and resident memory formation and function during an acute infection. *J Immunol*. (2016) 197:2079–89. doi: 10.4049/jimmunol.1501805
11. Rajasekaran K, Kumar P, Schuldt KM, Peterson EJ, Vanhaesebroeck B, Dixit V, et al. Signaling by Fyn-ADAP via the Carma1-Bcl-10-MAP3K7 signalosome exclusively regulates inflammatory cytokine production in NK cells. *Nat Immunol*. (2013) 14:1127–36. doi: 10.1038/ni.2708
12. May RM, Okumura M, Hsu CJ, Bassiri H, Yang E, Rak G, et al. Murine natural killer immunoreceptors use distinct proximal signaling complexes to direct cell function. *Blood*. (2013) 121:3135–46. doi: 10.1182/blood-2012-12-474361
13. Block H, Herter JM, Rossaint J, Stadtmann A, Kliche S, Lowell CA, et al. Crucial role of SLP-76 and ADAP for neutrophil recruitment in mouse kidney ischemia-reperfusion injury. *J Exp Med*. (2012) 209:407–21. doi: 10.1084/jem.20111493
14. Engelmann S, Togni M, Kliche S, Reinhold D, Schraven B, Reinhold A. The adhesion- and degranulation-promoting adaptor protein and its role in the modulation of experimental autoimmune encephalomyelitis. *Crit Rev Immunol*. (2015) 35:1–14. doi: 10.1615/CritRevImmunol.2014012162
15. Togni M, Engelmann S, Reinhold D, Schraven B, Reinhold A. The adapter protein ADAP is required for selected dendritic cell functions. *Cell Commun Signal*. (2012) 10:14. doi: 10.1186/1478-811X-10-14
16. Kasirer-Friede A, Moran B, Nagrampa-Orje J, Swanson K, Ruggeri ZM, Schraven B, et al. ADAP is required for normal alphaIIbbeta3 activation by VWF/GP Ib-IX-V and other agonists. *Blood*. (2007) 109:1018–25. doi: 10.1182/blood-2006-05-022301
17. Kasirer-Friede A, Ruggeri ZM, Shattil SJ. Role for ADAP in shear flow-induced platelet mechanotransduction. *Blood*. (2010) 115:2274–82. doi: 10.1182/blood-2009-08-238238
18. Kasirer-Friede A, Kang J, Kahner B, Ye F, Ginsberg MH, Shattil SJ. ADAP interactions with talin and kindlin promote platelet integrin αIIbβ3 activation and stable fibrinogen binding. *Blood*. (2014) 123:3156–65. doi: 10.1182/blood-2013-08-520627
19. Jarvis GE, Bihan D, Hamaia S, Pugh N, Ghevaert CJG, Pearce AC, et al. A role for adhesion and degranulation-promoting adapter protein in collagen-induced platelet activation mediated via integrin α(2) ß(1). *J Thromb Haemost*. (2012) 10:268–77. doi: 10.1111/j.1538-7836.2011.04567.x
20. Engelmann S, Togni M, Thielitz A, Reichardt P, Kliche S, Reinhold D, et al. T-cell independent modulation of experimental autoimmune encephalomyelitis in ADAP-deficient mice. *J Immunol*. (2013) 191:4950–9. doi: 10.4049/jimmunol.1203340
21. Miller SD, Karpus WJ, Davidson TS. Experimental autoimmune encephalomyelitis in the mouse. *Curr Protoc Immunol*. (2010) 88:15.1.1–20. doi: 10.1002/0471142735.im1501s88
22. Korn T, Bettelli E, Oukka M, Kuchroo VK. IL-17 and Th17 Cells. *Annu Rev Immunol*. (2009) 27:485–517. doi: 10.1146/annurev.immunol.021908.132710
23. Sie C, Korn T, Mitsdoerffer M. Th17 cells in central nervous system autoimmunity. *Exp Neurol*. (2014) 262:18–27. doi: 10.1016/j.expneurol.2014.03.009
24. Batoulis H, Addicks K, Kuerten S. Emerging concepts in autoimmune encephalomyelitis beyond the CD4/T(H)1 paradigm. *Ann Anat*. (2010) 192:179–93. doi: 10.1016/j.aanat.2010.06.006
25. Shemer A, Jung S. Differential roles of resident microglia and infiltrating monocytes in murine CNS autoimmunity. *Semin Immunopathol*. (2015) 37:613–23. doi: 10.1007/s00281-015-0519-z
26. Sinha S, Boyden AW, Itani FR, Crawford MP, Karandikar NJ. $CD8^+$ T-cells as immune regulators of multiple sclerosis. *Front Immunol*. (2015) 6:619. doi: 10.3389/fimmu.2015.00619
27. Matsumoto Y, Kohyama K, Aikawa Y, Shin T, Kawazoe Y, Suzuki Y, et al. Role of natural killer cells and TCR gamma delta T cells in acute autoimmune encephalomyelitis. *Eur J Immunol*. (1998) 28:1681–8. doi: 10.1002/(SICI)1521-4141(199805)28:05<1681::AID-IMMU1681>3.0.CO;2-T
28. Dungan LS, McGuinness NC, Boon L, Lynch MA, Mills KH. Innate IFN-γpromotes development of experimental autoimmune encephalomyelitis: a role for NK cells and M1 macrophages. *Eur J Immunol*. (2014) 44:2903–17. doi: 10.1002/eji.201444612
29. Langer HF, Choi EY, Zhou H, Schleicher R, Chung KJ, Tang Z, et al. Platelets contribute to the pathogenesis of experimental autoimmune encephalomyelitis. *Circ Res*. (2012) 110:1202–10. doi: 10.1161/CIRCRESAHA.111.256370
30. Skarnes WC, Rosen B, West AP, Koutsourakis M, Bushell W, Iyer V, et al. A conditional knockout resource for the genome-wide study of mouse gene function. *Nature*. (2011) 474:337–42. doi: 10.1038/nature10163
31. Rudolph JM, Guttek K, Weitz G, Meinke CA, Kliche S, Reinhold D, et al. Characterization of mice with a platelet-specific deletion of the adapter molecule ADAP. *Mol Cell Biol*. (2019) 39:e00365–18. doi: 10.1128/MCB.00365-18
32. Narni-Mancinelli E, Chaix J, Fenis A, Kerdiles YM, Yessaad N, Reynders A, et al. Fate mapping analysis of lymphoid cells expressing the NKp46 cell surface receptor. *Proc Natl Acad Sci USA*. (2011) 108:18324–9. doi: 10.1073/pnas.1112064108
33. Togni M, Swanson KD, Reimann S, Kliche S, Pearce AC, Simeoni L, et al. Regulation of *in vitro* and *in vivo* immune functions by the

cytosolic adaptor protein SKAP-HOM. *Mol Cell Biol*. (2005) 25:8052–63. doi: 10.1128/MCB.25.18.8052-8063.2005
34. Steinbrecher A, Reinhold D, Quigley L, Gado A, Tresser N, Izikson L, et al. Targeting dipeptidyl peptidase IV (CD26) suppresses autoimmune encephalomyelitis and up-regulates TGF-beta 1 secretion *in vivo*. *J Immunol*. (2001) 166:2041–8. doi: 10.4049/jimmunol.166.3.2041
35. Stoye D, Schubert C, Goihl A, Guttek K, Reinhold A, Brocke S, et al. Zinc aspartate suppresses T cell activation *in vitro* and relapsing experimental autoimmune encephalomyelitis in SJL/J mice. *Biometals*. (2012) 25:529–39. doi: 10.1007/s10534-012-9532-z
36. Buckland J, Pennington DJ, Bruno L, Owen MJ. Co-ordination of the expression of the protein tyrosine kinase p56(lck) with the pre-T cell receptor during thymocyte development. *Eur J Immunol*. (2000) 30:8–18. doi: 10.1002/1521-4141(200001)30:1<8::AID-IMMU8>3.0.CO;2-8
37. Clausen BE, Burkhardt C, Reith W, Renkawitz R, Forster I. Conditional gene targeting in macrophages and granulocytes using LysMcre mice. *Transgenic Res*. (1999) 8:265–77. doi: 10.1023/A:1008942828960
38. Abram CL, Roberge GL, Hu Y, Lowell CA. Comparative analysis of the efficiency and specificity of myeloid-Cre deleting strains using ROSA-EYFP reporter mice. *J Immunol Methods*. (2014) 408:89–100. doi: 10.1016/j.jim.2014.05.009
39. Mayo L, Quintana FJ, Weiner HL. The innate immune system in demyelinating disease. *Immunol Rev*. (2012) 248:170–87. doi: 10.1111/j.1600-065X.2012.01135.x
40. Woodberry T, Bouffler SE, Wilson AS, Buckland RL, Brustle A. The emerging role of neutrophil granulocytes in multiple sclerosis. *J Clin Med*. (2018) 7:E511. doi: 10.3390/jcm7120511
41. Sotnikov I, Veremeyko T, Starossom SC, Barteneva N, Weiner HL, Ponomarev ED. Platelets recognize brain-specific glycolipid structures, respond to neurovascular damage and promote neuroinflammation. *PLoS ONE*. (2013) 8:e58979. doi: 10.1371/journal.pone.0058979
42. Starossom SC, Veremeyko T, Yung AW, Dukhinova M, Au C, Lau AY, et al. Platelets play differential role during the initiation and progression of autoimmune neuroinflammation. *Circ Res*. (2015) 117:779–92. doi: 10.1161/CIRCRESAHA.115.306847
43. Hennet T, Hagen FK, Tabak LA, Marth JD. T-cell-specific deletion of a polypeptide N-acetylgalactosaminyl-transferase gene by site-directed recombination. *Proc Natl Acad Sci USA*. (1995) 92:12070–4. doi: 10.1073/pnas.92.26.12070
44. Wu JN, Gheith S, Bezman NA, Liu QH, Fostel LV, Swanson AM, et al. Adhesion- and degranulation-promoting adapter protein is required for efficient thymocyte development and selection. *J Immunol*. (2006) 176:6681–9. doi: 10.4049/jimmunol.176.11.6681
45. Fostel LV, Dluzniewska J, Shimizu Y, Burbach BJ, Peterson EJ. ADAP is dispensable for NK cell development and function. *Int Immunol*. (2006) 18:1305–14. doi: 10.1093/intimm/dxl063
46. Lysakova-Devine T, O'Farrelly C. Tissue-specific NK cell populations and their origin. *J Leukoc Biol*. (2014) 96:981–90. doi: 10.1189/jlb.1RU0514-241R
47. Yu J, Freud AG, Caligiuri MA. Location and cellular stages of natural killer cell development. *Trends Immunol*. (2013) 34:573–82. doi: 10.1016/j.it.2013.07.005
48. Goldmann T, Wieghofer P, Muller PF, Wolf Y, Varol D, Yona S, et al. A new type of microglia gene targeting shows TAK1 to be pivotal in CNS autoimmune inflammation. *Nat Neurosci*. (2013) 16:1618–26. doi: 10.1038/nn.3531
49. Spindler M, van Eeuwijk JMM, Schurr Y, Nurden P, Nieswandt B, Stegner D, et al. ADAP deficiency impairs megakaryocyte polarization with ectopic proplatelet release and causes microthrombocytopenia. *Blood*. (2018) 132:635–46. doi: 10.1182/blood-2018-01-829259
50. Hatfield JK, Brown MA. Group 3 innate lymphoid cells accumulate and exhibit disease-induced activation in the meninges in EAE. *Cell Immunol*. (2015) 297:69–79. doi: 10.1016/j.cellimm.2015.06.006
51. Casserly CS, Nantes JC, Whittaker Hawkins RF, Vallieres L. Neutrophil perversion in demyelinating autoimmune diseases: mechanisms to medicine. *Autoimmun Rev*. (2017) 16:294–307. doi: 10.1016/j.autrev.2017.01.013
52. Haribhai D, Luo X, Chen J, Jia S, Shi L, Schroeder JA, et al. TGF-beta1 along with other platelet contents augments Treg cells to suppress anti-FVIII immune responses in hemophilia A mice. *Blood Adv*. (2016) 1:139–51. doi: 10.1182/bloodadvances.2016001453

Conflict of Interest: The authors declare that the research was conducted in the absence of any commercial or financial relationships that could be construed as a potential conflict of interest.

frontiers in Immunology

REVIEW
published: 12 November 2019
doi: 10.3389/fimmu.2019.02642

CG-NAP/Kinase Interactions Fine-Tune T Cell Functions

Navin Kumar Verma[1]*, *Madhavi Latha Somaraju Chalasani*[2], *John D. Scott*[3] and *Dermot Kelleher*[1,4]

[1] Lee Kong Chian School of Medicine, Nanyang Technological University Singapore, Singapore, Singapore, [2] Autoimmunity and Inflammation Program, Hospital for Special Surgery, New York, NY, United States, [3] Department of Pharmacology, University of Washington School of Medicine, Seattle, WA, United States, [4] Departments of Medicine and Biochemistry and Molecular Biology, University of British Columbia, Vancouver, BC, Canada

CG-NAP, also known as AKAP450, is an anchoring/adaptor protein that streamlines signal transduction in various cell types by localizing signaling proteins and enzymes with their substrates. Great efforts are being devoted to elucidating functional roles of this protein and associated macromolecular signaling complex. Increasing understanding of pathways involved in regulating T lymphocytes suggests that CG-NAP can facilitate dynamic interactions between kinases and their substrates and thus fine-tune T cell motility and effector functions. As a result, new binding partners of CG-NAP are continually being uncovered. Here, we review recent advances in CG-NAP research, focusing on its interactions with kinases in T cells with an emphasis on the possible role of this anchoring protein as a target for therapeutic intervention in immune-mediated diseases.

Keywords: adaptor protein, kinases, CG-NAP, AKAP450, T cell motility, immune synapse

OPEN ACCESS

Edited by:
Kjetil Taskén,
Institute for Cancer Research, Oslo University Hospital, Norway

Reviewed by:
Noah Isakov,
Ben-Gurion University of the Negev, Israel
Tomas Brdicka,
Institute of Molecular Genetics (ASCR), Czechia

***Correspondence:**
Navin Kumar Verma
nkverma@ntu.edu.sg

Specialty section:
This article was submitted to T Cell Biology, a section of the journal Frontiers in Immunology

Received: *26 July 2019*
Accepted: *24 October 2019*
Published: *12 November 2019*

Citation:
Verma NK, Chalasani MLS, Scott JD and Kelleher D (2019) CG-NAP/Kinase Interactions Fine-Tune T Cell Functions. Front. Immunol. 10:2642. doi: 10.3389/fimmu.2019.02642

INTRODUCTION

T lymphocytes play a central role in immune defense by mounting specific responses to eliminate infections and transformed cells. To perform an immunosurveillance function, T cells continuously circulate throughout the body until they encounter specific antigen on the surface of the antigen presenting cell (APC, **Table 1**). Such contact with an APC triggers an initial activation of the T cell, which rapidly reorients its organelles and mobilizes signaling proteins to the contact site. This process is accompanied by dynamic structural and cytoskeletal changes within the T cell. An activated T cell undergoes an episode of rapid proliferation, cytokine secretion, differentiation into effector subtypes, and site-specific recruitment. These functional processes in T lymphocytes are precisely regulated and are critical for mounting an effective immune response.

Multiple stages of T cell functions, such as activation, differentiation, conjugate formation with APCs, homing and motility are crucially regulated by protein kinases (1, 2). As members of the kinase superfamily are widely distributed within cells and often have broad substrate specificity, a crucial element in signal transduction is local control of substrate specificity (3, 4). How is an individual kinase directed to connect with a single substrate or multiple components of a pool of downstream substrates? In some cases, kinase specificity is achieved by influencing substrate recognition. In this context, a class of proteins collectively known as "adaptor, anchoring and scaffolding proteins," have emerged as important mediators of signal transduction processes (5, 6). These proteins form specialized docking platforms that facilitate the formation of multicomponent signaling complexes, maintain static protein-protein interactions, position their kinase cargo in proximity to a subset of substrates, organize processes and components of protein kinase

cascades and thus streamline cell signaling responses (6–13). In T lymphocytes, these signal-organizing proteins allow signals to be transduced with precision in response to molecular instructions from the cell surface (14–16). Most importantly, these anchoring/adaptor proteins facilitate the phosphorylation and dephosphorylation of protein kinases, including trans- and auto-phosphorylations, which are important for the kinases to gain catalytically competent conformation in order to respond to intra- and/or extra-cellular signals (16, 17). Anchoring/adaptor proteins thus control numerous cellular processes in T lymphocytes, including cell fate decisions, activation, differentiation and various stages of development and functions (16–19). Herein, we review the involvement of such an anchoring protein "Centrosome and Golgi localized protein kinase N (PKN)-Associated Protein" (CG-NAP), also known as A-Kinase Anchoring Protein 450 (AKAP450) (20–22), in the regulation of protein kinase dynamics and functional outcomes in T cells.

A-KINASE ANCHORING PROTEINS (AKAPS)

AKAPs are a family of ubiquitously expressed structurally diverse signal-organizing proteins with tissue/cell-type specific expression patterns in human. So far, 41 AKAPs encoded by 41 genes have been experimentally validated in human cells and tissues (8, 23) (**Table 2**). Nine different AKAPs have been described in human T lymphocytes – AKAP1, AKAP2, AKAP5, AKAP8, AKAP9 (known as CG-NAP), AKAP11, Ezrin, RUNX1T1, and RUNX1T3 (24–26) and at least eight AKAPs with apparent molecular masses of 60, 75, 95, 120, 165, 190, 245, and 275 kDa were detected in mouse T lymphocytes (27); however, their involvements in the regulation of immune functions remain poorly understood.

Although members of the AKAP family differ greatly in their amino-acid sequences, structures, intracellular localizations and repertoire of protein binding partners, they all interact directly with the regulatory subunits of the protein kinase A (PKA) (28–33). However, the mechanism by which molecular interactions between specific AKAPs and PKA regulate normal and pathological signaling in human cells/tissues is just beginning to be understood.

AKAPs, through association with PKA, are involved in regulating T cell functions through the ubiquitous second messenger molecule cAMP (34–36), which controls cellular processes dictated by cell surface receptor-induced signaling (37–39). The interactions between AKAPs and PKA are complex as there are four distinct regulatory subunit isoforms of PKA – RIα, RIβ, RIIα, and RIIβ (7). These subunits differ in tissue distribution, cAMP sensitivity and AKAP-mediated localization, which fine-tune molecular signals depending on when and where PKA activity is applied (40). Most AKAPs bind to the RII isoform and a few dual-specific AKAPs can also interact with the RI isoform (33, 41). In addition, there are recent examples of RI selective AKAPs (42–44). Furthermore, most cell types simultaneously express multiple

TABLE 1 | A list of abbreviations used.

Abbreviations used	
AKAP	A-kinase anchoring protein
APC	Antigen presenting cell
cAMP	Cyclic adenosine monophosphate
CAMSAP2	Calmodulin regulated spectrin associated protein family member 2
CAMSAP3	Calmodulin regulated spectrin associated protein family member 3
CBFA2T3	CBFA2/RUNX1 partner transcriptional co-repressor 3
Cdk	Cyclin dependent kinase
CG-NAP	Centrosome- and Golgi-localized protein kinase N-associated protein
CHO	Chinese hamster ovary
CK1δ/ε	Casein kinase 1 delta/epsilon
CRISPR	Clustered regularly interspaced short palindromic repeats
EB1	End-binding protein 1
GM130	130 KDa cis-Golgi matrix protein
GTP	Guanosine triphosphate
HIV	Human immunodeficiency viruses
ICAM-1	Intercellular adhesion molecule 1
IL	Interleukin
IS	Immune synapse
JC virus	John Cunningham virus
KCNE1	Potassium voltage-gated channel subfamily E regulatory subunit 1
Kiz	Kizuna
LAT	Linker for activation of T cells
LFA-1	Lymphocyte function-associated antigen 1
MAPRE1	Microtubule associated protein RP/EB family member 1
MMG8	Myomegalin variant 8
MTCL1	Microtubule cross-linking factor 1
MTOC	Microtubule organizing center
NFAT	Nuclear factor of activated T cells
NFκB	Nuclear factor kappa B
PACT	Pericentrin-AKAP450 centrosomal targeting
PDE4D	Phosphodiesterase 4D
PKA	Protein kinase A
PKC	Protein kinase C
PKN	Protein kinase N
PLCγ1	Phospholipase C gamma 1
Plk1	Polo-like kinase 1
PP1	Protein phosphatase 1
PP2A	Protein phosphatase 2A
PR130	Serine/Threonine-protein phosphatase 2a 72/130 KDa regulatory subunit B
RAPGEF2	Rap guanine nucleotide exchange factor 2
RUNX1T1	RUNX1 partner transcriptional co-repressor 1
siRNAs	Small interfering RNA
TCR	T cell receptor
TGFβ	Transforming growth factor beta
TUBGCP	Tubulin gamma complex associated protein
γ-TuRC	Gamma tubulin ring complex

TABLE 2 | A list of AKAP family proteins.

S.N.	AKAPs	Name	Synonyms	HGNC ID (gene)	Chromosome
1.	AKAP1	A-kinase anchoring protein 1	PRKA1, AKAP121, AKAP149, SAKAP84, S-AKAP84, AKAP84, D-AKAP1, PPP1R43, TDRD17	HGNC:367	17q22
2.	AKAP2	A-kinase anchoring protein 2	PRKA2, AKAP-KL, KIAA0920, DKFZp564L0716, MISP2	HGNC:372	9q31.3
3.	AKAP3	A-kinase anchoring protein 3	FSP95, SOB1, AKAP110, CT82	HGNC:373	12p13.32
4.	AKAP4	A-kinase anchoring protein 4	p82, hAKAP82, AKAP82, Fsc1, HI, CT99	HGNC:374	Xp11.22
5.	AKAP5	A-kinase anchoring protein 5	AKAP75, AKAP79	HGNC:375	14q23.3
6.	AKAP6	A-kinase anchoring protein 6	KIAA0311, mAKAP, AKAP100, PRKA6, ADAP6	HGNC:376	14q12
7.	AKAP7	A-kinase anchoring protein 7	AKAP18, AKAP15	HGNC:377	6q23.2
8.	AKAP8	A-kinase anchoring protein 8	AKAP95, DKFZp586B1222	HGNC:378	19p13.12
9.	AKAP9	A-kinase anchoring protein 9	KIAA0803, AKAP350, AKAP450, CG-NAP, YOTIAO, HYPERION, PRKA9, MU-RMS-40.16A, PPP1R45, LQT11	HGNC:379	7q21.2
10.	AKAP10	A-kinase anchoring protein 10	D-AKAP2, PRKA10, MGC9414	HGNC:368	17p11.2
11.	AKAP11	A-kinase anchoring protein 11	KIAA0629, AKAP220, PRKA11, FLJ11304, DKFZp781I12161, PPP1R44	HGNC:369	13q14.11
12.	AKAP12	A-kinase anchoring protein 12	AKAP250, SSeCKS, gravin	HGNC:370	6q25.1
13.	AKAP13	A-kinase anchoring protein 13	LBC, Ht31, BRX, AKAP-Lbc, c-lbc, PROTO-LB, HA-3, ARHGEF13	HGNC:371	15q25.3
14.	AKAP14	A-kinase anchoring protein 14	AKAP28	HGNC:24061	Xq24
15.	AKAP17A	A-kinase anchoring protein 17A	CXYorf3, SFRS17A, XE7, XE7Y, DXYS155E, MGC39904, 721P, CCDC133	HGNC:18783	Xp22.33 and Yp11.32
16.	AKAP17BP	A-kinase anchoring protein 17B, pseudogene	AKAP16B, AKAP16BP	HGNC:38514	Xq24
17.	ACBD3	Acyl-CoA binding domain containing 3	GOLPH1, GOCAP1, GCP60, PAP7	HGNC:15453	1q42.12
18.	ARFGEF2	ADP ribosylation factor guanine nucleotide exchange factor 2	BIG2	HGNC:15853	20q13.13
19.	CHD8	Chromodomain Helicase DNA Binding Protein 8	HELSNF1, Helicase with SNF2 Domain 1, AUTS18, Duplin, KIAA1564	HGNC:20153	14q11.2
20.	CMYA5	Cardiomyopathy associated 5	C5orf10, SPRYD2, DKFZp451G223, TRIM76	HGNC:14305	5q14.1
21.	C2orf88	Chromosome 2 open reading frame 88	MGC13057, smAKAP	HGNC:28191	2q32.2
22.	EZR	Ezrin	VIL2, Villin 2, P81, Cytovillin	HGNC:12691	6q25.3
23.	GSKIP	GSK3B Interacting Protein	C14orf129	HGNC:20343	14q32.2
24.	ITGA4	α4 integrin	CD49D	HGNC: 6140	2q31.3
25.	MAP2	Microtubule associated protein 2	MAP2A, MAP2B, MAP2C	HGNC:6839	2q34
26.	MSN	Moesin	IMD50, HEL70, Membrane-Organizing Extension Spike Protein	HGNC: 7373	Xq12
27.	MYO7A	Myosin VIIA	USH1B, DFNB2, DFNA11, SRD2	HGNC:7606	11q13.5
28.	MYRIP	Myosin VIIA and Rab interacting protein	DKFZp586F1018, exophilin-8, MyRIP, SLAC2-C, SLAC2C	HGNC:19156	3p22.1
29.	NBEA	Neurobeachin	KIAA1544, BCL8B, FLJ10197, LYST2	HGNC:7648	13q13.3
30.	NF2	Neurofibromin 2	merlin, ACN, SCH, BANF	HGNC:7773	22q12.2
31.	OPA1	Optic Atrophy Protein 1	MyRIP, Optic Atrophy Protein 1, OPA1 Mitochondrial Dynamin Like GTPase, NTG, NPG, BERHS, LargeG, MTDPS14, KIAA0567, Dynamin-Like Guanosine Triphosphatase	HGNC: 8140	3q29
32.	PDE4DIP	Phosphodiesterase 4D Interacting Protein	MMGL, CMYA2, Myomegalin, Cardiomyopathy-Associated Protein	HGNC:15580	1q21.2
33.	PIK3CG	Phosphatidylinositol-4,5-Bisphosphate 3-Kinase Catalytic Subunit Gamma	P110γ, PI3Kγ, PI3CG, P120-PI3K	HGNC:8978	7q22.3
34.	RAB32	Ras-Related Protein Rab-32	Rab32	HGNC:9772	6q24.3
35.	RSPH3	Radial Spoke Head 3	RSP3, RSHL2	HGNC:21054	6q25.3
36.	RUNX1T1	RUNX1 Partner Transcriptional Co-Repressor 1	AML1T1, CBFA2T1, MTG8	HGNC:1535	8q21.3
37.	RUNX1T3	RUNX1 Partner Transcriptional Co-Repressor 3	CBFA2T3, ETO2, HMTG16, MTG8-Related Protein 2, MTG16, MTGR2, ZMYND4	HGNC:1537	16q24.3
38.	SPHKAP	SPHK1 interactor, AKAP domain containing	SKIP	HGNC:30619	2q36.3
39.	SYNM	Synemin	DMN, KIAA0353, SYN	HGNC:24466	15q26.3
40.	TNNT2	Troponin T2	c-troponinT, TnTC, CMPD2, LVNC6, CMD1D, CMH2	HGNC:11949	1q32.1
41.	WASF1	WAS protein family member 1	WAVE1, SCAR1, KIAA0269, WAVE	HGNC:12732	6q21

AKAPs (e.g., human T cells express at least 9 different AKAPs) (24–26).

It should be noted that the PKA-binding module of AKAPs denotes only one facet of their regulatory control. Apart from their interactions with PKA, AKAPs also interact with other downstream proteins and signaling enzymes, including protein kinase C (PKC) isoforms and PKN, protein phosphatases, phosphodiesterases, small GTPases (8) and substrates to integrate a diverse range of signals within distinct multivalent assemblies. The spatiotemporal interactions between enzymes and target substrates are important in the regulation of T cell functions as well as in the maintenance of T cell homeostasis (27).

CG-NAP: A GIANT MEMBER OF THE AKAP PROTEIN FAMILY

CG-NAP is a member of the AKAP family, prominently expressed in human T cells, in which this giant protein predominantly localizes to the centrosome (20). The human *CG-NAP* gene is located on the chromosome 7q21-22 and contains at least 50 exons (45–47). A total of 16 splice variants have been identified in the *CG-NAP* gene (**Table 3**). The cDNA derived from the *CG-NAP* gene contains 11.7 kb open reading frame coding the 3899 amino acid protein with a calculated molecular mass of 451.8 kDa (45). The CG-NAP protein has several stretches of coiled-coil structures and four leucine zipper-like motifs (**Figure 1**) and these structural motifs are involved in interactions with other signaling proteins (e.g., PKA, PKN and PKC isoforms) (45). Amino acid sequence comparison using BLAST analysis shows that regions of human CG-NAP share high homology with the rabbit AKAP120 and limited homology to the mouse pericentrin (48–50).

CG-NAP/PROTEIN KINASE INTERACTIONS IN T CELLS

The modular architecture of CG-NAP brings many protein kinases and their substrates in proximity within a cell and thus regulates the rate and magnitude of cytoplasmic catalysis. Since its initial characterization in 1999 (45) and the establishment of its role in regulating intracellular membrane trafficking and cell cycle progression (51), several interacting partners of CG-NAP have been identified in various cell types, including T lymphocytes (**Figure 2**).

Previous studies using co-immunoprecipitation approaches and deletion mutants to identify CG-NAP interacting partners revealed that CG-NAP functions as an anchoring molecular platform for protein kinases, including PKA (45). Using a yeast two-hybrid screening system, it has been demonstrated that CG-NAP interacts with the N-terminus of PKN (45). In addition, CG-NAP associates with the catalytic subunit of protein phosphatase 1 (PP1) (45), protein phosphatase 2A (PP2A) through its regulatory B subunit PR130 (45), casein kinase 1 delta and epsilon (CK1δ/ε) (52, 53), PKC isozymes (PKCβ, PKCδ, PKCε, PKCθ) (21, 54), calmodulin (55), the γ-tubulin ring complex (γ-TuRC) comprising of γ-tubulin, tubulin gamma complex associated proteins 2, 3, 4, 5 and 6 (TUBGCP2, TUBGCP3, TUBGCP4, TUBGCP5, and TUBGCP6) (55, 56), dynein/dynactin (57), Cdc42-interacting protein 4 (CIP4) (58), Ran (59), phosphodiesterase 4D (PDE4D) (45, 60), cyclin E/cyclin-dependent kinase (Cdk) 2 (61) and Golgin A2/GM130 (62) in various cell types (**Figure 2**). In cultured epithelial cells, CG-NAP forms a pericentrosomal complex with the EB1-binding-myomegalin protein complex and recruits calmodulin regulated spectrin-associated protein family member 2 and 3 (CAMSAP2 and CAMSAP3) and microtubule-associated protein RP/EB family member 1 (MAPRE1) to the Golgi (55, 63–66). Studies using various cell-types, including

TABLE 3 | A list of 16 splice variants (transcripts) of the CG-NAP gene in human.

S.N.	Name	Transcript ID	bp	Protein	Biotype	UniProt
1.	AKAP9-201	ENST00000356239.7	12471	3907aa	Protein coding	Q99996
2.	AKAP9-203	ENST00000359028.6	12247	3910aa	Protein coding	A0A0A0MRF6
3.	AKAP9-202	ENST00000358100.6	10309	3126aa	Protein coding	A0A0A0MRE9
4.	AKAP9-216	ENST00000619023.4	6006	1637aa	Protein coding	A0A087WX84
5.	AKAP9-204	ENST00000394534.6	5652	1769aa	Protein coding	H7BYL6
6.	AKAP9-206	ENST00000435423.1	1904	318aa	Protein coding	H0Y6Q0
7.	AKAP9-213	ENST00000491695.1	1389	282aa	Protein coding	A0A2R8Y590
8.	AKAP9-205	ENST00000394564.5	1356	314aa	Protein coding	Q6PJH3
9.	AKAP9-207	ENST00000438114.1	696	232aa	Protein coding	H7BZV6
10.	AKAP9-214	ENST00000493453.1	6020	No protein	Retained intron	–
11.	AKAP9-211	ENST00000487258.5	3983	No protein	Retained intron	–
12.	AKAP9-208	ENST00000463118.1	891	No protein	Retained intron	–
13.	AKAP9-212	ENST00000487692.1	869	No protein	Retained intron	–
14.	AKAP9-215	ENST00000493976.1	724	No protein	Retained intron	–
15.	AKAP9-209	ENST00000484815.1	671	No protein	Retained intron	–
16.	AKAP9-210	ENST00000486313.1	584	No protein	lncRNA	–

The list was prepared from the Ensembl database using the HGNC ID HGNC:379.

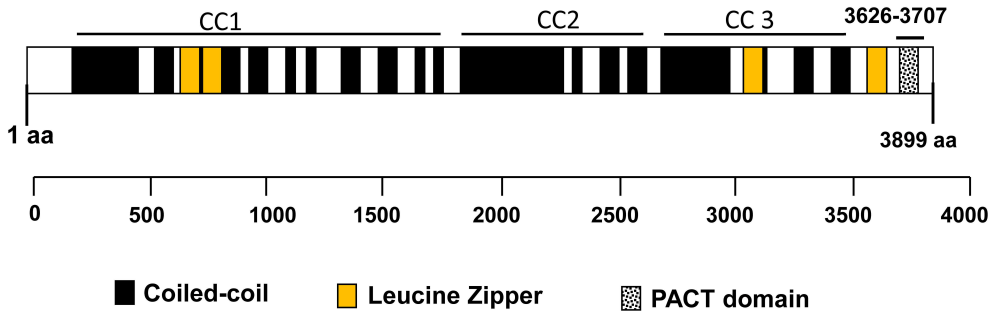

FIGURE 1 | An illustration of the domain organization of the CG-NAP. Modular structures of coiled-coil (CC1, CC2, and CC3), 4 Leucine Zippers and the PACT domain are shown schematically.

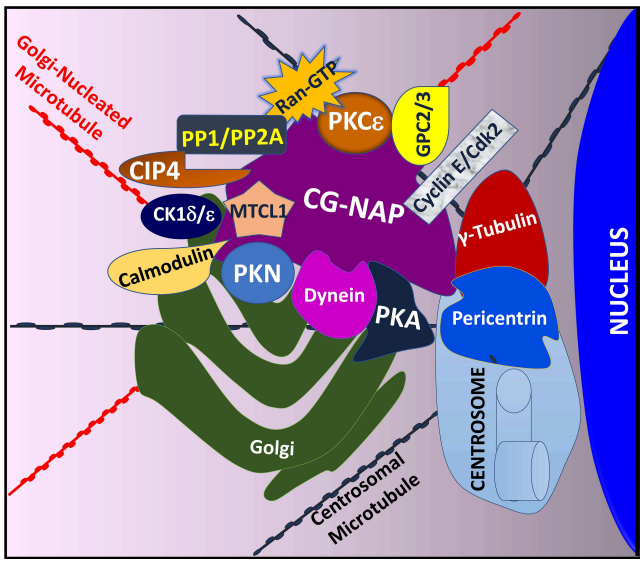

FIGURE 2 | An illustration showing T cell CG-NAP as an anchoring protein that provides a docking platform for several kinases and their substrates. In particular, the Golgi-localized CG-NAP interacts with PKA, PKN, PKC isoforms, dynein, pericentrin, γ-tubulin, MTCL1, PP1, PP2A, CK1, calmodulin, CIP4, cyclin E, and Cdk2 and regulates T cell functions, including activation, proliferation, IS formation and migration.

human T lymphocytes, further elucidate a role of CG-NAP in microtubule nucleation (20, 56, 67). These binding interactions with multiple proteins suggest a dynamic complexity in the active functions of CG-NAP.

In the context of T lymphocyte functions, crucial roles for CG-NAP have been demonstrated as (i) a component of the LFA-1-induced signaling complex, (ii) a mediator of T cell/APC immune synapse (IS) formation, (iii) an organizer of centrosomal re-localization, and *iv*) a facilitator of cytoskeletal rearrangement and motility (20–22). The LFA-1 β2 integrin plays multiple roles in the functioning of T lymphocytes, including migration to sites of inflammation/infection, proper functioning of the IS and functional programming for effector differentiation. In consequence, LFA-1-induced signals are critical in the pathogenesis of inflammatory diseases, such as psoriasis (68), and infectious diseases, including human immunodeficiency viruses (HIV) (69–71), Hepatitis C (72, 73) and John Cunningham (JC) virus (74). An active involvement of CG-NAP in mediating LFA-1 signaling suggests its potential implications for the above and other T cell-dependent diseases.

In prior studies, we have demonstrated that CG-NAP is an important component of the LFA-1 signaling complex for T lymphocyte migration (20, 21). These studies established that CG-NAP is expressed in T lymphocytes at the centrosome at rest and distributed both at the centrosome and along the trailing microtubules during migration (20, 21). CG-NAP co-immunoprecipitates with LFA-1 in activated migrating T cells (21). PKC isoforms, including PKCβ and PKCδ, also interact with CG-NAP in motile T cells (21). Hence, we concluded that the migratory signals in T lymphocytes induce the assembly of a multi-molecular protein complex involving CG-NAP, which serves as one of the docking platforms for PKCβ and PKCδ isoforms (21). PKCβ regulates LFA-1-mediated locomotion of activated T cells (75); whereas, PKCδ plays a critical role in TCR-induced negative regulation of IL-2 cytokine production and T cell proliferation (76).

Studies using cultured fibroblast cells demonstrated a direct association between CG-NAP and immature non- or hypo-phosphorylated PKCε at the Golgi and around the centrosome (54). Depending on environmental cues and upon phosphorylation, PKCε dissociates from the CG-NAP complex as a "mature" enzyme, which actively responds to second messenger signals (54). In human T cells, this PKC isoform regulates a diverse range of biological functions. In particular, PKCε modulates the TCR-associated signaling complex for T cell activation and cytokine secretion (77, 78), proliferation (79), sensitivity to TGFβ (79), development (80), gene expression (80), and survival (81, 82). PKCε directly activates the NFκB/NFAT/AP1 pathway in T cells leading to the up-regulation of IL-2 receptor expression and an increase in IL-2 production (83, 84). The LFA-1 signal for T cell migration activates PKCε, which phosphorylates the Rab GTPase Rab5a on Thr7, triggering a molecular cascade leading to the activation of the Rac1 protein and actin cytoskeletal rearrangements in motile T cells (85). Further studies are required to determine whether CG-NAP plays a role in the dynamic coordination of PKCε activities in human T cells.

CG-NAP/Kinase Interactions in T Cells at the Immune Synapse (IS)

Upon recognition of specific antigen on APCs and TCR engagement, a T cell undergoes a series of structural and molecular changes to form a flattened contact site, termed the "IS" (86). Within few seconds of T cell/APC contact, TCR signaling is triggered *via* an array of phosphorylation and de-phosphorylation cascades of membrane-proximal and -distal signaling elements. Within few minutes, the T lymphocyte rapidly reorients its cellular content to the intercellular contact zone. In particular, the stimulated T cell repositions its centromere from the uropod to the synapse at the contact site and dynamically orients cytoskeletal systems that allow asymmetric segregation of signaling and adhesive proteins toward the APC contact (87). This centrosomal polarization is important for the directional movement of recycling TCRs to the IS (88) and the positioning of the T cell secretory vesicles toward the APC (89). These molecular processes facilitate the polarized secretion of cytokines and cytolytic factors toward the bound target cell for effector immune responses (e.g., cell-mediated cytotoxicity and target cell destruction) (90), while preventing undesired bystander effects on neighboring cells. A single T lymphocyte is thus able to eliminate multiple target cells consecutively by integrin-mediated adhesion, rapid rearrangement of contacts and simultaneous formation of stimulatory and lytic synapses with defined central and peripheral signaling platforms. Moreover, the IS facilitates cell-to-cell communication between the T cell and the APC through exosomes and microvesicles (91, 92). After several hours of contact, T cell undergoes functional activation (93), and eventually differentiates to effector or memory T cells.

In the context of IS formation, CG-NAP coordinates dynamic interactions between protein kinases and their substrates at the centrosome in T cells. It colocalizes with a range of signaling molecules with implications for both the central supramolecular activation cluster (c-SMAC), which includes the TCR/CD3 complex and various costimulatory receptors, and the peripheral supramolecular activation cluster (p-SMAC) that incorporates LFA-1 (22). Functional consequences of CG-NAP loss in T cells during the IS formation, either by overexpression of a dominant-negative form or siRNA-mediated knockdown, include (i) impaired conformational activation and positioning of LFA-1 at the IS, (ii) defective segregation of LFA-1 at the p-SMAC ring, (iii) impaired LFA-1-associated signaling, (iv) reduced expression of the TCR CD3ϵ chain with decreased activation and clustering of TCR at the IS, (v) reduced phosphorylation of CD3ζ (Y83) in the TCR/CD3 complex, (vi) impaired recruitment of PKCθ to the IS, (vii) diminished phosphorylation of the phospholipase C gamma 1 (PLC-γ1), (viii) reduced activation of intracellular adaptor proteins, including the linker for activation of T cells (LAT) and Vav1, (ix) reduced phosphorylation of ERK1/2, (x) delocalization of the centrosome, (xi) defects in the translocation of microtubule organizing center (MTOC) toward the IS, and (xii) diminished production of IL-2 (22). The PKCθ isoform, PLC-γ1, ERK1/2, Vav1, and LAT play critical roles in TCR signaling. For example, activation of the TCR triggers PKCθ-mediated phosphorylation of the Rap guanine nucleotide exchange factor 2 (RAPGEF2) at Ser960, which regulates the adhesiveness of LFA-1 to its ligand ICAM-1 *via* Rap1 (94). Essential roles of PKCθ in regulating TCR-induced NFκB activation in mature thymocytes, inducible gene expression program in T cells, up-regulation and clustering of the LFA-1 on the T cell surface, adhesion capacity of T cells, effector T cell functions and protection from T cell-mediated autoimmune reactions have been documented (80, 95–97). An impaired PLC-γ1 activation in CG-NAP depleted T cells would impair diacylglycerol production, which is important for dynein function and MTOC translocation (22). TCR-induced phosphorylation of both LAT and Vav1 is critical for the functioning of the c-SMAC complex (22).

In the context of cytoskeletal reorganization at the IS, CG-NAP facilitates microtubule nucleation at the centrosome and non-centrosomal regions in human T cells (20). It coordinates PKA-mediated phosphorylation of dynein in motile T cells (20), which is crucial for centrosome repositioning at the IS (87, 98). Following APC/T cell contact, CG-NAP interacts with the kinase CK1δ that phosphorylates the microtubule plus-end binding protein EB1, which increases microtubule growth speeds (99) and has consequences for the IS. For example, T cell cytoskeletal remodeling elicits the APC to mobilize its intercellular adhesive molecules (ICAM-1 and−3) and subsequently the MHC-II molecules at the IS (100). Moreover, CG-NAP loss in human T cells impairs actin polymerization (22), which is crucial for the stabilization of APC/T cell contact at the IS (101).

CG-NAP mediates the activation of Aurora A protein kinase in human T cells (102), which is crucial for regulating signaling downstream of the TCR, such as activation of the Lck kinase and opening of the Ca^{2+} release-activated channels (CRAC)—both key signals involved in antigen-dependent T cell activation and in IS formation. Interestingly both knockdown and over-expression of CG-NAP significantly inhibit IL-2 secretion (22), suggesting multiple overlapping effects.

Thus, T cell CG-NAP contributes to the formation and maintenance of IS by serving as an intracellular scaffold for kinases and facilitating the organization and activation of receptor molecules.

CG-NAP/Kinase Interactions in T Cell Activation and Proliferation

The processes of T cell activation, proliferation and effector functions require several independent but coordinated molecular events initiated by TCR engagement (103). According to the clonal selection theory of adaptive immunity, the activation of a single lymphocyte clone provides sufficient function for an immediate immune response (i.e., proliferation of effector cells), as well as the regenerative capacity to maintain the selected lineage (i.e., development and differentiation of memory cells). In this context, CG-NAP is potentially involved in T cell proliferation and clonal expansion. While a direct role of CG-NAP in cell proliferation and cell cycle regulation has been identified in other cell types (51, 61, 104), further studies are required to dissect this role in T lymphocytes. Nonetheless some potential interactions may be inferred. For example, CG-NAP-depleted Chinese hamster ovary (CHO) cells and HeLa

cells over-expressing C-terminus CG-NAP are arrested at the G1 stage of cell-cycle followed by the induction of apoptosis in these cells (51, 61, 104). It has been shown in CHO cells that CG-NAP, by anchoring cyclin E/Cdk2 to the centrosome, drives centrosomal amplification and cell cycle progression (61). Further studies are required to determine whether CG-NAP-cyclin/Cdk complexes are involved in T cell proliferation.

At the centrosome, CG-NAP interacts with the centrosomal protein 72 kDa (Cep72) (105) and recruits the Kizuna (Kiz) protein, which is phosphorylated by the polo-like kinase 1 (Plk1) (106). The phosphorylation of Kiz enhances its association with the CG-NAP interacting protein, pericentrin (106). This association galvanizes the pericentriolar material, facilitates microtubule nucleation on the centrosome and allows for tubulin polymerization at the plus-end of the microtubules (107). CG-NAP associates with the dynein/dynactin motor complex and together with kendrin/pericentrin, anchors γ-TuRC at the centrosome through binding to its TUBGCP2 and/or TUBGCP3 subunits at the amino terminal regions (55). It provides new nucleation sites for *de novo* microtubule polymerization (55, 67, 108), which is important for cell cycle progression and proliferation of T lymphocytes. While many components of these interactions have been identified in T cells, further studies are required to determine the precise mechanisms whereby CG-NAP can regulate proliferation in human T cells.

CG-NAP also plays a crucial role in the regulation of endosomal trafficking of the TCR and is required for the effective re-stimulation of T cells (109). CG-NAP-dependent signaling and endosomal trafficking are important for the retention of T cells at sites of inflammation in mice (109). However, the viability of CG-NAP-knockout mice and the normal T cell counts in mice with conditional deletion of CG-NAP (109) suggest that CG-NAP may largely be dispensable or redundant for the maintenance of the resting T cell complement in the mouse. Loss of CG-NAP function in T cells would thus impair their sustained activation and have immunological consequences (109).

It is now clear that repeated and transient contacts of effector T cells with APCs are needed to functionally activate T lymphocytes in tissues. This suggests that signal integration between successive contacts is necessary to achieve activation. In contrast, the interactions between naïve T cells and DCs in the lymph node are relatively less dynamic and, typically, such interactions last for several hours (110, 111). It has also been speculated that the mechanisms of T cell activation at inflammation sites may vary from the primary activation of naïve T cells in lymph nodes (109). These tissue-specific differences in T cell activation may explain why depletion of CG-NAP does not significantly affect baseline T cell presence and differentiation in lymphoid tissues but may significantly impact T cell re-activation under suboptimal antigen-presenting conditions, such as re-activation in inflamed non-lymphoid tissue (109). Nevertheless, it has now been established that CG-NAP interacts with kinases (such as PKCβ, PKCδ, PKCε, PKCθ) (21, 54) and protein phosphatases (such as PP1, PP2A) (45) and transduces important signals *via* TCR (22) to regulate tissue-specific T cell activation and proliferation.

CG-NAP/Kinase Interactions in T Cell Migration

The recruitment of T cells to the tissue sites of infection or inflammation is critical to an effective immune response. Stimulated T lymphocytes leave lymphatic tissue and search the periphery for infected or transformed cells. When a T lymphocyte encounters an APC or a transformed cell, it mounts a specific immune response in a highly controlled manner. Blockade of the multi-step process of T cell motility can impair immune reactions, while uncontrolled migration can contribute to the development of autoimmunity.

In one pathway, T cell motility is dependent on the interactions between the T cell integrin LFA-1 and its ligand ICAM-1, which is expressed on endothelial surfaces during inflammation (112). LFA-1 engagement triggers a plethora of signaling cascades causing dynamic phosphorylation/de-phosphorylation of substrates by kinases and phosphatases and formation of macromolecular signaling complexes that culminate in cytoskeletal remodeling and T cell motility (112). CG-NAP is an integral component of these LFA-1-induced multi-molecular complexes and can serve to link the centrosome, microtubules and kinases, critical to the polarization and migration of T cells (5, 20, 21).

In human T lymphocytes, CG-NAP predominantly localizes in close proximity to the centrosome and the Golgi (20). This Golgi localization of CG-NAP is disrupted by microtubule depolarization (20). In HeLa-Kyoto cells, CG-NAP was found to recruit the microtubule cross-linking factor 1 (MTCL1), a molecule which crosslinks and stabilizes non-centrosomal microtubules to the Golgi membranes (113). Hence, we hypothesize a potential role of CG-NAP/MTCL1 interactions in T cell motility, a process which requires further investigation. Furthermore, as an AKAP, CG-NAP interacts with PKA and this complex consequently phosphorylates centrosomal proteins pericentrin and dynein in motile T cells (20). Dynein plays a crucial role in MTOC repositioning, cytoskeletal organization and the movement and processes of signaling complexes during T cell activation and motility (114, 115). In addition to PKA, several other kinases and phosphatases, including CK1, PKC, PP1 and PP2A, phosphorylate and dephosphorylate dynein in various cell types (116, 117) and all these enzymes are known to be anchored to the CG-NAP (45, 52, 53).

The functional significance of CG-NAP/kinase interactions for T cell motility is further underscored by the finding that the association between CG-NAP and LFA-1-induced signaling complex is greatly reduced when T cells are maintained at low temperature conditions (21). These data suggest a potential link between CG-NAP/kinase interactions and metabolic pathways in motile T cells. T cells overexpressing the C-terminal (aa 3699-3796) mutant form of CG-NAP fail to polarize and migrate (21). This CG-NAP C-terminus region contains the PACT (pericentrin-AKAP450 centrosomal targeting) domain, which binds additional proteins (50). For example, calmodulin binds to the C-terminus of CG-NAP in a calcium-independent manner (50). In addition, CG-NAP interacts with PKCβ and PKCδ (21), a process critical for signal transduction in motile T cells (75,

118). While *in vitro* knockdown of CG-NAP in human T cells significantly inhibited T cell migration and chemotaxis (20), no major impact of CG-NAP depletion on T cell motility was observed in T cell-specific CG-NAP knockout mice (109). The discrepancy between these findings could be attributed to the different model systems and experimental conditions.

It has been shown that the intracellular distribution of CG-NAP in LFA-1-stimulated motile T cells is different from that in cells stimulated to migrate through interactions with fibronectin (21). These data suggest that CG-NAP plays a unique role in β2 integrin-mediated T cell motility and may not have a similar role in adhesion and motility induced *via* different integrin families, such as, the β1 integrin. It has also been demonstrated that LFA-1-induced macromolecular signaling assemblies bring together molecules involved in intracellular transport and secretion. For example, LFA-1-induced formation of CG-NAP/kinase interactome containing PKCβ is crucial for T cell IL-2 production (21).

Microtubules are prominent elements of the cytoskeleton and dynamic cytoskeletal remodeling is essential for T cell motility. In addition to the cellular microtubule arrays emanating from the centrosome or the MTOC, secondary networks exist, in which microtubules are not anchored to the centrosome. While non-centrosomal microtubules are known to be present in differentiated cells (e.g., neurons, skeletal muscles, and epithelial cells), a recent report has demonstrated non-centrosomal microtubules emanating from CG-NAP in motile T cells (20). GapmeR-mediated knockdown of CG-NAP (119) disrupted both the centrosomal and non-centrosomal microtubule nucleation and inhibited post-translational tyrosination and acetylation of tubulin, illustrating the complexity of CG-NAP's role in coordinating microtubule dynamics and stability in migrating T cells (20).

PROSPECTS OF THERAPEUTIC TARGETING OF CG-NAP AND ASSOCIATED CHALLENGES

Immune-mediated diseases caused by T cell dysfunction are an increasing cause of mortality worldwide. While available therapeutic agents target T cell trafficking and immune hyperactivity, such treatment modalities are often accompanied by significant side effects. For example, while blocking LFA-1/ICAM-1 interaction has been proven to be effective in treating immune diseases, such as psoriasis (120), such immunosuppression can trigger the activation of JC-1 virus in the central nervous system leading to the development of fatal progressive multifocal leukoencephalopathy (121, 122). In prior studies, we have demonstrated that pre-activation through the LFA-1 pathway also alters the T cell programme, such that these stimulated T cells become refractory to TGFβ-mediated suppression and exhibit increased IL-17 secretion (123). Further studies are required to delineate whether specific interactions between CG-NAP and its docking partners may mediate specific migratory or secretory signals impacting on immune effector mechanisms. Fine-tuning of these interactions can provide functional selectivity and may offer exciting therapeutic approaches for a wide array of immune-mediated diseases.

One such fine-tuning strategy could be to alter a specific CG-NAP/kinase interaction by targeting a single protein-protein interaction. This could be achieved by either developing inhibitors against a specific kinase interaction in the CG-NAP interactome or by targeting CG-NAP/kinase interacting domain by blocking peptides (124). Although more likely to serve as a research tool, blocking peptides may assist in designing and developing small molecules targeting CG-NAP/kinase interactions, representing an interesting area of research and drug discovery. Further structural modeling of CG-NAP/kinase interactions should also identify suitable targets for small molecule inhibitors.

Targeting CG-NAP in its entirety would be challenging mainly because (i) this adaptor protein is expressed as several alternatively spliced transcripts and (ii) the degree of complexity of CG-NAP's involvement in multiple aspects of T cell signaling makes it difficult to elucidate each of their individual roles. One plausible strategy to understand the role of CG-NAP in T cell functioning would be to selectively displace interacting kinases and their subtypes from the CG-NAP docking platform. This would require the development of isoform-specific disruptors and other molecular tools to dissect individual pathway and CG-NAP/kinase interactions with high specificity. Exciting tools are available to silence individual gene in T lymphocytes that can be used to study functional involvement of specific interaction between CG-NAP and an individual kinase. These include the use of antisense GapmeR (119), siRNAs, gene correction and CRISPR-Cas9 editing techniques, which can be employed to overcome immune-mediated pathologies.

CONCLUSION

It is evident from the past two decades of research that CG-NAP regulates a plethora of biological processes by organizing supramolecular complexes and facilitating dynamic interactions between many different kinases and their substrates. In T cells, CG-NAP plays an important role in motility and participates in multiple interdependent pathways of T cell activation and effector functions. Thus, systematic studies are warranted to shed light on common or distinct binding partners and functions of CG-NAP and clarify to what extent CG-NAP/kinase interactions regulate T cell functions.

There is growing interest in developing protein-protein interaction disruptors, which would open new opportunities for therapeutic targeting of individual interactions between CG-NAP and specific kinases. A better understanding of CG-NAP/kinase interactions in T lymphocytes and their functional perturbations in immune response regulation is likely to lead to new frontiers in the treatment of T cell-mediated diseases.

AUTHOR CONTRIBUTIONS

NV and DK conceived the review idea. All authors contributed to the writing of this manuscript and approved the final manuscript version.

FUNDING

This work was supported, in part, by the Lee Kong Chian School of Medicine (LKCMedicine), Nanyang Technological University (NTU) Singapore Start-Up Grant (L0412290), the Singapore Ministry of Education (MOE) under its Singapore MOE Academic Research Fund (AcRF) Tier 2 Grant (MOE2017-T2-2-004) to NV, and NIH grants (DK119186 and DK119192) to JS.

REFERENCES

1. Finlay D, Cantrell D. The coordination of T-cell function by serine/threonine kinases. *Cold Spring Harb Perspect Biol*. (2011) 3:a002261. doi: 10.1101/cshperspect.a002261
2. Wells AD, Morawski PA. New roles for cyclin-dependent kinases in T cell biology: linking cell division and differentiation. *Nat Rev Immunol*. (2014) 14:261–70. doi: 10.1038/nri3625
3. Pawson T. Specificity in signal transduction: from phosphotyrosine-SH2 domain interactions to complex cellular systems. *Cell*. (2004) 116:191–203. doi: 10.1016/S0092-8674(03)01077-8
4. Li G, Qian H. Sensitivity and specificity amplification in signal transduction. *Cell Biochem Biophys*. (2003) 39:45–59. doi: 10.1385/CBB:39:1:45
5. Verma NK, Kelleher D. Adaptor regulation of LFA-1 signaling in T lymphocyte migration: Potential druggable targets for immunotherapies? *Eur J Immunol*. (2014) 44:3484–99. doi: 10.1002/eji.201344428
6. Flynn DC. Adaptor proteins. *Oncogene*. (2001) 20:6270–2. doi: 10.1038/sj.onc.1204769
7. Smith FD, Esseltine JL, Nygren PJ, Veesler D, Byrne DP, Vonderach M, et al. Local protein kinase A action proceeds through intact holoenzymes. *Science*. (2017) 356:1288–93. doi: 10.1126/science.aaj1669
8. Langeberg LK, Scott JD. Signalling scaffolds and local organization of cellular behaviour. *Nat Rev Mol Cell Biol*. (2015) 16:232–44. doi: 10.1038/nrm3966
9. Scott JD, Pawson T. Cell signaling in space and time: where proteins come together and when they're apart. *Science*. (2009) 326:1220–4. doi: 10.1126/science.1175668
10. Good MC, Zalatan JG, Lim WA. Scaffold proteins: hubs for controlling the flow of cellular information. *Science*. (2011) 332:680–6. doi: 10.1126/science.1198701
11. Zeke A, Lukács M, Lim WA, Reményi A. Scaffolds: interaction platforms for cellular signalling circuits. *Trends Cell Biol*. (2009) 19:364–74. doi: 10.1016/j.tcb.2009.05.007
12. Chen H, Jiang Z. The essential adaptors of innate immune signaling. *Protein Cell*. (2013) 4:27–39. doi: 10.1007/s13238-012-2063-0
13. Vajjhala PR, Ve T, Bentham A, Stacey KJ, Kobe B. The molecular mechanisms of signaling by cooperative assembly formation in innate immunity pathways. *Mol Immunol*. (2017) 86:23–37. doi: 10.1016/j.molimm.2017.02.012
14. Liu G, Dean A. Enhancer long-range contacts: the multi-adaptor protein LDB1 is the tie that binds. *BBA Gene Regul. Mech*. (2019) 1862:625–33. doi: 10.1016/j.bbagrm.2019.04.003
15. Zhang Q, Ding S, Zhang H. Interactions between hematopoietic progenitor kinase 1 and its adaptor proteins (Review). *Mol Med Rep*. (2017) 16:6472–82. doi: 10.3892/mmr.2017.7494
16. Rudd CE. Adaptors and molecular scaffolds in immune cell signaling. *Cell*. (1999) 96:5–8. doi: 10.1016/S0092-8674(00)80953-8
17. Jordan MS, Singer AL, Koretzky GA. Adaptors as central mediators of signal transduction in immune cells. *Nat Immunol*. (2003) 4:110–6. doi: 10.1038/ni0203-110
18. Koretzky GA, Myung PS. Positive and negative regulation of T-cell activation by adaptor proteins. *Nat Rev Immunol*. (2001) 1:95–107. doi: 10.1038/35100523
19. Kong MS, Hashimoto-Tane A, Kawashima Y, Sakuma M, Yokosuka T, Kometani K, et al. Inhibition of T cell activation and function by the adaptor protein CIN85. *Sci Signal*. (2019) 12:567. doi: 10.1126/scisignal.aav4373
20. Ong ST, Chalasani MLS, Fazil MHUT, Prasannan P, Kizhakeyil A, Wright GD, et al. Centrosome- and Golgi-localized protein kinase N-associated protein serves as a docking platform for protein kinase a signaling and microtubule nucleation in migrating T-cells. *Front Immunol*. (2018) 9:397. doi: 10.3389/fimmu.2018.00397
21. El Din El Homasany BS, Volkov Y, Takahashi M, Ono Y, Keryer G, Delouvee A, et al. The scaffolding protein CG-NAP/AKAP450 is a critical integrating component of the LFA-1-induced signaling complex in migratory T cells. *J Immunol*. (2005) 175:7811–8. doi: 10.4049/jimmunol.175.12.7811
22. Robles-Valero J, Martin-Cofreces NB, Lamana A, Macdonald S, Volkov Y, Sanchez-Madrid F. Integrin and CD3/TCR activation are regulated by the scaffold protein AKAP450. *Blood*. (2010) 115:74–4184. doi: 10.1182/blood-2009-12-256222
23. Smith FD, Omar MH, Nygren PJ, Soughayer J, Hoshi N, Lau HT, et al. Single nucleotide polymorphisms alter kinase anchoring and the subcellular targeting of A-kinase anchoring proteins. *Proc Natl Acad Sci USA*. (2018) 115:E11465–74. doi: 10.1073/pnas.1816614115
24. Wehbi VL, Taskén K. Molecular mechanisms for cAMP-mediated immunoregulation in T cells - role of anchored protein kinase A signaling units. *Front Immunol*. (2016) 7:222. doi: 10.3389/fimmu.2016.00222
25. Fukuyama T, Sueoka E, Sugio Y, Otsuka T, Niho Y, Akagi K, et al. MTG8 proto-oncoprotein interacts with the regulatory subunit of type II cyclic AMP-dependent protein kinase in lymphocytes. *Oncogene*. (2001) 20:6225–32. doi: 10.1038/sj.onc.1204794
26. Schillace RV, Andrews SF, Liberty GA, Davey MP, Carr DW. Identification and characterization of myeloid translocation gene 16b as a novel a kinase anchoring protein in T lymphocytes. *J Immunol*. (2002) 168:1590–9. doi: 10.4049/jimmunol.168.4.1590
27. Williams RO. Cutting edge: A-kinase anchor proteins are involved in maintaining resting T cells in an inactive state. *J Immunol*. (2002) 168:5392–6. doi: 10.4049/jimmunol.168.11.5392
28. Colledge M, Scott JD. AKAPs: from structure to function. *Trends Cell Biol*. (1999) 9:216–21. doi: 10.1016/S0962-8924(99)01558-5
29. Edwards AS, Scott JD. A-kinase anchoring proteins: protein kinase A and beyond. *Curr Opin Cell Biol*. (2000) 12:217–21. doi: 10.1016/S0955-0674(99)00085-X
30. Wong W, Scott JD. AKAP signalling complexes: focal points in space and time. *Nat Rev Mol Cell Biol*. (2004) 5:959–70. doi: 10.1038/nrm1527
31. Carr DW1, Stofko-Hahn RE, Fraser ID, Bishop SM, Acott TS, Brennan RG, et al. Interaction of the regulatory subunit (RII) of cAMP-dependent protein kinase with RII-anchoring proteins occurs through an amphipathic helix binding motif. *J Biol Chem*. (1991) 266:14188–92.
32. Newlon MG1, Roy M, Morikis D, Carr DW, Westphal R, Scott JD, et al. A novel mechanism of PKA anchoring revealed by solution structures of anchoring complexes. *EMBO J*. (2001) 20:1651–62. doi: 10.1093/emboj/20.7.1651
33. Gold MG, Lygren B, Dokurno P, Hoshi N, McConnachie G, Taskén K, et al. Molecular basis of AKAP specificity for PKA regulatory subunits. *Mol Cell*. (2006) 24:383–95. doi: 10.1016/j.molcel.2006.09.006
34. Arumugham VB, Baldari CT. cAMP: a multifaceted modulator of immune synapse assembly and T cell activation. *J Leukoc Biol*. (2017) 101:1301–16. doi: 10.1189/jlb.2RU1116-474R
35. Taskén K, Stokka AJ. The molecular machinery for cAMP-dependent immunomodulation in T-cells. *Biochem Soc Trans*. (2006) 34:476–9. doi: 10.1042/BST0340476
36. Kortum RL, Samelson LE. Priming the pump: adhesion enhances T cell antigen receptor-induced signaling. *Immunity*. (2009) 30:3–5. doi: 10.1016/j.immuni.2008.12.007
37. Mosenden R, Taskén K. Cyclic AMP-mediated immune regulation–overview of mechanisms of action in T cells. *Cell Signal*. (2011) 23:1009–16. doi: 10.1016/j.cellsig.2010.11.018

38. Grader-Beck T, van Puijenbroek AA, Nadler LM, Boussiotis VA. cAMP inhibits both Ras and Rap1 activation in primary human T lymphocytes, but only Ras inhibition correlates with blockade of cell cycle progression. *Blood*. (2003) 101:998–1006. doi: 10.1182/blood-2002-06-1665
39. Ramstad C, Sundvold V, Johansen HK, Lea T. cAMP-dependent protein kinase (PKA) inhibits T cell activation by phosphorylating ser-43 of raf-1 in the MAPK/ERK pathway. *Cell Signal*. (2000) 12:57–563. doi: 10.1016/S0898-6568(00)00097-8
40. Ould Amer Y, Hebert-Chatelain E. Mitochondrial cAMP-PKA signaling: What do we really know? *BBA Bioenerg*. (2018) 1859:68–877. doi: 10.1016/j.bbabio.2018.04.005
41. Jarnaess E, Ruppelt A, Stokka AJ, Lygren B, Scott JD, Taskén K. Dual specificity A-kinase anchoring proteins (AKAPs) contain an additional binding region that enhances targeting of protein kinase A type I. *J Biol Chem*. (2008) 283:33708–18. doi: 10.1074/jbc.M804807200
42. Means CK, Lygren B, Langeberg LK, Jain A, Dixon RE, Vega AL, et al. An entirely specific type I A-kinase anchoring protein that can sequester two molecules of protein kinase A at mitochondria. *Proc Natl Acad Sci USA*. (2011) 108:E1227–35. doi: 10.1073/pnas.1107182108
43. Burgers PP, Bruystens J, Burnley RJ, Nikolaev VO, Keshwani M, Wu J, et al. Structure of smAKAP and its regulation by PKA-mediated phosphorylation. *FEBS J*. (2016) 283:2132–48. doi: 10.1111/febs.13726
44. Burgers PP, Ma Y, Margarucci L, Mackey M, van der Heyden MA, Ellisman M, et al. A small novel A-kinase anchoring protein (AKAP) that localizes specifically protein kinase A-regulatory subunit I (PKA-RI) to the plasma membrane. *J Biol Chem*. (2012) 287:43789–97. doi: 10.1074/jbc.M112.395970
45. Takahashi M, Shibata H, Shimakawa M, Miyamoto M, Mukai H, Ono Y. Characterization of a novel giant scaffolding protein, CG-NAP, that anchors multiple signaling enzymes to centrosome and the golgi apparatus. *J Biol Chem*. (1999) 274:17267–74. doi: 10.1074/jbc.274.24.17267
46. Schmidt PH, Dransfield DT, Claudio JO, Hawley RG, Trotter KW, Milgram SL, Goldenring JR. AKAP350, a multiply spliced protein kinase A-anchoring protein associated with centrosomes. *J Biol Chem*. (1999) 274:3055–66. doi: 10.1074/jbc.274.5.3055
47. Witczak O, Skalhegg BS, Keryer G, Bornens M, Tasken K, Jahnsen T, et al. Cloning and characterization of a cDNA encoding an A-kinase anchoring protein located in the centrosome, AKAP450. *EMBO J*. (1999) 18:1858–68. doi: 10.1093/emboj/18.7.1858
48. Westphal RS, Tavalin SJ, Lin JW, Alto NM, Fraser ID, Langeberg LK, et al. Regulation of NMDA receptors by an associated phosphatase-kinase signaling complex. *Science*. (1999) 285:93–6. doi: 10.1126/science.285.5424.93
49. Dransfield DT, Yeh JL, Bradford AJ, Goldenring JR. Identification and characterization of a novel A-kinase-anchoring protein (AKAP120) from rabbit gastric parietal cells. *Biochem J*. (1997) 322:801–8. doi: 10.1042/bj3220801
50. Gillingham AK, Munro S. The PACT domain, a conserved centrosomal targeting motif in the coiled-coil proteins AKAP450 and pericentrin. *EMBO Rep*. (2000) 1:524–9. doi: 10.1093/embo-reports/kvd105
51. Keryer G, Witczak O, Delouvée A, Kemmner WA, Rouillard D, Tasken K, et al. Dissociating the centrosomal matrix protein AKAP450 from centrioles impairs centriole duplication and cell cycle progression. *Mol Biol Cell*. (2003) 14:2436–46. doi: 10.1091/mbc.e02-09-0614
52. Sillibourne JE, Milne DM, Takahashi M, Ono Y, Meek DW. Centrosomal anchoring of the protein kinase CK1delta mediated by attachment to the large, coiled-coil scaffolding protein CG-NAP/AKAP450. *J Mol Biol*. (2002) 322:785–97. doi: 10.1016/S0022-2836(02)00857-4
53. Giamas G, Hirner H, Shoshiashvili L, Grothey A, Gessert S, Kuhl M, et al. Phosphorylation of CK1delta: identification of Ser370 as the major phosphorylation site targeted by PKA *in vitro* and *in vivo*. *Biochem J*. (2007) 406:389–98. doi: 10.1042/BJ20070091
54. Takahashi M, Mukai H, Oishi K, Isagawa T, Ono Y. Association of immature hypophosphorylated protein kinase cepsilon with an anchoring protein CG-NAP. *J Biol Chem*. (2000) 275:34592–6. doi: 10.1074/jbc.M005285200
55. Takahashi M, Yamagiwa A, Nishimura T, Mukai H, Ono Y. Centrosomal proteins CG-NAP and kendrin provide microtubule nucleation sites by anchoring gamma-tubulin ring complex. *Mol Biol Cell*. (2002) 13:3235–45. doi: 10.1091/mbc.e02-02-0112
56. Wu J, de Heus C, Liu Q, Bouchet BP, Noordstra I, Jiang K, et al. Molecular pathway of microtubule organization at the Golgi apparatus. *Dev Cell*. (2016) 39:44–60. doi: 10.1016/j.devcel.2016.08.009
57. Kim HS, Takahashi M, Matsuo K, Ono Y. Recruitment of CG-NAP to the Golgi apparatus through interaction with dynein-dynactin complex. *Genes Cells*. (2007) 12:421–34. doi: 10.1111/j.1365-2443.2007.01055.x
58. Larocca MC, Shanks RA, Tian L, Nelson DL, Stewart DM, Goldenring JR. AKAP350 interaction with cdc42 interacting protein 4 at the Golgi apparatus. *Mol Bio Cell*. (2004) 15:2771–81. doi: 10.1091/mbc.e03-10-0757
59. Keryer G, Di Fiore B, Celati C, Lechtreck KF, Mogensen M, Delouvee A, et al. Part of Ran is associated with AKAP450 at the centrosome: involvement in microtubule-organizing activity. *Mol Biol Cell*. (2003) 14:4260–71. doi: 10.1091/mbc.e02-11-0773
60. Terrin A, Monterisi S, Stangherlin A, Zoccarato A, Koschinski A, Surdo NC, et al. PKA and PDE4D3 anchoring to AKAP9 provides distinct regulation of cAMP signals at the centrosome. *J Cell Biol*. (2012) 198:607–21. doi: 10.1083/jcb.201201059
61. Nishimura T, Takahashi M, Kim HS, Mukai H, Ono Y. Centrosome-targeting region of CG-NAP causes centrosome amplification by recruiting cyclin E-cdk2 complex. *Genes Cells*. (2005) 10:75–86. doi: 10.1111/j.1365-2443.2005.00816.x
62. Rivero S, Cardenas J, Bornens M, Rios RM. Microtubule nucleation at the cis-side of the Golgi apparatus requires AKAP450 and GM130. *EMBO J*. (2009) 28:1016–28. doi: 10.1038/emboj.2009.47
63. Wang Z, Zhang C, Qi RZ. A newly identified myomegalin isoform functions in Golgi microtubule organization and ER-Golgi transport. *J Cell Sci*. (2014) 127:4904–17. doi: 10.1242/jcs.155408
64. Wang J, Xu H, Jiang Y, Takahashi M, Takeichi M, Meng W. CAMSAP3-dependent microtubule dynamics regulates Golgi assembly in epithelial cells. *J Genet Genomics*. (2017) 44:39–49. doi: 10.1016/j.jgg.2016.11.005
65. Yang C, Wu J, de Heus C, Grigoriev I, Liv N, Yao Y, et al. EB1 and EB3 regulate microtubule minus end organization and Golgi morphology. *J Cell Biol*. (2017) 216:3179–98. doi: 10.1083/jcb.201701024
66. Bouguenina H, Salaun D, Mangon A, Muller L, Baudelet E, Camoin L, et al. EB1-binding-myomegalin protein complex promotes centrosomal microtubules functions. *Proc Natl Acad Sci USA*. (2017) 114:E10687–96. doi: 10.1073/pnas.1705682114
67. Petry S, Vale RD. Microtubule nucleation at the centrosome and beyond. *Nat Cell Biol*. (2015) 17:1089–93. doi: 10.1038/ncb3220
68. Lebwohl M, Tyring SK, Hamilton TK, Toth D, Glazer S, Tawfik NH, et al. Efalizumab study group. a novel targeted T-cell modulator, efalizumab, for plaque psoriasis. *N Engl J Med*. (2003) 349:2004–13. doi: 10.1056/NEJMoa030002
69. Starling S, Jolly C. LFA-1 engagement triggers T cell oolarization at the HIV-1 virological synapse. *J Virol*. (2016) 90:9841–54. doi: 10.1128/JVI.01152-16
70. Tardif MR, Tremblay MJ. Regulation of LFA-1 activity through cytoskeleton remodeling and signaling components modulates the efficiency of HIV type-1 entry in activated CD4+ T lymphocytes. *J Immunol*. (2005) 175:926–35. doi: 10.4049/jimmunol.175.2.926
71. Hioe CE, Chien PC Jr, Lu C, Springer TA, Wang XH, Bandres J, et al. LFA-1 expression on target cells promotes human immunodeficiency virus type 1 infection and transmission. *J Virol*. (2001) 75:1077–82. doi: 10.1128/JVI.75.2.1077-1082.2001
72. Volkov Y, Long A, Freeley M, Golden-Mason L, O'Farrelly C, Murphy A, Kelleher D. The hepatitis C envelope 2 protein inhibits LFA-1-transduced protein kinase C signaling for T-lymphocyte migration. *Gastroenterology*. (2006) 130:482–92. doi: 10.1053/j.gastro.2005.10.047
73. Petrovic D, Dempsey E, Doherty DG, Kelleher D, Long A. Hepatitis C virus–T-cell responses and viral escape mutations. *Eur J Immunol*. (2012) 42:17–26. doi: 10.1002/eji.201141593
74. Schwab N, Ulzheimer JC, Fox RJ, Schneider-Hohendorf T, Kieseier BC, Monoranu CM, et al. Fatal PML associated with efalizumab therapy: insights into integrin αLβ2 in JC virus control. *Neurology*. (2012) 78:458–67. doi: 10.1212/WNL.0b013e3182478d4b
75. Volkov Y, Long A, McGrath S, Ni Eidhin D, Kelleher D. Crucial importance of PKC-beta(I) in LFA-1-mediated locomotion of activated T cells. *Nat Immunol*. (2001) 2:508–14. doi: 10.1038/88700

76. Gruber T, Barsig J, Pfeifhofer C, Ghaffari-Tabrizi N, Tinhofer I, Leitges M, et al. PKCdelta is involved in signal attenuation in CD3+ T cells. *Immunol Lett.* (2005) 96:291–3. doi: 10.1016/j.imlet.2004.08.011
77. Keenan C, Volkov Y, Kelleher D, Long A. Subcellular localization and translocation of protein kinase C isoforms zeta and epsilon in human peripheral blood lymphocytes. *Int Immunol.* (1997) 9:1431–9. doi: 10.1093/intimm/9.10.1431
78. Genot EM, Parker PJ, Cantrell DA. Analysis of the role of protein kinase C-alpha, -epsilon, and -zeta in T cell activation. *J Biol Chem.* (1995) 270:9833–9. doi: 10.1074/jbc.270.17.9833
79. Mirandola P, Gobbi G, Masselli E, Micheloni C, Di Marcantonio D, Queirolo V, et al. Protein kinase Cε regulates proliferation and cell sensitivity to TGF-1β of CD4+ T lymphocytes: implications for Hashimoto thyroiditis. *J Immunol.* (2011) 187:4721–32. doi: 10.4049/jimmunol.1003258
80. Lim PS, Sutton CR, Rao S. Protein kinase C in the immune system: from signalling to chromatin regulation. *Immunology.* (2015) 146:508–22. doi: 10.1111/imm.12510
81. Bertolotto C, Maulon L, Filippa N, Baier G, Auberger P. Protein kinase C theta and epsilon promote T-cell survival by a rsk-dependent phosphorylation and inactivation of BAD. *J Biol Chem.* (2000) 275:37246–50. doi: 10.1074/jbc.M007732200
82. Pfeifhofer-Obermair C, Thuille N, Baier G. Involvement of distinct PKC gene products in T cell functions. *Front Immunol.* (2012) 3:220. doi: 10.3389/fimmu.2012.00220
83. Szamel M, Appel A, Schwinzer R, Resch K. Different protein kinase C isoenzymes regulate IL-2 receptor expression or IL-2 synthesis in human lymphocytes stimulated via the TCR. *J Immunol.* (1998) 160:2207–14.
84. Simon AK, Auphan N, Pophillat M, Boyer C, Ghosh S, Rincón M, et al. The lack of NF-κB transactivation and PKC epsilon expression in $CD4^+CD8^+$ thymocytes correlates with negative selection. *Cell Death Differ.* (2000) 7:1253–62. doi: 10.1038/sj.cdd.4400760
85. Ong ST, Freeley M, Skubis-Zegadło J, Fazil MHUT, Kelleher D, Fresser F, et al. Phosphorylation of Rab5a protein by protein kinase Cε is crucial for T-cell migration. *J Biol Chem.* (2014) 289:19420–34. doi: 10.1074/jbc.M113.545863
86. Bromley SK, Burack WR, Johnson KG, Somersalo K, Sims TN, Sumen C, et al. The immunological synapse. *Annu Rev Immunol.* (2001) 19:375–96. doi: 10.1146/annurev.immunol.19.1.375
87. Yi J, Wu X, Chung AH, Chen JK, Kapoor TM, Hammer JA. Centrosome repositioning in T cells is biphasic and driven by microtubule end-on capture-shrinkage. *J Cell Biol.* (2013) 202:779–92. doi: 10.1083/jcb.201301004
88. Cesari F. TCR–CD3 recycling to the synapse. *Nat Rev Immunol.* (2009) 9:820–1. doi: 10.1038/nri2680
89. Stinchcombe JC, Majorovits E, Bossi G, Fuller S, Griffiths GM. Centrosome polarization delivers secretory granules to the immunological synapse. *Nature.* (2006) 443:462–5. doi: 10.1038/nature05071
90. Stinchcombe JC, Salio M, Cerundolo V, Pende D, Arico M, Griffiths GM. Centriole polarisation to the immunological synapse directs secretion from cytolytic cells of both the innate and adaptive immune systems. *BMC Biol.* (2011) 9:45. doi: 10.1186/1741-7007-9-45
91. Mittelbrunn M, Gutierrez-Vazquez C, Villarroya-Beltri C, Gonzalez S, Sanchez-Cabo F, Gonzalez MA, et al. Unidirectional transfer of microRNA-loaded exosomes from T cells to antigen-presenting cells. *Nat Commun.* (2011) 2:282. doi: 10.1038/ncomms1285
92. Choudhuri K, Llodra J, Roth EW, Tsai J, Gordo S, Wucherpfennig KW, et al. Polarized release of T-cell-receptor-enriched microvesicles at the immunological synapse. *Nature.* (2014) 507:118–23. doi: 10.1038/nature12951
93. Iezzi G, Karjalainen K, Lanzavecchia A. The duration of antigenic stimulation determines the fate of naive and effector T cells. *Immunity.* (1998) 8:89–95. doi: 10.1016/S1074-7613(00)80461-6
94. Letschka T, Kollmann V, Pfeifhofer-Obermair C, Lutz-Nicoladoni C, Obermair GJ, Fresser F, et al. PKC-theta selectively controls the adhesion-stimulating molecule Rap1. *Blood.* (2008) 112:4617–27. doi: 10.1182/blood-2007-11-121111
95. Sun Z, Arendt CW, Ellmeier W, Schaeffer EM, Sunshine MJ, Gandhi L, et al. PKC-theta is required for TCR-induced NF-kappaB activation in mature but not immature T lymphocytes. *Nature.* (2000) 404:402–7. doi: 10.1038/35006090
96. Brezar V, Tu WJ, Seddiki N. PKC-theta in regulatory and effector T-cell functions. *Front Immunol.* (2015) 6:530. doi: 10.3389/fimmu.2015.00530
97. Freeley M, Long A. Regulating the regulator: phosphorylation of PKC θ in T cells. *Front Immunol.* (2012) 6:227. doi: 10.3389/fimmu.2012.00227
98. Hashimoto-Tane A, Yokosuka T, Sakata-Sogawa K, Sakuma M, Ishihara C, Tokunaga M, et al. Dynein-driven transport of T cell receptor microclusters regulates immune synapse formation and T cell activation. *Immunity.* (2011) 34:919–31. doi: 10.1016/j.immuni.2011.05.012
99. Zyss D, Ebrahimi H, Gergely F. Casein kinase I delta controls centrosome positioning during T cell activation. *J Cell Biol.* (2011) 195:781–97. doi: 10.1083/jcb.201106025
100. de la Fuente H, Mittelbrunn M, Sánchez-Martín L, Vicente-Manzanares M, Lamana A, Pardi R, et al. Synaptic clusters of MHC class II molecules induced on DCs by adhesion molecule-mediated initial T-cell scanning. *Mol Biol Cell.* (2005) 16:3314–22. doi: 10.1091/mbc.e05-01-0005
101. Fuller CL, Braciale VL, Samelson LE. All roads lead to actin: the intimate relationship between TCR signaling and the cytoskeleton. *Immunol Rev.* (2003) 191:220–36. doi: 10.1034/j.1600-065X.2003.00004.x
102. Blas-Rus N, Bustos-Morán E, Martín-Cófreces NB, Sánchez-Madrid F. Aurora-A shines on T cell activation through the regulation of Lck. *Bioessays.* (2017) 39:1600156. doi: 10.1002/bies.201600156
103. Guy CS, Vignali DA. Organization of proximal signal initiation at the TCR:CD3 complex. *Immunol Rev.* (2009) 232:7–21. doi: 10.1111/j.1600-065X.2009.00843.x
104. Mattaloni SM, Ferretti AC, Tonucci FM, Favre C, Goldenring JR, Larocca MC. Centrosomal AKAP350 modulates the G/S transition. *Cell Logist.* (2013) 3:e26331. doi: 10.4161/cl.26331
105. Oshimori N, Li X, Ohsugi M, Yamamoto T. Cep72 regulates the localization of key centrosomal proteins and proper bipolar spindle formation. *EMBO J.* (2009) 28:2066–76. doi: 10.1038/emboj.2009.161
106. Fabbro M, Zhou BB, Takahashi M, Sarcevic B, Lal P, Graham ME, et al. Cdk1/Erk2- and Plk1-dependent phosphorylation of a centrosome protein, Cep55, is required for its recruitment to midbody and cytokinesis. *Dev Cell.* (2005) 9:477–88. doi: 10.1016/j.devcel.2005.09.003
107. Paz J, Lüders J. Microtubule-organizing centers: towards a minimal parts list. *Trends Cell Biol.* (2018) 28:176–87. doi: 10.1016/j.tcb.2017.10.005
108. Tovey CA, Conduit PT. Microtubule nucleation by γ-tubulin complexes and beyond. *Essays Biochem.* (2018) 62:765–80. doi: 10.1042/EBC20180028
109. Herter JM, Grabie N, Cullere X, Azcutia V, Rosetti F, Bennett P, et al. AKAP9 regulates activation-induced retention of T lymphocytes at sites of inflammation. *Nat Commun.* (2015) 6:10182. doi: 10.1038/ncomms10182
110. Rothoeft T1, Balkow S, Krummen M, Beissert S, Varga G, Loser K, et al. Structure and duration of contact between dendritic cells and T cells are controlled by T cell activation state. *Eur J Immunol.* (2006) 36:3105–17. doi: 10.1002/eji.200636145
111. Garcia Z, Pradelli E, Celli S, Beuneu H, Simon A, Bousso P. Competition for antigen determines the stability of T cell-dendritic cell interactions during clonal expansion. *Proc Natl Acad Sci USA.* (2007) 104:4553–8. doi: 10.1073/pnas.0610019104
112. Smith A, Stanley P, Jones K, Svensson L, McDowall A, Hogg N. The role of the integrin LFA-1 in T-lymphocyte migration. *Immunol Rev.* (2007) 218:135–46. doi: 10.1111/j.1600-065X.2007.00537.x
113. Sato Y, Hayashi K, Amano Y, Takahashi M, Yonemura S, Hayashi I, et al. MTCL1 crosslinks and stabilizes non-centrosomal microtubules on the Golgi membrane. *Nat Comm.* (2014) 5:5266. doi: 10.1038/ncomms6266
114. Lim WM, Ito Y, Sakata-Sogawa K, Tokunaga M. CLIP-170 is essential for MTOC repositioning during T cell activation by regulating dynein localisation on the cell surface. *Sci Rep.* (2018) 8:17447. doi: 10.1038/s41598-018-35593-z
115. Benzing C, Rossy J, Gaus K. Do signalling endosomes play a role in T cell activation? *FEBS J.* (2013) 280:5164–76. doi: 10.1111/febs.12427
116. Carnegie GK, Means CK, Scott JD. A-kinase anchoring proteins: from protein complexes to physiology and disease. *IUBMB Life.* (2009) 61:394–406. doi: 10.1002/iub.168
117. Wirschell M, Yamamoto R, Alford L, Gokhale A, Gaillard A, Sale WS. Regulation of ciliary motility: conserved protein kinases and phosphatases are targeted and anchored in the ciliary axoneme. *Arch Biochem Biophys.* (2011) 510:93–100. doi: 10.1016/j.abb.2011.04.003

118. Quann EJ, Liu X, Altan-Bonnet G, Huse M. A cascade of protein kinase C isozymes promotes cytoskeletal polarization in T cells. *Nat Immunol*. (2011) 12:647–54. doi: 10.1038/ni.2033
119. Fazil MHUT, Ong ST, Chalasani ML, Low JH, Kizhakeyil A, Mamidi A, et al. GapmeR cellular internalization by macropinocytosis induces sequence-specific gene silencing in human primary T-cells. *Sci Rep*. (2016) 6:37721. doi: 10.1038/srep37721
120. Li S, Wang H, Peng B, Zhang M, Zhang D, Hou S, et al. Efalizumab binding to the LFA-1 alphaL I domain blocks ICAM-1 binding via steric hindrance. *Proc Natl Acad Sci USA*. (2009) 106:4349–54. doi: 10.1073/pnas.0810844106
121. Carson KR, Focosi D, Major EO, Petrini M, Richey EA, West DP, et al. Monoclonal antibody-associated progressive multifocal leucoencephalopathy in patients treated with rituximab, natalizumab, and efalizumab: a Review from the Research on Adverse Drug Events and Reports (RADAR) Project. *Lancet Oncol*. (2009) 10:816–24. doi: 10.1016/S1470-2045(09)70161-5
122. Lin EJ, Reddy S, Shah VV, Wu JJ. A review of neurologic complications of biologic therapy in plaque psoriasis. *Cutis*. (2018) 101:57–60.
123. Verma NK, Dempsey E, Long A, Davies A, Barry SP, Fallon PG, et al. Leukocyte function-associated antigen-1/intercellular adhesion molecule-1 interaction induces a novel genetic signature resulting in T-cells refractory to transforming growth factor-β signaling. *J Biol Chem*. (2012) 287:27204–16. doi: 10.1074/jbc.M112.376616
124. Wang Y, Ho TG, Bertinetti D, Neddermann M, Franz E, Mo GC, et al. Isoform-selective disruption of AKAP-localized PKA using hydrocarbon stapled peptides. *ACS Chem Biol*. (2014) 9:635–42. doi: 10.1021/cb400900r

Conflict of Interest: The authors declare that the research was conducted in the absence of any commercial or financial relationships that could be construed as a potential conflict of interest.

frontiers in Immunology

ORIGINAL RESEARCH
published: 22 January 2020
doi: 10.3389/fimmu.2019.03144

ADAP Promotes Degranulation and Migration of NK Cells Primed During *in vivo Listeria monocytogenes* Infection in Mice

Martha A. L. Böning[1,2,3], Stephanie Trittel[4], Peggy Riese[4], Marco van Ham[5], Maxi Heyner[5‡], Martin Voss[2], Gerald P. Parzmair[2,3‡], Frank Klawonn[5], Andreas Jeron[1,3], Carlos A. Guzman[4], Lothar Jänsch[5], Burkhart Schraven[2†], Annegret Reinhold[2†] and Dunja Bruder[1,3*†]*

[1] Infection Immunology Group, Institute of Medical Microbiology, Infection Control and Prevention, Health Campus Immunology, Infectiology and Inflammation, Otto-von-Guericke University Magdeburg, Magdeburg, Germany, [2] Institute of Molecular and Clinical Immunology, Health Campus Immunology, Infectiology and Inflammation, Otto-von-Guericke University Magdeburg, Magdeburg, Germany, [3] Immune Regulation Group, Helmholtz Centre for Infection Research, Braunschweig, Germany, [4] Vaccinology and Applied Microbiology, Helmholtz Centre for Infection Research, Braunschweig, Germany, [5] Cellular Proteome Research, Helmholtz Centre for Infection Research, Braunschweig, Germany

The adhesion and degranulation-promoting adaptor protein (ADAP) serves as a multifunctional scaffold and is involved in the formation of immune signaling complexes. To date only limited and moreover conflicting data exist regarding the role of ADAP in NK cells. To extend existing knowledge we investigated ADAP-dependency of NK cells in the context of *in vivo* infection with the intracellular pathogen *Listeria monocytogenes* (*Lm*). *Ex vivo* analysis of infection-primed NK cells revealed impaired cytotoxic capacity in NK cells lacking ADAP as indicated by reduced CD107a surface expression and inefficient perforin production. However, ADAP-deficiency had no global effect on NK cell morphology or intracellular distribution of CD107a-containing vesicles. Proteomic definition of ADAPko and wild type NK cells did not uncover obvious differences in protein composition during the steady state and moreover, similar early response patterns were induced in NK cells upon infection independent of the genotype. In line with protein network analyses that suggested an altered migration phenotype in naïve ADAPko NK cells, *in vitro* migration assays uncovered significantly reduced migration of both naïve as well as infection-primed ADAPko NK cells compared to wild type NK cells. Notably, this migration defect was associated with a significantly reduced expression of the integrin CD11a on the surface of splenic ADAP-deficient NK cells 1 day post-*Lm* infection. We propose that ADAP-dependent alterations in integrin expression might account at least in part for the fact that during *in vivo* infection significantly lower numbers of ADAPko NK cells accumulate in the spleen i.e., the site of infection. In conclusion, we show here that during systemic *Lm* infection in mice ADAP is essential for efficient cytotoxic capacity and migration of NK cells.

Keywords: ADAP, natural killer cells, cytotoxicity, *Listeria monocytogenes*, *in vivo* infection, migration, IL-10, CD11a

OPEN ACCESS

Edited by:
Navin Kumar Verma, Nanyang Technological University, Singapore

Reviewed by:
Arun K. Bhunia, Purdue University, United States
Laurel L. Lenz, School of Medicine, University of Colorado, United States

***Correspondence:**
Burkhart Schraven
burkhart.schraven@med.ovgu.de
Dunja Bruder
dunja.bruder@med.ovgu.de

† These authors have contributed equally to this study

‡ Present address:
Maxi Heyner, Omikron Systems GmbH, Braunschweig, Germany
Gerald P. Parzmair, Vakzine Projekt Management GmbH, Hannover, Germany

Specialty section:
This article was submitted to Molecular Innate Immunity, a section of the journal Frontiers in Immunology

Received: *25 July 2019*
Accepted: *27 December 2019*
Published: *22 January 2020*

Citation:
Böning MAL, Trittel S, Riese P, van Ham M, Heyner M, Voss M, Parzmair GP, Klawonn F, Jeron A, Guzman CA, Jänsch L, Schraven B, Reinhold A and Bruder D (2020) ADAP Promotes Degranulation and Migration of NK Cells Primed During in vivo Listeria monocytogenes Infection in Mice. Front. Immunol. 10:3144. doi: 10.3389/fimmu.2019.03144

INTRODUCTION

The coupling of transmembrane receptors to intracellular signaling pathways is mediated by adapter proteins that are made up of various protein domains without enzymatic or transcriptional activity. Adaptor proteins are central players involved in a number of cellular processes including cell proliferation, migration, and cell cycle regulation (1). The Adhesion and degranulation-promoting adapter protein ADAP, also known as Fyn-binding protein (Fyb) or SLAP-130 serves, amongst others, as a scaffold adapter protein specific for the hematopoietic lineage that so far has been mainly studied in the context of the activation of and effector functions in T cells (2). ADAP consists of several domains that can associate with proteins involved in cell migration, cellular adhesion and re-arrangement of the cytoskeleton in T cells (3). Moreover, ADAP plays an important role in T cell receptor- and chemokine receptor-mediated activation of integrins (inside-out signaling) and mediates signals derived from the interaction of integrins on T cells with ligands on target cells (outside-in signaling) (4, 5). ADAP-deficient T cells show reduced migration toward chemokines (6), impaired formation of the immunological synapse (4, 5) and impaired activation, differentiation and resident memory formation during acute infections (6, 7).

Next to its well-documented expression in T cells, ADAP is also expressed in other cells of the hematopoietic lineage including platelets, myeloid cells (8, 9) unconventional T cells, such as NKT, CD8α, and TCRγδ T cells (10) as well as in Natural Killer (NK) cells (11–13). NK cells are large granular lymphocytes which play a crucial role in the innate immune responses toward tumors and intracellular pathogens (14, 15). NK cells are able to identify malignant and infected cells and their activation occurs following integration of signals delivered by multiple activating and inhibitory receptors expressed on their surface (16, 17). In case the activating signals predominate, target cell death is induced by delivery of the cytolytic effector molecules perforin and granzymes (18). In addition to their inherent cytotoxic function, NK cells exhibit the capacity to produce effector cytokines and chemokines (19, 20), with IFN-γ being the principal NK cell cytokine produced early on during infections (21, 22). IFN-γ plays a central role for the activation of other immune cells needed for effective immunity to pathogens (23, 24). Thus, NK cells act as important immune regulators during infection and inflammation (25). In order to effectively fulfill their immunological functions, numerous cytokines, such as Interleukin (IL)-15, IL-18 (26, 27), IL-2, IL-4, IL-21 (27), and type I interferons (28) secreted by other immune cells are needed to prime NK cell activation, proliferation, and their differentiation into fully armed effector cells (29, 30).

NK cells develop from the same common lymphoid precursor as $CD8^+$ T cells (31) and both cell types share hallmark features like cytotoxicity and effector cytokine secretion. In light of their common ancestry, the fundamental role of ADAP in T cells and the usage of similar signaling pathways in T cells and NK cells, Fostel et al. proposed a similar requirement for ADAP in NK cell development and function. In direct contrast to their expectation, loss of ADAP in NK cells did neither affect NK cell development and function, nor cytotoxicity, IFN-γ production, anti-tumor response, and LFA-1-dependent conjugate formation with target cells (13). Several years later another study came to the opposite conclusion that NK cell activation would rely on ADAP. Here the authors demonstrated both impaired IFN-γ production and cytotoxicity of NK cells lacking ADAP (32). Only shortly later, Rajasekaran et al. uncovered a striking and ADAP-dependent uncoupling of cytokine secretion and cytotoxicity in NK cells (12). Using an experimental model system of CD137 and NKG2D induced *in vitro* stimulation of NK cells in combination with comprehensive analysis of the molecular signaling machinery utilized during NK cell activation the authors convincingly demonstrated that upon stimulation ADAP connects to the CBM signalosome consisting of the proteins Carma1, Bcl-10, and MALT1. This ADAP-CBM complex was essential for the production of cytokines and chemokines but not for cytotoxicity in murine and human NK cells (12). Taken together, available data regarding the role of ADAP in NK cells are conflicting ranging from a crucial role of ADAP in both pro-inflammatory cytokine production and cytotoxicity (32), an ADAP-dependent uncoupling of cytokine production and cytotoxicity with only cytokine production being dependent on ADAP (12) and the finding that ADAP in NK cells is fully dispensable for their function (13).

While the above mentioned studies utilized different experimental settings and NK cell stimulating ligands they all have in common that ADAP-dependency of principal NK cell functions was largely characterized either in primary or IL-2-activated NK cells following *in vitro* stimulation of selected NK cell activating receptors. To our knowledge no published data exist regarding the involvement of ADAP in NK cell functions *in vivo*. Given the fact that under physiological conditions NK cell activation is not induced by the stimulation of a single receptor but is the consequence of integration of signals derived by multiple activating and inhibitory receptors, NK cell activation *in vivo* is likely more complex than activation induced under *in vitro* conditions. Thus, we sought to extend existing knowledge regarding the role of ADAP in NK cell function to an *in vivo* setting. *Lm* is a facultative intracellular pathogen causing systemic infections that is frequently used as model pathogen. *In vivo* infection of mice with *Lm* is known to induce effective NK cell activation (33, 34) in a process involving a complex cellular network of macrophages, neutrophils, and dendritic cells as well as a plethora of soluble mediators derived from these cells (35, 36). Thus, *Lm* infection, that is well-established in our laboratory (6), represents a suitable tool to study the role of ADAP in NK cell priming, cytokine production and cytotoxicity during *in vivo* infection.

MATERIALS AND METHODS

Mice

ADAP wild type and knock out (ADAPko) mice have been described before (37) and were bred in the animal facility at the Helmholtz Center for Infection Research in Braunschweig (Germany) or in the animal facility of the Medical Faculty of the Otto-von-Guericke University Magdeburg (Germany).

Mice were kept under specific pathogen-free conditions in environmentally-controlled clean rooms and were used at 8–24 weeks of age. If not otherwise stated, experiments were performed using male mice and were approved by the local government agencies (Niedersächsisches Landesamt für Verbraucherschutz und Lebensmittelsicherheit and Landesamt für Verbraucherschutz, Sachsen-Anhalt). Mice containing the knockout first allele C57BL/6N-Fyb$^{tm1a(EUCOMM)Hmgu}$/Cnrm (38) were sourced from the EUCOMM project and were purchased from the European Mouse Mutant Archive EMMA. In this so called "knockout-first strategy" the ADAP allele is modified up- and downstream of its critical exon 2, the largest exon of ADAP. The lacZ and neomycin-resistance cassettes were both removed by breeding with transgenic mice expressing a Flp recombinase resulting in floxed alleles (containing *loxP* sites) and restoring the wild type (9). To generate conditional knockout mice with deletion of ADAP in the NK cell lineage, mice with floxed alleles were crossed with NKp46-iCre knock-in mice kindly provided by Prof. Eric Vivier (39). The presence or absence of the *FRT* sites, the *loxP* sites, the gene of interest, and the respective Cre transgene were checked routinely by PCR using genomic DNA isolated from ear tissue. To investigate specific effects of ADAP deletion and to exclude off-target effects of Cre recombinase, ADAP$^{wt/wt}$ × Cre^{het}, and ADAP$^{fl/fl}$ × Cre^{het} were always used as littermates. NK cell maturation in the bone marrow as well as distribution of mature NK cells in spleen and peripheral blood was similar in both genotypes (40).

Listeria Monocytogenes Infection

The *Listeria monocytogenes* (*Lm*) strain 10403S expressing ovalbumin was used for mouse infection experiments as described before (6, 41). Frozen stocks of *Lm* were thawed and subsequently diluted in brain heart infusion medium (BHI) followed by overnight growth on agar plates. One day before the infection, an overnight liquid culture (BHI) was prepared which was diluted with fresh medium (1:5) and cultivated at 37°C for 4 h before bacteria were harvested. Bacterial numbers were determined by measuring OD_{600} using a spectrophotometer and based on a previously established OD/cell-density correlation curve the suspension was further diluted in sterile PBS to the desired infection dose per mouse. Mice were infected by intravenous injection into the tail vein with the calculated dose of 2.5×10^4 bacteria suspended in 100 µl of PBS. To determine the actual infectious dose serial dilutions were plated on BHI agar followed by an overnight incubation of the plate at 37°C. The colonies were counted on the next day which, corrected for the dilution factor, showed the actual number of bacteria that had been applied to the mice. Body weight loss (infection dose: 5×10^4 bacteria) as an indicator for disease severity was measured daily over a period of 8 days. To determine colony forming units (CFU) in the organs of infected animals, mice were sacrificed at the indicated time points, spleens were collected and half of the spleens was homogenized in lysis buffer (PBS containing 0.2% IGEPAL CA-630). Ten microliters of 10-fold serial dilutions were plated on BHI agar plates. The bacterial count (CFU) was obtained by counting the colonies after incubation for 24 h at 37°C.

TABLE 1 | Primers used for qRT-PCR.

Gene symbol	Forward primer sequence (length)	Reverse primer sequence (length)	Annealing temp. (°C)
Ccl3	TGCCCTTGCTGT TCTTCTCT(20)	GTGGAATCTTCC GGCTGTAG(20)	60
Ccl4	CCCCTCTCTCTC CTCTTGCT(20)	GAGGGTCAGAGC CCATTG(18)	60
Ccl5	TGCAGAGGACTC TGAGACAGC(21)	GAGTGGTGTCCG AGCCATA(19)	60
Il-2	CAAGCAGGCCAC AGAATTGAAA(22)	GGCACTCAAATG TGTTGTCAGA(22)	58.4
Il-12b	GTAACCAGAAAG GTGCGTTCC(21)	GAACACATGCCC ACTTGCTG(20)	59.8; 59.4
Il-15	GGTCCTCCTGCA AGTCTCTC(20)	GGTGGATTCTTT CCTGACCTCTC(23)	61.4; 62.4
Il-18	GAAAGCCGCCTC AAACCTTC(20)	CCAGGTCTCCAT TTTCTTCAGG(22)	59.4; 60.3
Il-21	ATCTTCTTGGGG ACAGTGGC(20)	AGTGCCCCTTTA CATCTTGTGG(22)	59.4; 60.3
Rps9	CTGGACGAGGGC AAGATGAAGC(22)	TGACGTTGGCGG ATGAGCACA(21)	58.0

Quantitative RT-PCR

RNA was isolated from splenocytes using the RNeasy Mini Kit (Qiagen, Hilden, Germany) according to the manufacturer's instructions. RNA was eluted in 100 µl nuclease-free water. RNA content was determined with the NanoDrop ND-1000 spectrophotometer (Thermo Fisher Scientific, Massachusetts, USA). For cDNA synthesis ∼1 µg of RNA was transcribed using the Maxima First Strand cDNA Synthesis Kit for RT-qPCR according to the manufactures instructions (Thermo Fisher Scientific). cDNA was used as a template for real-time PCR using SYBR Green I (Roche). RPS9 was used as a housekeeping gene for normalization. Quantitative RT-PCRs were run in duplicates in the LightCycler 480 system II using the primers summarized in **Table 1**. mRNA sequences were derived from ncbi gene database and intron spanning real time PCR primers were designed accordingly using the web based assay design center (https://lifescience.roche.com/en_de/brands/universal-probe-library.html#assay-design-center) tool from Roche company. All primers were used in a final concentration of 500 nmol/l. The relative expression of the investigated target genes was calculated in relation to the housekeeping gene with the aid of the ΔΔCt method and the LightCycler480 software.

Serum Preparation and Cytokine Analyses

Mice were sacrificed and blood was obtained by puncture of the heart. Samples were incubated for 30 min at room temperature and for another 30 min at 4°C. After short centrifugation (14,000 rpm) the supernatant was collected and stored at −20°C. For the detection of IL-1α, IL-1β, IL-2, IL-4, IL-10, IL-12p40, IL-12p70, IL-15, IL-18, IL-21, IFN-γ, TNF-α and IFN-β in serum samples a flow cytometry based custom multiplex detection assay

(custom LegendPlex, mouse, BioLegend) was used according to the manufacturer's recommendations.

Proteome Analyzes

FACS-sorted NK cells ($NKp46^+$) were lysed in a buffer containing 1% SDS, 1× Complete protease inhibitor cocktail (Roche), 50 mM HEPES pH 8.5, 10 mM DTT for 5 min at 95°C, and rested for 5 min on ice. Benzonase was added and samples were incubated at 37°C for 30 min. After incubation, 5 mM tris(2-carboxyethyl)phosphine (TCEP) was added for 30 min, and 10 mM methyl methanethiosulfonate (MMTS) for 5 min, to reduce and protect cysteine residues, respectively. Protein purification, protein digestion and peptide purification was performed according to a slightly adapted Single-Pot Solid-Phase-enhanced Sample Preparation (SP3) protocol (42, 43). Sequencing grade trypsin (Promega, Fitchburg, WI, USA) was added at a ratio of 1:20 weight per weight in 50 mM HEPES pH 8. After < 14 h incubation at 37°C, samples were slightly acidified using formic acid (FA) shaken and incubated overnight at RT after raising the acetonitrile concentration to at least 95%. Beads containing the adsorbed peptides were washed once with pure acetonitrile and were dried by air. Peptides were eluted in a first step with 20 µl 2% DMSO for 30 min, and in a second step with 20 µl 0.065% FA, 500 mM KCl in 30% acetonitrile (ACN) for 30 min. Peptides were vacuum dried and dissolved in 0.2% trifluoroacetic acid/3% ACN for subsequent ultracentrifugation (50,000× g, 30 min, RT). LC-MS/MS analyses of purified and desalted peptides were performed on a Dionex UltiMate 3000 n-RSLC system connected to an Orbitrap Fusion™ Tribrid™ mass spectrometer (Thermo Scientific, Waltham, MA, USA). Peptides of each sample were loaded onto a C18 precolumn (3 µm RP18 beads, Acclaim, 0.075 × 20 mm), washed for 3 min at a flow rate of 6 µl/min and separated on a C18 analytical column (3 mm, Acclaim PepMap RSLC, 0.075 mm × 50 cm, Dionex, Sunnyvale, CA, USA) at a flow rate of 200 nl/min via a linear 120 min gradient from 97% MS buffer A (0.1% FA) to 25% MS buffer B (0.1% FA, 80% ACN), followed by a 30 min gradient from 25% MS buffer B to 62% MS buffer B. The LC system was operated with the Chromeleon software (version 6.8, Dionex) embedded in the Xcalibur software suite (version 3.0.63, Thermo Scientific). The effluent was electro-sprayed by a stainless steel emitter (Thermo Scientific). Using the Xcalibur software, the mass spectrometer was controlled and operated in the "top speed" mode, allowing the automatic selection of as many doubly and triply charged peptides in a 3 s time window as possible, and the subsequent fragmentation of these peptides. Peptide fragmentation was carried out using the higher energy collisional dissociation mode and peptides were measured in the ion trap (HCD/IT). MS/MS raw data files were processed via the Proteome Discoverer program (version 2.3, Thermo Scientific) using Mascot (version 2.4.1, Matrix Science) as search machine and fasta files from the Swiss-Prot/UniProt database from January 2018. Used Mascot search parameters were: maximum missed cleavage site: 1, precursor mass tolerance: 10 ppm, fragment mass tolerance: 0.05 Da. Oxidation of methionine was set as a variable modification and modification of cysteine by MMTS was set as fixed modification. Filters used in Proteome Discoverer were peptide confidence: high, search engine rank: 1, and false discovery rate: 1%. The entire mass spectrometry proteomics data have been deposited to the ProteomeXchange Consortium via the PRIDE partner repository with the data set identifier PXD016305.

Microscopy

FACS sorted NK cells were seeded onto poly-L-lysine (Sigma) coated coverslips and allowed to adhere for 30 min. Cells were fixed by using 4% paraformaldehyde (Sigma) in PBS for 20 min followed by washing with PBS. Cells were permeabilized using 0.15% Triton-X100 (Sigma) in PBS for 5 min followed by blocking using 1% BSA (Sigma) in PBS containing 0.05% Tween-20 (Roth) for 1 h. Antibodies (anti-α-tubulin: ab52866/Abcam; FITC-labeled anti-CD107a: clone 1D4B/BioLegend; Alexa594-labeled anti-rabbit: A11037/Invitrogen) were applied in blocking solution and staining was performed for 2 h at RT. Cells were washed three times with PBS containing 0.05% Tween-20 followed by dehydration using first 70% and then 100% ethanol. Samples were dried by air and mounted using Mowiol (Roth). Light microscopy was carried out on an inverted microscope (ECLIPSE Ti-E; Nikon) with standard epifluorescence illumination (Intensilight C-HGFIE; Nikon) and 100×/NA1.4 plan-apochromatic objective. Images were acquired with a back-illuminated, cooled charge-coupled-device camera (DS2-Qi2; Nikon) driven by NIS-Elements (Nikon). Data acquisition was performed in NIS-Elements.

Flow Cytometry Analyzes

Spleens were flushed by heart perfusion with 10 ml PBS. Afterwards the spleens were meshed trough a cell strainer (100 µm) with a syringe plunger and splenocytes were pelleted by centrifugation (1,200 rpm, 10 min, 4°C). Erythrocyte lysis was performed with different concentration of sodium chloride (PBS containing 0.2 or 1.6% NaCl, respectively) and stopped with PBS. After centrifugation (see above) splenocytes were filtered through a cell strainer (30 µm), centrifuged and the single cell suspension was collected in IMDM-complete medium containing 10% FCS, 1% Penicillin/Streptavidin, 0.1% Gentamycin, and 0.1% 2-Mercaptoethanol. For flow cytometric analysis single cell suspensions were treated with anti-CD16/32 (BioLegend) to reduce unspecific antibody binding. For live/dead discrimination the Fixable Viability Dye (eFlour780, eBioscience) was used followed by staining with the following antibodies: anti-CD3ε (FITC, 145-2C11), anti-CD8a (FITC, 53-6.7), anti-Ly6C (PerCP-Cy5.5, HK1.4), anti-Ly6G (BV510, 1A8), anti-NK1.1 (PE-Cy7, PK136), anti-CD11b (BV421, M1/70), anti-CD49b (APC, DX5) (all Biolegend) as well as anti-CD27 (PE, LG.3A10, eBioscience). Afterwards, cells were fixed with 2% paraformaldehyde and analyzed with a BD FACSCanto II (BD Biosciences). Flow cytometric data were analyzed using the BD FACS Diva v6.1.3 software.

Integrin Expression on NK Cells

Spleens were harvested from *Lm* infected or naïve $ADAP^{wt/wt}$ × $NKp46\text{-}Cre^{het}$ and conditional $ADAP^{fl/fl}$ × $NKp46\text{-}Cre^{het}$ mice and processed into single cell suspension. For flow cytometric analysis single cell suspensions were treated with anti-CD16/32 (BioLegend). Cell suspensions were furthermore surface stained

with a lineage mix (anti-CD3e, 145-2C11; anti-CD4, GK1.5; anti-CD8, 53-6.7; anti-CD19, 6D5; and anti-TER-119, TER-119; all FITC from BioLegend, except anti-TER-119 which was from Thermo Fisher). Furthermore, the following antibodies were used: anti-NK1.1 (APC-Cy7, PK136), anti-CD122 (PE-Cy7, TM-ß1), anti-CD11b (BV510, M1/70), anti-CD18 (AF647, M18/2), anti-CXCR4 (APC, L276F12), anti-CD29 (PE, HMß1-1) all from BioLegend as well as anti-NKp46 (V450, 29A1.4, BD Biosciences), and anti-CD11a (PE, 2D7, BD Pharmingen). Afterwards, cells were analyzed with a BD LSR Fortessa (BD Biosciences). Flow cytometric data were analyzed using the BD FACS Diva v6.1.3 software.

IL-10 Expression on NK Cells

Livers were harvested from *Lm* infected or naïve $ADAP^{wt/wt}$ × $NKp46\text{-}Cre^{het}$ and conditional $ADAP^{fl/fl}$ × $NKp46\text{-}Cre^{het}$ mice and cells were isolated using the mouse liver dissociation Kit (Miltenyi Biotech) and the gentleMACS dissociator device (Miltenyi Biotech) according to the manufactures instructions and processed into single cell suspension. Afterwards, each cell suspension was stimulated for 4 h at 37°C with phorbol myristate acetate (20 ng/ml, Sigma-Aldrich) and ionomycin (1 μg/ml, Sigma-Aldrich) in medium (IMDM-complete). After 1 h brefeldin A (1,000×, BioLegend) and Monensin (1,000×, BioLegend) were added. For flow cytometric analysis single cell suspensions were treated with anti-CD16/32 (BioLegend) after 4 h of stimulation. For live/dead discrimination the Fixable Viability Dye (eFlour780, eBioscience) was used followed by staining with the following antibodies: anti-B220 (FITC, RA3-6B2, BioLegend), anti-CD4 (FITC, RM4-5, BioLegend), anti-CD8 (FITC, 53-6.7, BioLegend), anti-CD3 (BV510, 17A2, BioLegend), anti-NK1.1 (PE, PK136, BD Pharmingen), anti-NKp46 (eFlour660, 29A1.4, Invitrogen). Cells were fixed with the Fixation/Permeabilization Kit (Thermo Fisher Scientific, Massachusetts, USA) and followed by intracellular staining for anti-IL-10 (BV421, JES5-16E3, BioLegend) for 30 min at 4°C. Cells were than analyzed using an Attune NxT Flow Cytometer (Thermo Fisher Scientific).

NK Cell Isolation

Spleens were harvested from *Lm* infected or naïve mice and processed into single cell suspension without erythrocyte lyses. Untouched NK cells were isolated using the mouse NK cell Isolation Kit (Miltenyi Biotech) and the autoMACS device (Miltenyi Biotech) according to the manufactures instructions or were sorted using a BD FACSAria (BD Biosciences) cell sorter. The purity of autoMACS isolated NK cells was >86 and >88% after FACSAria cell sorting. For untouched cell sorting, NK cells were stained for live/dead discrimination with Fixable Viability Dye (eFlour780, eBioscience) followed by staining with the following antibodies: anti-CD3ε (FITC, 145-2C11), anti-Ly6G (BV510, A18), anti-CD11b (BV421, M1/70), anti-NK1.1 (Biotin, PK136), anti-CD49b (APC, DX5) (all BioLegend), and anti-CD27 (PE, LG.3A10, eBioscience) or with anti-CD3ε (APC, 145-2C11, BioLegend), anti-CD8a (PerCP-Cy5.5, 53-6.7, BioLegend), anti-CD4 (BV510, RM4-5, BioLegend), and anti-NK1.1 (PE, PK136, BD Bioscience). Biotinylated antibodies were counterstained with streptavidin (PE-Cy7, BioLegend).

In vitro NK Cell Stimulation

Ninety-six-well U-bottom plates were coated overnight with anti-NK1.1 (1 μg/ml, Biotin, PK139, BioLegend) diluted in phosphate-buffered saline (PBS) at 4°C. Isolated NK cells (untouched) were added after removal of excessive anti-NK1.1 antibody. If indicated either IL-2 (3,000 Units/ml, BioLegend) and IL-12 (1 ng/ml, BioLegend) or phorbol myristate acetate (20 ng/ml, Sigma-Aldrich) and ionomycin (1 μg/ml, Sigma-Aldrich) were added to the wells and NK cells were stimulated for 4 h at 37°C. Controls were cultured in medium (IMDM-complete) without further stimulation. After 2 h brefeldin A (5 μg/ml, BioLegend) was added to all wells including the control wells. After 4 h *in vitro* stimulation NK cells were treated for live/dead discrimination with Fixable Viability Dye (eFlour780, eBioscience) and anti-CD16/32 (BioLegend) followed by staining with the following antibodies: anti-CD3ε (FITC, 145-2C11, BioLegend), anti-CD107a (Biotin, 1D4B, BioLegend), anti-CD49b (APC, DX5, BioLegend), anti-CD11b (PerCP-Cy5.5, M1/70, BioLegend). Cells were fixed with the Fixation/Permeabilization Kit (Thermo Fisher Scientific, Massachusetts, USA) followed by intracellular staining for anti-IFN-γ (BV421, XMG1.2, BioLegend) according to the manufacturer's instructions. Cells were than analyzed using an Attune NxT Flow Cytometer (Thermo Fisher Scientific). Biotinylated antibodies were counterstained with streptavidin (PE-Cy7, BioLegend).

In vitro NK Cell Migration Assay

For *in vitro* migration assay a transwell system (Costar; Corning, USA) was used. Here, the NK cell attracting chemokine CXCL12 (250 ng/ml, R&D Systems) was added to the lower chamber in a total volume of 600 μl chemotaxis medium (RPMI containing 25 mM HEPES and 0.5% BSA). Total splenocytes obtained from untreated and *Lm* infected mice, respectively, were loaded to the upper chamber at a density of 5×10^5 cells in 100 μl chemotaxis medium. Cells were allowed to migrate across the pores of the transwell inserts (pore size 5 μm) at 37°C and 5% CO_2. After 4 h, transmigrated cells from a pool of three wells were harvested by centrifugation (5 min, 300 ×g), resuspended in 100 μl PBS containing 2 mM EDTA, stained with trypan blue and counted using a hemocytometer. The percentage of NK cells before and after transmigration was analyzed by flow cytometry. Briefly, cells were first incubated with anti-CD16/CD32 (2.4G2, BD Pharmingen) for 10 min on ice followed by incubation with anti-CD3ε (FITC, 145-2C11, BD Pharmingen), anti-NK1.1 (APC-Cy7, PK136, BioLegend), anti-NKp46 (BV450, 29A1.4, BD Bioscience) for 30 min on ice. After washing, analysis was performed on a BD LSRFortessa (BD Biosciences) flow cytometer. Data are expressed as percentage of input calculated by the following equation: migrated NK cell number/input NK cell number.

Degranulation Assay

For the functional assessment of NK cells splenocytes were co-incubated with YAC-1 target cells at an effector:target ratio of 10:1 for a total incubation time of 6 h at 37°C and 5% CO_2 in medium containing anti-CD107a antibody (BV421, 1D4B, BioLegend). After 1 h of the incubation, the co-culture was supplemented with

5 μg/ml monensin and brefeldin A (Sigma-Aldrich) to prevent receptor internalization and cytokine secretion, respectively. Subsequently, the cells were stained for the identification of NK cells ($CD3^{-}NK1.1^{+}$), perforin, granzyme B (GrB), and IFN-γ using the following antibodies: anti-CD3ε (BUV395, 17A2, BD Biosciences), anti-NK1.1 (APC, PK136, eBioscience), anti-perforin (PE, S16009B, BioLegend), anti-GrB (FITC, NGZB, eBioscience), and anti-IFN-γ (BV785, XMG1.2, BioLegend). For intracellular staining of perforin, GrB and IFN-γ, cells were permeabilized and fixed using the Cytofix/Cytoperm kit from BD according to the manufacturer's protocol. Briefly, cells were incubated in fixation buffer and subsequently stained with the antibodies diluted in permeabilization buffer.

Statistics

All statistical analyses were performed using the GraphPad Prism Software v5 and v8 (GraphPad Software, Inc., La Jolla, USA) and $p < 0.05$ was considered as significant.

RESULTS

Cytotoxic Capacity of NK Cells Primed During *In vivo Listeria monocytogenes* Infection Requires ADAP

To first confirm the role of ADAP in cytokine production by naïve NK cells, they were isolated from the spleen of naïve wild type and conventional ADAPko mice and were stimulated *in vitro* with anti-NK1.1 alone or in combination with IL-2/IL-12 or with PMA/ionomycin followed by flow cytometric analysis of IFN-γ production. As shown in **Figure 1A**, secretion of the effector cytokine IFN-γ by NK cells from ADAPko mice was significantly impaired compared to NK cells from ADAP sufficient mice. Importantly, wild type mice did not only exhibit higher frequencies of IFN-γ^{+} NK cells (% IFN-γ^{+} NK cells, **Figure 1A**, middle panel), but NK cells from wild type mice as well produced higher levels of IFN-γ (MFI IFN-γ NK cells, **Figure 1A**, right panel). We next analyzed whether, in addition to effector cytokine production, ADAP deficiency would also affect the cytotoxic capacity of naïve NK cells. To this end, splenic NK cells from naïve wild type and ADAPko mice were stimulated *in vitro* as described before followed by the quantification of surface expression of CD107a on NK cells as an indicator for preceeding NK cell degranulation (44). While under these experimental conditions ADAP deficiency significantly impaired IFN-γ production, it did not affect the degranulation capacity of naïve NK cells (**Figure 1B**) which is well in line with published data (12). We next extended our analyses to an experimental setting allowing NK cell priming within their natural environment, i.e., during *in vivo* infection, and to a more physiological NK cell *in vitro* stimulation set-up using YAC-1 target cells. To this end, wild type and conventional ADAPko mice were sublethally infected with *Lm*. Subsequently, NK cells were isolated from the spleen of wild type and conventional ADAPko mice on day 3 post *Lm* infection, together with NK cells from uninfected mice (day 0) serving as internal control. In contrast to our data obtained with antibody/cytokine stimulation, YAC-1-mediated stimulation of naïve NK cells uncovered a striking and ADAP-dependent degranulation defect as indicated by significantly reduced CD107a expression on ADAPko compared to wild type NK cells (**Figures 2A**,**B**). This phenotype became evident not only in YAC-1 stimulated naïve NK cells but was detectable as well in NK cells that were primed during *in vivo Lm* infection. While *in vitro* re-stimulation of NK cells from infected wild type animals with YAC-1 target cells stimulated a highly significant degranulation of these cells, YAC-1 cells did not induce further degranulation of *in vivo* primed ADAPko NK cells (**Figures 2A**,**B**). Consistent with their increased degranulation capacity *Lm* infection triggered NK cells to produce elevated levels of perforin and strikingly, this acquisition of NK cell effector function was significantly impaired in mice lacking ADAP as indicated by the reduced frequency of perforin^{high} ADAPko NK cells (**Figures 2A**,**C**). As for CD107a and perforin, there was a clear increase in the frequency of granzyme B (GrB) and IFN-γ producing NK cells on day 3 post-infection compared to uninfected controls, indicative for efficient *in vivo* priming, but no genotype-dependent differences were observed (**Figures 2D**,**E**).

To rule out the possibility that the striking differences observed for NK cell degranulation and perforin production was the consequence of inefficient NK cell priming in the ADAP-deficient host rather than an intrinsic effect of ADAP-deficiency in NK cells we compared serum concentrations of cytokines that have been described in the context of NK cell activation (26, 27, 45, 46). Serum cytokine levels on day 1 post-*Lm* infection were, with the exception of IL-1α, largely comparable in wild type and ADAPko mice. Interestingly, for several analytes known to be important for the stimulation of cytotoxicity in NK cells we even observed elevated serum concentrations in ADAPko mice on day 3 post-infection (**Supplementary Figure 1A**). Additionally performed quantitative gene expression analysis for the major NK cell activating cytokines IL-2, IL-12, IL-15, IL-18, and IL-21 in splenocytes from *Lm* infected mice revealed equal expression levels of these NK cell activating cytokines (**Supplementary Figure 1B**). Taken together, we show here that *Lm* infection in ADAP-deficient hosts induces a cytokine response largely comparable or even slightly stronger than in wild type animals and we thus conclude that the cytotoxic capacity of NK cells primed during *in vivo Lm* infection is intrinsically dependent on ADAP.

ADAP-Deficiency Does Not Affect NK Cell Morphology, Intracellular Vesicle Distribution and the Overall Pattern of Protein Abundances in NK Cells During *Listeria monocytogenes* Infection

While we observed a clear impact of ADAP-deficiency on NK cell degranulation this effect became apparent only after YAC-1-mediated but not after antibody- and cytokine-mediated *in vitro* stimulation of NK cells (**Figures 1**, **2**). Since ADAP deficiency in T cells prevents microtubule-organizing center (MTOC) translocation upon activation (47), we wondered whether ADAP-deficiency *per se* would affect NK cell morphology, microtubule network structures and

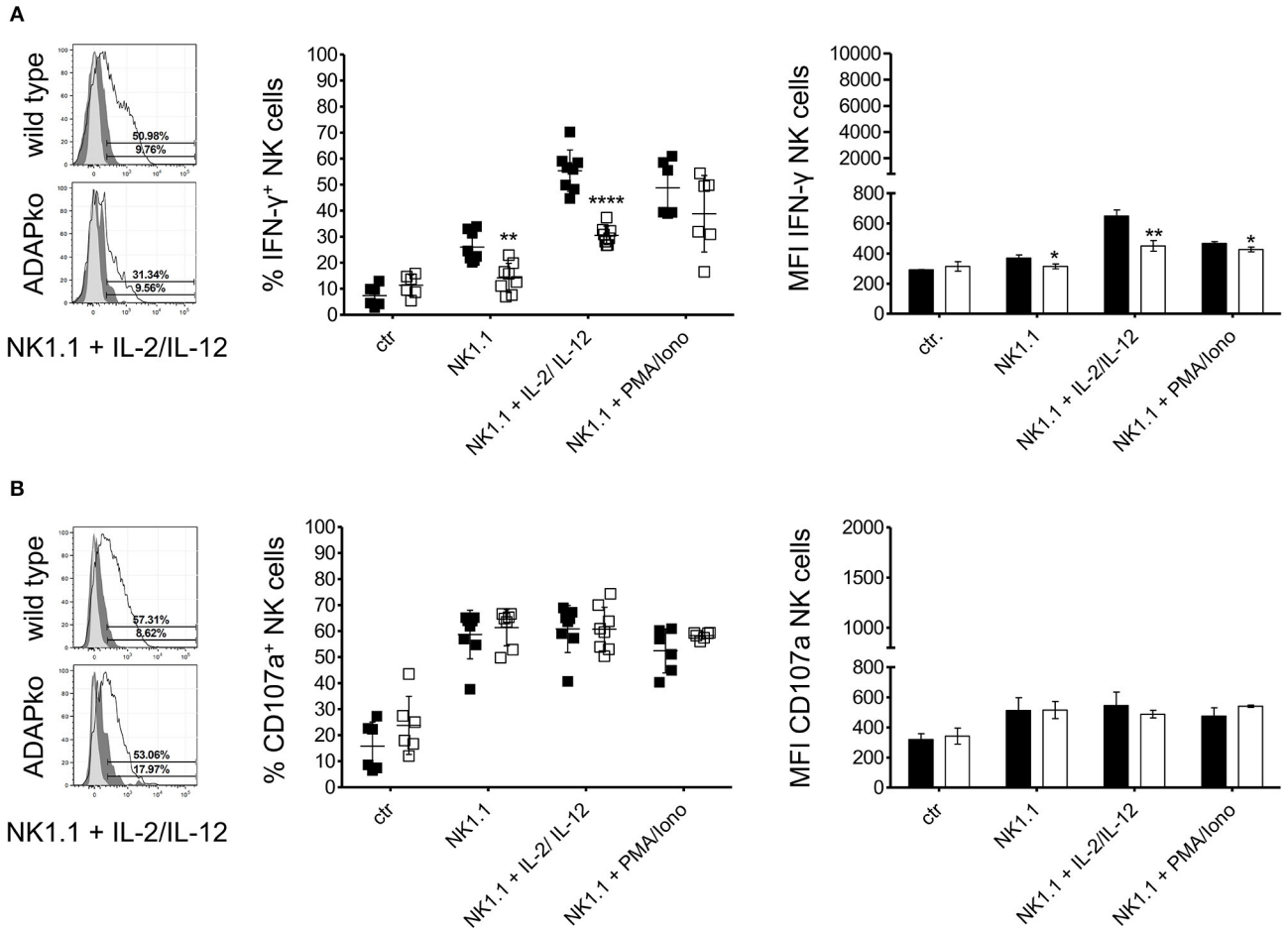

FIGURE 1 | IFN-γ production in naïve NK cells depends on ADAP. Naïve NK cells from the spleen of wild type (black symbols) and ADAPko (open symbols) mice were either stimulated *in vitro* with anti-NK1.1 (plate bound) alone or in combination with IL-2/IL-12 or PMA/ionomycin for 4 h or were left unstimulated (ctr). Subsequently, frequency of **(A)** IFN-γ producing NK cells and **(B)** frequency of NK cells exhibiting CD107a surface expression as indicator for degranulation was analyzed by flow cytometry. Representative histograms (left panels) are shown for re-stimulation with anti-NK1.1 in combination with IL-2 and IL-12 (light gray: unstained and untreated; dark gray: stained and untreated; open: stained and treated). Mean ± SD of IFN-γ^+ and CD107a$^+$ CD3$^-$CD49$^+$ NK cells (middle panels) and mean fluorescence intensity (MFI, right panels) of IFN-γ in and CD107a on NK cells is shown with $n = 6$–8 individually analyzed mice per group out of three independent experiments. Groups were compared by unpaired two-tailed *t*-test with Welch's correction (*$p < 0.05$, **$p < 0.01$, ****$p < 0.0001$).

distribution of vesicles, and whether such effect would become visible early on during *in vivo* infection. To analyze this, NK1.1$^+$ NK cells were sorted from the spleen of *Lm* infected mice (4 mice for each genotype) 1 day post-infection and analyzed by microscopy without any further *in vitro* stimulation. As shown in **Figure 3A**, independent of the genotype NK cells exhibited a well-structured microtubule network with single microtubules originating from the MTOC (visualized with a white arrow in **Figure 3A**). Interestingly, counterstaining for CD107a identified CD107a$^+$ vesicles (in green) distributed in the periphery of the MTOC, and again we did not observe differences in NK cells isolated from infected wild type or ADAPko mice (**Figure 3A**). Quantification of polarized CD107a distribution toward the MTOC in NK cells from *Lm* infected mice revealed indeed no differences. For both wild type and ADAPko mice, ∼65 to ∼90% of the NK cells showed MTOC-oriented CD107a distribution (**Figure 3B**). Similarly, NK cells isolated from naïve wild type and ADAPko mice showed no differences in CD107a distribution (data not shown). Thus, *ex vivo* analysis of NK cells at an early phase of *Lm* infection did not uncover obvious ADAP-dependent differences regarding cellular morphology and CD107a localization in vesicle-like structures. In line with this, phalloidin staining of cytoskeletal F-actin in naïve NK cells stimulated *in vitro* with CXCL12 did not reveal any significant difference in terms of actin re-organization between the genotypes as well (data not shown).

We further extended our molecular phenotyping and applied unbiased high-resolution mass spectrometry in order to identify potential ADAP-dependent alterations of NK cell proteomes in infected and non-infected mice. As for confocal microscopy, splenic NK cells from wild type and ADAPko mice were

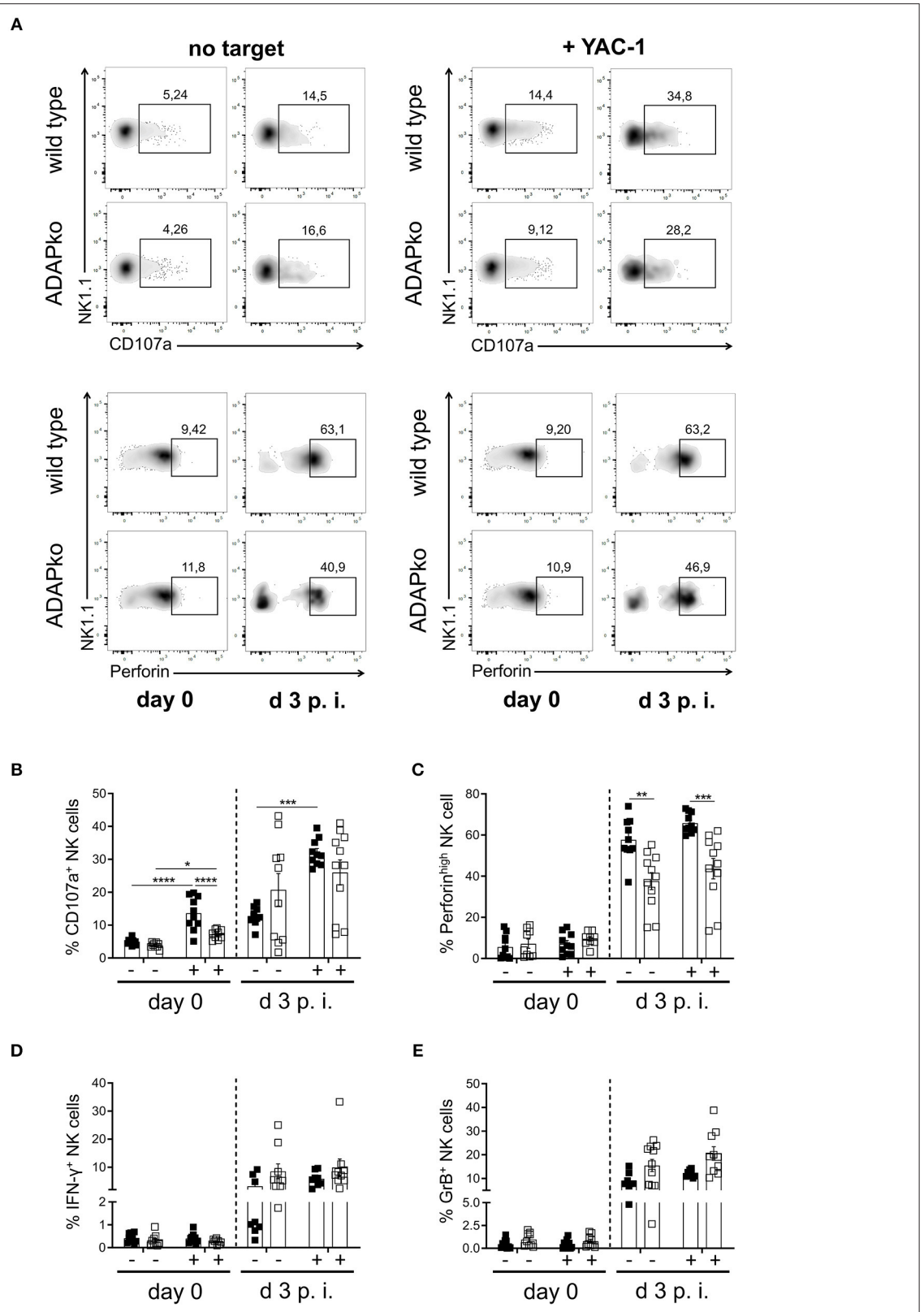

FIGURE 2 | Degranulation capacity and perforin production by NK cells during *Lm* infection depend on ADAP. Wild type (black symbols) and ADAPko (open symbols) mice were either infected with 2.5×10^4 CFU *Lm* or were left untreated (uninfected control, day 0) and were sacrificed at the indicated time points post infection.

(Continued)

FIGURE 2 | Splenocytes were isolated and incubated *in vitro* without targets (-) or with YAC-1 target cells (+). **(A)** Representative dot plots showing surface CD107a or intracellular perforin vs. NK1.1 expression on wild type and ADAPko splenocytes from naïve mice (day 0) as well as on day 3 post-*Lm* infection in the presence or absence of YAC-1 target cells. Frequency of **(B)** surface CD107a^{+}, **(C)** perforin^{high}, **(D)** IFN-γ^{+}, and **(E)** granzyme B (GrB)$^{+}$ CD3^{-}NK1.1^{+} NK cells in spleen of uninfected mice (day 0) and day 3 post-*Lm* infection after *in vitro* co-incubation with YAC-1 target cells. Data are presented as mean ± SEM of $n = 10$ individual mice per group out of two independent experiments. Groups were compared by two-way ANOVA with Bonferroni correction for multiple hypothesis testing (*$p < 0.05$, **$p < 0.01$, ***$p < 0.001$, ****$p < 0.0001$).

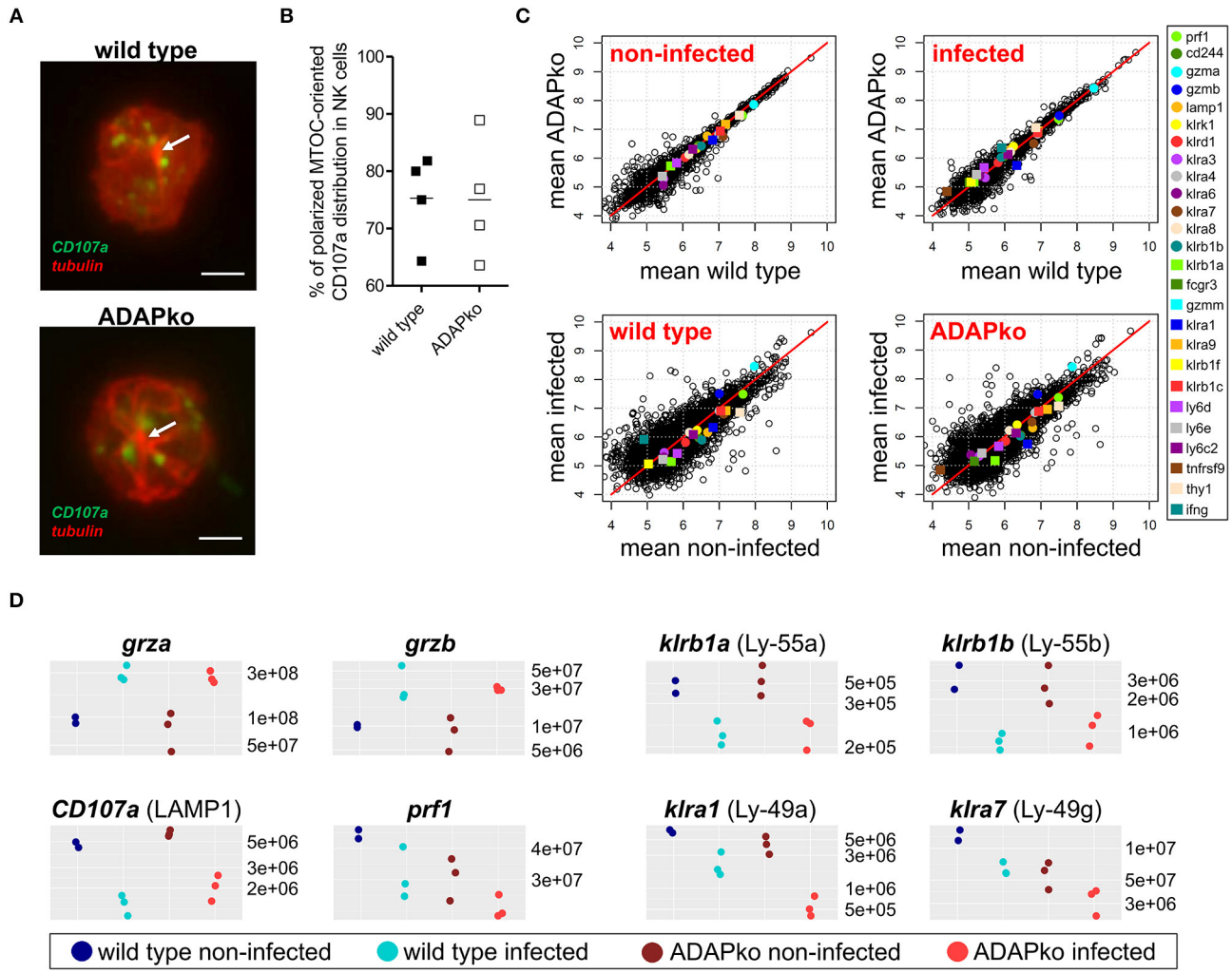

FIGURE 3 | CD107a distribution and global NK cell protein composition are similar in wild type and ADAPko NK cells. Wild type and ADAPko mice were either infected with 2.5 × 10^{4} CFU *Lm* or were left untreated (non-infected control, day 0). Mice were sacrificed and NK1.1^{+} NK cells were isolated by flow cytometry and prepared for microscopy or mass spectrometry. **(A)** NK cells were seeded onto poly-L-lysine coated coverslips and stained for CD107a (green) and α-tubulin (red). Representative images of NK cells from *Lm* infected mice are given as stacked images. Scale bars are 2 μm. **(B)** Quantification of CD107a distribution toward the MTOC in NK cells from *Lm* infected mice ($n = 4$; up to 25 cells per animal were analyzed). **(C,D)** NK cells were lysed and analyzed by high-resolution mass spectrometry after tryptic digestion. **(C)** Scatter plots depicting mean log10 abundances ($n = 3$; for wild type day 0: $n = 2$) of all detected proteins (circles and squares) and selected NK cell proteins are marked in colors (color code given on the right panel). **(D)** Dot plots depicting absolute abundances of selected NK cell proteins for each individual mouse in all four conditions.

isolated on day 1 post *Lm* infection and analyzed without further stimulation in comparison with corresponding NK cells from naïve wild type and ADAPko mice using a label-free quantitative proteomics approach (LC-MS). We analyzed NK cells of six individual ADAPko and five individual wild type mice and quantified relative abundance of in total 4,131 proteins. In the individual samples, we identified 3,365–3,705 proteins with a normal distribution in protein abundances indicating the robustness of our analytical workflow (**Supplementary Figure 2A**). As expected, mass spectrometry

identified ADAP exclusively in NK cells derived from wild type but not ADAPko mice (data not shown) underlining the accuracy of our analysis. Moreover, as a proof-of-concept, SKAP1, a protein that is co-regulated with ADAP expression (48), was undetectable in NK cells from infected ADAPko mice.

Computational cluster analysis of total NK cell proteomes clearly discriminated NK cells from infected and non-infected mice, but did not differentiate between NK cells from wild type and ADAPko mice (**Supplementary Figure 2B**). Likewise, comparison of protein intensities exhibited higher variation in NK cells from infected vs. non-infected mice (**Figure 3C**), underscoring that the infection-related *in vivo* priming of NK cells, but not the presence or absence of ADAP is decisive for the global changes observed in the proteome composition of NK cells. This held true for a number of prototypic NK cell proteins that were generally detectable at similar abundance in NK cells from non-infected wild type and ADAPko mice (**Figure 3D**). Among those the abundance of granzyme A and granzyme B increased upon *Lm* infection, while other proteins related to NK cell functions including CD107a, perforin and the Killer cell lectin-like receptor (KLR) subfamily members Ly-49a, Ly-49g, Ly-55a, and Ly-55b were detected with reduced abundance in NK cells from the infected host independent of the genotype (**Figure 3D**). In conclusion, unbiased *ex vivo* proteome profiling of splenic naïve NK cells and NK cells analyzed on day 1 post infection clearly revealed *in vivo* responsiveness of NK cells to *Lm* infection but did not uncover any obvious ADAP-dependent alterations in the effector molecule inventory involved in this process.

NK Cell Migration, but Not *Listeria monocytogenes*-Induced IL-10 Production, Is Dependent on ADAP

We finally asked if and how ADAP-deficiency in NK cells would affect the overall course of *Lm* infection. To rule out any effect of ADAP-deficiency in immune cells other than NK cells we used conditional knock out mice lacking ADAP specifically in NK cells ($ADAP^{fl/fl} \times NKp46\text{-}Cre^{het}$). Strikingly, health monitoring during infection revealed enhanced severity of the disease as indicated by a significantly higher body weight loss in conditional ADAPko mice compared to control animals (**Figure 4A**). This was, however, not due to impaired antibacterial immunity since both genotypes controlled pathogen growth equally well (**Figure 4B**). Since IL-10 produced by NK cells has been recently shown to enhance susceptibility of mice to Listeria infection (34) we analyzed whether ADAP-deficiency would affect the capacity of NK cells to produce IL-10. While NK cells from uninfected mice did not produce relevant concentration of IL-10, IL-10 production was induced in NK cells by day 3 following *Lm* infection (**Figure 4C**). This was however genotype independent, thus largely excluding the possibility that enhanced morbidity of conditional ADAPko mice is due to enhanced IL-10 production by ADAP-deficient NK cells.

Interestingly, lack of ADAP in NK cells was associated with considerably lower NK cell numbers in the spleen of conditional ADAPko compared to wild type mice. Notably, this was evident already in naïve mice (**Figure 5A**). While in wild type animals the number of NK cells steadily increased until day 5 post-*Lm* infection, the number of ADAPko NK cells in the spleen rose to a far lesser extend and reached the plateau already by day 2 post-*Lm* infection (**Figure 5A**). Flow cytometric analysis of NK cell maturation markers revealed only slight though in part significant differences in the maturation of ADAP-sufficient and -deficient NK cells in the spleen of *Lm* infected mice during the course of infection. However, the frequency of NK cells that reached the different maturation stages ($CD27^{-}CD11b^{-}$ (DN) $\rightarrow$ $CD27^{+}CD11b^{-}$ $\rightarrow$ $CD27^{+}CD11b^{+}$ (DP) $\rightarrow$ $CD11b^{+}CD27^{-}$) was the same by day 5 post-infection (**Supplementary Figure 3**) and as such impaired NK cell maturation was largely excluded as a reason for the pronounced ADAP-dependent differences in NK cell abundance in the spleen of *Lm* infected mice.

Since ADAP has been shown before to be involved in the migratory capacity of other immune cells (37, 49) and moreover protein network analyses of our proteome analyses identified three pathways potentially affected by ADAP-deficiency in NK cells to be related to cell migration (data not shown), we speculated that the observed phenotype might at least in part be the consequence of impaired migration of ADAPko NK cells to the spleen of *Lm* infected mice. To experimentally address this hypothesis we performed *in vitro* NK cell migration assays using splenocytes from naïve and *Lm* infected mice. Indeed and well in line with our expectation, NK cell migration toward a chemokine gradient was significantly impaired both in naïve as well as in ADAP-deficient NK cells pre-activated *in vivo* during *Lm* infection (**Figure 5B**). Of note, reduced *in vitro* migration of ADAPko NK cells toward the NK cell attracting chemokine CXCL12 was not the consequence of altered surface expression of the CXCL12 receptor CXCR4 as we observed similar CXCR4 expression levels on ADAP-deficient and –sufficient NK cells (**Figure 5C**). Since leukocyte entry into tissues is generally guided by the interaction of integrins with their respective ligands on endothelial cells we analyzed surface expression of selected integrins on splenic NK cells from *Lm* infected wild type and conditional ADAPko mice. While ADAP-deficiency did not affect expression levels of CD18, CD29, and CD11b on NK cells (data not shown), we observed a striking difference between ADAP-deficient and wild type NK cells with respect to CD11a surface expression on day 1 post *Lm* infection with significantly lower CD11a expression levels on NK cells lacking ADAP (**Figure 5D**). Together our data suggest that in addition to effector cytokine production and cytotoxic capacity ADAP is required for efficient migration of NK cells both *in vitro* and *in vivo* and that reduced NK cell cellularity in infected tissue of conditional ADAPko mice might be, at least in part, the consequence of reduced CD11a surface expression on ADAP-deficient NK cells.

DISCUSSION

We have studied for the first time ADAP-dependency of NK cell functions during *in vivo* infection. Our experimental approach is fundamentally different from previous studies as we studied

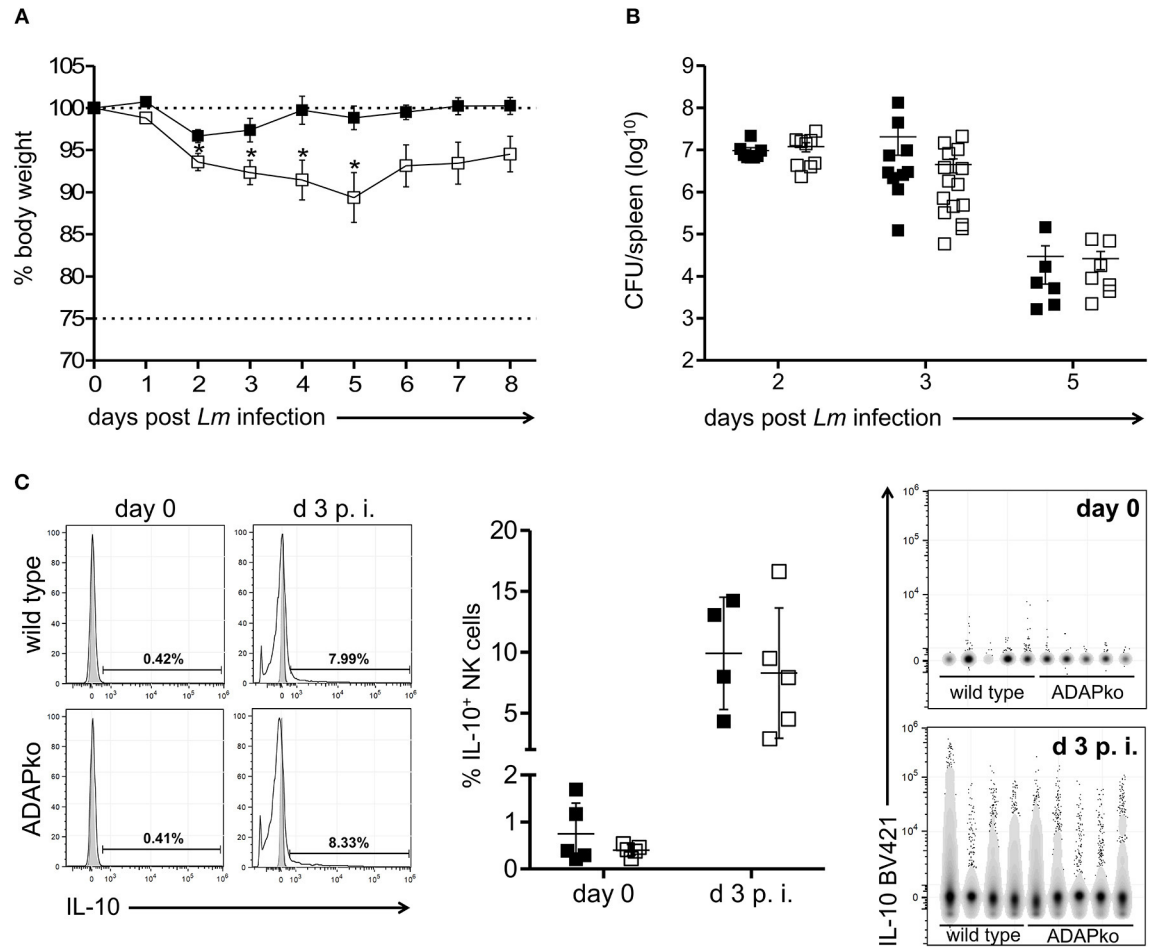

FIGURE 4 | Enhanced susceptibility of conditional ADAPko mice to *Listeria monocytogenes* infection is not associated with altered IL-10 production by NK cells. $ADAP^{fl/fl}$ × $NKp46\text{-}Cre^{het}$ (open symbols) mice lacking ADAP specifically in NK cells and respective littermate controls ($ADAP^{wt/wt}$ × $NKp46\text{-}Cre^{het}$, black symbols) were either infected with **(A)** 5×10^4 CFU *Lm*, **(B,C)** 2.5×10^4 CFU *Lm* or were left untreated (uninfected control, day 0). **(A)** Body weight loss of $ADAP^{wt/wt}$ × $NKp46\text{-}Cre^{het}$ control mice and conditional $ADAP^{fl/fl}$ × $NKp46\text{-}Cre^{het}$ mice during the course of *Lm* infection**. (B)** CFU was quantified in the spleen as a measure for the bacterial load. Data are presented as mean ± SEM for $n = 6$–15 individually analyzed mice per group out of three independent experiments. **(C)** Representative histograms (left panels) are shown for hepatic $CD3^-NK1.1^+NKp46^+$ IL-10 producing NK cells (light gray: unstained and untreated; dark gray: respective stained fluorescence minus one control; open: stained liver sample) for naïve NK cells (day 0, female mice) and day 3 post-*Lm* infection. Summary plots (middle panel) show percentage of IL-10 producing NK cells in liver. Data are presented as mean ± SD with $n = 4$–5 individual mice per group out of one experiment. Data were constrained to alive singlet NK cells and are shown in columns side-by-side in a concatenated qualitative dot plot (right panels) in which each column represents data of an individual mouse. Groups were compared by unpaired two-tailed *t*-test with Welch's correction (*$p < 0.05$).

the impact of ADAP on principal NK cell functions following their *in vivo* priming during infection, i.e., under physiological conditions involving a plethora of infection-induced cytokines as well as a complex network of NK cell-activating and inhibitory receptors. As such we feel that data from our *in vivo* study cannot directly be compared with the outcome from previous *in vitro* experiments but instead complement published knowledge and provides further clarification regarding the role of ADAP in infection-primed NK cells.

By extensively studying signaling events induced in NK cells by stimulation of the activating receptors CD137 or NKG2D, Rajasekaran et al. uncovered an ADAP-dependent signaling pathway exclusively responsible for the production of inflammatory cytokines but not for cytotoxicity (12). As an underlying mechanism for this striking dichotomy a unique interaction between Fyn and ADAP was discovered linking upstream signaling to the CBM module which, under the chosen experimental conditions, led to the production of IFN-γ and chemokines while not being responsible for cytotoxicity in murine and human NK cells (12). While applying antibody/cytokine-mediated *in vitro* stimulation of primed naïve NK cells confirmed these data (**Figure 1**), more physiological stimulation of naïve NK cells or infection-primed ADAPko NK cells with YAC-1 target cells uncovered impaired cytotoxicity of ADAP-deficient NK cells while their capacity to produce IFN-γ was not affected (**Figure 2**). Vivier et al. brought into consideration that the above mentioned study utilized IL-2-activated NK cells and that, given the plasticity of NK cells

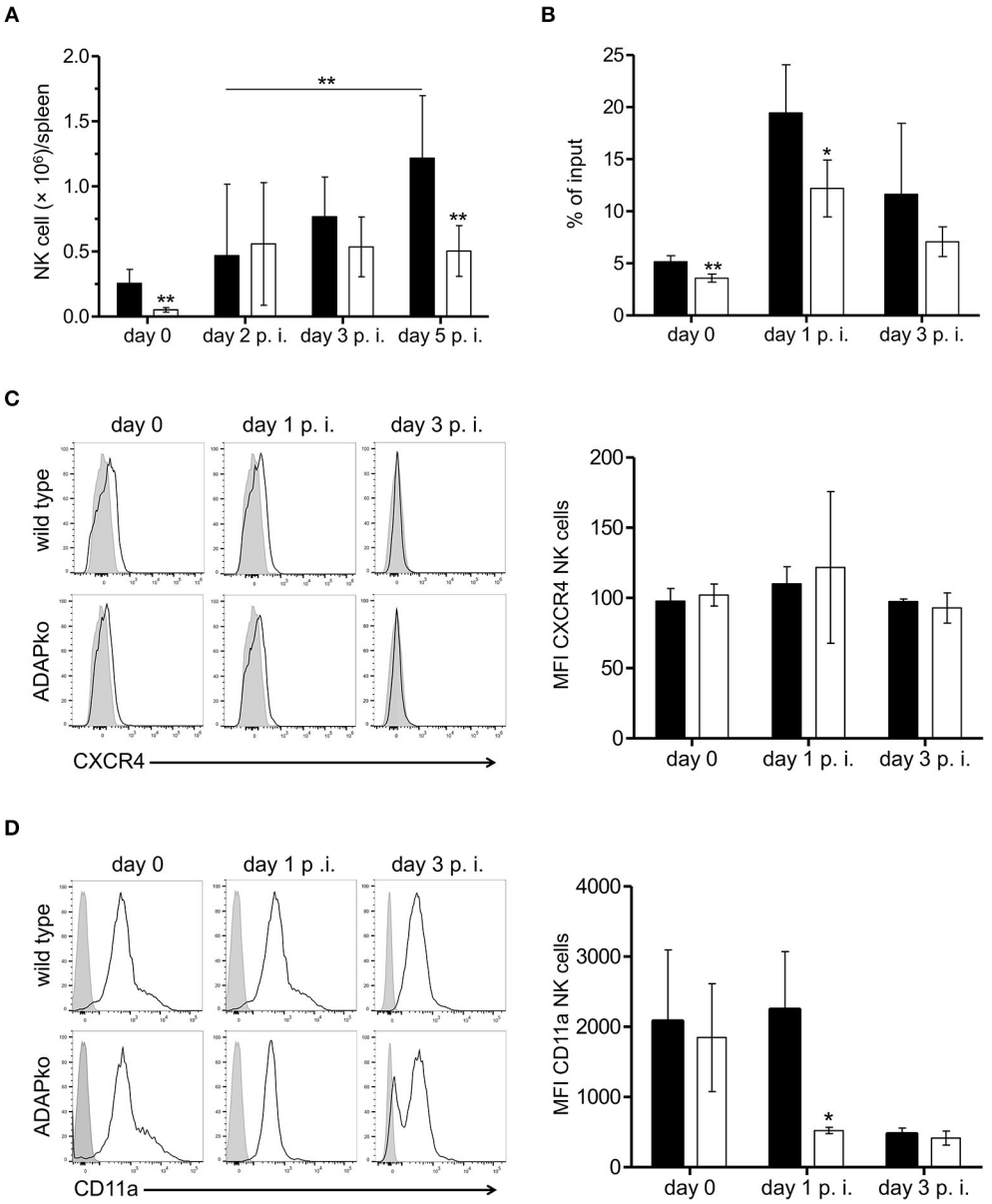

FIGURE 5 | Reduced accumulation in the spleen and impaired migratory capacity of ADAP-deficient NK cells of *Lm* infected mice. $ADAP^{fl/fl}$ × $NKp46\text{-}Cre^{het}$ (open bars) mice lacking ADAP specifically in NK cells and respective littermate controls ($ADAP^{wt/wt}$ × $NKp46\text{-}Cre^{het}$, black bars) were either infected with 2.5×10^4 CFU *Lm* or were left untreated (uninfected control, day 0). **(A)** $ADAP^{wt/wt}$ × $NKp46\text{-}Cre^{het}$ and conditional $ADAP^{fl/fl}$ × $NKp46\text{-}Cre^{het}$ mice were sacrificed at the indicated time points. Leukocytes were isolated from the spleen and NK cells were identified as $CD3^{-}NK1.1^{+}CD49b^{+}$ cells. Absolute NK cell numbers were calculated from the NK cell frequencies assessed by flow cytometry referred to the absolute leukocyte numbers as well as the frequencies of live cells. Data are presented as mean ± SD for $n = 4$–15 mice per group out of three independent experiments. **(B)** Splenocytes were seeded in the upper transwell chamber that was placed in medium containing the chemokine CXCL12 (250 ng/ml). After 4 h cells were recovered from the lower chamber, counted and analyzed by flow cytometry to determine the percentage of migrated NK cells (% of input). Data are presented as mean ± SD for $n = 4$ mice per group from two independent experiments. **(C)** Level of CXCR4 and **(D)** CD11a surface expression on NK cells. Depicted are representative histograms (left panels; light gray: respective stained fluorescence minus one control FMO; open: stained) and mean fluorescence intensity (MFI, right panels) ± SD of **(C)** CXCR4 and **(D)** CD11a on $NK1.1^{+}$ NK cells analyzed day 0 (female mice), day 1 and day 3 p.i. with $n = 4$–5 individually analyzed mice per group out of one to two experiments. Groups were compared by **(A–D)** unpaired two-tailed *t*-test with Welch's correction and additionally **(A)** by two-way ANOVA with Bonferroni correction for multiple hypothesis testing ($^{*}p < 0.05$, $^{**}p < 0.01$).

that is heavily dependent on their activation (50), it would be questionable if the findings by Rajasekaran et al. would generally apply to NK cells activated under different conditions (12). During Listeria infection various cytokines are induced that are known to permit NK cell activation (51) and indeed most of the known NK cell-activating cytokines were detectable in sera of *Lm* infected wild type and ADAPko mice (**Supplementary Figure 1**). Importantly, ADAPko mice did not exhibit an overall defect in

cytokine response to *Lm* infection (**Supplementary Figure 1**). Thus, we can largely exclude that impaired effector function in ADAPko NK cells is due to impaired priming in the ADAP-deficient host but is rather an inherent effect due to ADAP-deficiency in NK cells. Apart from the proteome analysis (**Figure 3**) we did not further analyze the influence of *Lm* infection on the expression of activating/inhibitory receptors on NK cells and the expression of the corresponding ligands on target cells, respectively. Anyway, we hypothesize that during infection the combination of cytokines and/or receptor-ligand pairs is ideal to prime NK cells for both, cytokine production and cytotoxicity and that under these optimized priming conditions the separation of the ADAP-dependent and -independent signaling pathways in NK cells is abrogated. Future studies are needed to clarify this aspect on the molecular level.

ADAPko NK cells exhibit reduced cytotoxic capacity (**Figure 2**). This phenotype was further confirmed by proteomic profiling that on the one hand revealed an overall decrease of intracellular perforin and CD107a upon infection suggesting the release of perforin from $CD107a^+$ granules following *in vivo* priming. Moreover, given that the applied LC-MS/MS analysis is particularly suitable for the detection of intracellular proteins, the observation of a slightly more pronounced decrease in CD107a protein abundance in ADAP-sufficient compared to ADAP-deficient NK cells during infection as well-hints at decreased cytolytic activity of ADAPko NK cells (**Figure 3D**).

Remarkably, independent of the genotype infection-priming of NK cells resulted in an overall decreased abundance of virtually all detectable prototypic NK cell proteins with the exception of granzyme A and granzyme B that were even found at higher abundances (**Figures 3C**,**D**). While at a first glance it might be counter-intuitive that priming of NK cells would result in increased granzyme A and granzyme B levels but at the same time decreased abundance of CD107a and perforin, several mechanisms could explain this finding. Already in previous studies we observed co-localization of CD107a with perforin but not with granzymes (Heyner et al., unpublished) and it has been shown that dependent on the activating signal used to stimulate NK cell function different cytotoxic vesicles are detectable within the cell. For instance, engagement of NKG2D or 2B4 on NK cells induces the co-localization of perforin with $Rab27a^+$ but not $Munc13\text{-}4^+$ vesicles. In direct contrast, antibody-dependent CD16 activation induces perforin localization to $Munc13\text{-}4^+$ vesicles but not to $Rab27a^+$ ones (52). Moreover, Munc13-4 and Rab27a have been described to be involved in granzyme B polarization to the immunological synapse (53). Thus, the observed differences regarding granzyme A/granzyme B vs. CD107a/perforin abundances might be a result of complex ligand/receptor binding events induced early on during infection leading to discrete maturation of lytic granules in NK cells. On the other hand, we cannot exclude that newly synthesized proteins, i.e., induced gene expression upon infection might also explain the differences of cytotoxic protein abundances. In this context, Fehniger et al. have shown that, well in line with our proteome data (**Figure 3D**), resting NK cells contain high levels of granzyme A but little granzyme B and perforin (54). Interestingly, they uncovered a clear discrepancy in terms of protein content *vs.* mRNA content, with mRNA being detectable in naïve NK cells at high abundance for all three genes. While naïve NK cells were *per se* granzyme A^+, stimulation with IL-15 increased the frequency of granzyme B and perforin expressing NK cells. Only in case of granzyme B this was associated with induced mRNA expression (54). While these data do not explain the inverse pattern of granzyme A/granzyme B and perforin in infection-primed NK cells they provide evidence for fundamental differences regarding the regulation of transcription and translation for these cytotoxic mediators in NK cells. Still, both granzyme B and perforin were shown to be required for efficient cytotoxicity *in vitro* and *in vivo* (54) and we show here that the abundance of one of them, i.e., perforin seems to be diminished in NK cells lacking ADAP (**Figure 2C**).

Interestingly, ADAP-deficiency in NK cells was associated with a more severe course of *Lm* infection (**Figure 4A**) which was not due to impaired antibacterial immunity (**Figure 4B**). Activated NK cells respond to *Lm* infection (19) in a complex process that requires crosstalk with macrophages, neutrophils and dendritic cells (35, 36). With this, NK cells are able to shape the immune response *via* pro-inflammatory cytokine and chemokine stimulation as well as due to cell-to-cell contacts (55, 56). Enhanced disease severity might be indicative for a critical role of ADAP in NK cells in the overall innate immune response induced during *Lm* infection. Apart from the role of ADAP in NK cells during listeriosis it is however even not clear whether NK cells exhibit a beneficial or detrimental role in immunity to *Lm*. An early study by Teixeira and Kaufmann revealed improved pathogen control in mice lacking NK cells (57). The deleterious role of NK cells in listeriosis was confirmed later by Viegas et al. demonstrating that although NK cells are not required for pathogen elimination *Lm* infected NK cell-deficient mice showed improved survival (58). Data from another study however implied that NK cells may rather be protective during *Lm* infection (51). By secretion of the pro-inflammatory cytokines IL-12, TNF-α, IL-1β, and IL-18 by *Lm* activated dendritic cells, NK cells are primed to produce IFN-γ. IFN-γ plays a pivotal role in innate and adaptive immunity to intracellular bacteria and indeed mice lacking the IFN-γ receptor are highly susceptible to *Lm* infection (59). Despite comparable IFN-γ production in infection-primed wild type and ADAPko NK cells (**Figure 2D**) IFN-γ serum concentration was increased by day 3 p.i. in ADAPko mice (**Supplementary Figure 1**). However, since in conventional ADAPko mice also immune cells other than NK cells are deficient for ADAP, we assume that IFN-γ produced by e.g., T cells, NKT cells, macrophages, B cells, or dendritic cells accounts for the observed difference. This is supported by our finding that in conditional ADAPko mice lacking ADAP exclusively in NK cells, IFN-γ serum concentration markedly increases by day 2 post-*Lm* infection, while we did not observe significant differences in infection-induced IFN-γ levels between wild type and conditional ADAPko mice (data not shown). It has recently been shown that infection-induced NK cell activation increases susceptibility to *Lm* infection independent from IFN-γ production by NK cells (34). As an underlying mechanism for the detrimental role of NK cells in listeriosis the authors uncovered that NK cells responding to *Lm* infection acquire

the ability to produce the immunosuppressive cytokine IL-10. In a follow-up study the same group identified that licensing of IL-10 production in NK cells requires IL-18 released by *Lm* infected Bat3$^+$ DCs (60). We did not observe any effect of ADAP-deficiency in NK cells on their capacity to produce IL-10 (**Figure 4C**). Combined with the finding, that neither the concentration of the immunosuppressive IL-10, nor the NK cell licensing cytokine IL-18 differed in sera of *Lm* infected wild type and ADAPko mice (**Supplementary Figure 1** and data not shown for conditional ADAPko mice), we exclude the possibility that IL-10 produced by NK cells would account for the enhanced morbidity of conditional ADAPko mice to *Lm* infection.

Within the early phase of *Lm* infection phagocytes are critically involved in immune containment of the pathogen (61). Infiltrating monocytes and especially neutrophils attracted to the site of infection may cause adverse side effects thus contributing to immunopathology (62, 63). Since infection-primed ADAPko NK cells exhibited impaired production of the phagocyte attracting chemokines CCL3, CCL4, and CCL5 (**Supplementary Figure 4**) we compared the number of monocytes and neutrophils in the spleen of *Lm* infected animals. However, no differences in the absolute numbers of monocytes and neutrophils were detectable (data not shown). Macrophages and neutrophils are considered the major source for IL-12 during listeriosis (64, 65). Notably, next to comparable numbers of these cells in the spleen of *Lm* infected wild type and conditional ADAPko mice we also did not find quantitative differences in serum IL-12 levels (data not shown) as a potential indicator for differential activation of phagocytes in mice lacking ADAP in NK cell. Taken together, enhanced body weight loss of infected conditional ADAPko mice most likely cannot be attributed to enhanced immunopathology exerted by phagocytes. However, the molecular/cellular mechanism by which ADAP-deficiency in NK cells promote disease severity during *Lm* infection remains elusive.

To the best of our knowledge, no data are available regarding the migration of ADAP-deficient NK cells. Utilizing an *in vitro* transwell system we could show for the first time that CXCL12-induced migration of ADAP-deficient NK cells is reduced compared to ADAP-sufficient NK cells. During infection, NK cells are recruited to the sites of inflammation in a chemokine-dependent manner. This is well-reflected by the observed increased migratory activity of *Lm* infection-primed compared to naïve NK cells (**Figure 5B**). CXCL12 is an important chemokine not only for T cells, but also for the chemo-attraction of NK cells (66). Since *Lm* infection in mice represents a complex disease model with different leukocyte subsets being recruited and activated to produce pro-inflammatory cytokines and chemokines during early innate immune activation, *in vitro* testing of CXCL12-induced migration of NK cells only insufficiently reflects the *in vivo* situation. Nevertheless, impaired migratory activity of ADAP-deficient NK cells might at least in part explain the reduced numbers of NK cells in the spleen of conditional ADAPko mice early after *Lm* infection (**Figure 5A**). In T cells, the inside-out signaling pathways leading to integrin activation after chemokine receptor stimulation are well-described (4) and we have recently shown that migration of both, CD4$^+$ and CD8$^+$ T cells, depends on ADAP (6). For NK cells, it is known that integrin-dependent activation is essential for migration and for cytotoxicity (67). Therefore, it seems likely that similar signaling complexes are formed in T cells and NK cells. Of note, compared to wild type NK cells, CD11a surface expression on infection-primed ADAPko NK cells was markedly reduced on day 1 post-infection (**Figure 5D**). Together with CD18, CD11a forms the heterodimeric adhesion molecule LFA-1 which upon interaction with its ligand ICAM on endothelial cells promotes entry of leukocytes from the bloodstream into tissues. In fact, an early study by Allavena et al. has shown that LFA-1 is crucial for NK cell adhesion to and migration through the vascular endothelium (68). Importantly, at least in T cells the intracellular domain of CD11a is directly linked to the signaling complex involving ADAP (69, 70). Thus, it is tempting to speculate that lack of ADAP in NK cells in NK cells and the associated reduced surface expression of CD11a on NK cells 1 day post *Lm* infection is mechanistically linked to the reduced accumulation of NK cells in the infected spleen of conditional ADAPko mice (**Figure 5A**). However, since differential CD11a expression on ADAPko vs. wild type NK cells was only transient and genotype-dependent differences in CD11a surface expression were lost by day 3 post-infection, most probably additional molecular factors will contribute to the observed phenotype. Yet, further studies are needed to dissect in more detail the molecular mechanism underlying reduced migratory activity of naïve and infection-primed ADAP-deficient NK cells.

DATA AVAILABILITY STATEMENT

The raw data supporting the conclusions of this article will be made available by the authors, without undue reservation, to any qualified researcher.

ETHICS STATEMENT

The animal study was reviewed and approved by Niedersächsisches Landesamt für Verbraucherschutz und Lebensmittelsicherheit, Germany and Landesamt für Verbraucherschutz, Sachsen-Anhalt, Germany.

AUTHOR CONTRIBUTIONS

MB designed and performed experiments and wrote the manuscript. ST, PR, MHa, MHe, MV, and GP designed and performed experiments. FK performed data mining and statistical analysis for proteome data. AJ contributed conception to the analyses. LJ contributed conception to the analysis, data interpretation, and provided research material. CG provided research material. BS, AR, and DB designed and supervised the research and wrote the manuscript. All authors contributed to manuscript revision, read, and approved the submitted version.

FUNDING

This work was funded by the Deutsche Forschungsgemeinschaft (DFG, German Research Foundation) - Project-ID 97850925 -

SFB 854 (BS B19, DB A23) and AR (RE 2907/2-2). MB and GP were supported by grants (SI2 and SI3) of the State of Saxony-Anhalt to BS.

ACKNOWLEDGMENTS

We thank F. Ewert, A. Sohnekind, G. Weitz, and U. Bröder for expert technical assistance, J. Rudolph for coordination of the ADAP$^{fl/fl}$ × NKp46-Cre^{het} breeding, I. Jorde, U. Kärst, and J. Wissing for technical support, S. Kliche for scientific advice as well as L. Gröbe and M. Höxter expert for cell sorting support.

SUPPLEMENTARY MATERIAL

The Supplementary Material for this article can be found online at: https://www.frontiersin.org/articles/10.3389/fimmu.2019.03144/full#supplementary-material

REFERENCES

1. Flynn DC. Adaptor proteins. *Oncogene*. (2001) 20:6270–2. doi: 10.1038/sj.onc.1204769
2. Veale M, Raab M, Li Z, da Silva AJ, Kraeft SK, Weremowicz S, et al. Novel isoform of lymphoid adaptor FYN-T-binding protein (FYB-130) interacts with SLP-76 and up-regulates interleukin 2 production. *J Biol Chem*. (1999) 274:28427–35. doi: 10.1074/jbc.274.40.28427
3. Peterson EJ. The TCR ADAPts to integrin-mediated cell adhesion. *Immunol Rev*. (2003) 192:113–21. doi: 10.1034/j.1600-065X.2003.00026.x
4. Kliche S, Worbs T, Wang X, Degen J, Patzak I, Meineke B, et al. CCR7-mediated LFA-1 functions in T cells are regulated by 2 independent ADAP/SKAP55 modules. *Blood*. (2012) 19:777–85. doi: 10.1182/blood-2011-06-362269
5. Mitchell JS, Burbach BJ, Srivastava R, Fife BT, Shimizu Y. Multistage T cell-dendritic cell interactions control optimal CD4 T cell activation through the ADAP-SKAP55-signaling module. *J Immunol*. (2013) 191:2372–83. doi: 10.4049/jimmunol.1300107
6. Parzmair GP, Gereke M, Haberkorn O, Annemann M, Podlasly L, Kliche S, et al. ADAP plays a pivotal role in CD4 + T cell activation but is only marginally involved in CD8 + T cell activation, differentiation, and immunity to pathogens. *J Leukoc Biol*. (2017) 101:407–19. doi: 10.1189/jlb.1A0216-090RR
7. Fiege JK, Beura LK, Burbach BJ, Shimizu Y. Adhesion- and degranulation-promoting adapter protein promotes CD8 T cell differentiation and resident memory formation and function during an acute Infection. *J Immunol*. (2016) 197:2079–89. doi: 10.4049/jimmunol.1501805
8. Kasirer-Friede A, Cozzi MR, Mazzucato M, De Marco L, Ruggeri ZM, Shattil SJ. Signaling through GP Ib-IX-V activates alpha IIb beta 3 independently of other receptors. *Blood*. (2004) 103:3403–11. doi: 10.1182/blood-2003-10-3664
9. Rudolph JM, Guttek K, Weitz G, Meinke CA, Kliche S, Reinhold D, et al. Characterization of mice with a platelet-specific deletion of the adapter molecule ADAP. *Mol Cell Biol*. (2019) 39:e00365–18. doi: 10.1128/MCB.00365-18
10. Dluzniewska J, Zou L, Harmon IR, Ellingson MT, Peterson EJ. Immature hematopoietic cells display selective requirements for adhesion- and degranulation-promoting adaptor protein in development and homeostatsis. *Eur J Immunol*. (2007) 37:3208–19. doi: 10.1002/eji.200737094
11. Coppolino MG, Krause M, Hagendorff P, Monner DA, Trimble W, Grinstein S, et al. Evidence for a molecular complex consisting of Fyb/SLAP, SLP-76, Nck, VASP and WASP that links the actin cytoskeleton to Fcgamma receptor signalling during phagocytosis. *J Cell Sci*. (2001) 114:4307–18.
12. Rajasekaran K, Kumar P, Schuldt KM, Peterson EJ, Vanhaesebroeck B, Dixit V, et al. Signaling by Fyn-ADAP via the Carma1-Bcl-10-MAP3K7 signalosome exclusively regulates inflammatory cytokine production in NK cells. *Nat Immunol*. (2013) 14:1127–36. doi: 10.1038/ni.2708
13. Fostel LV, Dluzniewska J, Shimizu Y, Burbach BJ, Peterson EJ. ADAP is dispensable for NK cell development and function. *Int Immunol*. (2006) 18:1305–14. doi: 10.1093/intimm/dxl063
14. Yokoyama WM, Kim S, French AR. The dynamic life of natural killer cells. *Annu Rev Immunol*. (2004) 22:405–29. doi: 10.1146/annurev.immunol.22.012703.104711
15. Lanier LL. NK cell recognition. *Annu Rev Immunol*. (2005) 23:225–74. doi: 10.1146/annurev.immunol.23.021704.115526
16. Di Santo JP. Natural killer cell developmental pathways: a question of balance. *Annu Rev Immunol*. (2006) 24:257–86. doi: 10.1146/annurev.immunol.24.021605.090700
17. Bryceson YT, Chiang SC, Darmanin S, Fauriat C, Schlums H, Theorell J, et al. Molecular mechanisms of natural killer cell activation. *J Innate Immun*. (2011) 3:216–26. doi: 10.1159/000325265
18. Trapani JA, Smyth MJ. Functional significance of the perforin/granzyme cell death pathway. *Nat Rev Immunol*. (2002) 2:735–47. doi: 10.1038/nri911
19. Humann J, Lenz LL. Activation of naive NK cells in response to *Listeria monocytogenes* requires IL-18 and contact with infected dendritic cells. *J Immunol*. (2010) 184:5172–8. doi: 10.4049/jimmunol.0903759
20. Prager I, Watzl C. Mechanisms of natural killer cell-mediated cellular cytotoxicity. *J Leukoc Biol*. (2019) 105:1319–29. doi: 10.1002/JLB.MR0718-269R
21. Zhang Y, Huang B. The development and diversity of ILCs, NK cells and their relevance in health and diseases. *Adv Exp Med Biol*. (2017) 1024:225–44. doi: 10.1007/978-981-10-5987-2_11
22. Martín-Fontecha A, Thomsen LL, Brett S, Gerard C, Lipp M, Lanzavecchia A, et al. Induced recruitment of NK cells to lymph nodes provides IFN-γ for TH1 priming. *Nat Immunol*. (2004) 5:1260–5. doi: 10.1038/ni1138
23. Boehm U, Klamp T, Groot M, Howard JC. Cellular responses to interferon-gamma. *Annu Rev Immunol*. (1997) 15:749–95. doi: 10.1146/annurev.immunol.15.1.749
24. Kak G, Raza M, Tiwari BK. Interferon-gamma (IFN-γ): exploring its implications in infectious diseases. *Biomol Concepts*. (2018) 9:64–79. doi: 10.1515/bmc-2018-0007
25. Narni-Mancinelli E, Jaeger BN, Bernat C, Fenis A, Kung S, De Gassart A, et al. Tuning of natural killer cell reactivity by NKp46 and helios calibrates T cell responses. *Science*. (2012) 335:344–8. doi: 10.1126/science.1215621
26. Lucas M, Schachterle W, Oberle K, Aichele P, Diefenbach A. Dendritic cells prime natural killer cells by trans-presenting interleukin 15. *Immunity*. (2007) 26:503–17. doi: 10.1016/j.immuni.2007.03.006
27. Nandagopal N, Ali AK, Komal AK, Lee SH. The critical role of IL-15-PI3K-mTOR pathway in natural killer cell effector functions. *Front Immunol*. (2014) 5:187. doi: 10.3389/fimmu.2014.00187
28. Stackaruk ML, Lee AJ, Ashkar AA. Type I interferon regulation of natural killer cell function in primary and secondary infections. *Expert Rev Vaccines*. (2013) 8:875–84. doi: 10.1586/14760584.2013.814871
29. Brady J, Carotta S, Thong RP, Chan CJ, Hayakawa Y, Smyth MJ, et al. The interactions of multiple cytokines control NK cell maturation. *J Immunol*. (2010) 185:6679–88. doi: 10.4049/jimmunol.0903354
30. Takeda K, Tsutsui H, Yoshimoto T, Adachi O, Yoshida N, Kishimoto T, et al. Defective NK cell activity and Th1 response in IL-18-deficient mice. *Immunity*. (1998) 8:383–90. doi: 10.1016/S1074-7613(00)80543-9
31. Sánchez MJ, Muench MO, Roncarolo MG, Lanier LL, Phillips JH. Identification of a common T/natural killer cell progenitor in human fetal thymus. *J Exp Med*. (1994) 180:569–76. doi: 10.1084/jem.180.2.569
32. May RM, Okumura M, Hsu CJ, Bassiri H, Yang E, Rak G, et al. Murine natural killer immunoreceptors use distinct proximal signaling complexes to direct cell function. *Blood*. (2013) 121:3135–46. doi: 10.1182/blood-2012-12-474361
33. Humann J, Bjordahl R, Andreasen K, Lenz LL. Expression of the p60 autolysin enhances NK cell activation and is required for *Listeria monocytogenes* expansion in IFN-gamma-responsive mice. *J Immunol*. (2007) 178:2407–14. doi: 10.4049/jimmunol.178.4.2407

34. Clark SE, Filak HC, Guthrie BS, Schmidt RL, Jamieson A, Merkel P, et al. Bacterial manipulation of NK cell regulatory activity increases susceptibility to *Listeria monocytogenes* Infection. *PLoS Pathog*. (2016) 12:e1005708. doi: 10.1371/journal.ppat.1005708
35. Newman KC, Riley EM. Whatever turns you on: accessory-cell-dependent activation of NK cells by pathogens. *Nat Rev Immunol*. (2007) 7:279–91. doi: 10.1038/nri2057
36. Vivier E, Tomasello E, Baratin M, Walzer T, Ugolini S. Functions of natural killer cells. *Nat Immunol*. (2008) 9:503–10. doi: 10.1038/ni1582
37. Peterson EJ, Woods ML, Dmowski SA, Derimanov G, Jordan MS, Wu JN, et al. Coupling of the TCR to integrin activation by SLAP-130/Fyb. *Science*. (2001) 293:2263–5. doi: 10.1126/science.1063486
38. Skarnes WC, Rosen B, West AP, Koutsourakis M, Bushell W, Iyer V, et al. A conditional knockout resource for the genome-wide study of mouse gene function. *Nature*. (2011) 474:337–42. doi: 10.1038/nature10163
39. Narni-Mancinelli E, Chaix J, Fenis A, Kerdiles YM, Yessaad N, Reynders A, et al. Fate mapping analysis of lymphoid cells expressing the NKp46 cell surface receptor. *Proc Natl Acad Sci USA*. (2011) 108:18324–9. doi: 10.1073/pnas.1112064108
40. Rudolph J, Meinke C, Voss M, Guttek K, Kliche S, Reinhold D, et al. Immune cell-type specific ablation of adapter protein ADAP differentially modulates EAE. *Front Immunol*. (2019) 10:2343. doi: 10.3389/fimmu.2019.02343
41. Frentzel S, Katsoulis-Dimitriou K, Jeron A, Schmitz I, Bruder D. Essential role of IκBNS for *in vivo* CD4+ T-cell activation, proliferation, and Th1-cell differentiation during *Listeria monocytogenes* infection in mice. *Eur J Immunol*. (2019) 49:1391–8. doi: 10.1002/eji.201847961
42. Hughes CS, Foehr S, Garfield DA, Furlong EE, Steinmetz LM, Krijgsveld J. Ultrasensitive proteome analysis using paramagnetic bead technology. *Mol Syst Biol*. (2014) 30:757. doi: 10.15252/msb.20145625
43. Sielaff M, Kuharev J, Bohn T, Hahlbrock J, Bopp T, Tenzer S, et al. Evaluation of FASP, SP3, and iST protocols for proteomic sample preparation in the low microgram range. *J Proteome Res*. (2017) 16:4060–72. doi: 10.1021/acs.jproteome.7b00433
44. Alter G, Malenfant JM, Altfeld M. CD107a as a functional marker for the identification of natural killer cell activity. *J Immunol Methods*. (2004) 294:15–22. doi: 10.1016/j.jim.2004.08.008
45. Abel AM, Yang C, Thakar MS, Malarkannan S. Natural killer cells: development, maturation, and clinical utilization. *Front Immunol*. (2018) 13:1869. doi: 10.3389/fimmu.2018.01869
46. Chaix J, Tessmer MS, Hoebe K, Fuséri N, Ryffel B, Dalod M, et al. Cutting edge: priming of NK cells by IL-18. *J Immunol*. (2008) 181:1627–31. doi: 10.4049/jimmunol.181.3.1627
47. Combs J, Kim SJ, Tan S, Ligon LA, Holzbaur EL, Kuhn J, et al. Recruitment of dynein to the jurkat immunological synapse. *Proc Natl Acad Sci USA*. (2006) 103:14883–8. doi: 10.1073/pnas.0600914103
48. Sylvester M, Kliche S, Lange S, Geithner S, Klemm C, Schlosser A, et al. Adhesion and degranulation promoting adapter protein (ADAP) is a central hub for phosphotyrosine-mediated interactions in T cells. *PLoS ONE*. (2010) 5:e11708. doi: 10.1371/journal.pone.0011708
49. Griffiths EK, Krawczyk C, Kong YY, Raab M, Hyduk SJ, Bouchard D, et al. Positive regulation of T cell activation and integrin adhesion by the adapter Fyb/Slap. *Science*. (2001) 293:2260–3. doi: 10.1126/science.1063397
50. Vivier E, Ugolini S, Nunès JA. ADAPted secretion of cytokines in NK cells. *Nat Immunol*. (2013) 14:1108–10. doi: 10.1038/ni.2737
51. Shtrichman R, Samuel CE. The role of gamma interferon in antimicrobial immunity. *Curr Opin Microbiol*. (2001) 4:251–9. doi: 10.1016/S1369-5274(00)00199-5
52. Wood SM, Meeths M, Chiang SC, Bechensteen AG, Boelens JJ, Heilmann C, et al. Different NK cell-activating receptors preferentially recruit Rab27a or Munc13-4 to perforin-containing granules for cytotoxicity. *Blood*. (2009) 114:4117–27. doi: 10.1182/blood-2009-06-225359
53. Zhang M, Bracaglia C, Prencipe G, Bemrich-Stolz CJ, Beukelman T, Dimmitt RA, et al. A Heterozygous RAB27A mutation associated with delayed cytolytic granule polarization and hemophagocytic lymphohistiocytosis. *J Immunol*. (2016) 196:2492–503. doi: 10.4049/jimmunol.1501284
54. Fehniger TA, Cai SF, Cao X, Bredemeyer AJ, Presti RM, French AR, et al. Acquisition of murine NK cell cytotoxicity requires the translation of a pre-existing pool of granzyme B and perforin mRNAs. *Immunity*. (2007) 26:798–811. doi: 10.1016/j.immuni.2007.04.010
55. Cella M, Miller H, Song C. Beyond NK cells: the expanding universe of innate lymphoid cells. *Front Immunol*. (2014) 5:282. doi: 10.3389/fimmu.2014.00282
56. Lanier LL. Up on the tightrope: natural killer cell activation and inhibition. *Nat Immunol*. (2008) 9:495. doi: 10.1038/ni1581
57. Teixeira HC, Kaufmann SH. Role of NK1.1+ cells in experimental listeriosis. NK1+ cells are early IFN-gamma producers but impair resistance to *Listeria monocytogenes* infection. *J Immunol*. (1994) 152:1873–82.
58. Viegas N, Andzinski L, Wu CF, Komoll RM, Gekara N, Dittmar KE, et al. IFN-γ production by CD27+ NK cells exacerbates *Listeria monocytogenes* infection in mice by inhibiting granulocyte mobilization. *Eur J Immunol*. (2013) 43:2626–37. doi: 10.1002/eji.201242937
59. Harty JT, Bevan MJ. Specific immunity to *Listeria monocytogenes* in the absence of IFN gamma. *Immunity*. (1995) 3:109–17. doi: 10.1016/1074-7613(95)90163-9
60. Clark SE, Schmidt RL, McDermott DS, Lenz LL. A Batf3/Nlrp3/IL-18 axis promotes natural killer cell IL-10 production during *Listeria monocytogenes* infection. *Cell Rep*. (2018) 23:2582–94. doi: 10.1016/j.celrep.2018.04.106
61. Pamer EG. Immune responses to *Listeria monocytogenes*. *Nat Rev Immunol*. (2004) 4:812–23. doi: 10.1038/nri1461
62. Thaler B, Hohensinner PJ, Krychtiuk KA, Matzneller P, Koller L, Brekalo M, et al. Differential *in vivo* activation of monocyte subsets during low-grade inflammation through experimental endotoxemia in humans. *Sci Rep*. (2016) 26:30162. doi: 10.1038/srep30162
63. Yang Q, Ghose P, Ismail N. Neutrophils mediate immunopathology and negatively regulate protective immune responses during fatal bacterial infection-induced toxic shock. *Infect Immun*. (2013) 81:751–63. doi: 10.1128/IAI.01409-12
64. Seki E, Tsutsui H, Tsuji NM, Hayashi N, Adachi K, Nakano H, et al. Critical roles of myeloid differentiation factor 88-dependent proinflammatory cytokine release in early phase clearance of *Listeria monocytogenes* in mice. *J Immunol*. (2002) 169:3863–8. doi: 10.4049/jimmunol.169.7.3863
65. Tripp CS, Wolf SF, Unanue ER. Interleukin 12 and tumor necrosis factor alpha are costimulators of interferon gamma production by natural killer cells in severe combined immunodeficiency mice with listeriosis, and interleukin 10 is a physiologic antagonist. *Proc Natl Acad Sci USA*. (1993) 90:3725–9. doi: 10.1073/pnas.90.8.3725
66. Bernardini G, Sciumè G, Bosisio D, Morrone S, Sozzani S, Santoni A. CCL3 and CXCL12 regulate trafficking of mouse bone marrow NK cell subsets. *Blood*. (2008) 111:3626–34. doi: 10.1182/blood-2007-08-106203
67. Barber DF, Faure M, Long EO. LFA-1 contributes an early signal for NK cell cytotoxicity. *J Immunol*. (2004) 173:3653–9. doi: 10.4049/jimmunol.173.6.3653
68. Allavena P, Bianchi G, Paganin C, Giardina G, Mantovani A. Regulation of adhesion and transendothelial migration of natural killer cells. *Nat Immun*. (1996) 15:107–116.
69. Verma NK, Kelleher D. Not just an adhesion molecule: LFA-1 contact tunes the T lymphocyte program. *J Immunol*. (2017) 199:1213–21. doi: 10.4049/jimmunol.1700495
70. Wang H, Rudd CE. SKAP-55, SKAP-55-related and ADAP adaptors modulate integrin-mediated immune-cell adhesion. *Trends Cell Biol*. (2008) 18:486–93. doi: 10.1016/j.tcb.2008.07.005

Conflict of Interest: The authors declare that the research was conducted in the absence of any commercial or financial relationships that could be construed as a potential conflict of interest.

Advantages of publishing in Frontiers

OPEN ACCESS
Articles are free to read for greatest visibility and readership

FAST PUBLICATION
Around 90 days from submission to decision

HIGH QUALITY PEER-REVIEW
Rigorous, collaborative, and constructive peer-review

TRANSPARENT PEER-REVIEW
Editors and reviewers acknowledged by name on published articles

Frontiers
Avenue du Tribunal-Fédéral 34
1005 Lausanne | Switzerland

Visit us: www.frontiersin.org
Contact us: info@frontiersin.org | +41 21 510 17 00

REPRODUCIBILITY OF RESEARCH
Support open data and methods to enhance research reproducibility

DIGITAL PUBLISHING
Articles designed for optimal readership across devices

FOLLOW US
@frontiersin

IMPACT METRICS
Advanced article metrics track visibility across digital media

EXTENSIVE PROMOTION
Marketing and promotion of impactful research

LOOP RESEARCH NETWORK
Our network increases your article's readership